A Data-driven Approach to Motion Diversification over Increases in Body Morphology

Thesis by
Satish Shewhorak, B.Sc., M.A.

Director of Studies: **Dr. Yifeng Zeng**
2nd Supervisor: **Dr. Shengchao Qin**

Submitted **April 2017**
In Partial Fulfilment of the Requirements for the
Degree of Doctor of Philosophy

School of Computing
Teesside University

This research was sponsored by the James Caldwell Scholarship. The views and conclusions contained in this document are those of the author and should not be interpreted as representing the official policies, either expressed or implied, of the sponsor.

ABSTRACT

Background: Generating locomotion for characters is a complex field with many challenges remaining for researchers to tackle. Whilst there has been various research undertaken into how to create diverse motion using physical simulation, inverse kinematics and motion capture, there is still little research on how to relate changes in virtual characters' body shape to the way they walk. This is important as audiences are capable of detecting repetition of character appearance and walking styles. By relating generated walk cycles to the body morphology of characters we can improve their believability. And to achieve this using a dynamic and automated system would save animators time when needing to create a variety of believable characters.

Objectives: This study will explore how people perceive gait to change over variations in body shape, how gait actually varies and whether it is possible to build a framework that believably correlates changes in gait parameters over changes in anthropometric parameters.

Implementing this framework could then produce a tool for animators that generates a variety of virtual characters with believable variations in walking styles.

The goal of this project is to improve the believability of virtual characters by relating virtual character's body shapes to an appropriate walk cycle.

Methods: 8 papers were analysed to generate 8 empirical appearance to motion trendline formulas. These formulas formed the basis of the scripted animation tool.

The animation tool was then used to create a point light survey testing 6 motion parameters to test people's perception of changes in motion over appearance.

n= 59 participants completed the perceptual online video surveys.

The animation tool's formulas were updated with the results of the point light survey and another survey was created using character meshes.

n= 69 participants completed the perceptual online video surveys.

28 adult male gait patterns were motion captured and analysed using a Vicon motion capture suite.

5 parameters were analysed to have the strongest appearance to motion correlation and were sorted by order of perceptual dominance. These parameters were implemented in the scripted animation tool and a final perceptual poll was conducted.
n= 96 participants validated the final animation tool using an online video survey.

Findings: The empirical data analysis identified speed, stride length, step width, stance/ step phase and foot progression as motion parameters that change over increases in Body Mass Index (BMI).
The point light perceptual survey found that changes to arm abduction, average arm bob and arm swing all produced motions associated with obese body morphologies.
The character mesh perceptual survey verified that speed and walking base were motion parameters associated with changes in body morphology, whilst verifying previous parameter strengths and combinations.
The actual motion capture sessions produced a framework of 5 appearance to motion formulas, ordered by perceptual dominance. The predictive correlations include:

1. Preferred walking speed over height
2. Average arm abduction over chest circumference
3. Walking base over waist-to-height ratio
4. Arm bob magnified over height
5. Arm swing over body fat percentage

A final perceptual video poll found that when asked to rank 4 different types of obese generated motion, participants voted the framework of anthropometric to locomotive parameters tool to be the most believable by a 38% majority.

Conclusions: This study identifies 5 gait parameters that people have identified as being perceptually dominant. The motion capture analysis highlighted 5 gait parameters with significant correlations to appearance parameters. When implementing the chosen combination of appearance to gait parameters a significant majority of people ranked this to more believably represent an obese character walk, than a lean, obese and keyframe obese walk. An efficient and believable method for generating diverse locomotion that relates to the body morphology of the character has been created and validated.

ACKNOWLEDGEMENTS

I would like to thank my team of supervisors including Dr. Yifeng Zeng and Dr. Shengchao Qin for their guidance. I would also like to thank Prof. James Caldwell for his generosity in sponsoring my PhD programme as well as his dedication and commitment to Teesside University's research within the School of Computing and Mathematics. I would like to thank Tom MacPherson in the School of Social Sciences, Business & Law for his support in using the Biomechanics Lab and Martin Davies, Matthew Graves and Stephie Johnson for their technical support. I would like to thank Gabrielle Kent for her patience and encouragement throughout.

CONTENTS

LIST OF FIGURES

LIST OF TABLES

LIST OF EQUATIONS

1. INTRODUCTION

In the field of animated films and games, there are often main characters that are individually modelled, animated or motion captured to imbue them with a sense of weight and believable motion.

However there is usually the need to populate these scenes with a range of cloned background characters. To give the impression of a believable range of different characters, we can take a single character and vary it in a number of different ways to save on modelling and animation time. These variations can include by texture (Thalmann et al., 2009), skin colour, clothing (Tecchia et al., 2002; Gosselin et al., 2005; de Heras Ciechomski et al., 2005; Dobbyn et al., 2006; Maïm et al., 2007) and motion (McDonnell et al., 2008).

However whilst much progress has been made into varying characters appearance and motion, a visual dissonance can occur when a cloned character has its body shape enlarged but its walking style is not adapted to match that change in a believable manner. A prominent researcher identified this as an area that is ripe for further study:

'Future challenges in Animation Variety [include] the adaptation of animation clips to the various morphologies. This means for example the adaptation of walking to tall people, to fat people.'

(Thalmann et al., 2009)

We therefore investigate how to vary a character's walking style to more naturally fit the shape of the bodies they are animating. For example modifying the walk cycle of a lean character to look like that of an obese one. This would retain the nuance of the base walking motion but modify it to look obese in an automated and efficient manner, saving animators time whilst retaining believability in the characters and the scene.

The intended use shall be for pre-rendered animation scenes, not real-time interactive environments, so we present a semi-automated approach to generating locomotion related to appearance.

1.1. Research Problem

The problem at the core of this investigation is how to automatically generate a variety of walking motions that believably relate to body shape. This is challenging as currently virtual characters reuse the same walking clips irrespective of their body shape as it is costly and time intensive to generate original and matching clips from scratch. However, applying a thin character's walk cycle onto an obese character can look incongruous and break the audience's belief in the realism of the animation.

To make this adaptation of one motion to another character (retargeting) more believable we need to understand the perceived and actual relationships between changes in body shape and gait. We can then modify gait parameters of that lean character's walk, like speed or step width, to give the moving perception of a differently weighted character.
Thalmann et al., (2009) highlighted that there is a limited understanding in how changes in people's body shape affects their walking gait, therefore there is a need to study and test these relationships to improve the dynamic generation of diverse, virtual characters' walking styles.

1.2. Why it is Important

Understanding the relationships between changing body morphology and walking gait is important, as animated films and games need to generate diverse characters that walk in a believable manner relating to their body shape. Walking is the motion primarily investigated as it is commonly used in many animation and crowd simulation systems and it has already been heavily researched in the field of gait analysis.

Humans are adept at identifying the naturalness of human motion (Ren et al., 2005) so when a lean character's walk animation is simply retargeted onto an obese character, the incongruity breaks their suspension of disbelief, in terms of the realism of the motion and the believability of the character. By studying these relationships we can assist animators by generating more believable characters driven by actual data, so that viewers are more likely to remain immersed within the virtual scenes and not become distracted by mismatched animation.

1.3. Research Contribution

By studying the perceived and actual changes in locomotion over increases in body morphology we can define the most perceptually dominant motion parameters and quantify the actual relationship between body shape and movement. This forms the basis of the locomotion model, which is a framework that predicts motion parameters based on given appearance parameters. Finally this can be implemented into an animation tool that automatically and believably generates locomotion based on real world data. This research therefore makes three main contributions to knowledge. These include:

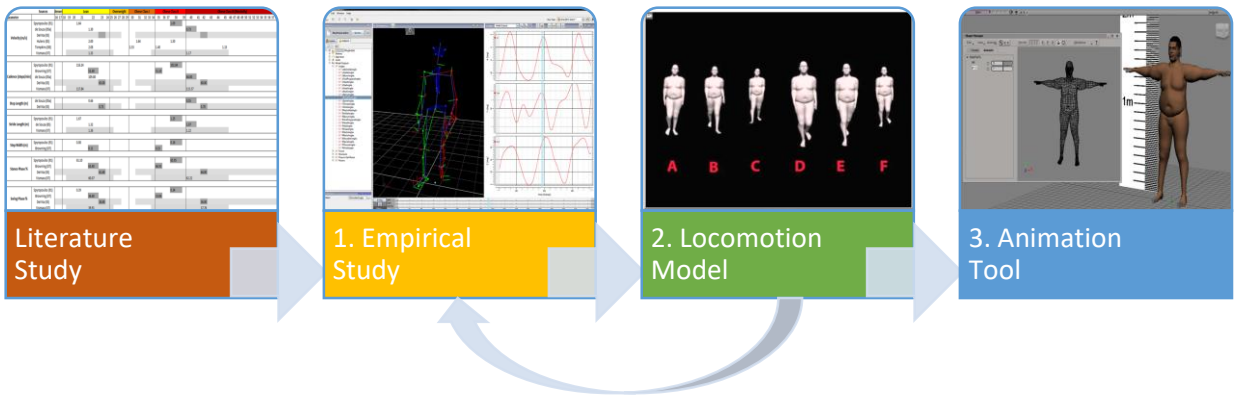

Figure 1-1 - Contribution to Knowledge

1. An empirical study defining the perceived and actual changes in full body gait over increases in obesity. By understanding the trends that relate changes in body shape to changes in locomotion, animators can improve their practise when creating a diversity of characters and their respective animations.
2. A relaxed model of locomotion that determines how changes in specific and generalised body anthropometrics affects generalised and specific aspects of walking gait. This model could be applied in a variety of fields and software uses to simulate a range of body shapes and walking styles. These appearance-to-gait relationships shall also be prioritised in order of those that are perceived to be most perceptually believable. This helps animators understand the most perceptually effective aspects of gait to focus on when creating or modifying characters.
3. An animation software tool developed, tested and validated that successfully implements the locomotion model to believably retarget lean walk cycles to appear to match the gait of an obese and/or taller looking characters. This will assist

animators and motion capture artists to efficiently retarget lean locomotion clips to more obese or taller characters in a scientifically accurate and believable manner.

1.4. Hypotheses

To address the research problem of how to automatically generate a data-driven variety of walking motions that believably relate to their body shape, a number of hypotheses are posed to focus the direction of the research project and methodologies:

- Some locomotive gait parameters are more perceptually dominant when viewing characters with different body morphology (e.g. obese /taller).
- A simplified model of locomotion can be derived from the analysis of walking gait data.
- A scripted animation tool can use the data-driven model of locomotion to automatically modify the walk cycle of a lean character to appear to be that of a character with differing body morphology.
- A data-driven model of locomotion can modify lean locomotion to a different body morphology, more efficiently and as believably using a scripted animation tool than motion capturing or key-framing new walk cycles.

1.5. Scope of Research

The primary research questions to be addressed by this project include:

- What is the order of priority for the most perceptually dominant motion parameters?
- What aspects of gait change over increases in body appearance?
- Is it possible to modify aspects of walking gait to efficiently and believably match the appearance of increasingly deformed character morphology?

Areas that are outside of the scope of this current research are:

- Complex non-locomotive motions such as jumping, fighting, dialogue etc.
- As work has already been undertaken in modelling internal muscular (Kohout et al., 2012), skeletal (Magnenat-Thalmann et al., 2004; Lee et al., 2009) and fat structures

(Lee, 1995; Boulic, 1995; Scheepers, 1997; Aubel, 2000) this shall not be necessary to explore.

- The generation of diverse characters and motions has applications in crowd simulation, however, the techniques related to this field such as path planning, steering, and decision making are outside of the scope of this current research.

1.6. Structure of Thesis

This document reports on the research conducted in exploration and support of the research problem and thesis. Chapter 2. analyses the current research in the related fields of Appearance Diversity, Motion Diversity and the Effects of Obesity on Gait. Chapter 3. explains early research using previously published data on the relationships between appearance and locomotion. Chapter 4. and 5. both assess the dominance of certain locomotion parameters on the perception of obese gait. Chapter 6 analyses the actual correlations between appearance and locomotion parameters. Chapter 7. compares the results from the previous three chapters to create the simplified, data-driven model of locomotion, ordered by perceptual dominance. Chapter 8. details the implementation of the animation framework into a scripted animation tool, its perceptual testing and validating results. Chapter 9. summarises all findings and potential for future work whilst Chapter 10. recommends areas for future work.

2. LITERATURE REVIEW

The following Literature Review explores research in the related field of virtual agents' diversification to provide an overview of its approaches, evaluation and necessity. Current research about techniques for varying appearance diversity and motion diversity, motion retargeting, human motion perception and the effects of obesity on gait are all reviewed.

The aim for virtual character diversification is to reduce the audience's ability to detect cloned characters and increase audience immersion. Whilst locomotion diversity not appearance diversity is the main focus of this research project, it is reviewed as it has a strong influence on the perception of variety. The most effective and adaptive approach to appearance diversity also needs to be determined as this needs to be modelled in conjunction with modelling motion diversification.

The latest research into motion diversification is then extensively reviewed to assess the most effective and adaptive, method to modify locomotion for the scripted animation tool. This is needed to test out our framework of anthropometric to locomotive parameters.

Perception of human motion is reviewed to prioritise the gait parameters that have the most dominant effects. This is to ensure we build a framework that can create diverse and believable motion.

Effects of obesity are subsequently reviewed to catalogue the previously recorded changes of gait parameters over increases in body morphology. This forms the first contribution to knowledge; an empirical study of the changes in gait over increases in body morphology. These trends are later analysed to inform the basis of the scripted animation tool and are tested for their perceptual strengths.

After summarising the limitations of the material reviewed, an extensive catalogue of metrics are reviewed to assess their appropriateness for measuring real world participants and for modelling on virtual characters.

2.1. Appearance Diversity

This section reviews the current research about people's ability to detect appearance clones and the techniques that have been explored to differentiate agents' appearance within virtual environments.

By reviewing appearance diversification techniques this can inform our methodology to change body morphology in a dynamic way that can drive changes to walking gait.

The perceptual impact of homogeneity in virtual crowds can lead to a break in viewers' suspension of disbelief as they identify repeated cloned patterns. We propose that this is important as a lack of belief in the authenticity of virtual characters undermines the belief and purpose of the scene and media that it is being used in.

Research has shown that modifying agents' appearance has an impact on viewers' perception and speed at detecting identical looking clones (McDonnell et al., 2008). In a matrix of twelve identical agents, the appearance clones could be picked out in an average time of 5.7 seconds whereas a modulation of garment colour more than doubled this time to 12.3 seconds. Diversification of appearance is proved to be important in reducing clone detection and therefore improving believability.

A method in varying agent appearance includes texture (Thalmann et al., 2009) and colour modulation of skin or clothing (de Heras Ciechomski et al., 2005; Dobbyn et al., 2006; Gosselin et al., 2005; Maïm et al., 2007; Tecchia et al., 2002). This is computationally efficient and effective at bringing perceptual variety to crowds, however, these techniques do not address body shape or motion variety so the agents are of the same shape and movement.

Thalmann et al., (2009) highlighted the problem of variety in order to simulate realistic crowds. Thalmann varied the height of human meshes by scaling the skeleton, bones and mesh. He discussed a FatMap technique to modify the body shape. This required the user to paint an extra grayscale UV texture of the character with darker areas representing increases of body fat and where the mesh would be deformed.

Figure 2-1 - Model and greyscale FatMap texture (Thalmann et al., 2009)

Whilst this saves time rather than manipulating each vertex, it is still a manual modification per character and is based only on the user's intuition of how characters vary in weight as opposed to any biological constraints. As the texture is grayscale this limits only 256 height values for each texel which means that the user must predefine maximum values on the 'fatScale', as opposed to having the freedom to select any value or by biological constraints. Theoretically these simplified height values could be used to modify the walk cycle. Direction of vertex deformation was also based upon the weighted normal of the bones influencing it. The drawback to this approach is that deformations are not necessarily rounded or based upon biologically realistic adiposity deposition patterns or topographies. Thalmann et al., (2009) concludes that the future challenge remains of how to modify body shape, gait and animation style to the 'fatWeight'.

Lyard and Magnenat-Thalmann (2008) presented methodologies to automatically create human body surfaces using a database of externally and internally scanned human bodies. A template model was used to identify landmarks and topographies of the scanned models. It was then possible to interpolate between all of these models. An algorithm then fits and rescales the template skeleton based on the distance between landmark areas. This, however, relies on cumbersome medical scanning technology and a variety of subjects available to be scanned to create a sample set. Also whilst the skeleton is rescaled to accommodate the interpolated models, there are no other correlation between increases in body mesh volume and its effects on locomotion.

Magnenat-Thalmann et al. (2004) explored methods for capturing the shapes of people, parameterization techniques to model the variety of body shapes and how the body moves. One method for modelling body shape variety, Spreadsheet Anthropometry Scaling System (SASS) (Azuola et al., 1994) used anthropometric data in spreadsheet form to automatically create characters. Similarly Seo et al. (2003) used statistics to drive body modifications using shape parameters like fat percentage. The technique of using body size data is to also be utilised in our proposed solution by using anthropometric data to scale body mesh regions.

The work of Kasap et al. (2007; 2008; 2009; 2010) has proven to be relevant as Kasap continues to explore the generation of human body models using anthropometric measurements. Kasap's approach is to divide the template into body segments corresponding to ISO-7250 and ISO-8559 standard clothing measurement landmarks. These segments are deformed using different methods depending upon their region and blended to the desired shape with the skinning information kept intact and the skeleton scaled accordingly. However, there is no guide as to the rates by which to deform body segments according to adiposity or muscle gain. Whilst Kasap's techniques for body segment deformations are useful, this approach still only generates a variety of agent body shapes, and does not address how increases in body deformation affects locomotion.

Assassi et al. (2012) presents an alternative to the skin deformation method using body scans, MRIs, motion capture data and physics simulations. Whilst the multi-layered approach sounds comprehensive, the muscles and fat are combined into a single tetrahedral mesh, which may not be accurate when modelling the motion of obese characters. No attempt at avoiding self-penetration of meshes is considered as the underlying motion is not altered.

Ramos & Larboulette (2013) presents a method where the movement of bones drives muscle contractions which dynamically deform and slide under skin surfaces. Whilst computationally efficient, the effect is not particularly novel and fails to take into account adipose tissue. Changes in body morphology or muscle mass are not reflected in changes to gait parameters. However this method could combine with our appearance to motion framework as part of a multi-layered approach encompassing bone, muscle, fat and skin.

Koo et al. (2015) proposes a statistical framework for parametric modelling of human body shapes. This uses linear anthropometric parameters for example-based synthesis. A database of 80 male and 80 female body scans was used for training to derive 63 landmarks and 15 joints to segment the body, parameterize body shapes and eventually generate a variety of poseable, body shape models. This combination of anthropometric landmarks derived from the large 'SizeKorea' database is undoubtedly richer than our sample set however crucially, no corresponding motion capture locomotion data is included for analysis.

Iwamoto et al. (2015) presents a voxel-based lattice model to deform characters at the bone, muscle, fat and skin layers. Whilst the multi-layered approach is more comprehensive than attempts by the likes of Assassi et al. (2012) the end result appears gelatinous and not structurally robust. Tension parameters could still be tightened however this method still fails to model biomechanical effects such as COM, balance and avoidance of self-penetration.

A review of these techniques demonstrates a range of methods to effectively create a diversity of characters that appear different. However, each technique to create or diversify appearance has no influence or relationship with the characters' walking style. By completing an empirical study into appearance diversification techniques we can create an appearance-locomotion model and apply it to an animation tool that not only diversifies appearance but also walking style.

2.2. Motion Diversity

This section reviews the current research about diversifying character motion within a virtual environment. Human's ability to identify cloned motion presents a challenge in how to bring believable locomotion amongst virtual crowds. Whilst creating new walk cycles, modifying existing ones or recording more motion capture data is time consuming, there is research into animating walk cycles procedurally. These techniques are assessed to understand their limitations and where there is opportunity to improve upon them and relate them to appearance.

Procedural animation is automated, flexible and less memory intensive than motion capture, however, it is also considered less believable and more CPU intensive than motion capture or animation (Hertzmann et al., 2009), so we shall not currently explore this approach.

Lyard and Magnenat-Thalmann (2008) tried to address deformations of motion based on deformations to the character's body. This approach adapts the template motion to avoid self-penetration with some added character rebalancing i.e. avoiding model clipping when a body is deformed, the way an obese person might adjust their movements to avoid chafing around their limbs. Ho et al. (2013) built on this with an IK system that avoids self mesh penetration by monitoring and regulating topology changes. This approach emulates some of the issues that obese face in avoiding real world chafing of body parts. However not all gait adjustments are due to this problem; e.g. increased step width, foot progression, spinal erectness and reduced walking speed may all be to better maintain balance and conserve energy. This is still an interesting approach that could marry our data driven framework with topology-based motion synthesis. Oshita (2017) proposed a lattice based method to deform human motion to avoid collision with objects. Whilst an interesting approach, this deals with external objects and not avoiding mesh self-penetration.

Gu et al. (2011) created dynamically changeable variations for motion captured clips such as walking, running and waiting, using the publicly available motion capture database from Carnegie Mellon University. This proved computationally expensive so the number of motion 'styles' was limited and they focused on how to spread motion styles contextually throughout a crowd. This approach is novel and effective in making clone detection more difficult, however, the motion variations bore no relation to the height or weight of the character, an area we are looking to improve.

Thalmann et al. (2009) used a motion capture based locomotion engine developed by Glardon to generate and adapt many different animations. Lack of crowd variety proved most noticeable in the foreground so Level of Detail (LoD) with the appearance of meshes was used. Thalmann deformed human meshes in the forefront, used pre-computed static meshes in the mid-ground and used pre-computed 'imposters' in the background. This

principle was dynamic and scalable and could be used to improve computational efficiency, however, by Thalmann's admission this method still did match the motion of certain characters to their appearance or weight.

A review of these techniques demonstrates a range of methods to modify motion or give the illusion of motion diversity. However, these techniques do not diversify a range of gait parameters in relation to anthropometric parameters.

2.3. Motion Editing

As we have previously reviewed techniques to modify appearance and motion we shall now focus further on the technique, limitations and opportunities of motion editing to see how it can be related to body morphology.

Motion editing is the act of changing the movement of an object (Gleicher, 2001). Through the process of changing an existing motion it would be necessary to preserve the original motion as well as adding new features to it. Constraint-based motion editing defines some of the features that are to be preserved or changed. Extending or adapting this technique when modifying motion by weight parameters would be useful to consider. A blending operation applied to a motion does change it (and is therefore an editing operation) preserving some aspects of the original, but does not explicitly describe the operation in terms of features of the motion. As we are initially focussing on locomotion we do not need to blend or concatenate different motion clips, however, this is worth considering for future use.

2.3.1. Key Frame Animation/ Densely Keyed Motion capture Animation

Traditional animation systems allow users to set key poses to be interpolated between. Gleicher (2001) refers to this as per-key inverse kinematics as the solver tackles the spatial constraints on each key, changing each pose individually and independently of other frames (although other frames may be considered). This method does not enforce or guarantee any constraints other than the keyframes. The animator can use a small number of key frames to describe the motion which can then be smoothly interpolated. However, this can prove problematic as these key frames are not always at semantically relevant places, making

temporal controls somewhat artificial. Whilst this may prove a useful approach when working with sparsely, and meaningfully keyed animation, this would prove a challenge to produce smooth modifications on densely keyed motions such as motion capture data.

Bindiganavale (2000) develops a representation for the unstructured data by identifying extreme motions as key poses, applying IK to them and interpolating between them. This means events can be preserved and not destroyed. However, this approach may overlook some of the believable subtleties of motion outside of extreme poses. As motion capture is densely keyed and we are aiming to modify gait parameters such as stride length then we shall need to identify extreme poses.

2.3.2. Motion Warping

Motion warping (Witkin and Popovic, 1995) is a technique for editing motion capture or key framed animation by warping the motion parameter curves using just a few keyframes. The modification can be efficient and radical. Gleicher (2001) describes it as motion warping plus inverse kinematics (MW+IK), as an IK solver must handle the spatial constraints once the motion warp is keyed. Whilst efficient there is only spatial control at keyframes and temporal constraints are also tied to the amount of spatial constraint keys. As motion warping is a geometric technique without any understanding of the motion's structure some warps can look distorted and unnatural. It can also be difficult to enforce geometric constraints between keys. Animation systems such as Softimage (2015) do provide simple curve fitting and control point adjustments for animation clips as a whole, but not deformation of individual limbs, which could limit our ability to fully relate motion diversification to body appearance.

Perlin (1995) used a motion blending technique to smoothly concatenate procedural motions using curves. Perlin suggested that this approach could be applied to motion captured data too. Whilst this was a consideration, the library of extreme motion clips that would be needed to be recorded, traversed and transitioned would be inefficient.

Rose et al. (1996) explored the generation of motion transition between segments of human body basis motions using spacetime and inverse kinematic constraints. Wang and

Bodenheimer (2004) went on to develop a method for determining a believable length for these motion transitions, finding that viewers preferred their automatically generated blend lengths over a fixed-length blend.

Hsu et al. (2005) developed a technique to translate motions into a different style by learning from input similar motions, matching similar poses and using iterative motion warping to modify them. Without accompanying anthropometric data we cannot understand and replicate the correlations with body morphology. Whilst this method allows the training for modification on trained generalised styles, specific gait parameters are not directly analysed or extracted.

Motion transitions are necessary for large libraries of different types of motion clips. However, we are immediately interested in only one type of motion; a looping two-step locomotion clip whose start and end point should be matched up with minimal linear blending. Once we have identified extreme poses we shall then use motion warping to evenly stretch the inbetween keyframes.

2.3.3. Per- Frame (sample) Method

Gleicher (2001) likens this method to the per-key method but where the keys are densely and regularly sampled such as an algorithmically generated animation or a motion capture recording keyed at every frame. The challenge in the per-frame method is to enforce constraints whilst modifying each frame individually. As our research is looking to record and then edit densely sampled motion capture data this presents a challenge that may need to consider hybridising some of the currently discussed motion editing approaches.

2.3.4. Online Motion Editing/ Retargeting

In games systems, virtual environments or performance animation, motion needs to be captured and edited in real time (Choi & Ko, 1999). These systems must work per-frame with inverse kinematic constraints being solved through linearization. Where there are little constraints the system tries to match joint angles as closely as possible from one character to another (Gleicher, 1988). As we look to base obesity related motion diversification on motion capture data of real subjects, this per frame motion retargeting technique will likely be required.

Shin et al. (2001) shows how to apply motion data to characters of differing sizes in a real time system. A Kalman filter technique reduces noise and enforces temporal constraints, a high performance inverse kinematic solver ensures end-effector constraints are met, and an importance metric is used to prioritise between tracking the end-effectors and joint angles. Unlike the system of Choi & Ko (1999), this only tracks end-effector positions when they are relevant, preferring to match postures at other times. If believability is maintained this could be considered as a more efficient approach to diversifying motion.

Hecker et al. (2008) introduced a system that retargets animated motions to characters created by users with highly varied morphologies and body structures. Animators create their animations and specify the semantic aspects of the animation. This data allows the motion to be generalized and then at runtime, specialized for retargeting onto different character morphologies. This method proved to be a highly sophisticated, flexible and effective animation system able to retarget animation to characters with completely new structures. The characters gaits, although tuned by animators and having procedural secondary motion added, were still synthesized using an inverse kinematic solver to pose the character at every frame. Whilst the motion adapted to new structural hierarchies this simulation did not reflect changes in body adiposity, as it did not recognise volume or boundaries. However, this method could possible by extended to incorporate such factors.

Neff & Kim (2009) introduced a system to edit motion by style. This was achieved by rotating wrist, ankle, COM and pelvis joints. Balance is adjusted with foot constraints. The system even allows correlations between modifying the position of body parts however this is more of an artistic or stylistic choice than one based on any kind of morphological trends. Whilst this is a flexible and accessible system even for non-animators, the number of editable motion parameters are limited for simplicity and the stylistic modifications are arbitrary and not based on any appearance to motion correlations.

Feng et al. (2013) created an automatic character animation pipeline which included a skeleton joint mapping system, motion retargeter, constraint enforcer and the ability to transfer stylised behaviour sets. However no behaviour set exists that correlates

anthropometric and obese variations in body morphology to gait variations. This remains a potentially useful future application for our appearance to motion framework.

For our research we will be looking to retarget the motion of lean character to an obese character with an identical structure (connectivity of limbs, types of joints degrees of freedom) whilst applying further motion editing and warping to it.

2.3.5. Spacetime Constraint/ Optimization

Spacetime constraints are a method for creating character animation. It does not look at individual frames but the solver computes an entire motion using equations considering constraints on the entirety of the clip. The animator specifies the character's physical structure, the physical resources and forces available to accomplish the motion, the space and timing that the action must take place within, constraints specifying the action, any obstacles of movements and how the movement should be carried out. It is then up to the physical system to use the constraints and Newton's Law to optimize a physically valid motion (Witkin and Kass, 1998; Gleicher, 1997).

Spacetime constraints can be useful to constrain footsteps at a given place. As weight gain affects parameters such as stride length and step length, a footstep constraint may be useful to implement, as may the peaks of non-contact cyclical movement such as arm swings. For the needs of our research problem, improving believability is the goal so that motion must be retargeted by data and not physically driven. However, a constraint could be mathematically derived and expressed from data analysis.

Simulating muscle forces is possible, however, the simulation of adipose tissue adds an extra layer of complexity in modelling the motion of the fat, its effect on the rest of the body and the muscular-skeletal reactionary forces involved. For larger crowd scenes this would continue to prove computationally taxing. The believability of motion depends on the correct modelling of all of the internal and external forces and constraints. Whilst we can try our best to model this as fully as possible, we would argue that only by recording actual motion captured data and modifying it based on trends can we provide a realistic and believable representation of motion changing over increases in weight.

Choi & Ko (1999) retargets the motion of one character to another in real-time using inverse rate control (Whitney, 1969) to compute the changes in joint angles according to the change in end effector positions. Kinematic redundancies of the animated model are used to minimize the joint angle differences in the original character, enabling Choi to preserve the original motion characteristics whilst performing slightly different motions to other character in real-time. This proved useful for previewing motion capture sessions on target characters to provide better results. Useful by-products of Choi's OMR algorithm also appeared to be an improvement in preservation of high frequency detail, accuracy in measurement of joint angles and end effector positions. As our research will need to measure biomechanical parameters accurately this technique could help with our measurement procedure.

Tak and Ko (2005) presents a constraint-based motion editing technique that converts a captured or animated motion to a physically plausible motion according to specified kinematic and dynamic constraints. This works on a Kalman filter per-frame basis rather that the whole of the clip which means it is much quicker and more suitable for real time applications. The Kalman filter handles position, velocity and acceleration as separate variables which can create errors in motion so a least-squares filter is added to smooth out jerkiness as it is a curve fitting procedure. This flexible method is worth exploring as the motion capture data we will capture will be sampled and modified per frame and may need to be modified by certain constraints.

Torresani et al. (2007) explores a method of motion sequences generated from space-time interpolation of motion capture data to learn motion styles. These motion styles are described using the Laban Movement Analysis notation form. Whilst this approach can generate stylistic variations of a given action, the LMA theory is not precise enough to meet spatio-temporal constraints or morphology to gait parameter correlations.

Kim & Neff (2012) generate new motion paths for input locomotion clips that adjust feet and blend lengths for the loops based on input walks. Their system automatically detects walk cycle loops based on foot -plants. This derives phases of locomotion, warping the

motion to paths and constraining foot placements to these phases. As our research focuses on simple locomotion clips, theoretically this could extend the use of our framework by allowing variations in paths, turns and speed. However without meaningful correlations between body morphology and gait parameters, these motion variations might appear unrealistic. There is the opportunity to complement this system with our appearance-motion framework 'style' to provide a greater degree of realism and flexibility.

As Perlin (1955) ultimately noted, physical based simulation is considered less natural. Whilst a hybrid data-driven, spacetime constraint method is an area worth further investigation, until further comparative studies are made we shall focus on data-driven methods.

A review of these techniques to modify locomotion shows a range of possible approaches to build upon when relating walking styles to body shapes. A solution for modifying motion in the animation tool would need to work with densely keyed data like motion capture. However, as our animation tool shall be based on specific motion parameters defined by our locomotion model, our approach shall also need to identify key poses and motion edit between them. Where there are spacetime constraints our tool shall need to use an IK solver to manipulate keyframes in a non-destructive manner.

We have reviewed a range of methods to effectively modify motion. However, each technique has little relationship with the characters' body morphology. By completing an empirical study into this relationship we can create an appearance-locomotion model and apply it to an animation tool that not only diversifies appearance but also walking style.

2.4. Perception of Human Motion

Understanding human perception is also important as we are trying to relate perceivable differences in walking styles to body shapes in a believable manner. This can help us prioritise which body areas have most perceptual impact when analysing and modifying their motion in our empirical study and locomotion model. As humans can detect identical looking characters in a crowd and are also able to detect characters with identical

movements, it is important we move beyond cloning walk cycles to creating more diverse and believable ones.

Research has shown that modifying agents' motion has an impact on perception, albeit to a lesser degree than appearance. This research also showed that particular characteristic walk cycles were significantly easier to detect (McDonnell et al., 2008). This indicates that the more extremely modified the characters, the more attention needs to be paid to differentiating or randomizing aspects of their movements. To optimize the process, fewer differentiations between motion modifications in more generic appearance modified characters may be less noticeable. This could be experimented with further to improve the speed of the animation tool.

We can perceive people's gait by the dimensions of their underlying skeleton and the dynamic qualities of its movement on point light figure displays, also referred to as biological motion stimuli, (Pittenger and Shaw, 1975; Shaw et al., 1974; Pollick et al., 2003). Humans are so adept at identifying locomotion that they can identify walk cycle styles from particular walkers (Cutting and Kozlowski, 1977; Kozlowski and Cutting, 1977; 1978) from twelve moving dots and can even identify the gender of such walkers (Johansson, 1973; 1976). As viewers can identify walking styles we see this is an opportunity to retarget motion not by gender but by weight gain to improve crowd diversity. These point light techniques shall be implemented within the empirical study to test viewers' abilities to identify obese locomotion parameters.

Familiarity cues can also have an effect on perception. These could include size and shape cues or the context of the environment (Cutting and Kozlowski, 1977). Viewers in Cuttings' experiment mentioned clues such as speed, bounciness, rhythm of the walker, arm swing and length of steps. Interestingly whilst many of these factors have since become staple measurements for lower body gait, bounciness (vertical hip variance) and arm swings do not appear to have been measured. These could be looked at again as parameters in our empirical study to determine perceptual changes in motion for our locomotion model.

Hodgins et al. (1998) tested motion perception of human figures comparing a variety of modelling and rendering styles. Hodgins et al. also measured torso rotation because it can provide cues for gender and subject recognition (Cutting et al., 1978). Their results indicate that the 'realer' the representation of the human character, the more sensitive the viewer was to changes in motion. This makes our research more challenging but useful to photoreal visualisations of crowds as opposed to abstract or stylized representations.

Reitsma and Pollard (2003) looked to develop a metric to measure human sensitivity to errors in animated human motion based on detection theory (Macmillan and Creelman, 1991). This could be utilised in the evaluation of our empirical study, particular if the sample size of testers is small. This study found that viewers were more sensitive to errors in acceleration than decelerations, which may prove useful for motions that are slowed down due to increases in obesity.

Ren et al. (2005) looked at whether it is possible to develop a machine learning based measure that quantifies the naturalness of human motion. The aim was to verify that a motion editing operation had not destroyed the naturalness of a motion capture or synthetic motion clip. Their test sets included edited motion capture clips, keyframed motions, clips with motion noise, motion transitions and un-cleaned motion capture data. If we had access to Ren's approach this could be useful to evaluate the naturalness of our modified locomotion clips, however, one of the drawbacks of this approach was that whilst it could judge perceptually unbelievable artefacts like foot-skating as unrealistic, it had trouble detecting motion that had been slowed down, particularly for behaviours that do not include a flight phase. As several of the parameters we will be measuring will likely need slowing down for the modifications, this evaluation approach may prove to be more difficult.

McDonnell et al. (2008) validated crowd simulations on their believability by testing how quickly appearance and motion clones could be detected against matrices of other clones. McDonnell found that appearance clones are easier to detect than motion clones but are harder to find when combined with random motions. She noted that whilst appearance clones were easier to detect in a close-up, in a larger crowd scenario the effect of motion

may have a stronger perceptual effect as individual appearances may be harder to detect. This indicates that we could expand our testing procedure from close-up comparisons to medium or wider angled, denser crowd scenes. She also found that appearance clones could be masked by randomising their orientation and motion. McDonell's methodology is highly relevant in isolating and testing aspects of character modifications so will form the basis of our methodology when conducting our empirical study.

Pražák et al. (2009) presented a perception based metric comparing human skeletal poses during locomotion. It described perceptually important differences of the data-driven locomotion between different subjects. Pražák et al. (2010) followed this research up with a perceptual evaluation of human animation timewarping, reinforcing McDonnell's earlier findings that speeding up motion produces perceptual artifacts whilst slowdown appears to be perceptually acceptable, however, his experiments looked at timewarping entire locomotion clips. Our research will look into the slowdown and modification of motion clips on a limb-by-limb basis.

Following our review of perception of human walkers we can summarise that whilst humans are more adept at identifying walkers with similar appearance, we are still very adept at differentiating between humans when viewing their isolated locomotion. In addition we can also identify changes in individual motion parameters. This shall enable us to modify gait parameters to test which are more perceptually dominant and therefore effective to modify to give the impression of distinctive, new motion.

2.5. Effects of Obesity on Gait

The research on the effects of obesity on gait provides some insight into the factors that are affected by real world changes in body shape. The following section explores those effects that obesity has on locomotion. The intention is not to simply offer the alternative of normal or obese characters but gradations between. Future research could be undertaken to discover the effects of emaciation on locomotion, so that we can deform motion in the opposite end of the scale.

The research presented on obesity related changes to gait are based on Body Mass Index, as opposed to Waist-Hip ratio or Waist Circumference, because this was the commonly used measurement in biomedical research (Spyropoulos et al., 1991; da Silva-Hamu et al., 2013; Hulens et al., 2003; DeVita and Hortobágyi, 2003; McGraw et al., 2000). However, BMI is an imprecise measurement of body weight (Deurenberg et al., 2001) so our research shall look to adopt an additional more representational metrics such as Body Fat Percentage.

Whilst there has been research conducting into modifying characters' body shape and motion for greater variety in crowd simulations, what is missing is the modification of motion in relation to the modification of body morphology. To start to understand to what extent body shape affects locomotion in the real world we looked at the following research. Research has demonstrated that the following locomotive parameters are affected by increases in obesity in adults:

- Slower preferred walking speed (Spyropoulos et al., 1991; DeVita and Hortobágyi, 2003; Hulens et al., 2003; Vismara et al., 2007; Tompkins et al., 2008; Lai et al., 2008; Browning, 2012; da Silva-Hamu et al., 2013; Pataky et al., 2014)
- Cadence- full walk cycles per minute (Spyropoulos et al., 1991; DeVita and Hortobágyi,, 2003; De Souza et al., 2005a; Browning and Kram, 2007; Vismara et al., 2007; da Silva-Hamu et al., 2013)
- Reduced step frequency (DeVita and Hortobágyi, 2003)
- Reduced step length (De Souza et al., 2005a; DeVita and Hortobágyi., 2003; Lai et al., 2008;)
- Shorter stride length (Hulens et al., 2003; Lai et al., 2008; da Silva-Hamu et al., 2013; Pataky et al., 2014)
- Wider step width (Spyropoulos et al., 1991; Browning and Kram, 2007; Sarkar et al., 2011; Wu et al., 2012; Vartiainen et al., 2012)
- Shorter swing phase (Spyropoulos et al., 1991; Lai et al., 2008)
- Longer stance phase duration (3%) (Spyropoulos et al., 1991; Lai et al., 2008)
- Wider lateral leg swing (Spyropoulos et al., 1991)
- More erect posture (McGraw et al., 2000)
- Wider Foot Progression (Sarkar et al., 2011)

2.6. Summary

The three key issues that emerged as a result of our literature review were believability, lack of relation between appearance and motion and the lack of automation and efficiency. These limitations are summarised below as opportunities for the proposed solution to fulfil.

Our ultimate goal is to improve believability of crowds of characters through diversity, however this has shown to be an issue which manifests in some of the methods for motion editing, warping and IK interpolation. The most significant limitation across all of the literature has been the lack of relation of body appearance to body motion. Approaches tend to modify appearance or motion separately but with limited correlation. After identifying some of the locomotive parameters that change as BMI increases we look to expand these with more detailed data capture, to unify them as a model and apply them to increasingly obese virtual characters to believably diversify their motion parameters. The other main limitation identified is the lack of automation and efficiency in certain techniques.

3. DATA-DRIVEN METHODOLOGY

To identify and simulate perceptually dominant correlations between body anthropometrics and motion parameters we first investigated what existing data and trends had been published previously. Some basic trendlines were analysed across these multiple sources to form the basis of our own perceptual investigation. By understanding published data that relates changes in body shape to changes in locomotion, we can use these as the basis for our animation tool but also verify these trends after assessing our own data. This forms the first contribution to knowledge; an empirical study of the changes in gait over increases in body morphology.

The next stage was to create a set of scripted appearance and motion modifiers. This enabled modifications to the base lean motion captured walk to test perceived changes to obesity. This set of scripted modifiers also serves as a prototype for future enhancements and uses. This forms another contribution to knowledge; the development of a scripted animation tool that implements the locomotion model to retarget walk cycles to appear to be those of larger people.

Once we had the means to modify appearance and motion, the next stage was to create a series of perceptual video surveys to validate previously established and hypothesised correlations between appearance and motion. By analysing the results of these perceptual video surveys this could then inform the perceptual priority and strengths of motion parameters.

Finally, real world appearance and motion data was collected using motion capture techniques. Correlations between the real world appearance and locomotion data was analysed to then compare and contrast with the results of what correlations people perceived to exist from the video surveys. This informed the creation of a model of locomotion that determines how changes in specific and generalised body anthropometrics affects generalised and specific aspects of walking gait. This model, which is the major contribution to knowledge, could be used to simulate a variety of body shapes and walking

styles. The results of these perceptual and actual data analyses could then inform the parameters of a scripted animation modifier.

The methodology was therefore comprised of seven main parts that shall be detailed further:

Empirical Data Analysis

Scripted Appearance and Motion Modifier

Point-Light Perceptual Survey

Character Mesh Perceptual Survey

Motion Capture Kinematic Gait Analysis

Data-driven Animation Modifier

This multifaceted approach was designed to not only test people's perceptual expectations of gait but to also compare it to actual gait data. Our methodology can be visualised as:

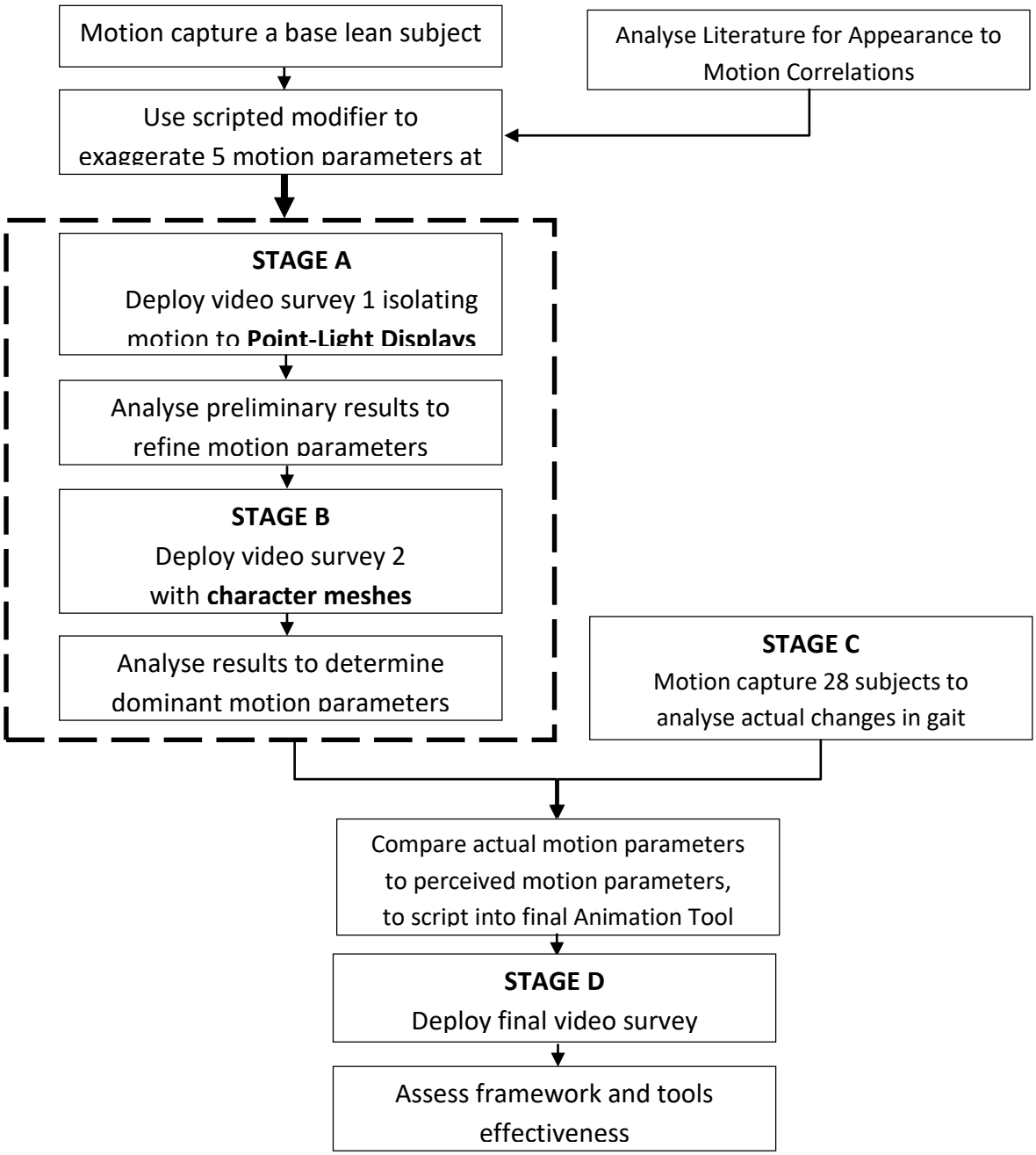

Figure 3-1 - Overview of the Perceptual and Practical Recordings of Gait Parameters

Figure 3-1 visualises this approach. A single lean participant's gait was motion captured used as the basis of all modifications. Empirical research observing changes of gait over increases in body morphology was analysed for overall trendlines for 5 parameters. Using these trendlines, 5 strengths of gait exaggeration were selected and fed into the scripted animation tool as part of the first point-light video survey.

Figure 3-1 represents the testing of the framework of anthropometric to locomotive parameters.

The results of the point-light survey were analysed and the results were used to inform the second character mesh survey. At the same time 28 participants had their appearance and gait captured. The analysis of the character mesh survey was then compared to the analysis of the motion captured participants.

A framework of affecting and perceptually dominant appearance to motion parameters was compiled and input into the scripted animation tool. A final poll was then conducted to test the effectiveness and efficiency of the scripted animation framework and tool at generating obese motion versus other methods.

3.1. Empirical Data Analysis

A review of previous publications on the correlations between obesity and gait surfaced a range of findings as summarised in Section 2.5. The first stage in our methodology was to analyse motion parameters over multiple papers to verify their trends and to create averaged trendlines. This would help inform strengths of the first perceptual survey. The following motion parameters were found to cover multiple motion parameters:

Table 3-1- Motion Parameters across Published Papers

Velocity (m/s)	Spyropoulos (1991) de Souza (2005a) DeVita (2003) Hulens (2003) Tompkins (2008) Vismara (2007) Lai (2008) Pataky (2014)
Cadence (steps/min)	Spyropoulos (1991) Browning (2007) de Souza (2005a) DeVita (2003) Vismara (2007)
Step Length (m)	de Souza (2005a) DeVita (2003)
Stride Length (m)	Spyropoulos (1991) de Souza (2005a) Vismara (2007) Lai (2008) Pataky (2014)
Step Width (m)	Spyropoulos (1991) Browning (2007) Sakar (2011) Wu (2012) Vartiainen (2012)
Stance Phase %	Spyropoulos (1991) Browning (2007) DeVita (2003) Vismara (2007) Lai (2008)
Swing Phase %	Spyropoulos (1991) Browning (2007) DeVita (2003) Vismara (2007)
HIP flexion° [HS]	Spyropoulos (1991)
Hip ROM°	Vismara (2007)
Pelvic Girdle	de Souza (2005b)
Knee ROM°	Vismara (2007)
Knee flexion° [HS]	Spyropoulos (1991) DeVita (2003)
Ankle plantar flexion° [HS]	Spyropoulos (1991) DeVita (2003) Vismara (2007)
Ankle ROM°	Vismara (2007)
Foot progression °	de Souza (2005a) Vismara (2007) Sakar (2011)
Cervical, Lumbar & Thoracic spine curvature	McGraw (2000) de Souza (2005b)

Motion parameters were only analysed if they had more than one published source. These were: velocity, cadence, stride length, step length, step width, stance phase, swing phase and foot progression.

Spyropoulos et al. (1991) sampled 12 men aged 31 to 47 years whose body weight ranged from 105.6kg to 151kg. Spyropoulos found obese persons walked slower, taking shorter strides and wider steps than non-obese persons. Obesity was 70% to 99% above ideal body weight (Metropolitan Life Insurance Table, 1956, cited in Spyropoulos et al. (1991). These were compared to 9 non obese men. This is a difficult metric to translate into BMI or Body Fat Percentage as the values were simply grouped into obese and non-obese. The motion parameters for these groups were also not presented in full but as mean and standard deviation values. For this reason we classified non-obese as 21 kg/m^2 and obese as 38 kg/m^2 on the BMI scale (Ravussin et al., 1982). Another potential limitation is that obese participants were aged 31 to 47 skewing results to middle aged men as opposed to a broader range or younger average. Gait can change with age (Seung et al., 2012) so a concentration on older males may skew the results.

De Souza et al. (2005a) sampled 34 obese adults, and found obese persons walked slower, with wider steps and reduced cadence and stride length than non-obese persons. However, 32 of them were female and gender affects gait so the results are less comparable with other sources. The mean age of participants was 47, so the results were once again skewed to older gaits. Individual walk data was not available but the mean BMI was 40.1 kg/m^2.

DeVita and Hortobagy (2003) sampled 21 obese adults (8 males and 13 females) and 18 lean adults (7 males and 11 females) and found obese persons reduced their walking speed, cadence and step length. As gender affects gait and because the results were not split by gender this makes them less comparable with other sources. BMI ranged from 32.4 to 58.7 kg/m^2. The obese group had a mean age of 39.5 which was significantly older than the lean group which were 20.8, however, the authors claim that there is no evidence that gait is effected within those age ranges.

Hulens et al. (2002) sampled 82 lean (BMI <_ 26 kg/m2), 85 obese (BMI >_ 27.5 kg/m^2) and 133 morbidly obese (BMI >_ 35 kg/m^2) and found obese women walked significantly slower than lean women. Participants were aged between 18 and 65. Whilst the quantity and age range is broad, all participants were female which are not comparable with male gait. Body

fat percentage was also recorded, however, body fat composition is not directly comparable with male body fat composition.

Tompkins et al. (2008) sampled 28 women and 2 men aged 31 to 58 with a mean BMI of 45.5 kg/m^2. They were then retested after gastric bypass surgery at the 3 month stage with a mean BMI of 35.7 kg/m^2 and then the 6 month stage with a mean BMI of 30.1 kg/m^2. As participants were mostly women, and gender affects gait, this makes it less comparable to publications that focus on males or separate genders. Participants were aged from 31 to 58 with a mean of 44. This skews to middle-aged walkers which could slightly differentiate gaits from young adults.

Speed was measured by recording the distance in metres walked in 6 minutes. Calculated walking speed was found to reduce over BMI. Walking speed was measured, but using the 6 minute walk test (6MWT) which is widely used by physical therapists as a measure of functional exercise tolerance (Gibbons et al., 2001). This could induce a degree of fatigue and slowdown in comparison to simply measuring participants preferred walking speed.

Vismara et al. (2007) sampled 5 male and 9 female obese patients with mean BMI of 39.2 kg/m^2 and 10 male and 10 female lean subjects. 19 Prader-Willi Syndrome (PWS) patients with a mean BMI of 41.3 kg/m^2 were also sampled, however, their obesity inducing condition is accompanied by a number of disorders such as scoliosis that were shown to affect gait, so they were not included in this study. Vismara found obese persons walked slower, had a reduced cadence and shorter stride length than non-obese persons.

Browning and Kram (2007) sampled 5 obese male with mean BMI 34.1 kg/m^2 and 5 obese female patients with mean BMI of 37 kg/m^2. 5 lean males (BMI 23.1 kg/m^2) and 5 lean female (BMI of 21.0 kg/m^2 were also sampled. They found obese persons had wider step widths and longer stance phases.

Lai et al. (2008) sampled 14 obese people mean age 35.4 (8.8) with BMI 33.06 (4.2) kg/m^2 and 14 non-obese subjects mean age 27.6 (8.6) with BMI 21.33 (1.5) kg/m^2. They found

obese persons reduced their walking speed and stride length. More time was spent on stance phase and double support in walking.

Pataky et al. (2014) sampled 36 women with a mean BMI 37 kg/m^2 and 10 women with a mean BMI 21.5 kg/m2 . They found obese persons reduced their walking speed, cadence and stride length. Age ranges weren't disclosed but participants were all female.

Sarkar et al. (2011) sampled 15 men with a mean BMI 21.97 kg/m^2 and 15 obese men with a mean BMI of 35.21 kg/m^2 aged 20-30. Sarkar et al. found obese males increase their step width and widened the degree of foot progression. They also sampled 15 lean and 15 obese women with similar findings in foot progression but no significant change in step width. We shall just analyse the male findings.

Vartiainen et al. (2012) sampled 13 people of a mean age 45.5(10.3) walking at 1.2m/s before weight loss BMI 42.2(3.9) kg/m^2 and after weight loss BMI 33.1(3.1) kg/m^2. Step width was observed to decrease over step width from 0.12m to 0.09m but this was considered anomalously low so it was not analysed.

3.1.1. Empirical Data Analysis

Multiple sources strongly correlate the trend that preferred walking speed is reduced over increases in BMI (Figure 4). Vismara et al. (2007) trendline appears anomalous in its gradient, as the listed walking speed was normalised by height.

Multiple sources correlate the trend that cadence is reduced over increases in BMI (Figure 3-3). Browning and Kram (2007) appears weak in its gradient, as preferred walking speed was not recorded but six walks at regular set speeds ranging from 0.5m/s to 1.75m/s. The mean cadence of all six speeds were used for obese and normal-weight participants. DeVita and Hortobágyi (2003) also demonstrated an even gradient, however, this may be because walking speeds for obese and lean were standardised at 1.5m/s.

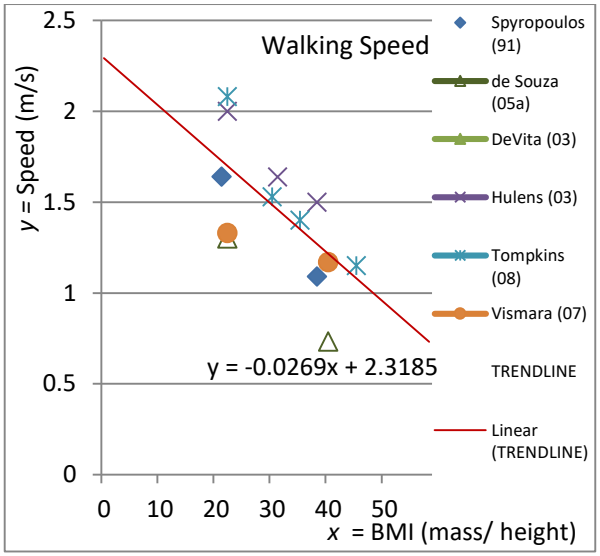

Figure 3-2- Empirical Analysis of Speed over BMI

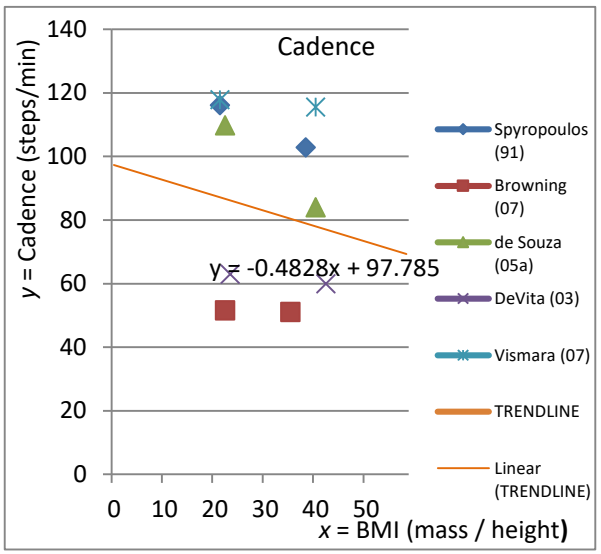

Figure 3-3- Empirical Analysis of Cadence over BMI

Multiple sources correlate the trend that Stride Length is reduced over increases in BMI (Figure 3-4). Vismara et al. (2007) may appear anomalously low as their data was normalized by height. Both sources demonstrate a decrease in step length over BMI (Figure 3-5). Further sources may have demonstrated this trend more clearly.

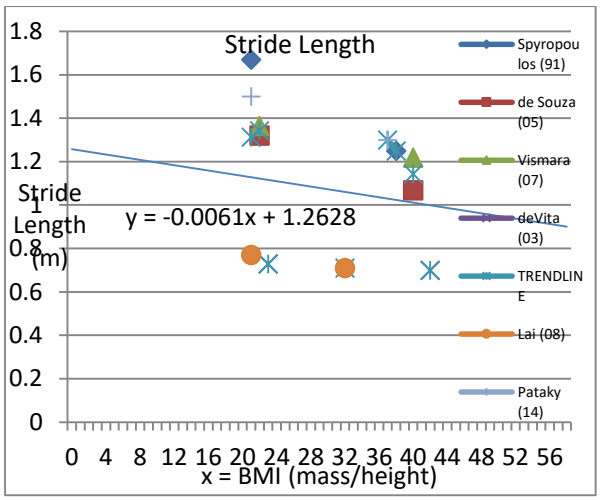

Figure 3-4- Empirical Analysis of Stride Length over BMI

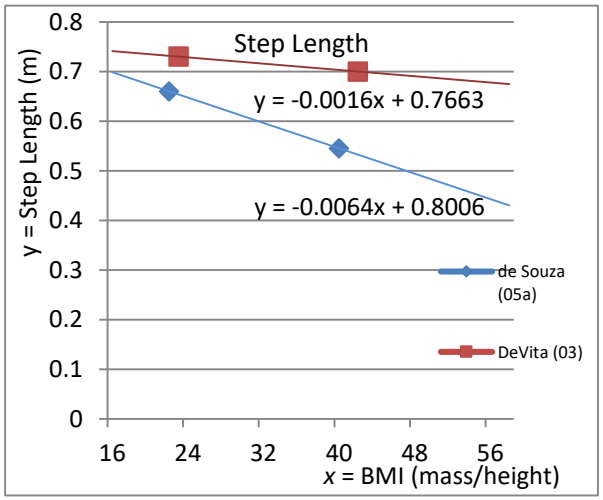

Figure 3-5- Empirical Analysis of Step Length over BMI

Both sources strongly correlate a widening in step width over BMI (Figure 3-6). Further sources may have demonstrated this trend more clearly. Multiple sources strongly correlate the trend that walkers spend longer in the Stance Phase over increases in BMI (Figure 3-7).

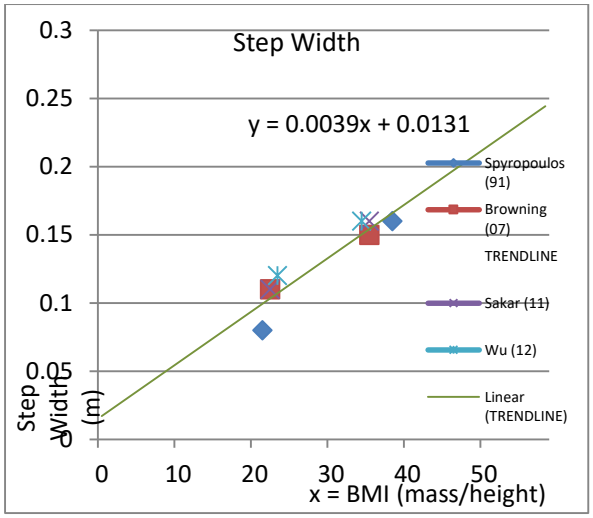

Figure 3-6- Empirical Analysis of Step Width over BMI

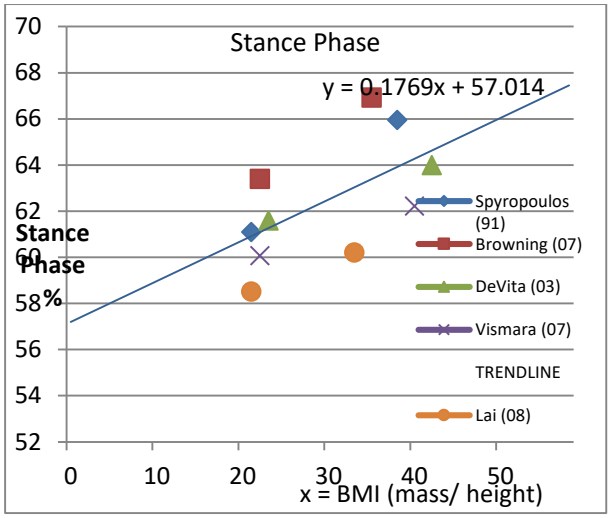

Figure 3-7- Empirical Analysis of Stance Phase over BMI

Multiple sources strongly correlate the trend that walkers spend less time in the Swing Phase over increases in BMI (Figure 3-8). Multiple sources strongly correlate increases in Foot Progression over increases in BMI (Figure 3-9).

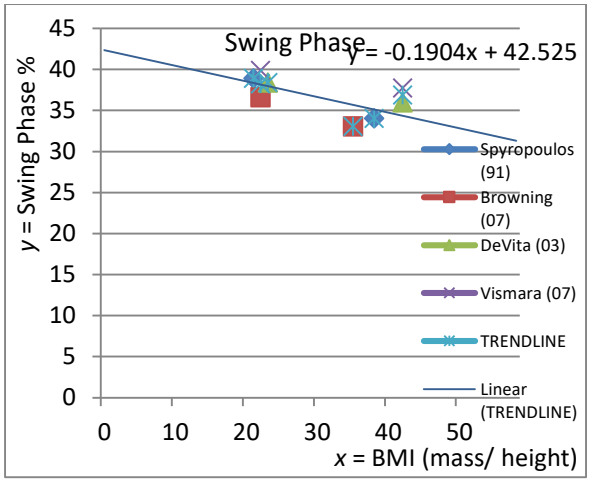

Figure 3-8- Empirical Analysis of Swing Phase over BMI

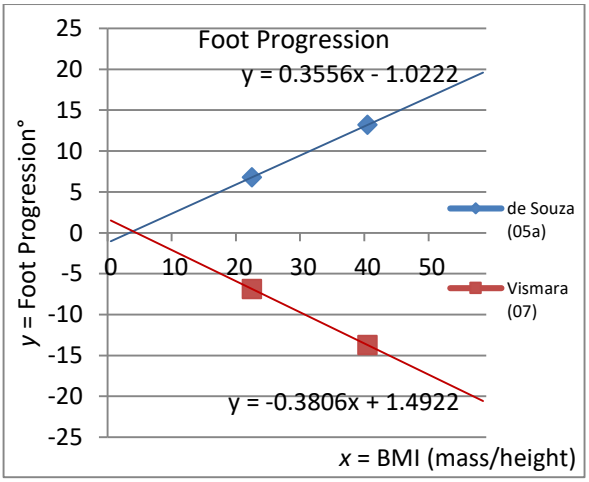

Figure 3-9- Empirical Analysis of Foot Progression over BMI

The regression formulas that resulted from this analysis formed the basis for the scripted motion deformations that were deployed in the perceptual video surveys.

3.1.2. Summary

By analysing published literature on the observed changes in gait parameters over increases in body morphology, we could verify eight trends against each other and provide a predictive formula. The main limitation of analysing these previous published data was that most listed data under two to three mean classifications of obesity as opposed to tracking

motion parameter changes over increments of BMI. This means richer trends are harder to map out.

3.2. Scripted Appearance and Motion Deformation Tool

3.2.1. Base Lean Motion Captured Locomotion

Once a round of early empirical data analysis had been conducted, the next stage was to implement the motion parameter trendlines into a scripted animation tool that could deform a lean character to have an increasingly obese appearance and gait parameter.

An early motion capture session provided walk data for an adult male 21 years old and 1.76m tall, the average height for an English male (Moody, 2013). He was also an ideal 12.1% body fat and a BMI of 23 kg/m^2 therefore suitable to utilise as the base motion capture data.

The base lean motion capture walk was captured using six MX13 Vicon cameras and using the Validated Vicon Marker Set (Kadaba et al., 1990; Winter et al., 1990; Davis et al., 1991). This process including calibration, range of motion tests, multiple takes and cleanup is described further in section 6.3.2.

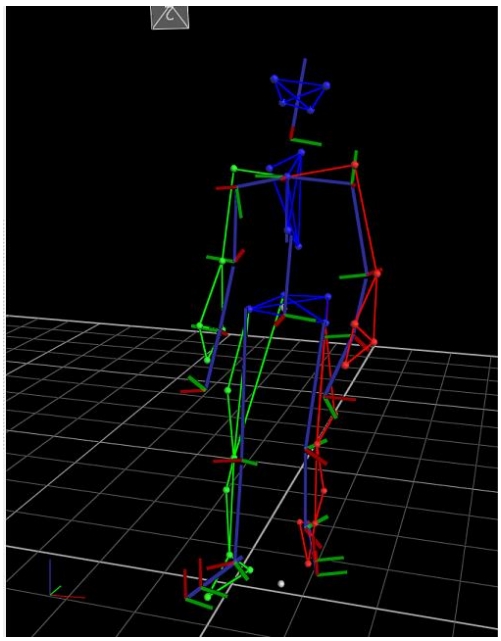

Figure 3-10- Captured and Cleaned Gait within Vicon Nexus 1.8.5

The base motion capture walk was exported from Vicon's Nexus 1.8.5 software as a .c3D file containing global positional marker data. This locomotion data was imported into Autodesk MotionBuilder where it was characterized onto the widely used default Forward Kinematic / Inverse Kinematic MotionBuilder rig. The characterization process interpreted the global marker positions from the motion capture data into local rotations on the following bones:

1.	Hips	6.	RightLeg	11.	LeftHand
2.	LeftUpLeg	7.	RightFoot	12.	RightArm
3.	LeftLeg	8.	Spine	13.	RightForeArm
4.	LeftFoot	9.	LeftArm	14.	RightHand
5.	RightUpLeg	10.	LeftForeArm	15.	Head

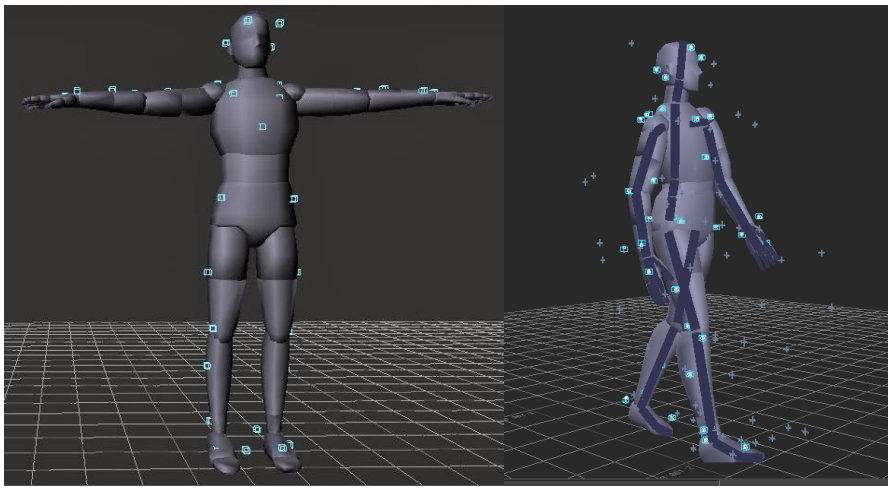

Figure 3-11- Characterization process with Autodesk's MotionBuilder 2013

The local bone rotations were exported using the .fbx file format. The lean motion captured walk animation was imported within Softimage (2015) and used to drive a MotionBuilder rig smoothly for five steps over two seconds. The walk was edited into a loopable walk cycle so as to retain as much data as possible.

3.2.2. Deformable Character Mesh

The lean motion captured walk cycle then needed to be applied to a lean character model.

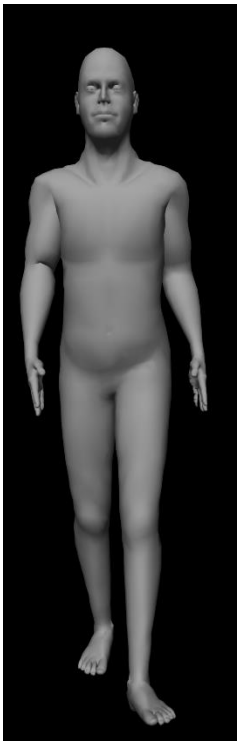

Figure 3-12 - Obese deformation of virtual human

The stock Softimage (2015) male character model was modified by height to fit the average height from the lean participant, which matched the average British male height (Moody, 2013). Abdominal muscles were also smoothed out to avoid visual exaggeration in body shape deformations. This modified male character model represented a base average lean body shape of 12% body fat.

An appearance deformation tool was then developed to enable the creation of a variety of differently shaped characters over increasing body fat percentage. Little research was uncovered about the linearity of adipose accumulation in certain body areas so we had to refer to photographic references of males at 3-40% body fat (Figure 3-13).

Using standard shape modelling and expert reference photography such as Perry (2012), the lean character model was deformed to look as though it had increased to approximately 35% body fat percentage (Figure 3-14).

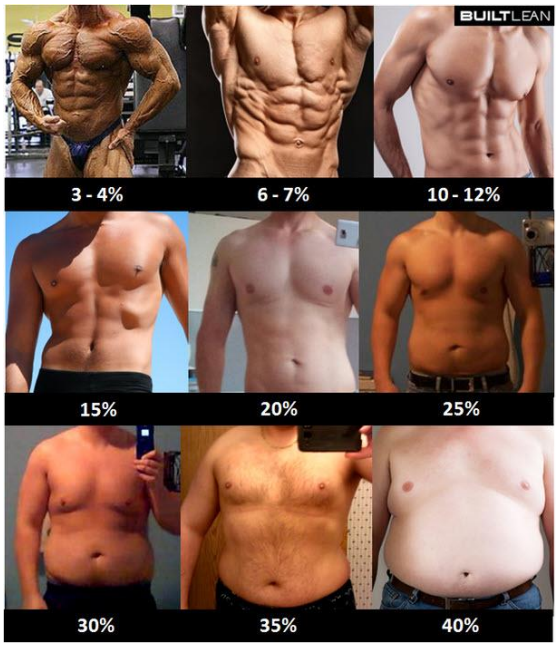

Figure 3-13- Photographic references of male body fat percentages (Perry, 2012)

Figure 3-14 - Obese deformation of virtual human

A slider was then created within Softimage (2015) to linearly blend between the lean model and the deformed obese model. There is no published evidence accurately defining or categorising the rates and areas where males put on weight, so a linear blend was chosen as a suggested profile. The deformation slider ranged from 12% to 35% as seen in Figure 3-15.

Figure 3-16 demonstrates on the left; the stock Softimage (2015) male character model with smoothed abdominal muscles representing 12% body fat, the character in the centre is deformed to represent 23.5% body fat and on the right; deformed to represent 35% body fat.

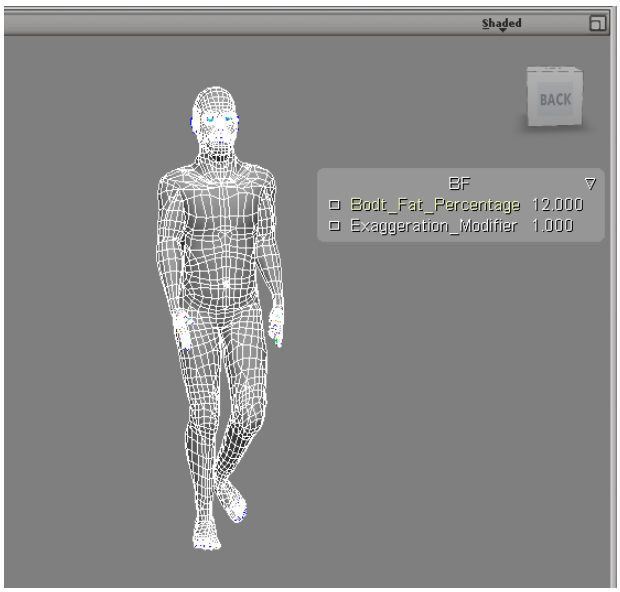

Figure 3-15- Appearance Deformation Slider

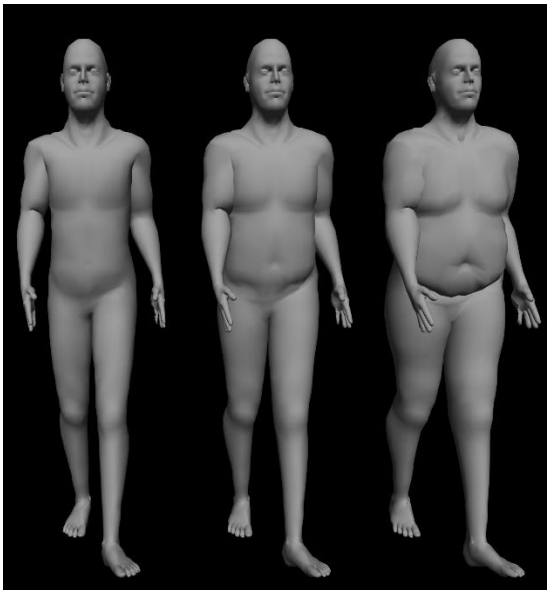

Figure 3-16- Character Mesh Linearly Deformed

The character mesh was fitted and weight painted onto the standard MotionBuilder skeletal rig with the intention to maximise compatibility with future imported motion capture walk files or keyframed animations.

The lean motion capture data from section 3.2 could then drive the lean character mesh. The appearance deformation slider was then driven by a series of motion deformation scripts.

3.2.3. Motion Deformation Scripts

Following early empirical data analysis a number of motion parameters were decided upon as being perceptually significant to modify and worth of scripted modification.

Average arm abduction, bob and twist, whilst not heavily researched, represents a large range of movement in the upper body half. As this is an area of the body that might be more visible than the lower half, we wanted to invest time into testing its perceptual effect and actual variance. Whilst spinal curvature was only measured by McGraw et al. (2000) and de Souza (2005b) it also represented a potentially variable and perceptually strong parameter in the upper half of the body. This included thoracic curvature but not abduction – adduction. For this reason torso twist was tested. As hip twist could move in contralateral to torso twist so this was also included. Speed was also modelled as it had been measured so frequently in literature it could prove to be of perceptual dominance.

A number of parameters were not scripted for a variety of reasons. Foot progression was considered too small and low to be perceptually visible. Varying stride length would also affect forward speed and cadence so it was opted to only change the latter two in unison. Percentage of time spent in stance and swing phase would have demanded motion warping phases of movement which if done incorrectly could create an unnatural stocatto effect of locomotion. This is a more demanding challenge for future iterations of the scripted tool. Pelvic Girdle tilt was tested but deemed perceptually hard to read. Knee range of motion was not modelled as we wished to free this up for the IK legs to allow the flexibility of other parameters. And finally ankle plantar flexion and range of motion were not modelled as they too were considered too small and low to be perceptually visible.

A full copy of all JavaScripts are available in Appendix D. All motion retargeting was performed on a per-key basis.

Average Arm Abduction

Average arm abduction was selected to be modified as the previous literature had not tracked these changes over obesity. As believability of character diversity is more important in small to medium sized crowds or camera shots (Zhou et al., 2010) we posit that upper body movement would be more visible than lower body. Abduction of the arms could produce the largest and most visible amount of movement. This parameter was also chosen as casual observation of obese people appears to show increased arm abduction.

Average arm abduction in biomechanical terms is more often referred to as average Lateral Shoulder Abduction. This is measured as the average upward movement of the arms away from the midline of the body. The scripted modifier was applied to the MotionBuilder rig in a manner analogous to how the real world measurement is taken.

The scripted modifier creates a duplicate of the base character so that changes to the original character are reversible, providing a non-destructive workflow.

Average arm position is defined as dataPosAvgDiff:

```
20  var dataPosAvgDiff      = 12.7742;      // F
```

Figure 3-17 - Average Arm Position Variable

Six absolute values were defined for the purpose of rendering multiple deformations for the perceptual video survey. This approach was followed for all of the scripts. These values were decided by manually raising the virtual arms to a level that represented a morbidly obese walker at 35% body fat as predicted by the trendlines from the empirical data analysis. One underweight value and two more extreme values above obese were used with even increases in arm abduction defined.

In this example the function ssModKey loops through each key on the duplicated character's left and right arm and adds the average arm position in the z rotation axis.

```
31  function    ssModKey(objectStringTo, avgMod)       // rig1, rig2, theor diff between avg pos, mag multiplier, actual average position
32  {
33      CurrentFrameNo          = FirstKey(objectStringTo);                         // After deletion current frame set back to start
34      aLastKey                = LastKey(objectStringTo);
35      var newKeyPos = 0;
36
37      while (CurrentFrameNo   <= aLastKey)
38          {
39          var CurrentKeyVal   = GetValue(objectStringTo, CurrentFrameNo);         // Gets current key value
40          newKeyPos           = CurrentKeyVal - avgMod;                           // Minus as arm is flipped
41          SaveKey(objectStringTo, CurrentFrameNo, newKeyPos );
42          CurrentFrameNo      = NextKey(objectStringTo, CurrentFrameNo);          // Increment frame no on Rig1
43          }
44  }
```

Figure 3-18 - ssModKey Algorithm

Line 40 shows the average value being subtracted, however, this demonstrates an oddity of the MotionBuilder rig.

The MotionBuilder rig was chosen as it was assumed that it represented a commonly used and compatible rig. However, upon development of the scripted mechanism, it became apparent that the orientation of multiple limbs appeared correct, but were working on inverted axes. The reasoning for this is unclear, however, the scripted mechanism had to compensate with multiple flipped axes.

Spinal Erectness

Spinal Erectness was selected to modify as McGraw et al. (2000) had claimed that posture changes over obesity but this was measured in prepubescent boys not adult males, therefore it was worth further investigation. Erectness of the spine could produce a significant change in upper body movement. This parameter was also chosen as casual observation of obese people appears to show distinctive increased spinal curvature in some, but not all walkers.

Spinal erectness in biomechanical terms is sometimes referred to as spinal curvature or erect posture, representing a combination of parameters including posterior thoracic tilt, lumbar lordosis, and anterior pelvic tilt.

The ssModKey function was reapplied to the lumbar bone to tilt the upper torso backwards.

Upper Magnitudes

Upper Magnitudes was a set of scripts that modified aspects of upper body movement as the previous literature had not tracked these changes over obesity.

Torso twist in biomechanical terms is referred to as Torso or 'Thorax Axial Rotation ROM'.

Torso bob is referred to as Torso or 'Thorax Lateral Flexion ROM'.

Arm bob is referred to as 'Lateral Shoulder Abduction and Adduction ROM'.

Whilst *Arm swing* is referred to as 'Shoulder Flexion and Extension ROM'.

These parameter were chosen as it was hypothesised that increased adiposity on the abdomen and torso produced larger ranges of inertia in their swing to counteract and maintain a steady centre of mass.

These functions required the average position of the swing to be found and then each keyframe position to be magnified along the local axis of rotation.

Average Arm Abduction and Arm Bob

This combined the average abduction of the shoulder with its Range of Motion (ROM) of the lateral abduction and adduction.

Average Arm Abduction and Swing

This combined the average abduction of the shoulder with its ROM of the arm flexion and extension.

Speed and Cadence

Walking speed is a product of cadence and step length. In the virtual world forward velocity can also be manipulated, however, if not done in tandem with cadence or step length, foot sliding will occur.

$$\textit{forward velocity (m/s) = cadence(steps/s) x step length(m)}$$

Equation 1 - Forward Velocity

For this reason we chose to manipulate forward velocity and cadence together whilst keeping step length the same.

Walking Speed in biomechanical terms is referred to as preferred walking speed or self-selected speed. Multiple sources, seen in Figure 3-2, had tracked its reduction over increases in obesity therefore it was a crucial parameter to model.

Cadence in biomechanical terms refers to the number of steps taken per minute. It was chosen as a motion parameter as da Silva-Hamu et al. (2013) had tracked these changes over obesity. If the number of steps per minute did decrease with obesity this could also drive a counterbalancing reduction in all other keys which would have a significant perceptual effect on the walking style of the character.

The scripted modifier for reducing the number of steps per minute involved duplicating the lean character and deleting all keyframes from the clone. A new function ssRetimeKey was then used to copy all of the keyframes from the lean bones rotational axes (and the Hips positional data), multiply it by the speedMod value and then to copy it onto the second character.

```
// RETIME INDIVIDUAL KEY FUNCTION ##########################################################################################################
// No rescaling or magnitude modifying
function ssReTimeKey(objectStringFrom, objectStringTo, timeMod)
    {
    try
        {   // DELETES all keys on rig2.
        var CurrentFrameNo      = FirstKey(objectStringTo);
        var aLastKey            = LastKey(objectStringTo);

        while (CurrentFrameNo   <= aLastKey)
            {
            RemoveKey(objectStringTo, CurrentFrameNo);
            CurrentFrameNo      = NextKey(objectStringTo, CurrentFrameNo );
            }
        }
    catch (err){}

    try //Retiming section ##############################################################################################################
        {
        CurrentFrameNo          = FirstKey(objectStringFrom);                   // After deletion current frame set back to start
        aLastKey                = LastKey(objectStringFrom);

        while (CurrentFrameNo   <= aLastKey)
            {
            var modFrameNo      = CurrentFrameNo / timeMod;                     // Divides frame no by scaleMod
            var CurrentKeyVal   = GetValue(objectStringFrom, CurrentFrameNo);   // Gets current key value
            SaveKey(objectStringTo, modFrameNo, CurrentKeyVal );
            CurrentFrameNo      = NextKey(objectStringFrom, CurrentFrameNo );
            }
        }
    catch (err){}
    }

```

Figure 3-19 - ssRetimeKey algorithm

Hip Twist

Hip twist was selected to modify as casual observation of obese walkers indicated some change in pelvic movement that could be a result of needing to maintain a counteractive balance to their centre of mass, or as a result of increased ground reaction force to heavier body mass.

Hip twist in biomechanical terms is referred to as the lateral and medial pelvic rotation ROM.

The scripted modifier for hip twist and the following lower body parameters required additional work to modify the motion capture data to avoid the problem of footskating. When importing the FK/IK MotionBuilder data into Softimage (2015) the local bone rotation data is baked onto the rig with forward kinematics.

To manipulate hip twists without moving feet positions the lower body had to be replaced with Inverse Kinematics legs. This was achieved by creating an IK leg chain in the same global position as the FK legs. The root of the IK legs were attached to the hips, as were the feet.

```
// RUN COMMANDS TO BUILD IK LEGS
// Left IK Leg
var IKLbone;
var IKLeff;
var IKLLegChain = Create2DSkeleton(lUpLegx, lUpLegy, lUpLegz, lKneex, lKneey, lKneez, 1, 0, 0, 4, IKLbone, IKLeff);        // Create Upper IK Leg() should contain or
var IKLLegShin  = AppendBone (IKLLegChain.Effector, lFootx, lFooty, lFootz);                                             // Append Lower IK Leg
ParentObj("MotionBuilder_Template.Hips", IKLLegChain.Root);                                                              // Parent whole IK Leg to FK Leg
var IKLFootbone;
var IKLFooteff;
var IKLFootChain = Create2DSkeleton(lFootx, lFooty, lFootz, lToex, lToey, lToez, 1, 0, 0, 4, IKLFootbone, IKLFooteff);     // Create IK Foot from heel to toe() shoul
ParentObj(IKLLegChain.Effector,IKLFootChain.Root);                                                                       // toeRoot to Heel end eff // Might not ne

// Left Leg Control Box
GetPrim("Null", null, null, null);                                  //get primitive null
SetValue("null.null.primary_icon", 4, null);                        // change icon to box
SetValue("null.Name", "left_leg_pos", null);                        // rename null "left_leg_pos"
MakeLocal("left_leg_pos.display", siNodePropagation);               // change colour to red for visability
SetValue("left_leg_pos.display.wirecolorr", 0.878, null);
SetValue("left_leg_pos.display.wirecolorg", 0, null);
SetValue("left_leg_pos.display.wirecolorb", 0, null);
MatchTransform("left_leg_pos", "MotionBuilder_Template.eff", siTrn, null);  // Match Control Box pos to IK heel eff pos

```

Figure 3-20 - Inverse Kinematic Leg Generation

The script then looped through and saved the global position of the IK ankles, matched to the global position of the FK ankle positions. The IK knees were then afforded some flexibility when the IK hips or feet were modified. The original FK leg keys were then removed.

A global position control box was also parented to the character and all positional and rotational data from the hips were copied to it, and then deleted from the hips. The hips

were then parented to the global position control box. This was to allow independent manipulation of the character's forward velocity and movement of the hips.

Walking Base

Walking base was selected to modify as it was hypothesised that as obesity or abdominal girth increased, a wider walking base would be needed to maintain a steadier centre of gravity.

Walking base in biomechanical terms is also known as stride width. It is the sum perpendicular distance between the two heels and the midline of the body.

The scripted modifier used the IK legs to increase the distance between the ankles and toes from their midline.

Combinations

The scripts were then able to have their values modified for testing purposes, multiple surveys and to combine parameters into multiples.

When speed and cadence were part of the multiple parameters this modification would have to be made on a third character duplication to avoid other modifier keys from being overwritten.

3.2.4. Summary

By taking the results of the early empirical data analysis, it was possible to use these trendlines as the base strengths and formulas for the scripted animation tool.

This required the development of an appearance deformer built using photographic reference. And a motion deforming script. This maintained the base motion capture data whilst using duplicate characters, FK retiming and IK translations across multiple parameters.

This was developed to enable the following phase of perceptual video survey tests as well as laying the technical foundation for the scripted animation tool.

4. POINT LIGHT PERCEPTUAL SURVEY

A video test was developed to assess the most perceptually dominant motion parameters. The first iteration of this video test involved the use of point-light walkers (Johansson, 1973) so that participants could try to identify motion without the bias of appearance. This test required a base lean model and five duplicates with one or more parameter exaggerated to varying strengths. Viewers then had to select which point-light walker most resembled an obese person's gait.

The lean motion capture walk was reused as a base model and then modified using the previously described scripted modifier. However, instead of using a character mesh, fifteen point-lights were attached to the skeleton. Troje (2002) determined that fifteen point lights located around joints of the body was enough to communicate the structure and dynamic movement of a human walker. This was done to disambiguate appearance bias:

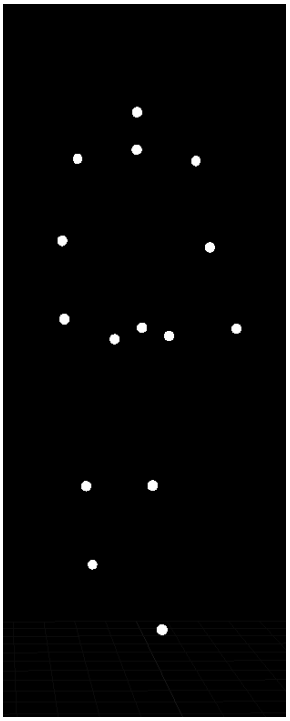

Figure 4-1- Point Light Walker configuration

The point-lights were spheres of 1.5 Softimage unit (SI) size that were comparable in relative prominence to the experiments by Cutting and Kozlowski (1977) and were judged to be visible enough against a black background. The spheres had a white constant texture

applied and were rendered against a black background with no external lighting to maximise contrast, clarity and readability of motion.

They were attached at the centre of the following locations on the MotionBuilder rig, which is similar to Troje (2002) configuration:

1. Hips
2. Left Upper Leg
3. Left Knee
4. Left Heel
5. Right Upper Leg
6. Right Knee
7. Right Heel
8. Left Shoulder
9. Left Elbow
10. Left Wrist
11. Right Shoulder
12. Right Elbow
13. Right Wrist
14. Torso
15. Head

4.1. Motion Parameter Strengths

The light perceptual survey tested five motion parameters and five combinations. Five motion parameters were selected based on availability of multiple sources of data and their representation of upper and lower body gait parameters. As velocity, cadence, step length and stride length are all related, we compounded them into walking speed and chose not to initially vary step/stride length. Cervical, lumbar & thoracic spine curvature was tested. Hip flexion (twist) was included but pelvic girdle was not as it was deemed too small and subtle a range of movement. As the virtual legs were made using inverse kinematics, this did not allow the direct manipulation of knee ROM, and knee flexion. Ankle plantar flexion and ROM was not altered to avoid issues of inaccurate foot plantation. Finally foot progression was not tested as it was lowest on the body therefore likely to have the least perceptual impact especially in a crowd. The five combinations were then paired by limb group, upper and lower body to see which had the strongest perceptual effect and then a complete combination to test their overall effectiveness. This combinations helped rank the comparative strength of perceptual dominance of each parameter and their combined effectiveness.

The number of parameter strengths was six as anymore produced confusion in early video tests. This range of strengths was designed to allow an under-exaggerated value, a value with no change from the base walker of 12% body fat, an overweight exaggeration, a target obese exaggeration of 35%, an over exaggeration and an extreme exaggeration. 25% body

fat on males is classified obese (ACE, 2003; Phillips et al., 2013) in males so 35% was selected to represent a morbidly obese level.

To test these motion parameters, relative bone rotations and global positions needed to be exaggerated. This was achieved within the Softimage (2015) scripting environment by writing JavaScript code to manipulate the bone rotation by average position, offset position, swing magnitude and the timing of all keyframes.

Analysis was made on quantitative data from eight existing, cited dataset (Spyropoulos, 1991; de Souza, 2005a; de Souza, 2005b; DeVita and Hortobágyi, 2003; Hulens et al., 2003; Tompkins et al., 2008; Vismara, 2007; Browning and Kram, 2007) on the changes in motion parameters over increases in BMI. The most common BMI values were 22 (lean) and 38 (severe to morbidly obese) which we consider to be equivalent to 35% Body Fat.
As velocity and cadence had the most sources to derive a regression formula this was used to calculate the expected reduction in speed for an obese walker from the base lean walker's speed:

$$Walking\ speed = -0.0269 \times BMI + 2.3185$$

Equation 2 - Prediction of Walking Speed

The other 35% body fat values were created by manually adjusting each relevant gait parameter of the lean character's walk cycle to appear to be that of an obese person from the animator's perception. Values were then interpolated between an unchanged value at 12% body fat (the original lean walker's position) and this value set at 35%. The combinations then reused the values from the other individual parameters. Table 4-1 lists the motion parameters, the bone names (and corresponding references in software packages) movement axes, modification type and strength values:

Table 4-1 - Point Light Survey's Motion Parameter Strengths

						Body Fat Percentage Values					
Survey No.	**Angle View**	**Video Test Parameters**	**Bone**	**Movement**	**Mod Type**	**0.5%**	**12%**	**23.5%**	**35%**	**46.5%**	**58%**
1	**45°**	**Increased Hip (twist) & Torso (twist)**									
		a. Increased hip (twist)	Hips	local.roty	Swing Magnitude	-0.8	1	2.8	4.644041	6.5	8.3
		b. Increased torso (twist)	Chest	local.rotx	Swing Magnitude	-0.8	1	2.8	4.644041	6.5	8.3
2	**45°**	**Upper body combination**									
		a. Increased hip (twist)	Hip	local.roty	Swing Magnitude	-0.8	1	2.8	4.644041	6.5	8.3
		b. Increased torso (twist)	Chest	local.rotx	Swing Magnitude	-0.8	1	2.8	4.644041	6.5	8.3
		c. Increased arm abduction	Upper Arm	local.rotz	Average Position	-3.19355	0	3.19355	6.3871	9.58065	12.7742
		d. Increased arm (bob)	Upper Arm	local.rotz	Swing Magnitude	0.6	1	1.4	1.895681	2.3	2.8
		e. Increased arm (swing)	Upper Arm	local.roty	Swing Magnitude	0.5	1	1.5	2	2.5	3
3	**45°FL**	**Lower body combination**									
		a. Reduced walking speed	Hips	global.posz	Retime	1.1	1	0.9	**0.805026**	0.7	0.6
		b. Reduced cadence	ALL	ALL	Retime All	1.1	1	0.9	**0.805026**	0.7	0.6
		c. Increased hip (twist)	Hips	local.roty	Swing Magnitude	-0.8	1	2.8	4.644041	6.5	8.3
		d. Increased walking base	Heels	local.posx	Offset	-1	0	1	2	3	4
4	**45°**	**Increased Arm Abduction & (swing)**									

		a. Increased arm abduction	Upper Arm	local.rotz	Average Position	-3.19355	0	3.19355	6.3871	9.58065	12.7742
		b. Increased arm (swing)	Upper Arm	local.roty	Swing Magnitude	0.5	1	1.5	2	2.5	3
5	**45°FL**	**Whole body combination**									
		a. Reduced walking speed	Hips	global.posz	Retime	1.1	1	0.9	**0.805026**	0.7	0.6
		b. Reduced cadence	ALL	ALL	Retime All	1.1	1	0.9	**0.805026**	0.7	0.6
		c. Increased hip (twist)	Hips	local.roty	Swing Magnitude	-0.8	1	2.8	4.644041	6.5	8.3
		d. Increased torso (twist)	Chest	local.rotx	Swing Magnitude	-0.8	1	2.8	4.644041	6.5	8.3
		e. Increased walking base	Heels	local.posx	Offset	-1	0	1	2	3	4
		f. Increased arm abduction	Upper Arm	local.rotz	Average Position	-3.19355	0	3.19355	**6.3871**	9.58065	12.7742
		g. Increased arm (bob)	Upper Arm	local.rotz	Swing Magnitude	0.6	1	1.4	**1.895681**	2.3	2.8
		h. Increased arm (swing)	Upper Arm	local.roty	Swing Magnitude	0.6	1	1.3	1.6	1.9	2.2
6	**90°**	**Increased Arm (swing)**	Upper Arm	local.roty	Swing Magnitude	0.5	1	1.5	2	2.5	3
7	**90°**	**Increased Spinal Erectness**	Lower Spine	local.roty	Average Position	-5	0	5	10	15	20
8	**45°FL**	**Reduced Walking Speed/ Cadence**	ALL								
		a. Reduced walking	Hips	global.pos	Retime	1.1	1	0.9	**0.80502**	0.7	0.6

		speed			z				**6**			
			b. Reduced cadence	ALL	ALL	Retime All	1.1	1	0.9	**0.805026**	0.7	0.6
9	**0°**	**Increased Arm Abduction & (bob)**										
		a. Increased arm abduction		Upper Arm	local.rotz	Average Position	-3.19355	0	3.19355	6.3871	9.58065	12.7742
		b. Increased arm (bob)		Upper Arm	local.rotz	Swing Magnitude	0.6	1	1.4	1.895681	2.3	2.8
10	**0°**	**Increased Arm Abduction**		Upper Arm	local.rotz	Average Position	-3.19355	0	3.19355	6.3871	9.58065	12.7742

The code for all motion modifying scripts can be found in Appendix D.

4.2. Survey Design

The video survey was developed using Google Forms; a flexible, free, online method that enabled survey results to be directly output to Google's spreadsheets for analysis. An online survey was used as it was an efficient method to reach a larger number of participants in a short amount of time and reduced the requirements on participants' time and travel. The survey was promoted through social media channels such as Facebook, Twitter and email with the incentive of a randomly selected animation or games related prize. The survey was anonymous, however, those who wished to participate in the random prize draw supplied their email address, which was stored securely in accordance with the Data Protection Act (1998).

Whilst viewing conditions could not be controlled it was possible to fix video dimensions to 585 x 573 pixels. The video surveys can be viewed online at (Shewhorak, 2014a; 2014b).

The survey consisted of fourteen linked webpages, which were estimated to take approximately 10 minutes to complete. Previous prototypes were longer but feedback included complaints at the length as it induced viewer fatigue that could be detrimental to the quality of responses. A progress bar also helps participants track their completion progress.

The first two pages briefly introduced the project and required participants to list their age. Under eighteens were not permitted to continue due to ethical requirements. Participants were introduced to the survey format with an example video of five point light walkers and a visual representation of the obese target weight they were attempting to identify. Accompanying text instructed participants without inferring expected responses.

Following the introductory pages were the testing pages containing embedded YouTube videos. Twenty videos were initially tested but early feedback reduced this to ten as testers noted the survey length was too fatiguing. Their design and layout is detailed further in section 4.3. Videos were set to play at the maximum page dimensions possible with instructions to click and watch the videos at full screen, before selecting a radio button to

indicate which walker looked like an obese person. The radio buttons allowed only one selected option.

The final page also had options for participants to type feedback notes and to enter their email addresses if they wished to be entered into the prize draw.

4.3. Video Design

For the ten pages of video tests a row of six point-light walkers were centred in each video frame with bold, capitalised, red lettering beneath each identifying them to their radio button response. One point-light walker was the unchanged lean walker whilst the other five were exaggerated by different strengths. The order of the six walkers were randomised so that participants would not be able to select the lean walker through relative ordering. The base lean walk cycle lasted three seconds and involved five steps. The entire clip was looped to a length of thirty seconds, as opposed to trimming a two-step walk cycle to retain as much visual information possible, however, this did introduce a slight jump when transitioning from the end of the clip to the start of it. Forward movement along the z-axis was typically deleted so the walker appeared to be walking on the spot. To capture each walker the virtual camera was distanced so that the walker filled the frame and was angled slightly below eye level for a distortion less, natural gaze. To most clearly demonstrate each parameter or combination of parameters, the camera was rotated slightly differently.

Early prototype video designs displayed a 2 x 6 matrix of the parameter from 0° front view on the top row and the same parameter but with the camera rotating 360° on the bottom row. This was designed in reference to McDonnell et al. (2008) with the purpose to show the parameter from multiple angles.

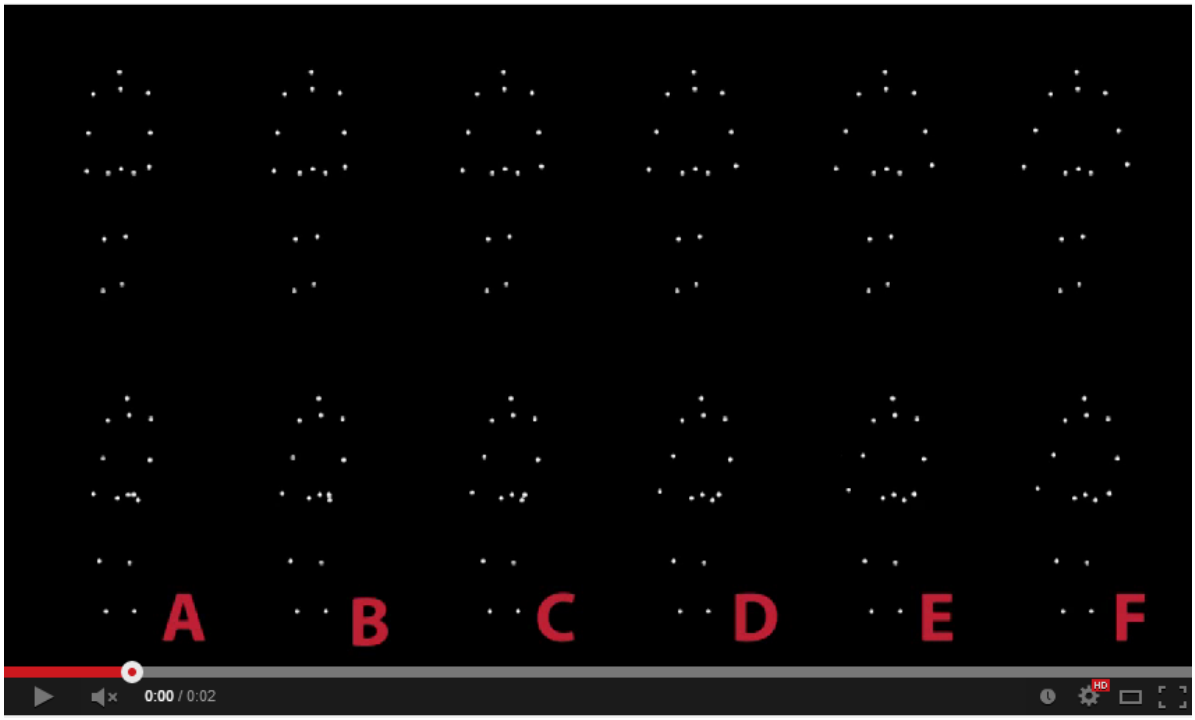

Figure 4-2- Point light walker matrix prototype

However, feedback was negative with users noting that the rotating camera view was too fast and confusing and the set of twelve point-light walkers became a “less distinguishable cloud of points”, with the fatiguing effect worsening with each new video. Therefore a switch to a row of six point-light walkers with a fixed camera angle was implemented.

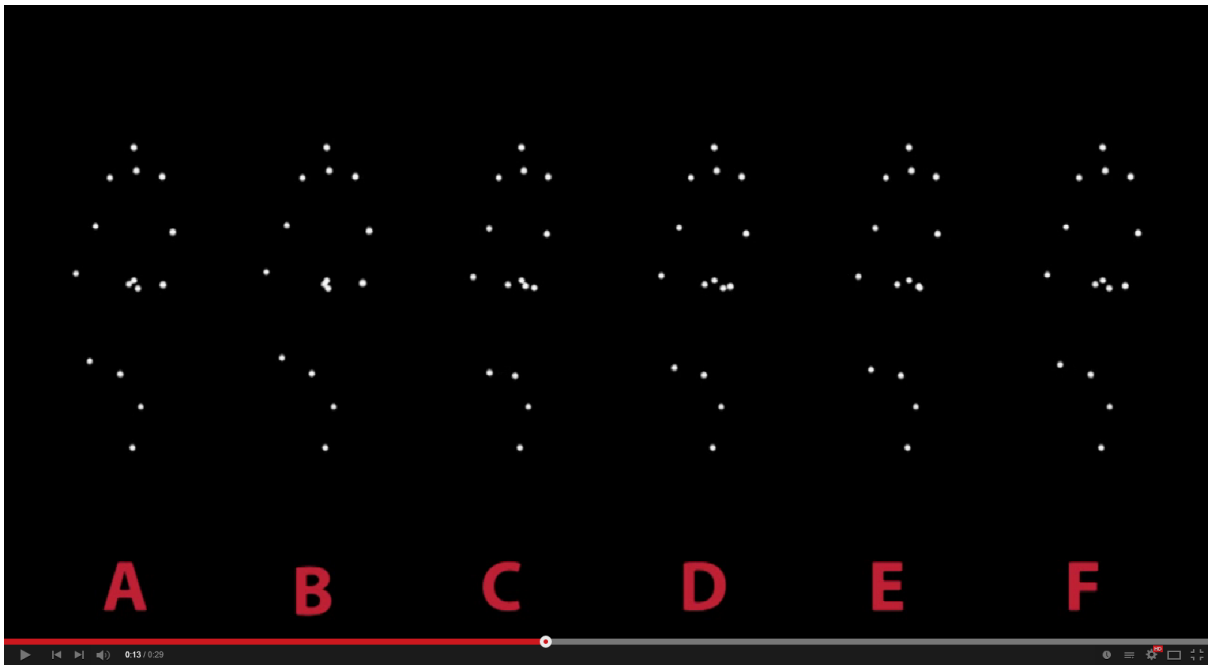

Figure 4-3 - Simplified point light walker matrix

Most videos showed characters walking at 45° from the camera (as seen above in to give a view of the front and side profiles. Two videos were at 45° but took up the Full Length (FL) of the horizontal frame, as they needed to demonstrate changes in speed so the walkers did not walk on the spot. Two videos were orthogonal side on at 90° and two front on at 0°. Those parameters and their angle of view is listed in Table 4-2:

Table 4-2 – Angle and order of point light walker matrices

Survey Order	Point Light Video Parameters	Angle of View
1	Increased Hip (twist) & Torso (twist)	45°
2	Upper body combination	45°
3	Lower body combination	45° FL
4	Increased Arm Abduction & (swing)	45°
5	Whole body combination	45° FL
6	Increased Arm (swing)	90°
7	Increased Spinal Erectness	90°
8	Reduced Walking Speed/ Cadence	45° FL
9	Increased Arm Abduction & (bob)	0°
10	Increased Arm Abduction	0°

Early prototype designs featured a single loop of the walk cycles but the feedback response was that the clips were too short and some effort was needed to keep pressing the replay button. So the walk cycles were rendered again with loops extended to thirty seconds, which prototype feedback had estimated would be enough time to make an informed selection. Participants were also free to loop the embedded thirty second video multiple times.

4.4. Point-Light Perceptual Survey Results

This section presents the results of our point light perceptual survey to try and discern the strengths and order of perceptual dominance for motion parameters.

We do this by analysing the number of respondents who associated a motion parameter exaggeration (or combinations of) with the character deformed to represent 35% Body Fat Percentage. These are presented in the forms of categorical bar charts.

Individual motion parameters that feature a single value of offset or magnitude amplification may feature those values across graphs x axis. However, when multiple motion parameters are tested, analysed and presented, the x axis features categorical labels such as A, B, C, D, E, F or the 0.5%, 12%, 23.5%, 35%, 46.5% or 58% Body Fat values the combined parameters are being tested as a representative of.

The video survey was promoted from 13/02/14 through social media and in classes at Teesside University with a £20 voucher incentive. Participants' (*n*=59) mean age was 23.3, 31 who identified as having experience in animation or games development, one identified as having experience in sports sciences or biomechanics and twenty seven who identified themselves as simply members of the public (layman viewers).

The first perceptual survey tested the following motion parameters listed previously in Table 4-2. This mixture of parameters was chosen to represent the potentially large ranges of movement or perceptually outstanding aspects of the upper body; arm abduction, swing, bob, spinal erectness. They were also chosen to represent the more traditionally studied lower body gait; walking speed/ cadence and hip and torso twist. Further justifications for their selection for surveying and scripting can be found in section 3.2.3 and 4.1.

Modification values of offset or multiplications are listed on each graphs horizontal axis. When multiple parameters are tested, their results are categorised into 'A' – 'F' or '0.5%' – '58%' bars, whose values can be found in Table 4-1. The results, however, shall be discussed in a more logical order of upper body, lower body then combined parameters as follows:

4.4.1. Increased Average Arm Abduction

It was hypothesized that as body morphology increased, viewers expected average arm abduction to increase to avoid chafing with the torso. The results, as seen in Figure 4-4,

confirm this hypothesis with significant identification of obese walkers with increased angle of arm abduction.

4.4.2. Increased Spinal Erectness

It was hypothesized that as body morphology increased, viewers expected spinal erectness to increase, as observed by McGraw et al. (2000) and de Souza (2005b). The results, as seen in Figure 4-5, are mixed. Removing strengths -5 and 5 as outliers could present an upward trend of viewers perceiving increased spinal erectness in obese walkers. Upon reviewing the videos, however, it would appear that spinal erectness was poorly modelled using flexion-extension of only the lowest spine bone. A better representation of the motion parameter may have been Spinal Curvature that includes flexion-extension of multiple spinal bones. For this reason, the motion parameter and survey results for spinal erectness are no longer to be considered valid.

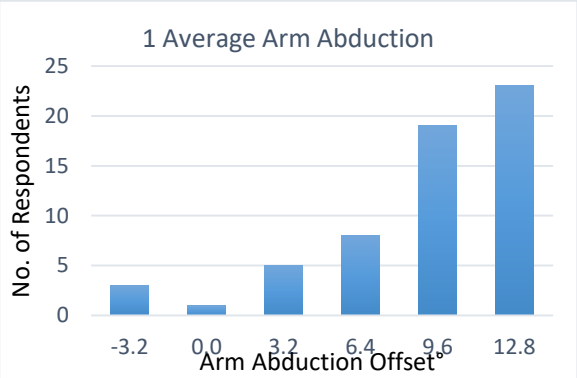

Figure 4-4- Increased Arm Abduction point-light results

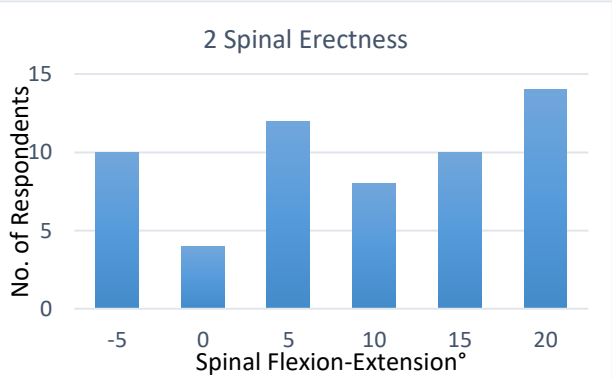

Figure 4-5- Spinal Erectness point-light results

4.4.3. Increased Arm Flexion - Extension (swing)

It was hypothesized that as body morphology increased, viewers expected arm swing to increase.

The results as seen in Figure 4-6 show a significant trend of identification of under exaggerated arm swing with an obese walk. This indicates that viewers perceive obese walkers to reduce their arm swing magnitude. This could be to reduce the movement of the COM to maintain balance and conserve energy.

4.4.4. Increased Average Arm Abduction & Abduction - Adduction (bob)

It was hypothesized that as body morphology increased, viewers expected average position of arm abduction and bob magnitude to increase. The results as seen in Figure 4-7 shows a significant increase in preference for positively exaggerated arm abduction and bob in the perception of obese gait. Increasing arm abduction to avoid chafing with the torso and increasing arm bob could be a passive kinematic reaction to increased ground reaction forces. However, as the arm abduction has already been shown to be more believable when increasing, increasing arm bob may simply be a less dominant parameter. For this reason, arm bob needed to be tested in isolation in survey two.

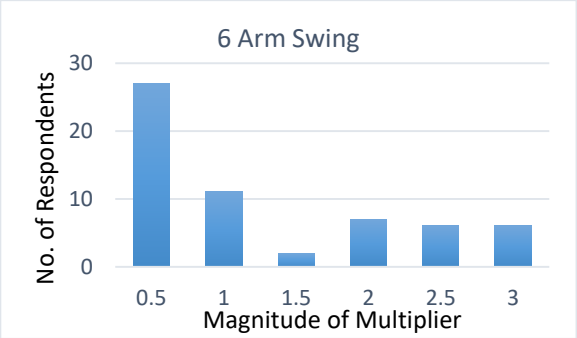

Figure 4-6- Arm Swing point-light results

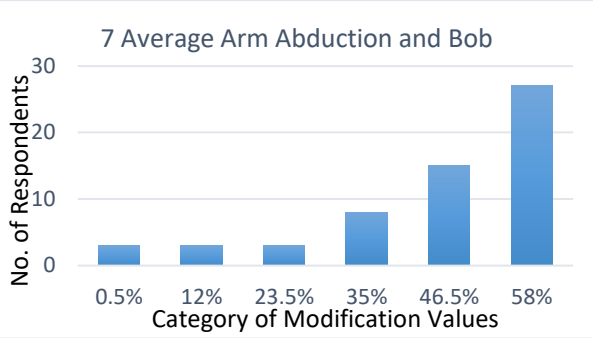

Figure 4-7- Average Arm Abduction and Bob point-light results

4.4.5. Increased Average Arm Abduction & Extension – Flexion (swing)

It was hypothesized that as body morphology increased, viewers expected average arm abduction and swing magnitude to increase. The results, as seen in Figure 4-8, show mixed results. Previous survey results had demonstrated viewer preference for increased arm abduction, and decreased arm swing magnitude, which explains the mixed results.

4.4.6. Reduced Walking Speed/ Cadence

It was hypothesized that as body morphology increased, viewers expected preferred walking speed to decrease. The results as seen in Figure 4-9 were inconclusive with no trending preference. As previous research by Spyropoulos et al. (1991) had determined a correlation between increases in obesity and decreases in walking speed this suggests that the full length 45° angle of the video experiment did not allow viewers to compare changes in distance and needed retesting at a different angle in survey two.

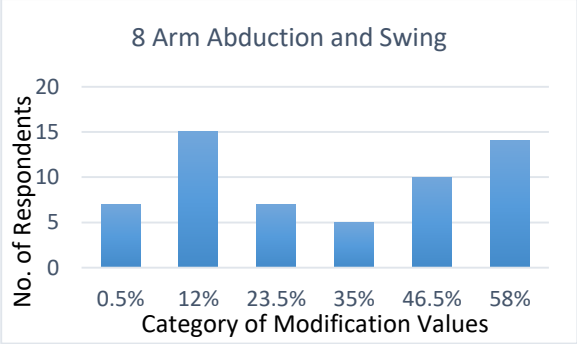

Figure 4-8- Arm Abduction and Swing point-light results

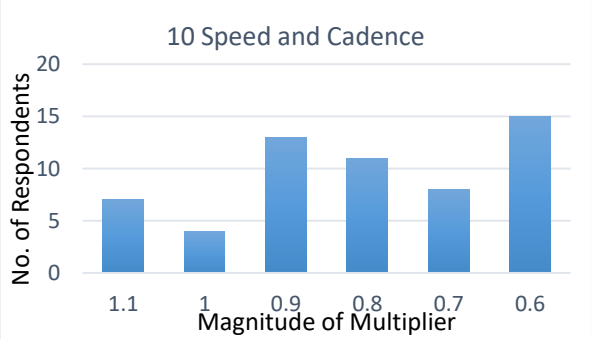

Figure 4-9- Speed and Cadence point-light results

4.4.7. Increased hip twist & torso twist (thorax axial rotation)

It was hypothesized that as body morphology increased, viewers expected hip and torso twist magnitude to increase. The results, as seen in Figure 4-10, appear mostly mixed with some preferences at the under exaggerated and over exaggerated strengths with the largest choice being the unchanged original. This suggests that viewers possibly expect no change, or a decrease in hip and torso twist. The spike at 8.3 magnitude could have been selected as an outlier. As the hip and torso body parts exhibit less movement than other limbs, the point-light method abstracts a lot of the effect of this subtler motion parameter. For this reason this parameter was retested in survey two using surface topology.

4.4.8. Upper body combination

It was hypothesized that as body morphology increased, viewers expected hip and torso twist, arm abduction, bob and swing to increase. The results as seen in Figure 4-11 shows a mixed preference with seventeen people selecting under exaggeration and seventeen people selecting over exaggeration. This suggests that more than one parameter is contradictory. Increased arm abduction and bob had previously shown to be perceptually

preferable whilst decreased arm swing had been shown to be preferable. Isolating or reversing arm swing magnitude exaggeration in survey two would clarify this.

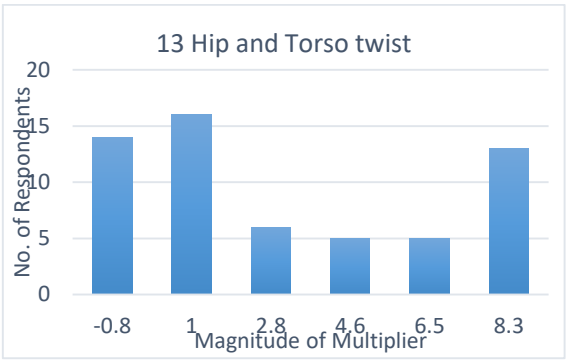

Figure 4-10- Hip and Torso Twist point-light results

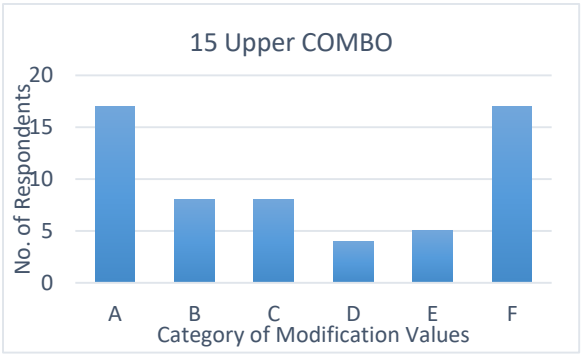

Figure 4-11- Upper Body Combination point-light results

4.4.9. Lower body combination

It was hypothesized that as body morphology increased, viewers expected walking speed to decrease, hip twist and walking base to increase. The results as seen in Figure 4-12 show a strong preference for the most exaggerated combination of values configured at '58%'. As walking speed and hip twist had not yet appeared to be dominant (given the angle and presentation) the results suggest that increased walking base has a significant effect of the perception of obese walkers.

4.4.10. Whole body combination

It was hypothesized that as body morphology increased, viewers expected walking speed to decrease and hip twist, torso twist, walking base, arm abduction, arm bob and arm swing to increase.

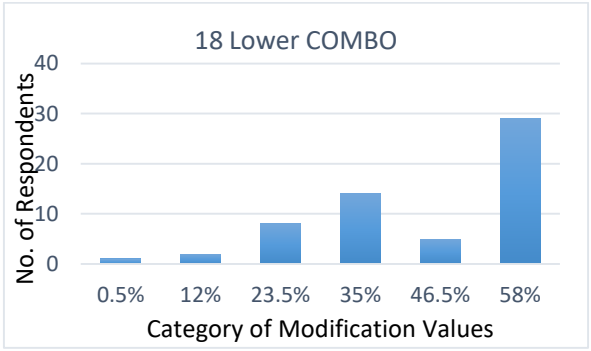

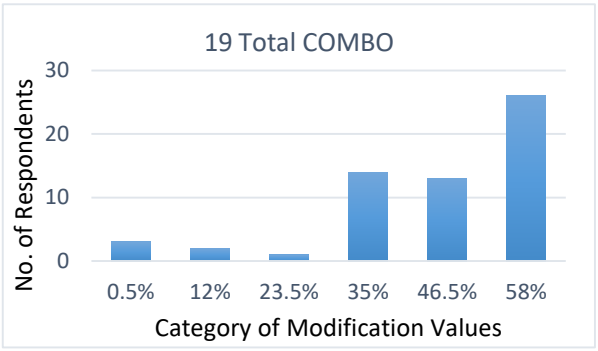

Figure 4-12- Lower Body Combination point-light results

Figure 4-13- Total Combination point-light results

It was hypothesized that as body morphology increased, viewers expected walking speed to decrease and hip twist, torso twist, walking base, arm abduction, arm bob and arm swing to increase. The results as seen in Figure 4-13 show a strong preference for the most exaggerated combinations.

Considering some parameters needed to be presented differently, this suggests that parameters such as arm abduction, arm bob and walking base were more dominant than others. Or it could suggest that the combination of these and weaker presented parameters was enough to provide a strong visual perception of obese walkers.

4.5. Summary

With the prototyping of a scripted animation deformation tool, it became possible to modify 5 individual and 5 combinations of parameters at 6 strengths of exaggeration. This was deployed in a survey with the intention of better understanding people's perception of

obese gait and potentially how it may differ to actual variations in real life. Whilst this chapter presented the results of the point-light survey, they shall be analysed in comparison to the character mesh survey in Chapter **Error! Reference source not found.**. The following chapter shall describe the process of a second round of perceptual surveys using character meshes as opposed to point light displays.

5. CHARACTER MESH PERCEPTUAL SURVEY

Following the first point-light survey another survey was developed. Two surveys were used to test a wider range of parameters without fatiguing the same participants with one excessively long survey. The first point-light survey was also analysed to optimise the second survey's presentation format, angle of viewing, to verify questionable parameters, introduce new parameters and combinations.

Whilst the first survey used point-light walkers some users' feedback had noted that they found it difficult to differentiate motion amongst the cloud of lights. Certain parameters such as torso twist were also much more difficult to perceive from just the point lights. For this reason a switch to displaying character meshes was made.

Figure 5-1 - Obese deformation of virtual human

The scripted parameter modifications still worked on the new character in the same way as before, however, now the movement could be seen through surface topology as opposed to fifteen point lights.

5.1. Motion Parameter Strengths

The mesh based perceptual survey tested five motion parameters and five combinations. Following analysis of the results from the first survey, a number of parameters were retested, reoriented, isolated or modified as summarised in Table 5-1:

Table 5-1 - Motion parameter changes

	Video Parameter	**Parameter Changes from Point Light Survey**
1	Upper body combination	Torso twists and arm swing magnitude decreased in strengths
2	Lower body combination	Hip twists decreased in strengths
3	Increased walking base	Walking base was isolated as a parameter as it had not previously been tested on its own
4	Torso (swagger)	Torso swagger was added as this parameter was observed in a distinctive overweight motion capture participants.
5	Increased Arm (bob)	Arm bob was isolated as a parameter as the first surveyed tested arm bob and abduction combined, so there was a need to test the perceptual dominance of arm bob alone.
6	Reduced Walking Speed/ Cadence	Preferred walking speed and cadence was retested from a front-on view as the previous 45° full length view returned feedback that it was hard to judge.
7	Increased Hip (twist) & Torso (twist)	Increasing hip and torso twist was retested. The point light version may have been too subtle for participants to read the changes so the test was repeated with the 3D character mesh with the hope that surface topology deformations would be easier to see.
8	Decreased Hip (twist)	Hip twist magnitude decreased in strengths.
9	Whole body combination	Hip and torso twists and arm swing magnitude decreased in strengths
10	Increased Arm Abduction & (swing)	Arm swing magnitude decreased in strengths

Arm abduction and swing was retested as the scripted tool had failed to implement the changes correctly. Spinal erectness was tested in the first survey but on reflection the modelling was judged to be too simplistic whereas a curvature to the whole spine would have been more accurate. Whilst McGraw et al. (2000) and de Souza (2005b) states that spinal curvature increases over obesity, the constraints of the motion capture process meant capturing spinal curvature over taut areas of the compression suit, especially with obese participants, would have been highly inaccurate. For these reasons, this parameter was abandoned in this second survey.

Table 5-2 lists the motion parameters, the bone names (and corresponding references in software packages) movement axes, modification type and strength values. Whilst the combination values carry over values from the previous survey or other parts of the survey, the individual parameters being tested or retested had their values decided as follows:

Walking base is tested again on its own with values manually modified in to be a perceived obese width of 4 Softimage units from the line of progression at 35% body fat, and then other values were interpolated equally between that and the unchanged base value of 0 offset at the lean 12%.

Torso swagger was a distinctive movement noticed anecdotally in one person so its magnitude in the lateral y axis was manually exaggerated to a degree that was believed could be an obese person at 35% body fat and then other values were interpolated equally between that and the unchanged multiplication of 1 at the lean 12% base value.

Arm bob was retested on its own with 35% set at an expanded magnification of 3.7 and 0.5% dipping into the negative direction of -0.8. This was manually altered to try and detect a preference trend in one direction or the other for what was seeming to be a perceptually weak parameter.

Hip twist was retested on its own but now on a decreasing scale with 35% body fat magnifying rotation by only 0.25. This was manually altered to see if people perceived less movement over body fat percentage.

The combinations were an opportunity to retest parameters, the direction of their exaggeration or scales of modification.

Increased arm abduction was retested but with arm swing now decreasing over a smaller scale as the previous survey gave inconclusive results. The values were decided by decreasing from a subtler scale of 1.25 magnitude of amplification at 0.5% body fat down to unchanged at 58% we hoped to see some more refined results.

Lower combination kept the speed values and walking base but we opted to try the newer values from the hip twist test to compare the combined effectiveness

Upper combination utilises the values for the decreased hip twist and also keeps them for torso twist assuming a contralateral action would change in unison. Arm abduction's values are kept unchanged as the results indicated they were effective. Arm bob values were kept the same as they were being tested separately, and arm swing reuses the newer values.

Whilst the total combination utilised values from the lower and upper body combinations to test their overall effectiveness.

Table 5-2 - Obese Mesh Survey's Motion Parameter Strengths

							Body Fat Percentage Values					
Survey No.	**Script No.**	**Angle View**	**Video Test Parameters**	**Bone**	**Movement**	**Mod Type**	**0.5%**	**12%**	**23.5%**	**35%**	**46.5%**	**58%**
1	15	**45°**	**Upper body combination**									
			a. Decreased hip (twist)	Hip	local.roty	Swing Magnitude	**1.25**	**1**	**0.75**	**0.5**	**0.25**	**0**
			b. Decreased torso (twist)	Chest	local.rotx	Swing Magnitude	**1.25**	**1**	**0.75**	**0.5**	**0.25**	**0**
			c. Increased arm abduction	Upper Arm	local.rotz	Average Position	-3.19355	0	3.19355	6.3871	9.58065	12.7742
			d. Increased arm (bob)	Upper Arm	local.rotz	Swing Magnitude	0.6	1	1.4	1.895681	2.3	2.8
			e. Decreased arm (swing)	Upper Arm	local.roty	Swing Magnitude	1.25	1	0.75	0.5	0.25	0
2	18c	**0° FL**	**Lower body combination**									
			a. Reduced walking speed	Hips	global.posz	Retime	1.1	1	0.9	**0.805026**	0.7	0.6
			b. Reduced cadence	ALL	ALL	Retime All	1.1	1	0.9	**0.805026**	0.7	0.6
			c. Decreased hip (twist)	Hips	local.roty	Swing Magnitude	**1.25**	**1**	**0.75**	**0.5**	**0.25**	**0**
			d. Increased walking base	Heels	local.posx	Offset	-1	0	1	2	3	4
3	16	**0°**	**Increased walking base**									
			a. Increased walking base	Heels	local.posx	Offset	-1	0	1	2	3	4
4	22	**0°**	**Torso (swagger)**									

			a. Increased torso swagger	Chest	local.roty	Swing Magnitude	0.8	1	1.2	1.4	1.6	1.8
5	5	**0°**	**Increased Arm (bob)**									
			a. Increased arm (bob)	Upper Arm	local.rotz	Swing Magnitude	-0.79136	0.104319	1	1.895681	2.791363	3.687044
6	10	**0° FL**	**Reduced Walking Speed/ Cadence**									
			a. Reduced walking speed	Hips	global.posz	Retime	1.1	1	0.9	**0.805026**	0.7	0.6
			b. Reduced cadence	ALL	ALL	Retime All	1.1	1	0.9	**0.805026**	0.7	0.6
7	13	**45°**	**Increased Hip (twist) & Torso (twist)**									
			a. Increased hip (twist)	Hips	local.roty	Swing Magnitude	-0.8	1	2.8	4.644041	6.5	8.3
			b. Increased torso (twist)	Chest	local.rotx	Swing Magnitude	-0.8	1	2.8	4.644041	6.5	8.3
8	11a	**45°**	**Decreased Hip (twist)**									
			a. Decreased hip (twist)	Hips	local.roty	Swing Magnitude	**1.25**	**1**	**0.75**	**0.5**	**0.25**	**0**
9	19	**0° FL**	**Whole body combination**									
			a. Reduced walking speed	Hips	global.posz	Retime	1.1	1	0.9	**0.805026**	0.7	0.6
			b. Reduced cadence	ALL	ALL	Retime All	1.1	1	0.9	**0.805026**	0.7	0.6
			c. Decreased hip (twist)	Hips	local.roty	Swing Magnitude	**1.25**	**1**	**0.75**	**0.5**	**0.25**	**0**
			d. Decreased torso (twist)	Chest	local.rotx	Swing Magnitude	**1.25**	**1**	**0.75**	**0.5**	**0.25**	**0**

			e. Increased walking base	Heels	local.posx	Offset	-1	0	1	2	3	4
			f. Increased arm abduction	Upper Arm	local.rotz	Average Position	-3.19355	0	3.19355	6.3871	9.58065	12.7742
			g. Increased arm (bob)	Upper Arm	local.rotz	Swing Magnitude	0.55	1	1.45	**1.895681**	2.34	2.79
			h. Decreased arm (swing)	Upper Arm	local.roty	Swing Magnitude	1.25	1	0.75	0.5	0.25	0
10	8	**45°**	**Increased Arm Abduction & (swing)**									
			a. Increased arm abduction	Upper Arm	local.rotz	Average Position	-3.19355	0	3.19355	6.3871	9.58065	12.7742
			b. Decreased arm (swing)	Upper Arm	local.roty	Swing Magnitude	1.25	1	0.75	0.5	0.25	0

5.2. Video Design

Whilst the survey design remained largely identical to the first. There were some slight alterations to the video design.

The following parameters were changed from full length walks at 45° to full length walks at 0°. This was because survey participants had noted that they had found it difficult to judge distance, especially with the point light displays.

Table 5-3 - Obese Mesh Survey's Change in Angle of View

Obese Mesh Video Parameters	Changed Angle of View
Lower body combination	0° FL
Reduced Walking Speed/ Cadence	0° FL
Increased Arm Abduction & (swing)	0° FL

The video matrix now featured full mesh characters instead of point-light ones.

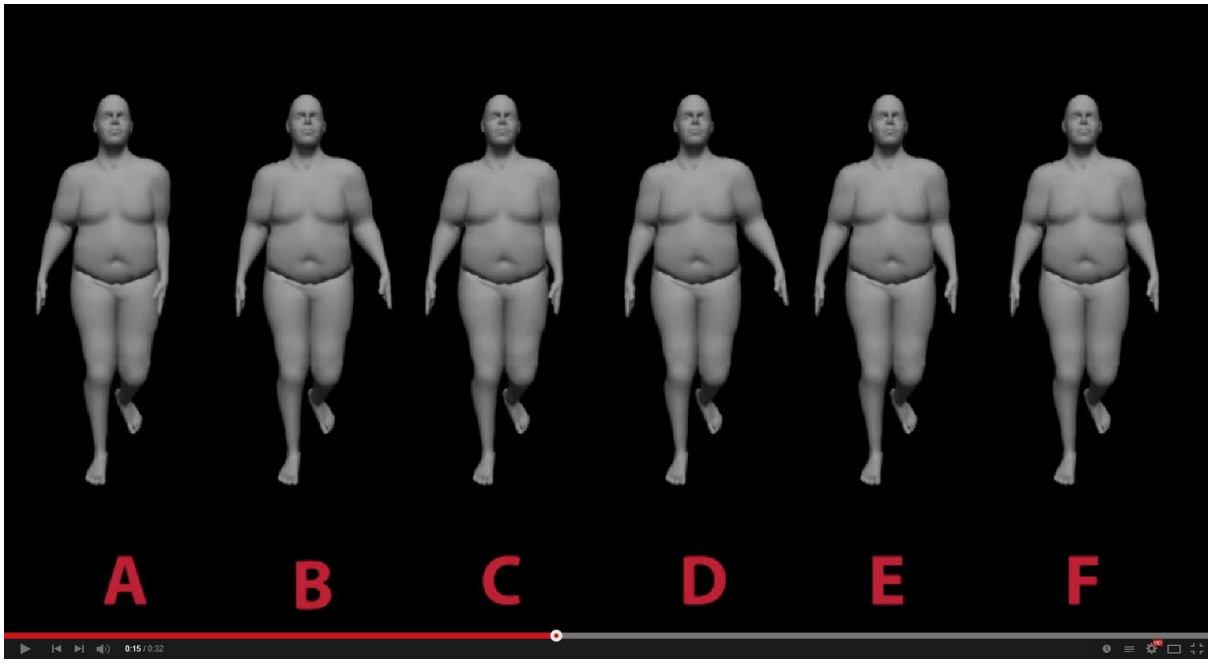

Figure 5-2- Obese mesh walker matrix

5.3. Character Mesh Perceptual Survey Results

The second separate survey was developed and deployed a couple of months after the first survey, and a month after the second round of mocap data collection, from 25/04/14. This was to cover more parameters without fatiguing previous participants with one lengthy survey. It also allowed an iterative approach to testing the first set of parameters by allowing verification of parameters in the following ways:

- The abstracted presentation method of point-light walkers was switched to surface topology, meshed obese characters. This was due to feedback that multiple point-light walkers had appeared confusing and at times looked like a "cloud of points". When testing hip and torso twist, the rotational effect on the two spherical lights was deemed too abstract and subtle. Deformation of surface topology would be more representational.

- Initially arm bob magnitude was tested in combination with average arm abduction position.

  Whilst results were positive, it was deemed important to assess which parameter was more dominant and when separated, assess the weaker parameter's effect in isolation.

- Arm swing magnitude was to be tested in decreasing strength

- Walking speed and upper and whole body combinations were to be retested in survey two from a front on angle so distance travelled in time could be more comparatively judged.

The video survey was promoted through social media and in classes at Teesside University with a £20 voucher incentive. Participants' (*n*=67) mean age was 28.3, thirty who identified as having experience in animation or games development, three identified as having

experience in sports sciences or biomechanics and thirty four who identified themselves as simply members of the public (layman viewers).

The second perceptual survey tested the following motion parameters:

Table 5-4 - Order of Obese Mesh Tests

Survey Order	Video Parameter
1	Upper body combination
2	Lower body combination
3	Increased Walking Base
4	Increased Torso Twist
5	Increased Arm Bob
6	Decreased Walking Speed/ Cadence
7	Increased Hip & Torso Twist
8	Decreased Hip Twist
9	Whole body combination
10	Increased Arm Abduction & decreased Arm Swing

The values for each of these parameters and combinations of parameters can be found in Table 5-2. The results, however, shall be discussed in a more logical order of upper body, lower body then combined parameters as follows.

5.3.1. Increased Arm Bob

It was hypothesized that as body morphology increased, viewers expected arm bob to increase. The results as seen in Figure 5-3 are inconclusive with no apparent trending preference. In Figure 4-7 we saw an upward trend of preference for Increased Arm Abduction and Bob taken from the same front on view of 0°. This indicates that arm abduction is a more dominant motion parameter whilst increased arm bob does not contribute to the perception of increased obese morphology.

5.3.2. Increased Average Arm Abduction & Decreased Arm Swing

It was hypothesized that as body morphology increased, viewers expected average arm abduction to increase and arm swing to decrease, as demonstrated in Figure 4-8. The results as seen in Figure 5-4 appear mixed which indicates a mismatch in the strengths of the two parameters. However, the viewer preference was for the strongest value 'f' which supports the trends presented.

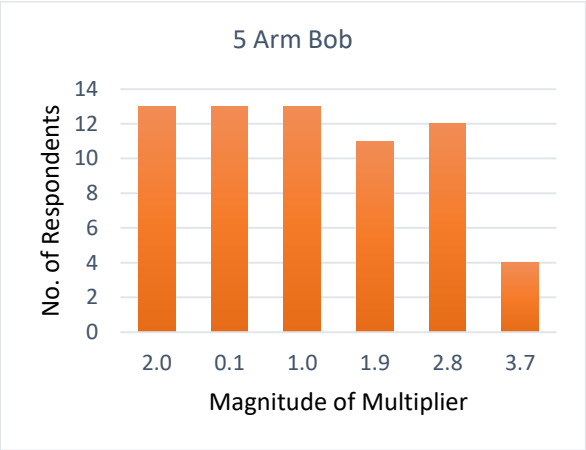

Figure 5-3 Arm Bob obese mesh results

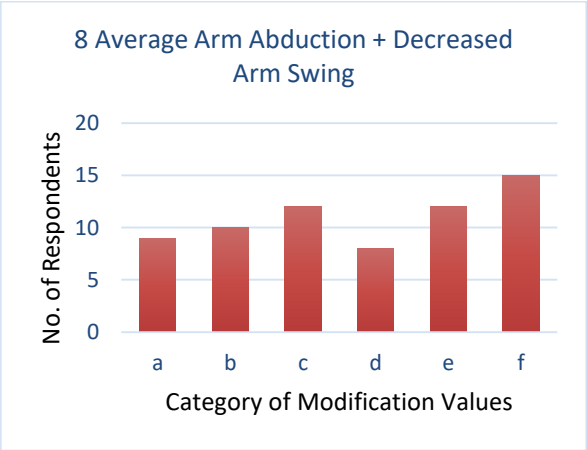

Figure 5-4- Arm Abduction and Arm Swing obese mesh results

5.3.3. Increased torso swagger (thorax lateral rotation)

It was hypothesized that as body morphology increased, viewers expected torso swagger to increase. The results as seen in Figure 5-5 partially support this hypothesis with a preference for exaggerations of 1.6. However, the rest of the selections are approximately equal which suggests this is a perceptually less significant motion parameter.

5.3.4. Increased Hip & Torso Twist

It was hypothesized that as body morphology increased, viewers expected hip and torso twist to increase. The results as seen in Figure 5-6 appear too mixed to support this hypothesis or to indicate a trend in either direction.

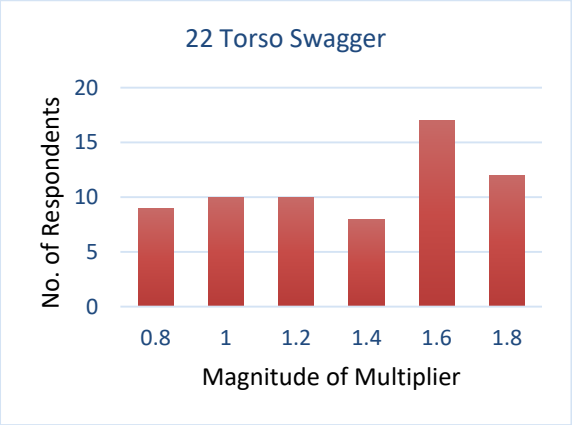

Figure 5-5- Torso Swagger obese mesh result

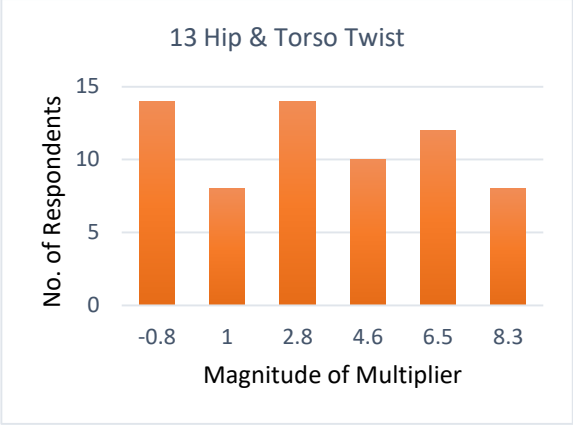

Figure 5-6- Hip and Torso Twist obese mesh results

5.3.5. Upper body combination

It was hypothesized that as body morphology increased, viewers expected decreased hip and torso twist and increased arm abduction, bob and swing to increase. The results as seen in Figure 5-7 significantly support this hypothesis with an upward trend of identification of obese walkers. Looking at the results of previous parameter videos suggests an order of perceptual dominance of: arm abduction, swing, bob, hip and torso twist.

5.3.6. Decreased Hip Twist

It was hypothesized that as body morphology increased, viewers expected hip twist to decrease. The results as seen in Figure 5-8 shows mixed results with increased hip twist having the strongest identification with obese motion.

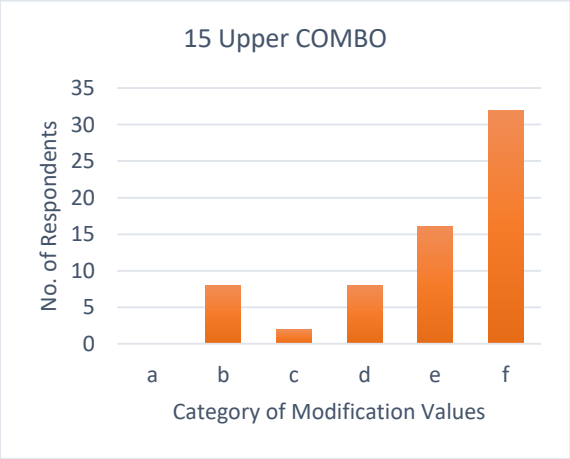

Figure 5-7- Upper Body Combination obese mesh results

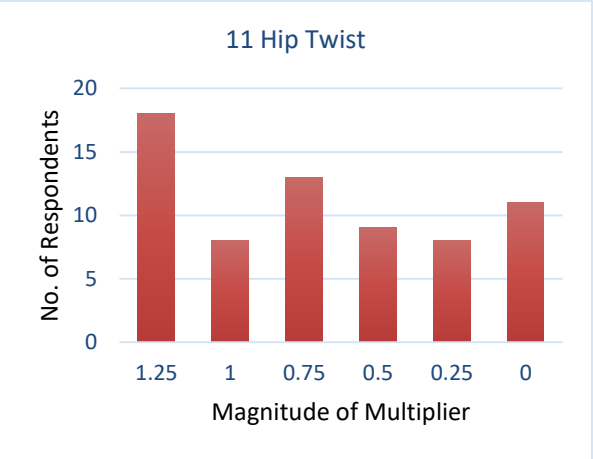

Figure 5-8- Hip Twist obese mesh result

5.3.7. Decreased Walking Speed/ Cadence

It was hypothesized that as body morphology increased, viewers expected preferred walking speed to decrease out of fatigue. The results as seen in Figure 5-9 supports this hypothesis with an upward trend of identification of obese walkers peaking at a slowdown rate of 80%.

5.3.8. Increased Walking Base

It was hypothesized that as body morphology increased, viewers expected walking base to increase to provide a wider and more stable base of support. The results, as seen in Figure 5-10, support this hypothesis with an upward trend of identification of obese walkers with widened walking base. However, values 0 and 2 are reduced in preference.

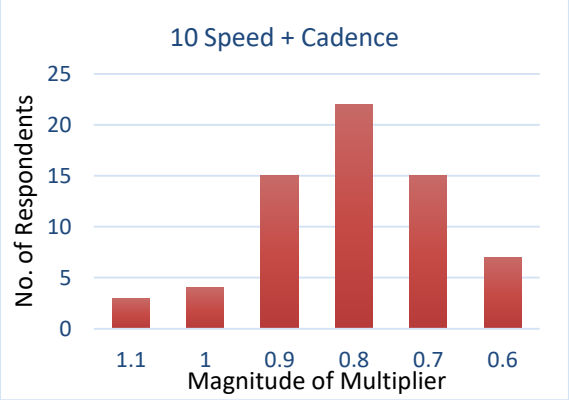

Figure 5-9- Speed and Cadence obese mesh results

Figure 5-10- Walking Base obese mesh results

5.3.9. Lower body combination

It was hypothesized that as body morphology increased, viewers expected walking speed and hip twist to decrease and walking base to increase. The results, as seen in Figure 5-11, appear to support this hypothesis with a significant increasing trend of identification of obese walkers with values at strongest preference peaking at 'D', which follows the results of preferred walking speed, suggesting that this is the more dominant parameter. Increased walking base skewed more results to the 'e' and 'f' values suggesting it as a strong secondary parameter.

5.3.10. Whole body combination

It was hypothesized that as body morphology increased, viewers expected walking speed, hip and torso twist and arm swing to decrease whilst walking base, arm abduction and bob to increase. The results, as seen in Figure 5-12, appear to strongly support this hypothesis with an upward trend of identification of obese walkers.

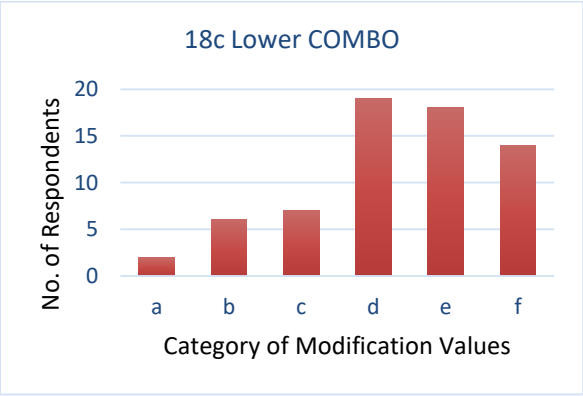

Figure 5-11- Lower Body Combination obese mesh results

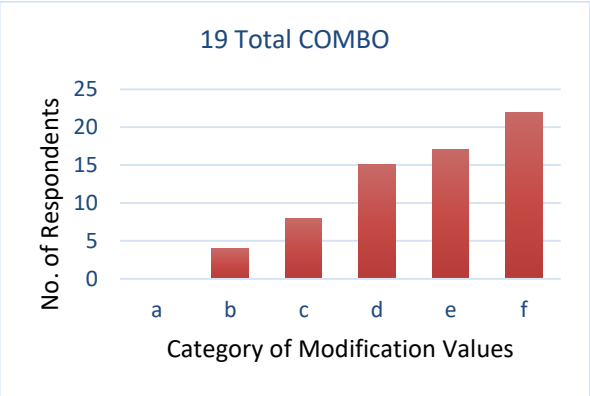

Figure 5-12- Total Combination obese mesh results

5.4. Summary

Following feedback from the point light survey a second character mesh survey was created to test new parameters, and retest previous parameters at different strengths and angles. This two-staged approach reduced visual fatigue and enable the validation of previous trendlines. By the end of this process we then had a set of motion parameters that could be listed by perceptual dominance and compared to the point-light results as well as the actual motion capture results.

6. MOTION CAPTURE GAIT ANALYSIS

Following the two perceptual surveys for expectant changes in motion parameters, an empirical study of real world gaits was undertaken. Before undertaking this, a methodology was carefully devised based upon its requirements, and where possible, justified against comparable published research. Here we shall review a range of metrics, their appropriateness for measuring body shape and how they have been used in existing research. The key questions asked when reviewing each index were:

a) How well does each index represent body shape?
b) How well does each index measure physical people and virtual characters?
c) Is the measurement convenient, accurate or comfortable to measure?

The following sections shall review the different types of anthropometrics and kinematic measurements and summarise their suitability and selection.

6.1. Anthropometrics

Anthropometry is the measurement of physical properties and dimensions of the human body. When trying to assess the level of a person's obesity there have been numerous indices developed to measure and categorise body shapes. Linear anthropometrics are used to measure or predict physical properties of the body. Sometimes this is a direct measurement or an index derived from population data. Linear anthropometrics have been established since Roman times, are quick and easy to measure and there is a huge range of anthropometric tables and recorded population data to take advantage of.

A more recent alternative to linear anthropometry is surface anthropometry. This describes the size and shape of the 3D surface of the body but can also be used to measure internal structures. This type of anthropometry has only recently been made possible with modern technologies such as 3D, MRI, CT, CAT, ultrasound and laser scanners. Whilst more detailed, this approach is costlier and more complex.

The usefulness of each index has improved over time with some being more relevant to different industries such as health insurance, paediatrics, bariatrics, garment fitting, sports

training and surgical procedures. These indices cannot only be judged on their correlations with body shape but also their accuracy and ease of measurement.

For our purposes we shall be looking to record externally perceivable body shapes using the equipment available within Teesside University. We shall summarise some of these metrics as absolute masses, circumferences, ratios, linear anthropometry and surface anthropometry before deciding which are of use to measure body shapes.

6.1.1. Mass

Total Body Weight is actually body mass measured in (kg). This includes adipose tissue, muscles and skeletal mass. Strictly speaking this should be measured without clothing or shoes, however, in practicality it is typically measured with clothing. The average UK adult male weight is 84kg (Welsh Health Survey, 2009). The drawback of solely recording body weight is that it does not take height into account, which is an important perceptual factor when perceiving body shape.

Fat Mass (FM) is the total mass of adipose tissue in the body, measured in (kg). This includes two different classifications of adipose tissue; Visceral Adipose Tissue and Subcutaneous Adipose Tissue.

The following parameters are discussed further in Appendix C:

Visceral Adipose Tissue (VAT) was considered in regards to its relation to Waist Circumference and Waist to Hip Ratio however since it is internal fat it is not visible. **Subcutaneous Adipose Tissue** (SAT) was considered as it is used in skinfold calliper pinches to estimate overall BF%. Whilst it has an effect of the perception of external body fat volume and circumferences, it is challenging to accurately measure. **Fat Free Mass** (FFM) was also considered, however as it is just one component of body morphology it was not used.

6.1.2. Circumferences

Another type of measurement for body shapes relates to circumferences of particular body areas. Circumferences of body areas can represent the volumetric size of characters and are

measurable in real life as well as virtually. The following measurements were considered and expanded in Appendix C:

Hip Circumference (HC) also helps measure central abdominal fatness in (cm). It is measured around the widest portion of the buttocks, with the tape parallel to the floor (WHO, 2011).

Waist circumference (WC) is measured midway between the uppermost border of the iliac crest and the lower border of the rib cage (WHO, 2008 cited in WHO, 2011). WC is a useful metric as it is more effective at predicting abdominal fat than WtHR or BMI. Waist circumference does not take into account height, which can bias people taller or shorter than the national average.

Thigh Circumference (ThC) helps measure lower body shape in (cm). A tape measure is used to measure the midpoint of the thigh. Increased thigh muscles could have a direct effect on gait parameters.

Sum of Five circumferences (CSum) is simply the sum total of the HC, WC, ThC, arm and calf circumference. These expand with, and can loosely represent body volume. Waist, hip and arm/ calf circumferences had the highest associations with whole-body VAT, SAT and skeletal muscle volumes respectively (Heymsfield et al., 2008).

6.1.3. Ratios

Aside from absolute measurements of mass and circumference lengths, there also exist ratios that can measure relative body shape.

Waist-to-Hip Ratio (WtHR) is the ratio of the waist circumference to that of the hips. It is also abbreviated to WHpR or WHR. This ratio provides a useful estimation of the proportion of abdominal or upper-body fat (Kissebah and Krakower, 1994; Björntorp, 1984; Björntorp, 1985). In medical terms this relative representation of body shapes with larger abdominal areas turns out to be a better indicator of cardiovascular diseases than BMI (Dobbelsteyn et al., 2001). Ashwell et al. (2012) also found WtHR to be a more reliable indicator of

cardiovascular disease than BMI or WC and devised a chart of norms as seen in Table 6-1. This is a useful measurement as it can assess body shape independent of height. WtHR has a stronger effect when it comes to the perception of a more attractive female body shape than BMI so it is of perceptual significance (Wetsman and Marlowe, 1999).

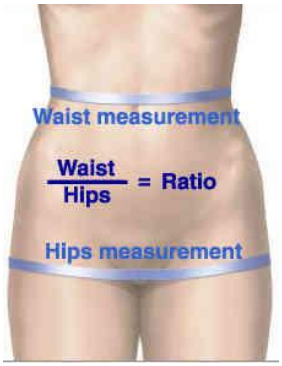

Figure 6-1- Waist-to-hip Ratio (Simon, 2013)

Table 6-1- Waist to Hip Ratio Norms

Waist-to-Hip Ratio (WHR) Norms				
Gender	**Excellent**	**Good**	**Average**	**At Risk**
Males	<0.85	0.85–0.89	0.90–0.95	≥0.95
Females	<0.75	0.75–0.79	0.80–0.86	≥0.86

Waist to Height Ratio (WHtR) is the ratio of the waist circumference to height. This ratio provides a useful estimation of the distribution of body fat over the whole body. It is also useful, as recommended boundaries can be classified independent of age, ethnicity or gender. Ashwell et al. (2012) created a Shape Chart which is expanded in Figure 12-1 in Appendix C alongside the **Waist to Chest Ratio** (WCR).

6.1.4. Linear Anthropometric Indecises

Numerous formulas exist that are meant to represent body shape and create a scale towards ideal body weight. Formulas such as the Quetelet Index (QI) and the Metropolitan Life tables are expanded in Appendix D.

Body Mass Index (BMI) was based on the Quetelet Index , however, it was re-termed BMI in 1972 when it was reviewed in the context of increasing health concerns over obesity (Keys et al., 1972).

$$BMI = Mass / Height^2$$

Equation 3- Body Mass Index

At the time it was found to be the best proxy for body fat percentage and due to its simplicity it overtook the insurance tables as the most popular measurement for body measurement.

Table 6-2 - BMI adult male classifications (WHO, 1995; 2000)

BMI	Classification
Below 18.5	Underweight
18.5–24.9	Normal weight
25.0–29.9	Pre-obesity / Overweight
30.0–34.9	Obesity class I / Obese
35.0–39.9	Obesity class II / Morbidly Obese
Above 40	Obesity class III / Extremely Obese

From BMI BF% can be predicted, using age and sex-specific formulas (Durnin-Womersley, 1974; Deurenberg et al., 1991; Gallagher et al., 1996; Deurenberg-Yap et al., 2000). The formulas are, however, specific to ethnic populations (Deurenberg et al., 1998).

However, a number of problems persist with BMI. Keys et al. (1972) noted that it was more appropriate for population studies and inappropriate for individual evaluation. A study by Deurenberg et al. (2001) found that 8% of all men and 7% of all women were incorrectly classified as obese using standard BMI cutoff points. BMI does not scale well to body frame size meaning people with a small frame but more fat may be classified as normal whereas a person with minimal fat mass but a larger frame may be erroneously classified as overweight. It does not take into account body circumferences to determine classification for a given height. BMI does not take into account the differences between muscle and fat mass, meaning that short bodybuilders will be misclassified as overweight. As it does not provide information on body fat distribution it is also not a great proxy for body shape.

Body Fat Percentage (BF%) is the percentage of fat mass per total body mass. This fat mass includes essential fat and storage fat such as visceral (VAT) and subcutaneous (SAT). As women have sex-specific fat in the breasts, pelvis, hips and thighs, the classifications for body fat ranges differ as seen below in Table 6-3:

Table 6-3 - Recommended Ranges of BF% (Muth, 2009)

Description	Women	Men
Essential fat	10–13%	2–5%
Athletes	14–20%	6–13%
Fitness	21–24%	14–17%
Average	25–31%	18–24%
Obese	32%+	25%+

A minimum level of fat is required to function effectively which is listed as 'Essential fat' in Table 6-3 above. It is noteworthy that higher levels of BF% increases the risk of cardiovascular diseases (Christou et al., 2005). SAT distribution also differs with ethnicity as Wang et al. (1994) observed that Asians had more subcutaneous fat and different fat distributions than Caucasians. There are numerous methods to measure BF% that vary in accuracy, convenience, and comfort. These include Underwater Weighing (UWW), Whole-body Air Displacement Plethysmography (ADP), Dual energy X-ray absorptiometry (DXA), estimation from BMI, estimation from BAI, skinfold testing, bioelectrical impedance analysis (BIA), and height and circumference methods. The first three methods for body fat measurement required facilities that were not available at Teesside University. In some cases a combination a multi-compartment model can be used to avoid systematic bias of each method e.g. measuring FM, FFM, SMM (Baumgartner et al., 1991; Gallagher et al., 1996).

Densitometry is the measurement of body density (mass/volume) and distinguishes FM and FFM on the assumptions that their densities are constant at 0.9kg/l and 1.1 kg/1 respectively. Its accuracy is affected by sex, age and race (Wang et al., 1991).

Both underwater weighing (UWW) and air displacements are methods for densitometry. These, along with Internal Body Composition measuring techniques such as DXA, MRI and CAT scans, are explored further in Appendix C.

6.1.5. Body Shape Scales / Surface Anthropometrics

A variety of indices and scales have been developed over the years to measure and classify body shape, volume and surface. Some of these build upon previous linear anthropometrics by including a third dimension such as hip or waist circumference that better models body shape.

The following anthropometrics were considered and are expanded upon in Appendix C:

- Somatypes (Sheldon et al., 1940)
- Body Build and Posture Scales (Douty, 1968)
- Body I.D. Scale (August and Count, 1981)
- Body Surface Area (BSA) (Boyd, 1935; Dubois and DuBois, 1916; Gehan and George, 1970; Haycock et al., 1978; Mosteller, 1987)
- Volume Height Index (VHI)
- Body Adiposity Index (BAI) (Bergman et al., 2011)
- A Body Shape Index (ABSI) (Krakauer and Krakauer, 2012).
- Body Roundness Index (BRI)
- Body Shape Assessment Scale (BSAS©) (Connell et al., 2006)
- Body Volume Index (BVI) (Tahrani et al., 2008)

6.1.6. Measurements

To measure body shape and composition there are numerous methods we can employ. Dissecting and examining a cadaver is the most accurate method of determining total body composition, however, there are obvious impracticalities.

There are numerous methods to record body weight, however, analogue or digital scales are sufficient. Care must be taken when processing self-reported data as people have a tendency of underreporting their actual weight, waist and hip circumference (Rimm et al., 1990). BMI and height measurement errors are difficult to quantify, but parametric prediction models can be used to address these biases (Stommel and Scheonborn, 2009).

There are cheap and easy techniques to measure linear anthropometrics in-vivo such as BF% using BIA and skinfold calipers. Imaging technologies such as MRI and CT scanners can help us visualise and analyse internal body compositions, whilst BVI scanners can help measure external body shape volumes.

Skinfold testing is a viable option for accurately predicting BF%. It involves pinching the SAT with Skinfold Calipers (Figure 6-2) at seven standardized body landmarks and entering their width (mm) through formulas such (Durnin-Womersley, 1977; Jackson and Pollock, 1985; Siri, 1961; Brožek, 1963).

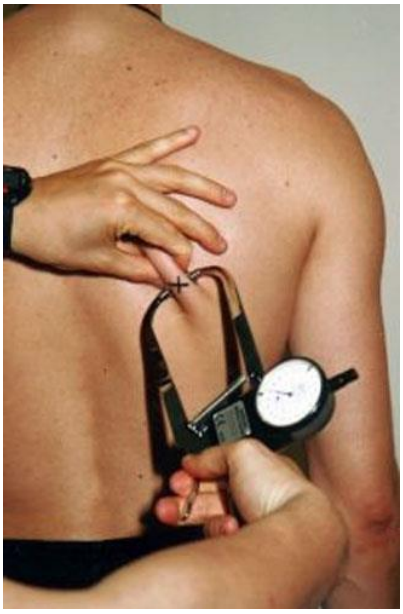

Figure 6-2 - Harpenden Skinfold Calipers (Baty, 2015)

Figure 6-3 - Bioelectrical Impedance machine (Inbody 720, 2014)

However, ISAK training is required to consistently measure accurate readings and in severely obese patients it can become harder to find landmarks and to differentiate between SAT and muscle mass. Skinfold measurements also go through two measurements methods (Durnin and Womersley, 1977; Jackson and Pollock, 1985; Siri, 1961; Brožek, 1963) carrying the cumulative error of both.

Furthermore these formulas are based on population data so that individuals often simply track their skinfold widths as a direct measure of fatness rather than attempting to convert it into BF% estimations. The use of skinfold calipers also requires costly IZAK training for accurate readings as inconsistent compression can affect skinfold measurements (Ward and Anderson, 1993). Skinfold compressibility is affected by water levels at different times of measurement (Becque et al., 1986) and also varies between individuals (Martin et al., 1992). Large measurement errors can be problematic for interpretation (Ulijaszek and Kerr, 1999). In addition, pinching participant's bodies can be embarrassing and it can get more difficult to differentiate between SAT and muscle mass with increasingly large rolls of adipose tissue.

Bioelectrical Impedance Analysis (BIA) predicts an individual's BF% as well as VAT, SAT, WtHR and WC. To achieve this, the meter passes a small, harmless, electric current through the body and measures the resistance (NIH, 1994). It then calculates an approximate value taking into account the person's weight, height, age, and sex. The calculation measures the total volume of water in the body (lean tissue and muscle contain a higher percentage of water than fat), and estimates the percentage of fat by understanding the density of body tissue masses. BIA machines (Figure 6-3) can provide a convenient, automated estimation of BF% and a variety of other body composition parameters. It also minimises the discomfort of disrobing or physical contact with the examiner.

Yet, its estimations are based off population data and the accuracy can vary depending upon how much liquids have been consumed. A study by Deurenberg et al. (2001) found that 5% of all men and 4% of all women were incorrectly classified as obese, however, this is an improvement upon BMI's error rates.

6.1.7. Summary

The following table of metrics categorises the availability of resources to measure them, whether the metrics can be applied to virtual characters, pros and cons as well as how well they represent body shape.

Table 6-4- Table of Body Shape Metrics and Suitability for Modelling

Metric	**Available**	**Virtual**	**Advantages/ Disadvantages**
Mass	Yes	No	Simple but no differentiation between FM & FFM. Can't measure/ model virtually.
Hip Circumference	Yes	Yes	Direct measurement of lower body shape. Doesn't represent shape of abdominal obesity.
Waist Circumference	Yes	Yes	Direct measurement of abdominal adiposity. Only a single metric representing upper body.
Thigh Circumference	Yes	Yes	Direct measurement of upper limb. Only a single metric representing lower body.
CSum	Yes	Yes	Sum value could be considered volumetric but without definition of body parts.
Waist-to-Hip Ratio (WtHR)	Yes	Yes	Abdominal obesity shape independent of height. Stronger perception of female attractiveness than BMI.
Waist-to-Height Ratio (WHtR) / Ashwell Chart	Yes	Yes	Abdominal obesity shape estimates distribution over height. Shape categories not validated.
Waist-to-Chest Ratio (WCR)	Yes	Yes	Estimates upper body/ torso shape. Stronger perception of male attractiveness than BMI or WtHR.
Metropolitan Life Insurance Tables	Yes	No	Sourced from large but specific sample population. No longer used as frame size too difficult to measure.
BMI	Yes	No	Simple. But doesn't differentiate frame size, SMM & FMM. Doesn't indicate shape or distribution. Virtual shape requires estimation.
Body Fat Percentage	Yes	Yes	Distinguishes between FM and FFM. Doesn't indicate shape or distribution of fat or muscle tissue. Virtual shape requires estimation.

Body Surface Area (BSA)	Yes	Yes	Simpler than measuring volume. Physical calculation estimated on weight.
Volume Height Index (VHI)	No	Yes	More related to shape than weight based indices Physical measurement requires water displacement.
Body Adiposity Index (BAI)	Yes	Yes	Estimates body fat using HC & Height.
A Body Shape Index (ABSI)	Yes	No	Like BMI but takes WC into account as a representation of body fat and shape.
Body Roundness Index (BRI)	Yes	Yes?	Estimates body shape using height, WC & HC
BSAS	No	No	Estimates body shape on multi parameter scale Not available.
Body Volume Index (BVI)	No	No	Automatically measures and assesses body shape and volume. Not available.

To decide which indices to use in the research project, it was necessary to review them against the initial stated criteria:

a) How well does each index represent body shape?
b) How well does each index measure physical people and virtual characters?
c) Is the measurement convenient, accurate or comfortable to measure?

Linear anthropometrics can't usually measure or model body surface or shape geometry, however, they are the easiest to record and can rely on a large range of published data for comparison. These anthropometrics include Mass, Height, BMI and BF%. Measuring mass alone cannot differentiate between FM and SMM, nor can it represent body shape distribution, however, when combined with height it can provide BMI, which is not a perfect representation of body fat or shape but it is supported by a large body of published data. BF% is a better representation of FM than BMI, however, it still does not provide the clearest definition on body shape distribution. Whilst a variety of methods for estimating BF% are available, skinfold callipers and U.S Naval equations are too inaccurate whilst most densitometry methods are too costly or inaccessible. BIA is the most suitable method to

easily, consistently and automatically acquire BF% data. It also has the benefit of providing a range of other body composition data such as FM, FFM, SMM and others.

If our primary criteria is to utilise indices that represent body shapes then CSum, WtHR, WHtR, WCR, BSA, VHI, ABSI, BRI, BSAS, BVI all take into account more than one dimension to measure anthropometrics such as height, surface or volume.

CSum is easy to measure and could represent body shape, however, the five circumferences are summed and lose their individual measurements. A more defined model would combine all five circumferences into separate virtual cylinders with the height measurement.

WtHR is easy to measure and can represent abdominal adiposity, which is a prominent feature of obese body shape but does not take height into consideration. WHtR is easier to measure and does takes height into consideration, which is a dimension that can alter the perception of body shape, when only looking at one index such as waist circumference. In some ways BRI combines these three measurements of WC, HC and Height into a somewhat elliptical based metric. However, no other supportive studies have utilised this metric.

WCR is easy to measure but not commonly tracked in literature which makes early analysis of published data much more difficult.

BSA is analogous to a volumetric measurement, however, it cannot differentiate body composition or distribution and it would require uncomfortable water displacement. VHI would be a more direct measurement of volume but would still not measure adipose distribution and would also require uncomfortable water displacement or inaccurate volume estimation.

BAI estimates body fat using HC and Height, however, it has been challenged as not being as representative as BMI (Freedman et al., 2012). Body fat can be more directly measured physically.

ABSI is a body shape index that takes into account WC, Height. However, as virtual characters have no discernible mass this would be difficult to apply. BSAS and BVI are also direct measurements of body shape, however, their body scanning hardware is not readily available.

The following anthropometrics shall therefore be recorded:

1. Five Circumferences
2. Mass
3. Height
4. BMI
5. HC
6. WC
7. WtHR
8. BF%

With the capability to analyse the additional parameters if needed:

- CSum
- WHtR
- WCR
- BSA
- BAI
- ABSI
- BRI

6.2. Gait Parameters

Gait is a series of rhythmical, alternating movements of the trunk and limbs resulting in the forward movement of the centre of gravity and body. Walking is also described as a series of controlled falls (Rosenbaum, 2009)

Gait analysis is often used for identifications of health related abnormalities. In our instance we shall measure aspects of gait that change over variations in body shape. To do this we must understand the components of gait and select those that shall most perceptibly change and can be modified on virtual characters. The key questions asked when reviewing each parameter were:

- How perceivable is each parameter when altered?
- How accurately can each parameter be measured using the techniques available?
- How effectively can each parameter be modified on virtual characters?

The following sections shall review the different types of gait parameters. In section 3.1 we review the published research on the parameter changes over increases in obesity.

Gait parameters can be classified as either spatial or temporal which are expanded upon below.

6.2.1 Spatial Parameters /Distance Variables

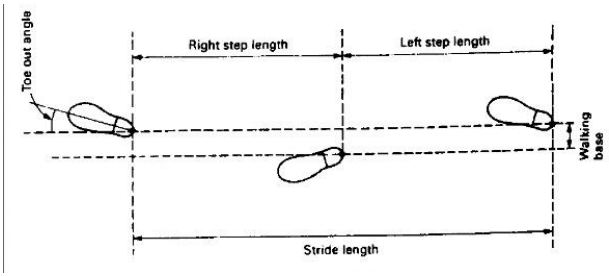

Figure 6-4- Distance Variables (Kaur, 2014)

Step Length is the distance between the point of initial contact of one foot and the point of initial contact of the opposite foot. In normal gait, right and left step lengths are similar.

Stride Length is the distance between successive points of initial contact of the same foot. Right and left stride lengths are normally equal. Step length and stride length are both related to each other and show the positional differences of the feet, which are easily measured using motion capture. Changes in step length and steps per minute produce a change in walking speed which is perceptibly significant (Pražák et al., 2010) These parameters are not easily modified on densely keyed motion captured characters, however, it is possible by replacing the lower body with an IK rig.

Walking Base or Step Width is the sum of the perpendicular distances from the points of initial contact of the right and left feet to the line of forward progression. This is easily measured using the spatial differences between the feet and if the virtual character's lower body has been replaced with IK legs it would be simple to offset their positions. The perception of changes to walking base would be more apparent from the front than the side

Foot Progression or toe out describes an angle between the line of progression and a line drawn between the midpoints of the calcaneus and the second metatarsal head. This can be measured using motion capture and modified by rotating the virtual character's heel, however, the perception of changes to foot progression may be limited due to the small degrees of change and limited effect on the rest of the body.

6.2.2 Temporal Parameters /Time Variables

Velocity (speed) the product of cadence and step length, is expressed in units of distance per time (m/s). As instantaneous velocity varies during locomotion we use an average velocity. Recording speed physically would involve measuring the positional movement of

the hips over time. Modifying velocity could be achieved by time warping the entire walking clip to alter forward movement and cadence, otherwise footskating would occur.

Cadence or walking rate is calculated in steps per minute. This can be measured physically by counting the number of steps per captured walking time. To modify this virtually would simply require time warping the walking clip so that cadence and velocity are both altered.

Stance Time is the amount of time taken during the stance phase of a gait cycle (a single stride) including single support and double support. Typically the stance phase takes 60% of the time whilst the swing phase takes 40% of the time. As walking speed decreases, percentage of time spent in the stance phase increases (Sarmini, 2005) which could provide the impression of a plodding walking style.

Swing Time is the amount of time taken during the pendulum-like swing phase of a gait cycle (Sarmini, 2005). It is possible to measure the stance and swing time by counting the duration between heel strike and toe-off. It would also be possible to apply these phase time modifications to the feet of a virtual character, however, without modelling changes to forward hip movement, locomotion could appear staggered.

Step Time is the amount of time spent during a single step; between the heel strike of one leg and the heel strike of the contra-lateral leg (Essa, 2012). Assuming normal gait, the step time for left and right legs should be equal.

Stride Time is the amount of time taken to complete one gait cycle (Essa, 2012). Step time and stride time are easily measured and can be applied to virtual characters, however, they are actually expressions of speed and stride length.

6.2.3 Determinants of Gait

The following spatial variables interact dynamically to have an effect on the displacement of the centre of mass (COM). Movement of COM beyond a normal range increases energy expenditure (Saunders et al., 1953).

- **Pelvic Rotation** in the transverse plane is when the pelvis rotates forwards on the swing side whilst rotating backwards on the stance side.

- **Lateral Pelvic Tilt** in the frontal plane is when one side of the pelvis is elevated higher than the other
- **Lateral Pelvic Displacement** is the horizontal shift of the pelvis.
- **Knee Flexion** during mid-stance is the angle between the lower leg to the back of the thigh.
- **Knee range of motion** is the range in degrees from full extension to full flexion

Pelvic movement can be captured physically using motion capture and modified virtually, however, the degrees of movement may be too subtle to be perceived.

Knee flexion and range of motion can be measured physically but modifying it virtually can produce foot skating. Controlling knee flexion directly may also conflict with stride length modifications, which would require a replacement IK lower body rig which would preclude direct control of the knee joints.

6.2.4 Additional Gait Parameters

The ankle is subject to the weight of the entire body and the force impact with the ground. The joint is constantly moved through mechanical extremes during gait and it is essential for walking on any surface.

Ankle Plantar Flexion is when the foot points downward.

Ankle range of motion is typically 0-50° flexion and 0-20° dorsiflexion (upwards)

Ankle flexion is a relatively smaller joint rotation which only affects the relative rotation of the toes so modification of its movement on a virtual character, whilst possible, may have minimal perceptual effect.

In addition to lower body gait parameters there are a range of upper body gait parameters less commonly recorded. 2/3 of the body mass in the head, arms and trunk (HAT) is located 2/3 of the body height above the ground which makes maintaining a balance with the COG challenging (Winter et al., 1990).

The lower spine section, lumbar, bears the weight of the body whilst the upper spine, thoracic, holds the rib cage and has a lower range of motion.

De Souza et al. (2005b) observed that spinal posture was altered in obese patients, however, their study observed patients standing still.

6.2.5 Summary

Most gait parameters are measurable using the motion capture technology available with the possible exception of spinal curvature. Therefore we shall build our choice of gait parameters on those previously studied to change over increases in obesity as seen in section 3.1. Velocity, cadence and stride length are all essential components of walking speed. Knee flexion shall not be explored as this would cause foot skating and the use of IK legs would remove direct control. Hip movement shall also be tested to verify how perceivable its motion modifications are. Ankle rotation shall not be modified as its movements would be too small and subtle to notice. Spinal curvature shall be explored with some caution due to the constraints of the motion capture equipment. Finally arm abduction, swing and abducting bob shall also be tested as they represent perceptually large upper body movements that have not yet been tracked over increases in body shape.

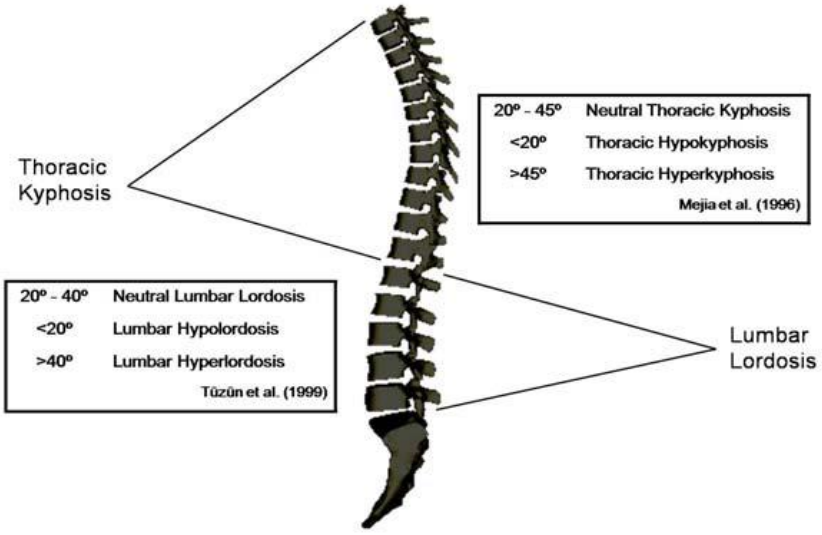

Figure 6-5- Angle references for thoracic kyphosis and lumbar lordosis (Muyor et al., 2011)

Measuring trunk motion can prove complex as the spine is comprised of 33 vertebrae bones typically in an S shape, as seen in Figure 6-5. Spinal curvature is difficult to measure physically as motion capture suits will stretch taut over spinal curvature gaps making it difficult to measure. To apply it to virtual characters would also need to take into account the counteracting relationship with hip movements.

Upper body limbs, like arms, can swing under the influence of gravity with or without muscle assistance. Whilst leg swings are prevented from swinging backwards by footstrike, arms are not.

Arm swing is the combination of shoulder extension and flexion. It is the motion that each arm swings with the motion of the opposing leg. The pendulum-like motion of arm swings is not essential for walking, but can improve the stability and energy efficiency in human locomotion. These variables can vary over increases in body mass. Changes in arm swing range of motion can be measured using motion capture and modified on virtual characters. The range of movement in arm swing from the rotating shoulder down to the tips of the fingers can be as large as some people's leg swings so it is arguable that this could have a large effect on perception of motion changes.

Arm abduction is the angle at which the arms are raised from the side of the body in the plane of the torso. Arm abduction could raise with increased adipose or muscle tissue in upper arms or torso. This parameter can be measured physically and can be modified easily on virtual characters. It could also have a significant perceptual effect on changes in motion.

6.3. Motion Capture Methodology

The motion capture sessions were promoted through social media channels such as Twitter and Facebook. Twenty-eight male volunteers without gait related health problems or pacemakers were recruited, mostly from Teesside University. Participants were sent an information guide and consent form to read which explained the project, the process and benefit. Both documents are available to read in Appendix A and B. Upon arrival participants would be shown the facility, talked through the procedure, and it would be checked that they had read the information guide and given signed consent. A final check would be made on whether participants had any remaining questions or health issues.

The motion capture session was comprised of two sections that tackle the core of this thesis; appearance capture and motion capture.

6.3.1. Appearance Capture

The appearance capture took place in Teesside University's Olympia Building, within the Physiology Lab which contained the required equipment.

There are multiple options to select for when trying to accurately capture body morphology such as body scanning (Wang et al.2006; Tahrani et al., 2008), hydrostatic weighing (Siri, 1961), BMI (Keys et al., 1972), BVI (Tahrani et al., 2008) and Body Fat Percentage. Body scanning was considered, however, the topology of the scanned mesh was considered to be too high density and disorganized to be useful for modelling or automated anthropometric measurements. Using the Konica Minolta Vi-700's field of view only permitted scanning half a body at a time which proved insufficient.

The hydrostatic weighing method measures a participant's mass, however, this would require them to undress and immerse themselves in water which many (especially obese participants) would find embarrassing. There are only limited facilities in the UK that house water displacement units and Teesside University does not currently have one.

A combination of appearance capture methods was chosen. Ten appearance measurements were recorded. Sports science technicians in Teesside University's School of Health advised on measurement techniques.

Height was recorded using a wall-mounted height rod as this measurement was necessary to calculate BMI. Participants were instructed to stand straight against a wall and to take a breath before the height was recorded.

Weight and body fat percentage was recorded without jackets or shoes using the InBody 720 scales. The typical procedure involved cleaning the plates with sterilizing wipes, asking the participant to remove their socks, stand on the floor plate and grip the handles whilst their details were entered. The participants were then asked to stand still for a minute with their arms slightly away from their body, so as not to interrupt the path of the electrical flow, and to maintain a steady balance.

The InBody 720 machine was assessed by Ogawa et al. (2011) and found to a more convenient substitute for Computed Tomography with significantly correlated results (R = 0.759). Alternative methods to measuring body fat percentage included the U.S. Naval tape measure method (Hodgdon and Beckett, 1984), were tested, but were deemed to be too inaccurate. However, height, neck, waist and hip circumference were measured on all participants so future analysis could compare the differences in methods.

Skinfold testing is a popular method for measuring body fat percentage, and was initially tested. However, this was ultimately rejected for a number of reasons. The primary assessor was not ISAK accredited to measure skinfolds to a high enough level of precision. The accuracy of skinfold measurements also becomes more difficult to accurately measure as adipose deposits increase with obesity. Early feedback with skin calliper measurements also noted that participants felt that the method may be too intrusive or embarrassing for others.

The bio-electrical impedance method is safe, non-invasive and easy to use (Houtkooper et al., 1986), however, readings can vary depending on hydration levels (Lukaski et al., 1986), meal consumption (Slinde and Rossander-Hulthen, 1986) and exercise (Kushner et al, 1986). Ultimately this method was considered to have the most suitable balance of accuracy, consistency, ease of use and non-invasiveness. The bio-electrical impedance meter used was the InBody 720 machine seen in Figure 6-6:

Figure 6-6 – InBody 720 Body Composition Analyser

Figure 6-7- InBody 720 Body Composition Report

Following the measurement participants received a free Body Composition Report seen in Figure 6-7 which they were recommended to take to a personal trainer or qualified health practitioner if they wished to improve their fitness and health. The report also displays a wide range of interesting but extraneous data such as Skeleton Muscle Mass and Visceral Fat. This study relates to the external appearance parameters that are perceptually viewable. Analysing changes to motion based on skeletal muscle mass and visceral fat data, whilst of value, could not be applied to virtual characters with only surface topology modelling.

The final set of anthropometric measurements taken were body circumferences. The circumferences represent the major limbs, some of which correspond to measurements taken using the U.S. Naval method (Hodgdon and Beckett, 1984) and U.S. Army (2011) for estimating body fat composition. This is a useful combination of measurements to take as they are a simplified volumetric measurement. They are quicker, easier and cheaper to take than a 3D volumetric laser scan. The same circumference measurements can also be taken from virtual characters.

They were recorded using a Myotape Body Tape with measurement guidance from ISAK accredited sports science technicians, and consistently measured by the same assessor, Satish Shewhorak, on the right side of participants' relaxed bodies. Circumference metrics and landmarks are listed in Table 6-5 below:

Table 6-5 - Circumference metrics and landmarks

	Anthropometric Girth	Landmark
1	Neck	Across laryngeal prominence (Adam's apple)
2	Chest	Across nipples
3	Bicep/ arm girth relaxed	50% between elbow and shoulder cliff
4	Waist/ Abdomen	Across navel
5	Hips	Across deepest gluteal girth
6	Thigh	50% between hips and knee
7	Calf	Largest girth of the calf

6.3.2. Motion Capture

Once all appearance measurements had been taken participants moved onto the motion capture phase. The motion capture session took place in the Biomechanics Lab, close to the previously used Physiology Lab, which featured six MX13 Vicon cameras in a capture volume with the following settings (mm):

-3500, -3500, -100 (min vector x,y,z)

3500, 3500, 3000 (min vector x,y,z)

Participants were asked to change, using the fitting area, into a black compression suit. The suit came in three sizes; small, medium and large, with most lean participants using the largest suit. Elasticated material bands with prefixed markers were also strapped around the wrists and head. Thirty five optic markers were positioned on the body following the Validated Vicon Marker Set as seen in Figure 6-8. This marker set was selected as it had been validated by biomechanics as a suitable configuration to model full body gait to a research standard (Kadaba et al., 1990; Winter et al., 1990; Davis et al., 1991). As it is commonly used in other published biomechanical research papers, this makes the results easy to compare and replicate.

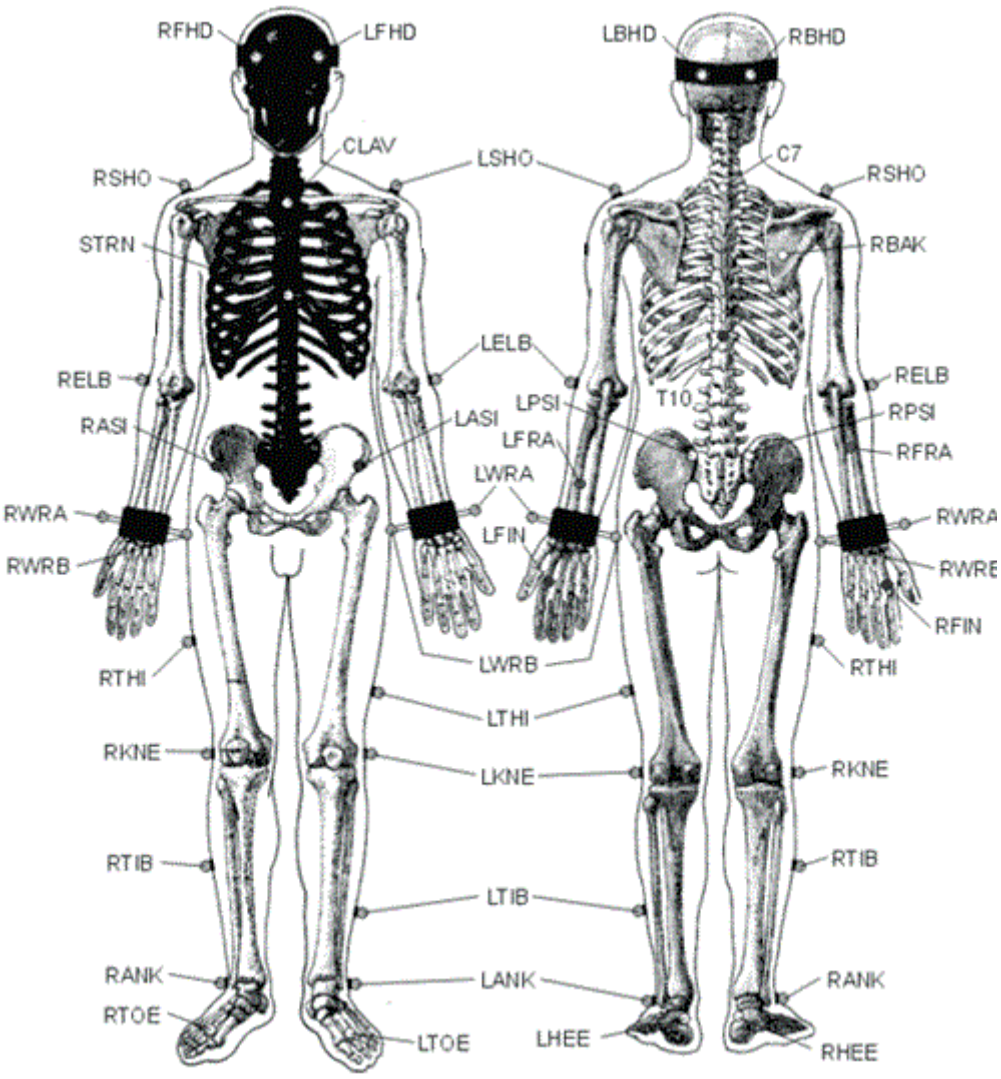

Figure 6-8- Validated Vicon Marker Set

The optic markers with Velcro bases were attached to the compression suit using bony landmarks as reference as seen in Figure 6-8. Markers were attached to the base of the fingers and the outside of the shoes using double sided tape. Participants were motion captured wearing shoes as most people viewed in a real or virtual crowd would be expected to be wearing shoes and this could affect their gait. Larger participants who could not fit the compression suit top were requested to wear their own tight fitting t-shirt and optic markers were attached using double sided tape. Climbing harnesses and tape across the upper body were tested to minimise marker movement on clothing, however, these methods proved restrictive and uncomfortable to participants. These methods produced unnatural movements so were abandoned in favour of adhesive marker placement on t-shirts and skin.

Figure 6-9- Motion Capture T-Pose

A series of calibration tests were needed for each session. This included a room calibration using an L-Frame to calculate the inclination of the floor against the position of the cameras. The cameras and volume were also calibrated using the 3-Marker wand (240mm). Error rates were recorded for participants and camera calibrations were repeated and adjusted until they fell below 0.18 which is considered by Vicon to be an acceptable level of error suitable to research purposes. Finally the participant held a T-pose as seen above in Figure 6-9 to take a single frame static calibration to aid the system in marker recognition.

The rigidity and adhesion of the optic markers was rechecked after the static calibration phase and after each take. Participants were asked to take part in a Range of Motion test which would help verify the orientation of the bones. They were asked to hold a T-pose, then rotate their right arm in two axes, their right torso in two axes and their right upper leg in two axes.

Before participants were recorded walking they were asked to start walking back and forth along the centre of the capture volume at a preferred walking speed until they were comfortable. This was to acclimatise participants to walk in a natural style of gait along the central line and to ensure the attached optic markers were secure.

Participants were then asked to walk at five different self-selected speeds:

1. Slowest natural speed
2. Slower than preferred walking speed
3. Preferred walking speed
4. Faster than preferred walking speed
5. Fastest natural walking speed

Each speed was recorded at least two times to ensure alternate takes were available if there were unforeseen problems or marker occlusions that could not be filled.

Finally, all participants were asked to walk at a fixed speed of 1.2m/s. This was achieved by marking out a distance of 7m and asking participants to hit the end marker on 5.83 seconds. They were then allowed several practise attempts with a timer on a large screen to help them get the pacing right. Once they had achieved a natural walk at the required speed, the timer was removed so there was some deviation in the speed around the 1.2m/s. For this reason two to four walks were captured so that the speed closest to 1.2m/s could be selected.

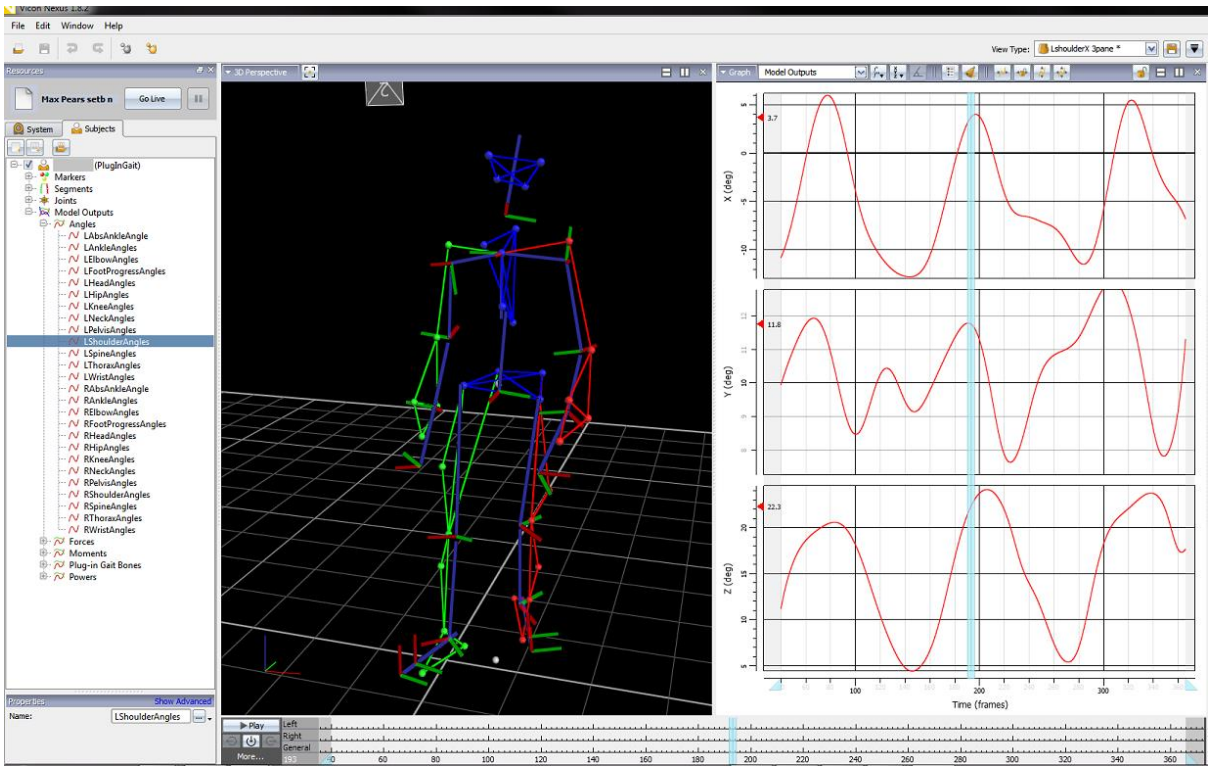

Figure 6-10- Vicon Nexus cleanup processs

Vicon's Nexus 1.8.5 software was used to cleanup each walk clip's data. This involved manually retagging any markers that had been incorrectly identified e.g. the system often disorientated the hand so the left [LWRI] and right [RWRI] markers might need swapping around.

The other cleanup requirement was gap filling, typically caused by marker occlusion e.g. hand markers passing past hip markers. For small gaps of one to three frames a linear join could be used but for longer gaps a spline filling may be considered to be smoother or more accurate.

6.3.3. Limitations and Assumptions

This study primarily focuses on appearance and motion relationships in males as female gait differs significantly with wider hips and shoulders (Kozlowski and Cutting, 1977). Five females volunteered and completed the appearance and motion capture sessions, however, the sample group was not considered large enough to be of useful analysis.

Whilst male participants ranged in weight between 59.1 - 115kg there were only eight who would be classified as obese on the BMI scale, seven classified as obese on the BF% scaler or

five who would be classified ‘at risk’ on the WtHR scale. This was due to recruitment largely taking place from a presumably fit and active student population. However, this also reduced the range in ages to 19-62.

Body Mass Index was recorded but there are known problems with this measurement as it does not differentiate between fat and muscle mass e.g. short but muscular people can be incorrectly classified as obese.

Body Fat Percentage was therefore recorded but it does not take height into account, which is an influential perceptual parameter. It also takes internal visceral fat and edema levels into account, which are not externally perceivable.

The motion capture walks were recorded at preset speeds by using a timed bleep to accustom participants to hit a mark within the time limit. It was assumed that gauging timing by asking participants to watch an onscreen clock could cause a small amount of anxiety that could affect gait, whilst following another person walking at the correct speed would encourage mimicry in gait style. Therefore we assume that our method of practising to hit a distance at a timed beep was the least abnormal.

The compression suit for the motion capture procedure was suitable for most lean people, however, for more overweight participants we had to switch to adhering markers to their clothing. We assume that the improved comfort created less abnormality of gait than increased marker movement due to looser clothing.

6.4. Range of Motion Capture Data

Once both perceptual video surveys had been deployed, real world data capture was needed to understand the correlations between body morphology parameters and motion parameters.

An initial batch of motion capture data was collected, before any perceptual surveys were conducted, between 28/03/13 and 23/05/13. A second round of motion capture was then collected after the point-light perceptual survey had been deployed, between 10/03/14 and 16/04/14.

Local participants were attracted through social media and from Teesside University but no monetary incentive was offered, however, an anthropometric feedback report and their personal motion capture data was available upon request.

When collecting data to determine a reliable regression model between anthropometric and motion parameters, as large a sample size as possible would be preferable.

A common rule of thumb is 10-15 cases of data per predictor, so for 5 anthropometric variables 50-75 would be a target sample size. However, Green (1991) recommends when testing the overall fit of our regression model:

$$\textit{Minimum sample size} = 50 + (8 * \textit{no. of predictors})$$

Equation 4 - Green's Minimum Sample Size for Overall Fit (1991)

Or when testing individual predictors within the model (*b*-values):

$$\textit{Minimum sample size} = 104 + \textit{no. of predictors}$$

Equation 5 - Green's Minimum Sample Size for Individual Predictor's (1991)

Which would require a sample size of 90 or 109. As we're interested in both uses, Green recommends using the largest value (109).

However, when compared to related studies the typical sample size is much lower than 75 or 109.

Table 6-6 - Comparison of Sample Sizes in Related Studies

Source	Sample Size n
Browning and Kram (2007)	20
DeVita and Hortobágyi, (2003)	39
Hulens et al. (2003)	218
McGraw et al. (2000)	20
da Silva-Hamu et al. (2013)	48
de Souza (2005a)	34
Spyropoulos et al. (1991)	21
Tompkins et al. (2008)	30
Vismara et al. (2007)	34
Troje (2002)* *males*	20
Lai et al. (2008)	14
Pataky et al. (2014)	46
Sarkar et al. (2011)	30
Wu et al. (2012)	10
Vartiainen et al. (2012)	13

By comparing fifteen related publications in Table 6-6 we can estimate a mean sample size (*n*=40). However, as Hulens et al. (2003) used a significantly larger samples size we can also consider the median sample size (*n*=30).

However, due to the sensitivity of obese participants and the lengthy time it took to recruit, measure and analyse appearance and locomotion, a slightly smaller sample size of participants (*n*=28) was obtained and are reported for exploratory purposes to validate existing research and guide further research.

n=28 participants were recruited providing a range of 59 - 115kg in body **mass** measurements.

The mean body mass of the twenty-one participants was 86.4kg against the UK male bodyweight of 84kg (Welsh Health Survey, 2009).

n=28 Participants ranged between 1.65 - 1.91m in **height**. The mean height of the participants was 1.8m against the average UK male height of 1.77m (Moody, 2013).

n= 26 participants ranged between 0.8 – 1.06 in **waist-to-hip ratio** when recorded**.** The mean waist-to-hip ratio of the participants was 0.89 against the recommended mean of 0.93.

n= 28 participants ranged between 19.3 – 33.8 in **body mass index**. The mean BMI of the twenty-one participants was 26.7 against the average UK male BMI of 21.7 (Moody, 2013).

n= 28 participants range between 5.8 – 37.3% in **body fat percentage**. The mean body fat percentage of the participants was 23.8% against the recommended male body fat percentage of 21% (WHO, 1995; 2000).

6.5. Motion Capture Results

For each motion capture participant, five walking clips at different speeds were captured, cleaned up and exported in Vicon Nexus software as described in the previous sections.

Each participant's exported data was collected into anonymised, individual spreadsheets containing multiple tabs of data. The anthropometric data was stored in the first tab, and then the positional and rotational data for each walk clip was also contained in subsequent tabs.

The LASI:Y positional data was used to calculate each walks average speed by dividing the waists distance travelled over time. Primarily the preferred walking speed was verified to check how close to the control speed of 1.2m/s they were. Variations in speed of 0.1m/s were considered acceptable.

By analysing the positional and rotational data from each participant's 1.2m/s walks, a number of motion parameters could be analysed and compared against the anthropometric measurements.

SPSS was used for linear regression analysis and all results presented had passed the five assumptions needed for them to provide valid predictions:

1. A linear relationship between the two variables (or transformed to linearity).
2. No significant outliers or influential points.
3. Independence of errors (residuals).
4. Homoscedasticity of residuals (equal error variances).
5. Errors (residuals) are normally distributed.

6.5.1. Average Arm Abduction Position

Arm abduction occurs when the arms are held at the sides, parallel to the length of the torso, and then raised sideways. In the real world the angle of arm abduction would be measured using a universal goniometer and a standing, stabilized participant. To measure arm abduction position during locomotion, the average position had to be calculated from the motion captures output for the LShoulderAngles:Y rotational data over the length of the walk clip. It is hypothesized that Average Arm Abduction raises over increases in anthropometric parameters.

Figure 6-11 shows average arm abduction visualised against increases in body fat percentage. Linear regression (r^2 = 0.33) indicates the body fat percentage has a medium effect (Cohen, 1988; 1992) on the average arm abduction position. Figure 6-12 shows average arm abduction visualised against increases in bicep circumference. Linear regression (r^2 = 0.36) indicates the bicep circumference has a medium effect on the average arm abduction position.

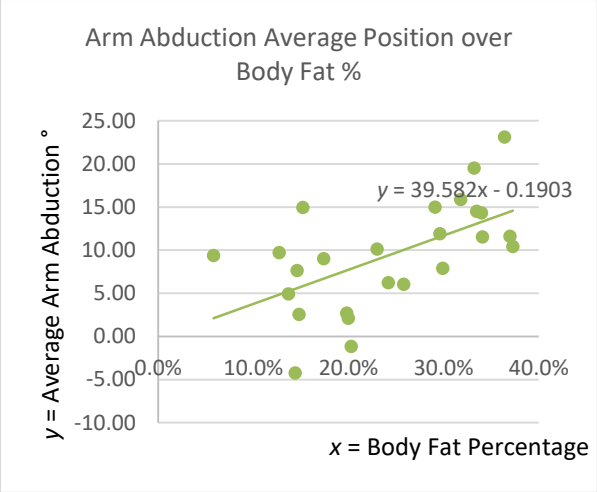

Figure 6-11- Increase of Arm Abduction over Body Fat Percentage

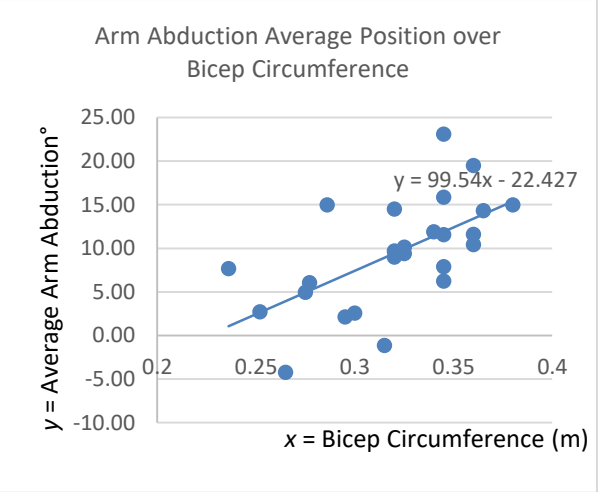

Figure 6-12- Increase of Average Arm Abduction over Bicep Circumference

Figure 6-13 shows average arm abduction visualised against increases in Body Mass Index. Linear regression (r^2 = 0.42) indicates the body mass index has a large effect on the average arm abduction position.

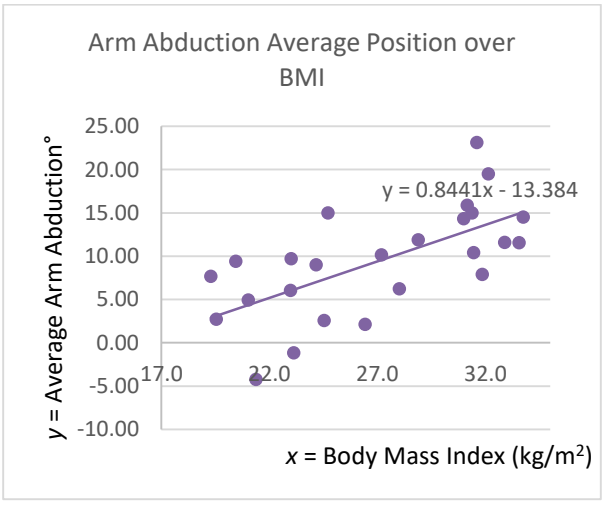

Figure 6-13- Increase of Arm Abduction over Body Mass Index

Figure 6-14 shows average arm abduction visualised against increases in chest circumference. This is the strongest correlation between any motion parameter and appearance parameter that was analysed. Linear regression (r^2 = 0.49) indicates the chest circumference has a large effect on the average arm abduction position.

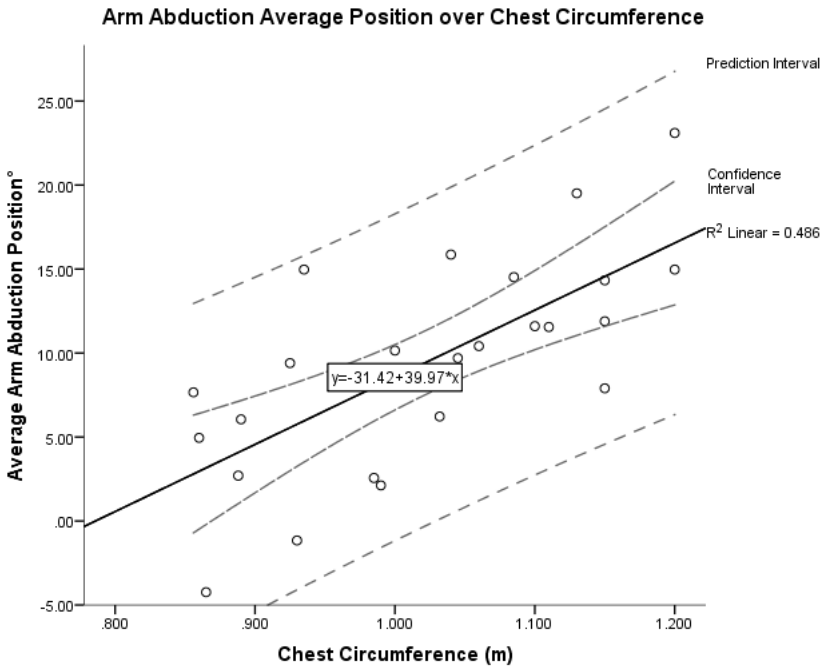

Figure 6-14- Increase of Average Arm Abduction over Chest Circumference

A linear regression established that statistically Chest Circumference could significantly predict Average Arm Abduction Position, $F(1, 23) = 21.773$, $p < .0005$ and Chest Circumference accounted for 48.6% of the explained variability in Average Arm Abduction Position. The regression equation was:

*Predicted Average Arm Abduction = 0.907 + (0.012 * Chest Circumference)*

Equation 6 - Average Arm Abduction

6.5.2. Arm Bob Magnitude

Arm bob magnitude refers to shoulder abduction and adduction range of motion. This is the range of lateral movement of the upper arm in the plane of the torso. To measure arm abduction magnitude during locomotion, the maximum and minimum rotation had to be differenced from the motion captures output for the LShoulderAngles:Y over the length of the walk clip. It is hypothesized that Average Bob Magnitude becomes more exaggerated over increases in anthropometric parameters.

Figure 6-15 shows arm abduction magnitude visualised against increases in body fat percentage. This suggests minimal or non-existent correlation between the motion parameter and the appearance parameter. Figure 6-16 shows arm abduction magnitude

visualised against increases in body mass. Linear regression (r^2 = 0.02) indicates body mass has a small effect on arm bob magnitude.

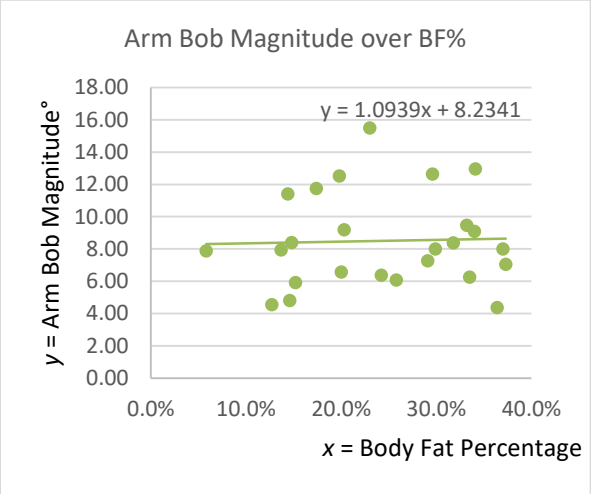

Figure 6-15- Increase In Arm Abduction Magnitude Over Body Fat Percentage

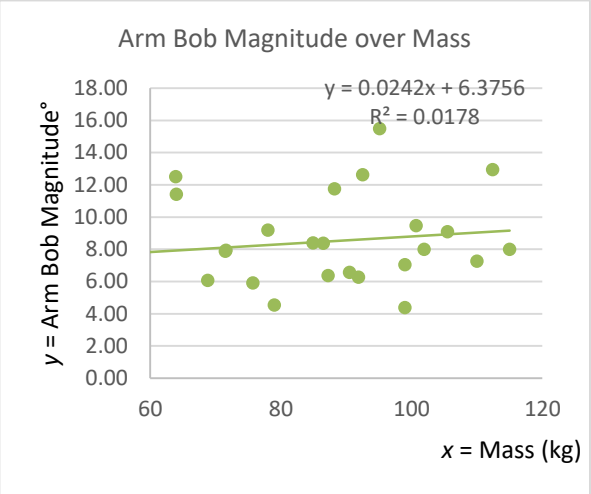

Figure 6-16- Increase In Arm Abduction Magnitude Over Body Mass

Figure 6-17 shows arm abduction magnitude visualised against increases in height. Height demonstrates the strongest correlation with arm bob magnitude.

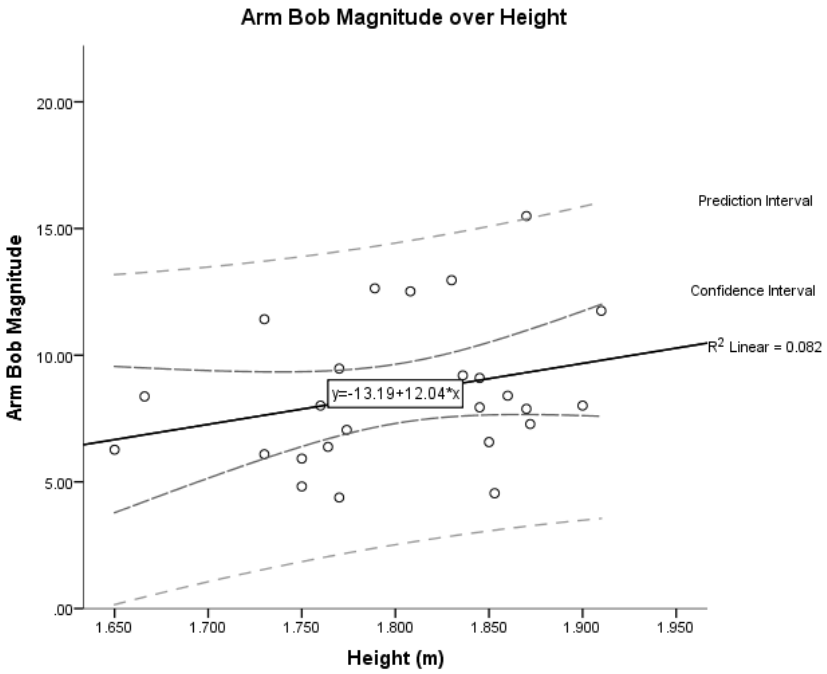

Figure 6-17- Increase In Arm Abduction Magnitude Over Height

A linear regression established that Height could statistically significantly predict Arm Bob Magnitude, F(1, 23) = 2.055, p < .0005 and Height accounted for 8.2% of the explained variability in Arm Bob Magnitude which Cohen considers a small effect size. The regression equation was:

*Predicted Arm Bob Magnitude = -13.19 + (12.04 * Height)*

Equation 7 - Arm Bob Magnitude

6.5.3. Arm Swing Magnitude

Arm swing known as shoulder flexion and extension occurs when the arms rotate out of the plane of the torso so that they swings anteriorly and posteriorly. To measure arm swing magnitude during locomotion, the maximum and minimum rotation had to be differenced from the motion captures output for the LShoulderAngles:X over the length of the walk clip. It is hypothesized that Average Swing Magnitude becomes more exaggerated over increases in anthropometric parameters.

Figure 6-18 shows arm swing magnitude visualised against increases in BMI. Linear regression (r^2 = 0.13) indicates the body mass index has a small effect on the arm swing magnitude. Figure 65 shows arm swing magnitude visualised against increases in height. This suggests that as people get taller their arm swing could reduce. However, linear regression (r^2 = 0.02) indicates that height only has a small effect on the arm swing magnitude so this requires further exploration.

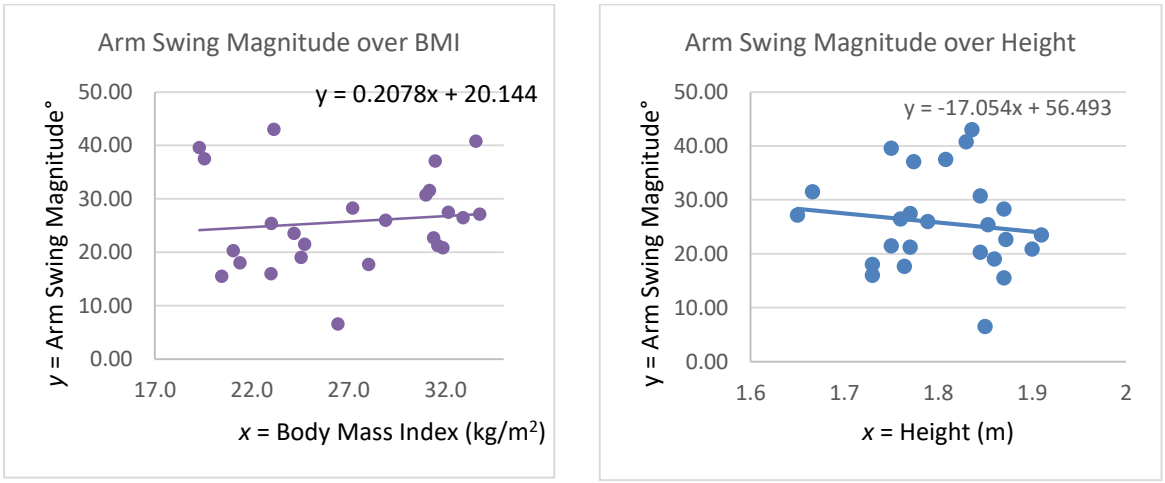

Figure 6-18- Increase In Arm Swing Magnitude Over BMI

Figure 6-19- Decrease In Arm Swing Magnitude Over Increase In Height

The following graph shows arm swing magnitude visualised against increases in body fat percentage. This suggests a correlation between increases in arm swing magnitude over increases in body fat percentage.

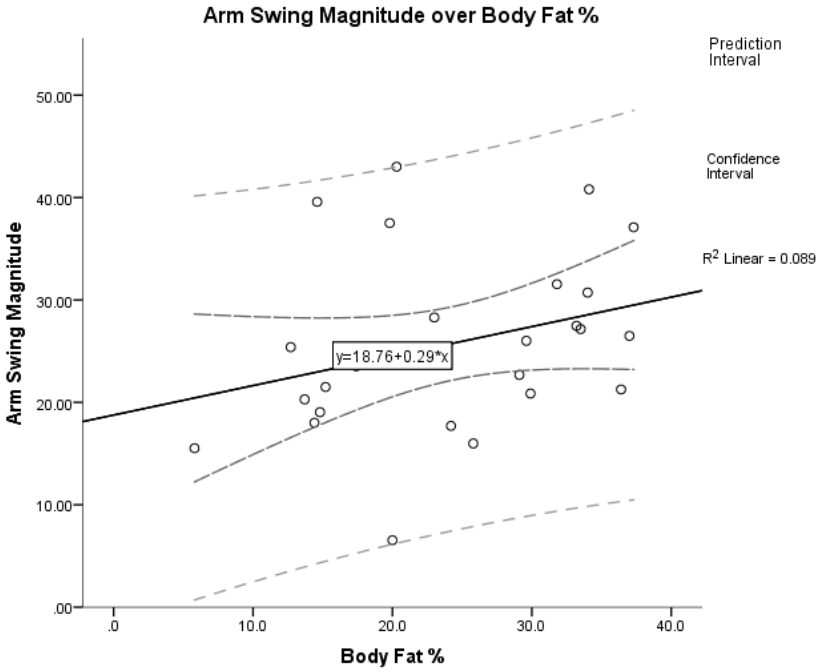

Figure 6-20- Increase in arm swing magnitude over body fat percentage

A linear regression established that statistically Body Fat % could significantly predict Arm Swing Magnitude, F(1, 23) = 2.237, p < .0005 and Body Fat % accounted for 8.9% of the explained variability in Arm Swing Magnitude which Cohen considers a small effect size. The regression equation was:

$$Predicted\ Arm\ Swing\ Magnitude = 18.76 + (0.29 * Body\ Fat\ \%)$$

Equation 8- Arm Swing Magnitude

6.5.4. Average Preferred Walking Speed

Preferred walking speed is the self-selected speed that participants feel comfortable walking at. Walking speed is determined by three elements; forward speed, cadence (steps per minute) and step length (distance between both heel strikes in a step). Average walking speed is measured using the motion capture data of the positional distance travelled by LASI:Y (waist) divided by the time taken to complete the walk. It is hypothesized that Average Preferred Walking Speed increases over increases in anthropometric parameters.

Figure 6-21 shows preferred walking speed visualised against increases in BMI. This suggests that there is no correlation between body mass index and speed. Figure 6-22 shows preferred walking speed visualised against increases in body fat percentage. Again we find a negligible or non-existent correlation between the body fat percentage and preferred walking speed.

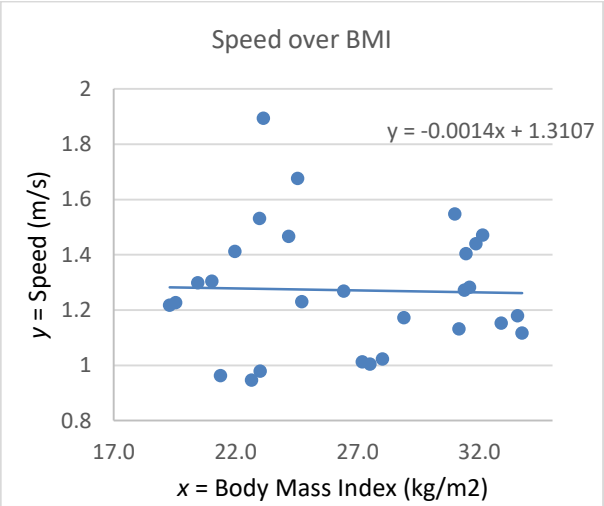

Figure 6-21- Increase Preferred Walking Speed Over BMI

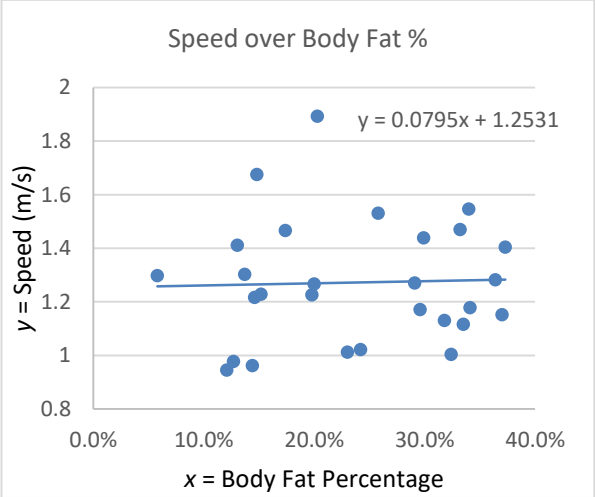

Figure 6-22- Increase Preferred Walking Speed Over Body Fat Percentage

Figure 6-23 shows preferred walking speed visualised against increases in body mass. This suggests a small correlation between the motion parameter and the appearance parameter.

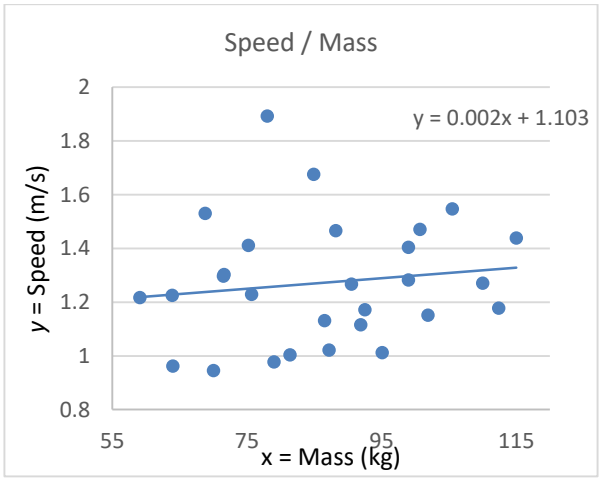

Figure 6-23- Increase In Preferred Walking Speed Over Body Mass

Figure 6-24 shows preferred walking speed visualised against increases in height. This demonstrates the strongest correlation between the motion parameter and the appearance parameter.

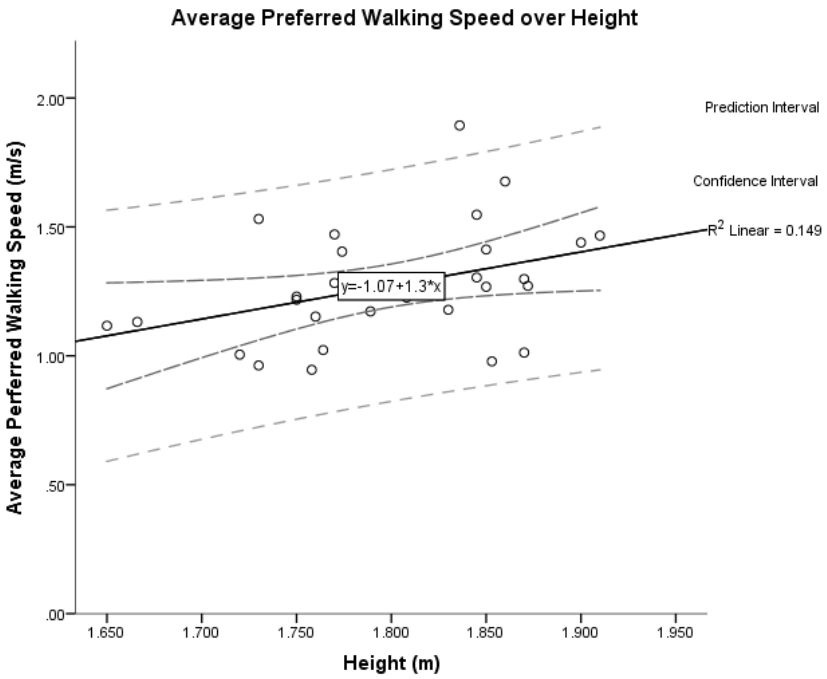

Figure 6-24- Increase In Preferred Walking Speed Over Height

A linear regression established that Height could statistically significantly predict Average Preferred Walking Speed, $F(1, 26) = 4.538$, $p < .0005$ and Height accounted for 14.9% of the explained variability in locomotion. The regression equation was:

$$\textit{Predicted Average Preferred Walking Speed} = -1.07 + (1.3 * \textit{Height})$$

Equation 9 - Average Preferred Walking Speed

6.5.5. Walking Base

Walking base is the width of a stride; the lateral distance between the line of both heels during the heel strike phase. It is hypothesized that Walking Base widens over increases in anthropometric parameters.

Figure 6-25 shows walking base visualised against increases in body fat percentage. Linear regression (r^2 = 0.17) indicates the body fat percentage has a small effect on the walking base. Figure 6-26 shows walking base visualised against increases in BMI. Linear regression (r^2 = 0.2) indicates the body mass has a small effect on the walking base.

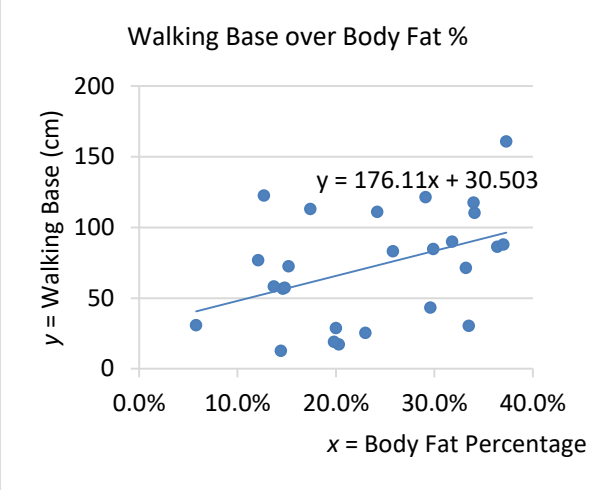

Figure 6-25- Increase In Walking Base Over Body Fat Percentage

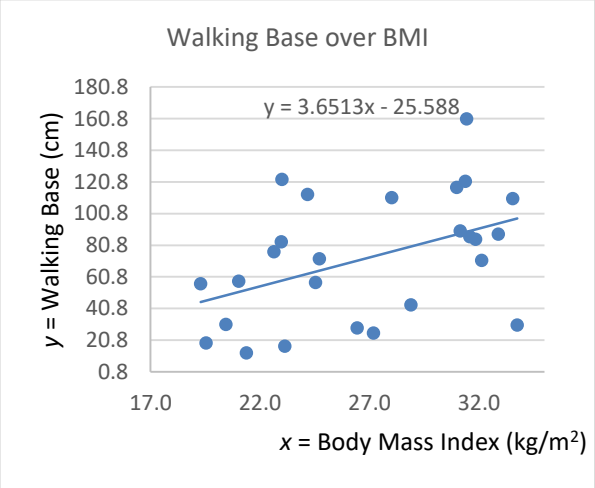

Figure 6-26- Increase In Walking Base Over BMI

Figure 6-27 shows walking base visualised against increases in total body part limb circumference. Linear regression (r^2 = 0.2) indicates the circumferences of key multiple body parts has a small effect on the walking base. Figure 6-28 shows walking base visualised against increases in waist-to-hip ratio. Linear regression (r^2 = 0.24) indicates the waist to hip ratio has a medium effect on the walking base.

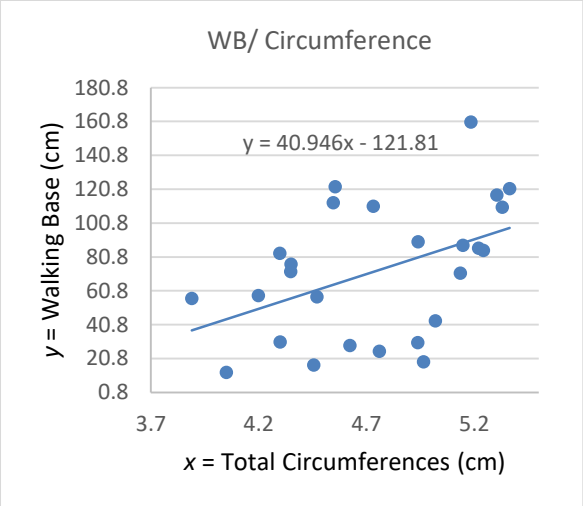

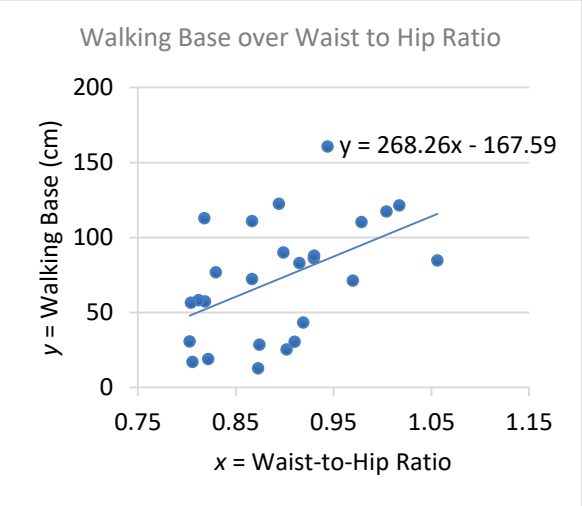

Figure 6-27- Increase In Walking Base Over Total Circumferences

Figure 6-28- Increase In Walking Base Over Waist-To-Hip Ratio

Figure 6-29 shows walking base visualised against increases in body mass. Linear regression (r^2 = 0.24) indicates that body mass has a medium effect on the walking base. Body Mass is the strongest correlation to walking base but multiple regression could be performed to incorporate waist to hip ratio which was almost equal in strength of fit.

Figure 6-29- Increase In Walking Base Over Body Mass

A linear regression established that body mass could statistically significantly predict walking base, F(1, 24) = 6.005, p < .0005 and body mass accounted for 23.6% of the explained variability in walking base. The regression equation was:

$$Walking\ Base = -32.11 + (1.2 * Body\ Mass)$$

Equation 10 - Walking Base

6.5.6. Step Length

Step length is the distance between the point of initial contact of one foot and the point of initial contact of the opposite foot. It was measured using the motion capture data of the positional distance between the LHEE: and RHEE: during a heel strike phase. It is hypothesized that Step Length increases over increases in anthropometric parameters.

Figure 6-30 shows step length visualised against increases in BMI. This suggests a negligible or non-existent negative correlation between the step length and body mass index. Figure 6-31 shows step length visualised against increases in body fat percentage. This suggests a negligible or non-existent negative correlation between the step length and body fat percentage.

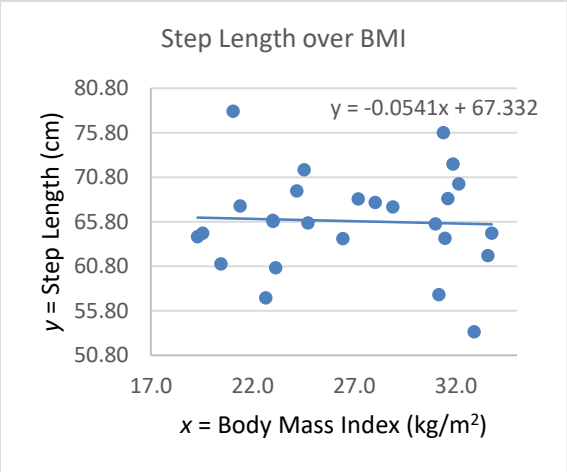

Figure 6-30- Decrease In Step Length Over BMI

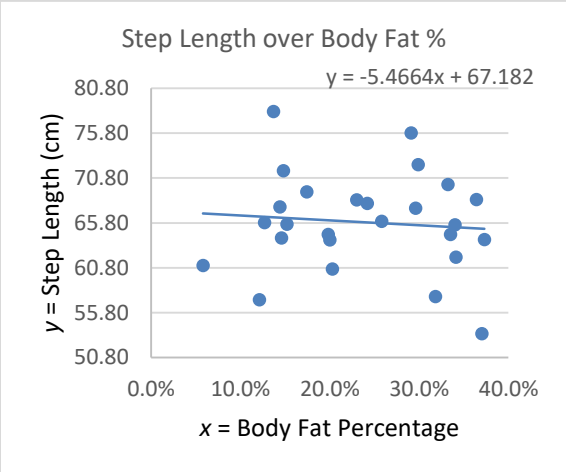

Figure 6-31- Decrease In Step Length Over Body Fat Percentage

Figure 6-32 shows step length visualised against increases in body mass. Linear regression (r^2 = 0.02) indicates the body mass has a small effect on the length of step. Figure 6-33 shows step length visualised against increases in height. Linear regression (r^2 = 0.18) indicates the body fat percentage has a small effect on the walking base.

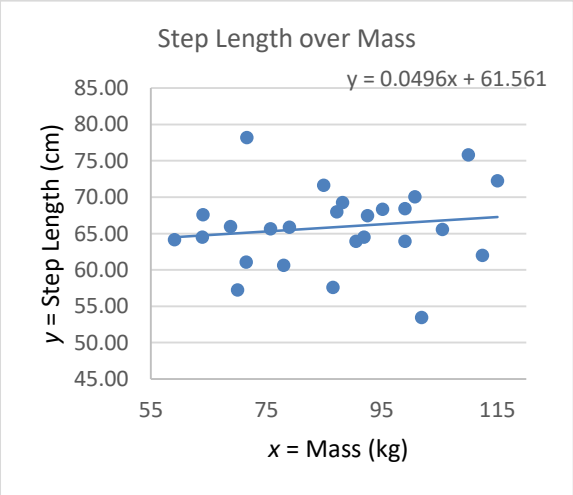

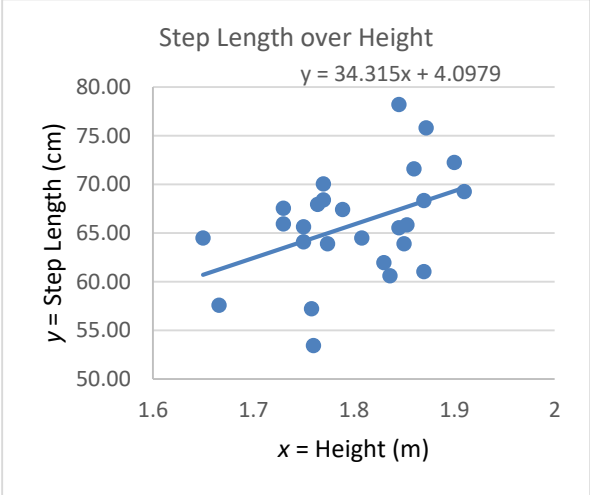

Figure 6-32- Secondary Anthropometric Correlation With Step Length

Figure 6-33- Dominant Anthropometric Correlation With Step Length

6.6. Summary

The methodology thoroughly reviewed a range of difference anthropometrics and kinematic metrics to determine which best represent body shape and gait for physical and virtual characters and which were practical to employ. Eight anthropometrics were decided upon to measure body morphology and seven further parameters could be derived from these.

The motion capture process allows the recording of full body movement and most gait parameters but the focus of analysis was eight gait parameters, three of which failed to return useful data. The remaining five parameters were correlated against anthropometrics. These will be further analysed in comparison to the results of the perceptual video tests in the following chapter.

This process resulted in the research contribution of a relatively small but rich dataset combing multiple anthropometric and locomotive data points. Unlike the KIT Whole-Body Human Motion Database, our richer database contains internal limb lengths as well as externally visible limb circumferences, height, weight and body fat percentage data. In addition we have collated five correlations between anthropometric and gait parameters that form the basis of an appearance to motion framework

7. ANALYSIS & OBSERVATIONS

The surveys were developed using Google forms which allows easy distribution online and embedding of fixed dimension videos. The video matrix of walkers was initially based on McDonnell et al. (2008) format but iterated upon for clarity, based on prototype feedback. The selection criteria for participants were loose; they had to declare that they were over the age of eighteen and were sourced broadly through social media channels such as Facebook and Twitter with a £20 voucher incentive to encourage participation. For more information on our survey methodology see section 4.2. Whilst the response rate to the point light survey was fair (*n=59*), we were able to double the confidence in our results by iterating a second character mesh survey (*n=67*) which helped cover more parameters. There is large range of other biomechanical parameters that could have also been modelled and tested, however we chose to cover those with the larger range of movements that we deemed most perceptually noticeable individually and within a crowd.

The survey results have been analysed using categorical bar charts. Whilst results from surveys' individual parameters could show the distribution of degrees of exaggeration, these were only displayed and selectable in discrete categorical values. In addition, combination videos had different parameters modified at different rates and in different directions so a categorical bar chart was the appropriate format for analysis.

Numerous public domain motion data sets were considered for analysis, such as Carnegie Mellon University's motion capture database, however whilst this source was rich in a variety of locomotion clips it was devoid of any corresponding anthropometric data. The KIT Whole-Body Human Motion Database, had some potentially useful anthropometric data however these were all structural lengths representing underlying bone sizes. Whilst we recorded many of the same measurements for calibration purposes, we were interested in more externally perceptual anthropometrics such as circumferences around muscular-adipose limb masses, weight, body fat percentage and height.

The motion capture data was analysed against anthropometric measurements using linear regression to provide predictive formulas for implementation into the final scripted animation tool. The sample size, whilst smaller than Green's (1991) formula recommended, was in the range of other highly cited anthropometric studies.

We shall analyse the results of our perceptual surveys and motion capture sessions to make observations on how the motion parameter trends correlate with appearance parameters, perceptually and actually. This shall help inform the structure of a framework that can be implemented in a believable character generation tool.

7.1. Observations

7.1.1. Average Arm Abduction Position

Changes in arm kinematics were predicted to be perceptually strong as they have a larger range of motion of compared to the torso and their movement could appear to be amplified by any rotation of the torso or hips. Average arm abduction was predicted to raise over increases in perceived obesity to avoid chafing of the upper arms and chest. The results as seen in Figure 4-4 confirm this with a clear upward trend of identification of obese walkers with increased angle of the average arm abduction.

Increased arm abduction is also demonstrated in combination with arm bob in Figure 4-7. However, when increased arm bob was surveyed in Figure 5-3 the results were broadly mixed and supported under exaggeration. This means that in Figure 4-7 arm abduction was significantly more perceptually dominant than (the incorrectly exaggerated) arm bob. This can be seen more clearly when the two survey results are compared in Figure 7-1:

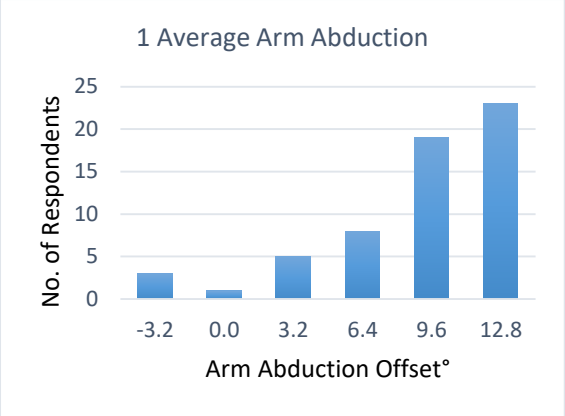

Figure 4-4- Increased Arm Abduction point-light results

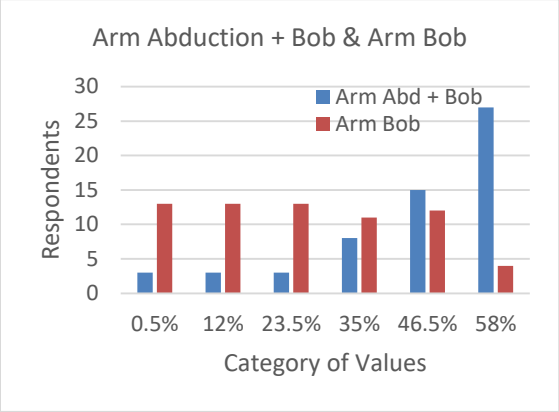

Figure 7-1 - Arm Abduction + Bob & Arm Bob Comparison

When increased arm abduction and arm swing were tested the results were mixed but not as evenly random, which suggested one or two of the parameters were correct but conflicting in some way. Figure 4-6 shows a viewer preference for under exaggerated arm swing. This can be seen more clearly when the two survey results are compared in Figure 7-2. In a similar conflict in Figure 4-7, arm abduction dominated the arm bob (which was exaggerated in the incorrect direction) whereas Figure 4-8 is mixed which suggests arm abduction is perceptually stronger than arm swing, which is perceptually stronger than arm bob. This can be seen more clearly when the two survey results are compared in Figure 7-3.

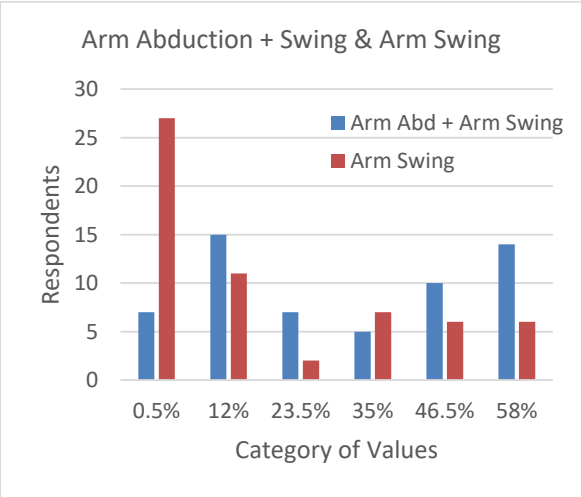

Figure 7-2 - Arm Abduction + Swing & Arm Swing Comparison

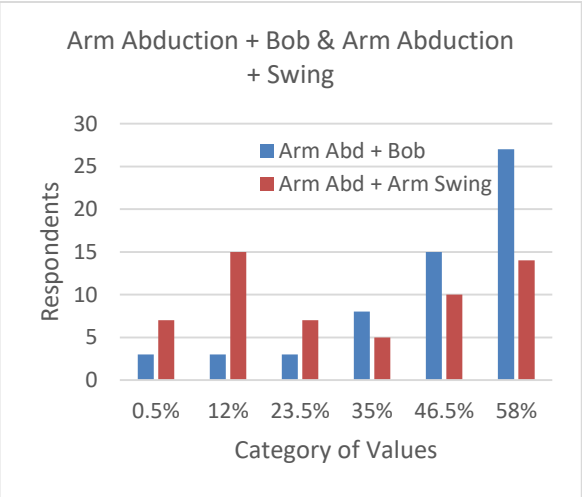

Figure 7-3 - Arm Abduction + Bob & Arm Abduction + Swing Comparison

Section 6.5.1 shows the actual changes in average arm abduction position over increases in obesity. The strongest appearance correlation is with increased chest circumference with a coefficient of (r^2=0.49) seen in Figure 6-14. This is the strongest correlation between an appearance parameter and motion parameter. Bicep girth also had a strong correlation with 0.3627 seen in Figure 6-12. This suggests the cause is avoidance of chafing of increased bicep girth with increased chest girth.

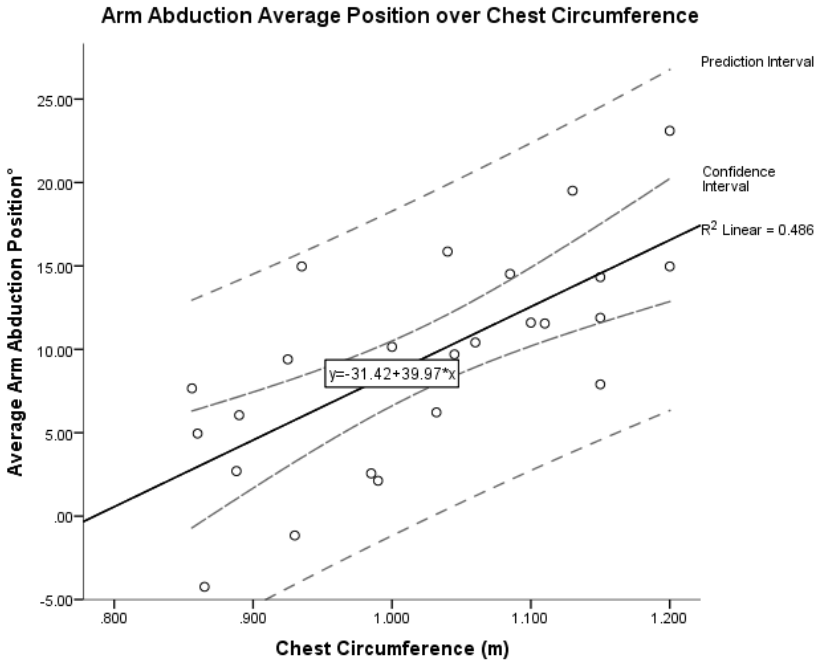

Figure 6-14- Increase of Average Arm Abduction over Chest Circumference

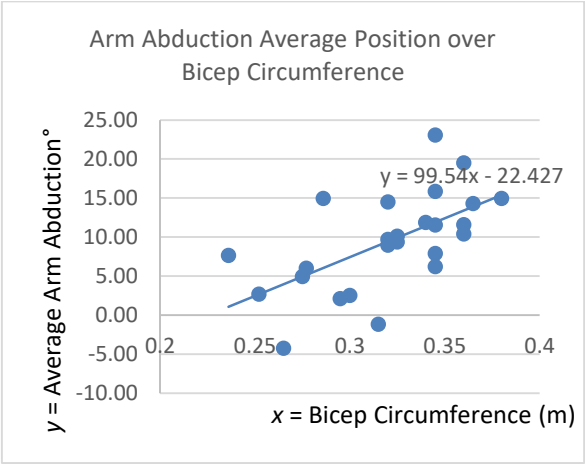

Figure 6-12- Increase of Average Arm Abduction over Bicep Circumference

7.1.2. Increased Arm (swing)

Arm swing magnitude was predicted to amplify over increases in perceived obesity as Cutting and Kozlowski (1977) had noted this change. It was hypothesised this would be in

counterbalance to a perceived increase in torso twist. Arm swing has a large range of motion of 175° which could be considered to be perceptually significant.

The results in Figure 4-6 appear to oppose this hypothesis with a decreasing trend of identification of obese walkers with increased arm swing magnitude. Viewers perceived arm swing magnitude to decrease in obese walkers. As previously discussed, the combined parameters in section 4.4.5 demonstrates 'correct' increases in arm abduction but 'incorrect' arm swing increases. As the results appear somewhat mixed this supports the trend for decreased arm swing over increases in obesity. This can be seen more clearly when compared to survey results preferring under-exaggerated arm swing compared in Figure 7-4.

Figure 5-4 combined increased arm abduction with decreased arm swing. Whilst the results were much less clear than increases in arm abduction alone, they still appeared to somewhat support a preference that supports decreased arm swing.

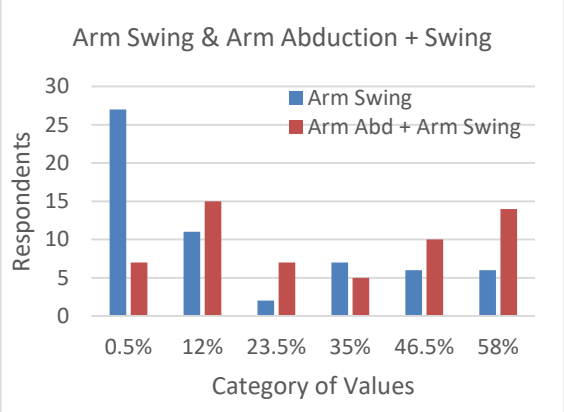

Figure 7-4 - Arm Swing & Arm Abduction + Arm Swing Comparison

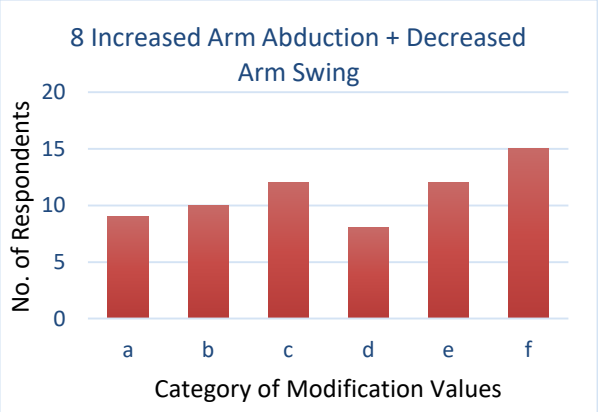

Figure 5-4- Arm Abduction and Arm Swing obese mesh results

Section 6.5.3 shows the actual changes in arm swing magnitude over increases in obesity. However, several correlations such as body fat percentage and BMI show an increase of arm swing magnitude. There were few direct correlations with appearance parameters, however, in Figure 6-19 increasing height is seen to have a small correlation of 0.0173 over decreasing arm swing. This could suggest that taller people reduce their arm swing to maintain a steady COG/ balance

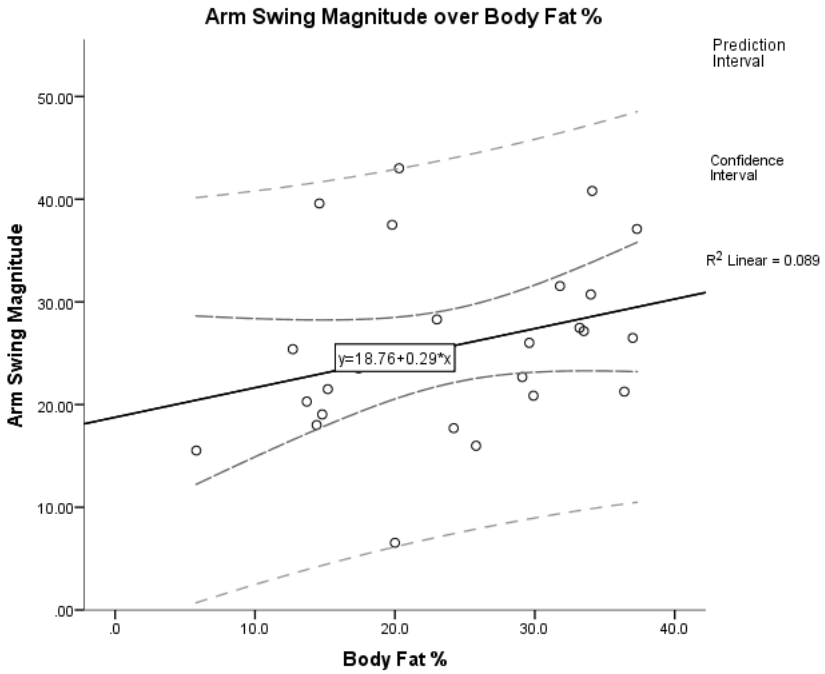

Figure 6-20- Increase in arm swing magnitude over body fat %

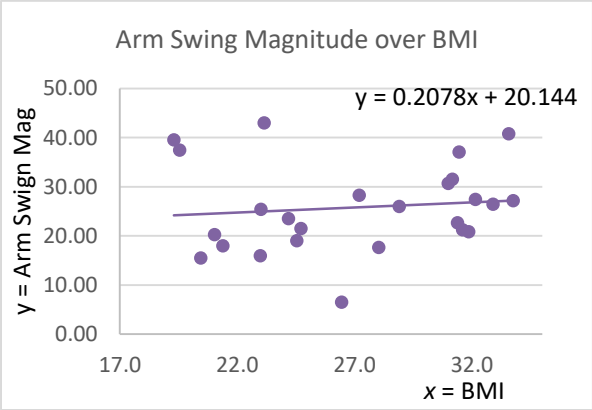

Figure 6-18- Increase In Arm Swing Magnitude Over BMI

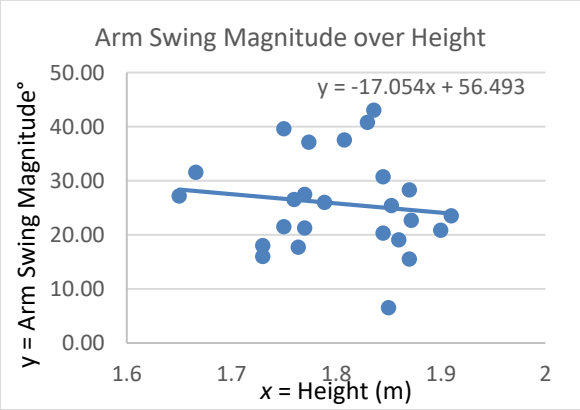

Figure 6-19- Decrease In Arm Swing Magnitude Over Increase In Height

7.1.3. Increased Arm bob

Arm bob magnitude was predicted to amplify over increases in perceived obesity. The results in Figure 5-3 appear to oppose this hypothesis with a slight downward trend of identification of obese walkers with increased arm bob. Whilst the responses to the first three strengths are equally distributed the last and strongest amplifications of arm bob magnitude received fewer preferences. To verify these subtle responses, we can check the

combined parameters of increased arm abduction and arm bob seen in Figure 4-7. The clarity of the upward trend suggests that either arm bob increases over obesity or the more likely trend, that its decrease is overpowered by the perceptual strength of arm abduction. This can be seen more clearly when the two survey results are compared in Figure 7-5.

Either way, the clear trend in the combined parameters of Figure 4-7 is so similar to arm abduction alone in Figure 4-4, as seen in Figure 7-6, that we can determine that arm bob is a perceptually weaker motion parameter.

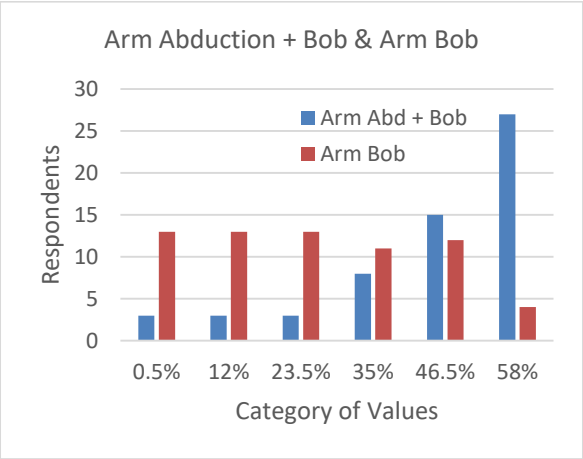

Figure 7-5 Arm Abduction + Bob & Arm Bob Comparison

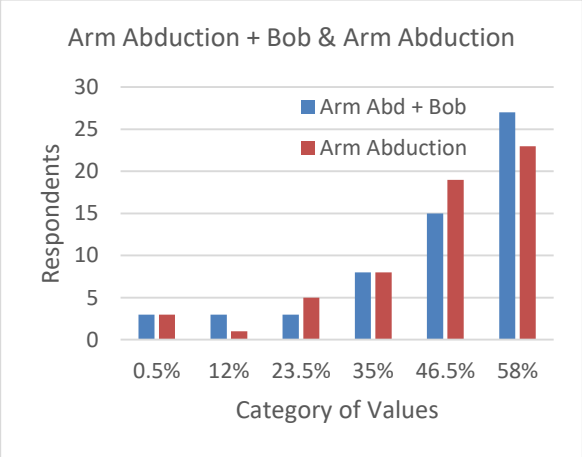

Figure 7-6 Arm Abduction + Bob & Arm Abduction Comparison

Section 6.5.2 shows the actual changes in arm bob magnitude over increases in obesity BF%.

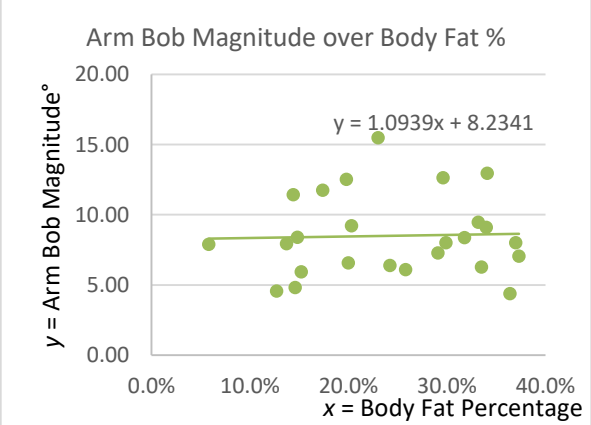

Figure 6-15- Increase in arm abduction magnitude over BF%

Like arm swing magnitude, the strongest arm bob correlation is over an increase in height with a (r^2=0.08) correlation seen in Figure 6-17:

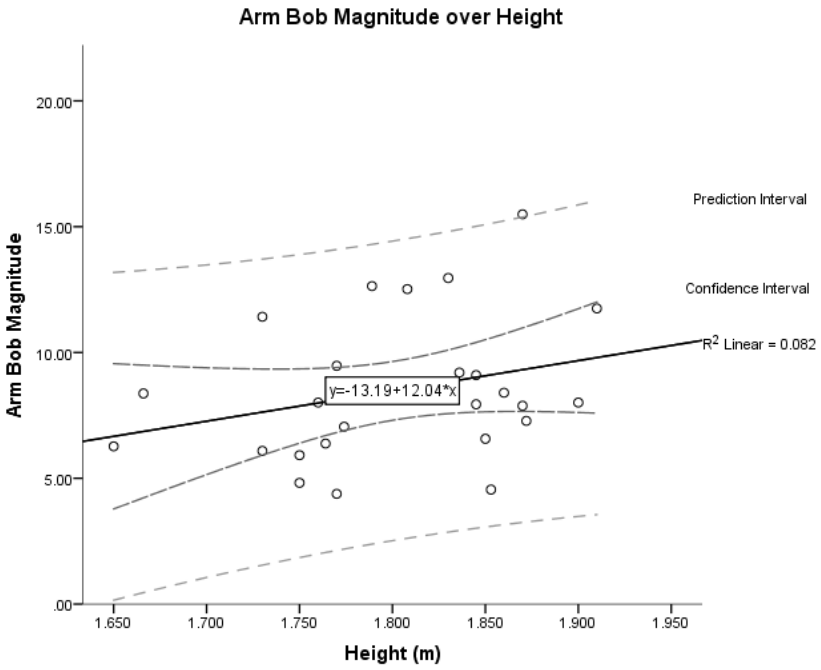

Figure 6-17- *Increase In Arm Abduction Magnitude Over Height*

Similarly to arm swing magnitude, this could suggest that taller people reduce their arm bob to maintain a steady COG/ balance.

7.1.4. Increased Spinal Erectness

Spinal erectness was predicted to increase over increases in perceived obesity, as (McGraw et al., 2000) had noted this change. The mixed perceptual results in Figure 4-5 unfortunately demonstrated that this parameter was poorly modelled.

Whilst the motion capture recording did capture C7 upper spine, T10 mid spine and Hip Angles which might have provided enough to analyse a three point spine curvature, the T10 marker was placed on an area of the suit that was often stretched taut over the actual spinal curvature so it would not have been accurate enough.

7.1.5. Hip and Torso (twist)

Hip and torso twist was predicted to increase over increases in perceived obesity. Figure 4-10 showed the point light results of hip and torso twist but the results appear mixed with stronger values at -0.8, 1 (the original lean walker) and 8.3. As the degree of rotation may have been difficult to ascertain from spherical lights with no affected body surface we also look at the retested hip and torso twist combination using body meshes in Figure 5-6. Unfortunately, this provides even less clear results.

The cause of this is unclear however hip and torso may simply be a subtle parameter as they are the closest body parts to the centre of gravity and less movement is needed to maintain balance. As they proved too subtle a set of parameters, gait analysis was not performed on the actual data.

7.1.6. Torso Swagger (thorax lateral rotation)

Torso swagger was predicted to increase over increases in perceived obesity. Torso swagger rotation is likely a counter balance to the opposite legs heel strike to maintain centre of gravity. The results in Figure 5-5 appears to somewhat support this hypothesis with a peak identification of obese walkers identified at 1.6.

This parameter was analysed as one tall, overweight walker had a characteristic torso swagger, however, not all tall or overweight walkers did, so this was not considered as clear a trend as others parameters and further gait analysis was not performed at this stage.

7.1.7. Reduced Walking Speed/ Cadence

Preferred walking speed was predicted to slow down over increases in perceived obesity. The results in Figure 4-9 appear too mixed to assess, as a result of the confusing presentation angle of 45° of the video. So when the parameter was retested in Figure 5-9 with mesh characters presented 0° towards the camera, the results demonstrated a clear bell curve with a preferred speed reduction of 0.8 expected over an increase in perceived

obesity. This can be seen more clearly when the two survey results are compared in Figure 7-7:

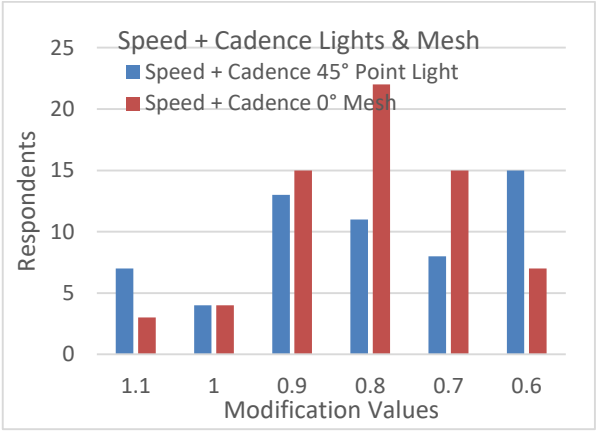

Figure 7-7 - Speed + Cadence Point Light & Mesh Comparison

Figure 6-21 and Figure 6-22 shows the recorded changes in walking speed over increases in obesity. However, the wide range in walking speed does not display a clear trendline over increase in either body fat percentage or body mass index despite literature demonstrating (Spyropoulos et al., 1991) a decrease in walking speed over increases in obesity.

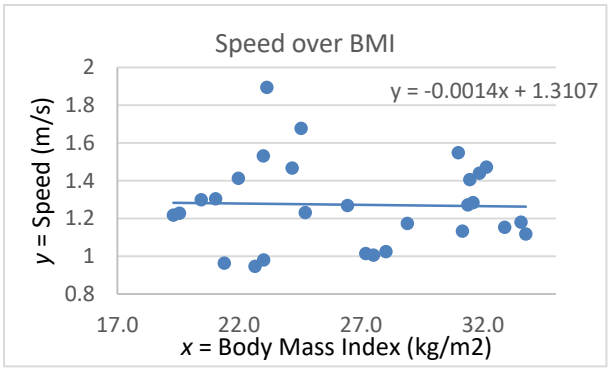

Figure 6-21- Increase Preferred Walking Speed Over BMI

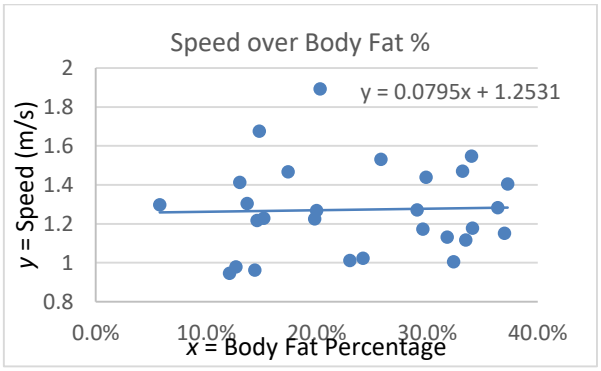

Figure 6-22- Increase Preferred Walking Speed Over Body Fat Percentage

Figure 6-24, however, does show a strong correlation of (r^2=0.1486) increasing preferred walking speed over height. Webb (1996) confirms this correlation of height with walking speed. The cause of this trend could be the taller the height, the longer the leg length and therefore the stride length.

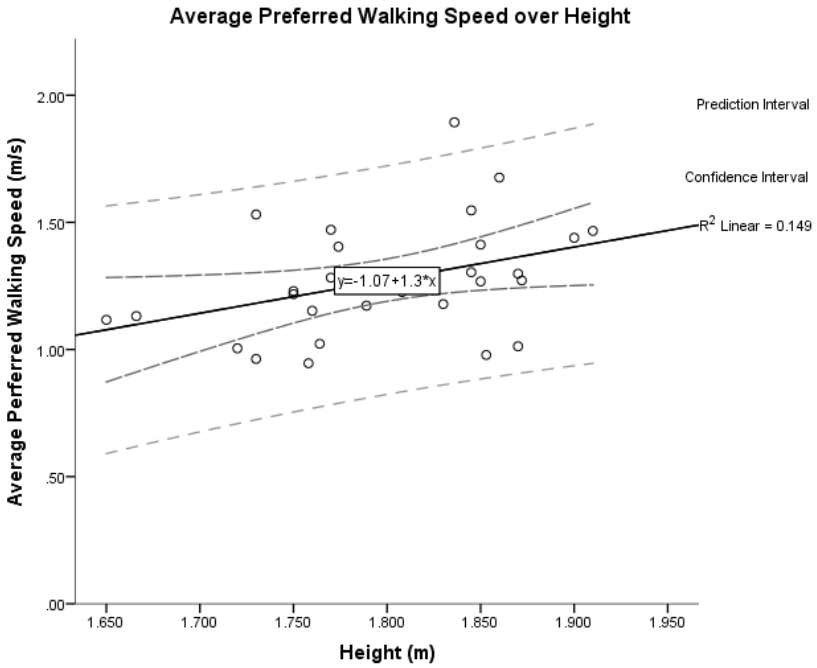

Figure 6-24- Increase In Preferred Walking Speed Over Height

However, when leg length was also analysed the correlation (r^2 = 0.0667) was weaker than overall height as seen in Figure 7-8.

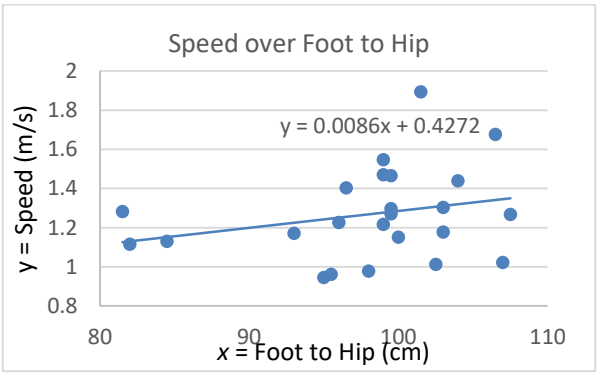

Figure 7-8 - Increased walking speed over Foot to Hip

Decreased walking speed/ cadence is considered to be a dominant motion parameter as Figure 5-9 demonstrated the clearest curve of identification for strengths of exaggeration.

It is considered more dominant a motion parameter than increased average arm abduction as preferred speed reduction requires a reduction by 0.8 (Figure 5-9) whilst arm abduction requires an increase of 12.8 (Figure 4-4) to reach the preferred exaggeration strengths for identification of obese walker i.e. a smaller degree of exaggeration is needed to reduce preferred walking speed than average arm abduction, therefore its effect is more dominant.

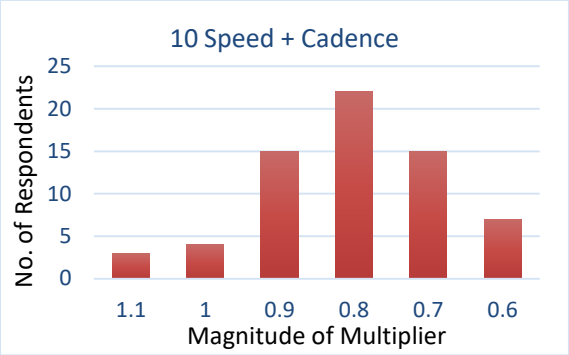

Figure 5-9- Speed and Cadence obese mesh results

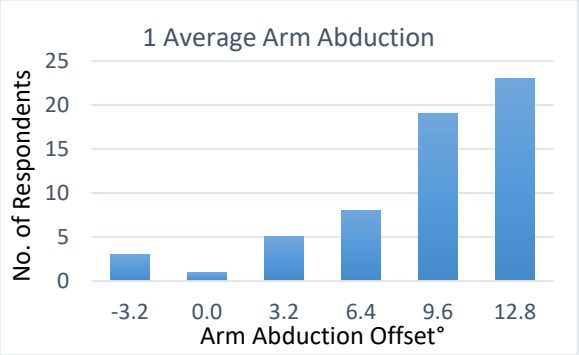

Figure 4-4- Increased Arm Abduction point-light results

7.1.8. Increasing Walking Base

Walking base was predicted to widen over increases in perceived obesity. The results in Figure 5-10 appear to support this hypothesis with an upward trend of identification of obese walkers with widening walking base.

Figure 5-10- Walking Base obese mesh results

Section 6.5.5 shows how the actual changes in walking base over increases in obesity. The strongest appearance correlation is with Body Mass (r^2= 0.2356) seen in Figure 6-29.

Figure 6-29- Increase in walking base over body mass

Waist to Hip Ratio also had a strong correlation of (r^2= 0.2349) seen in Figure 6-28. As Waist-to-Hip Ratio can be measured and modified on virtual characters this is the more useful parameter for our purposes.

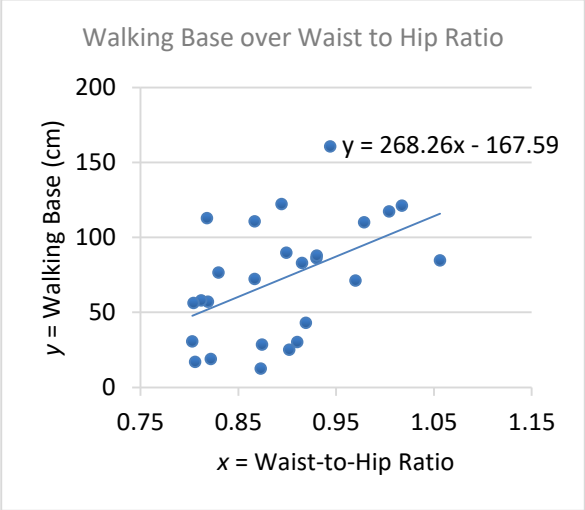

Figure 6-28- Increase In Walking Base Over Waist-To-Hip Ratio

This suggests that the larger the Waist-to-Hip Ratio the wider the legs spread apart to maintain a steadier support base.

Increased walking base is considered to be a moderately dominant motion parameter as eighteen people selected the most exaggerated width compared to twenty-three people who selected Arm Abduction's exaggerated width and twenty-two people who selected Speed/ Cadence's.

7.1.9. Upper body combination

It was expected that upper body movement would have a strong perceptual effect with arm abduction having the largest effect, arm swing having a medium effect, arm bob having a lesser effect and hip/torso rotation having the least effect. This could be seen in isolation Figure 4-4 where arm abduction has a clear upward trend. Arm abductions perceptual dominance is also determined by its overpowering over other parameters such as arm bob, as seen in Figure 7-1.

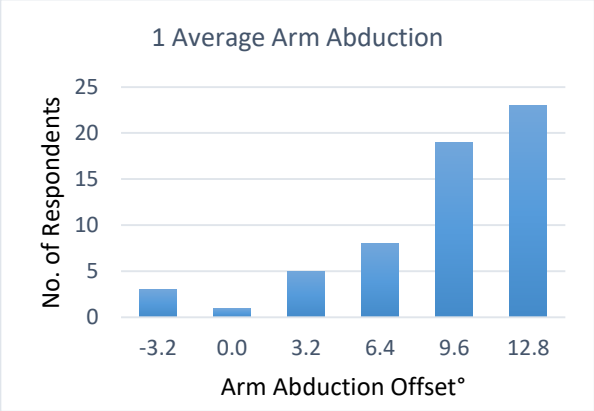

Figure 4-4- Increased Arm Abduction point-light results

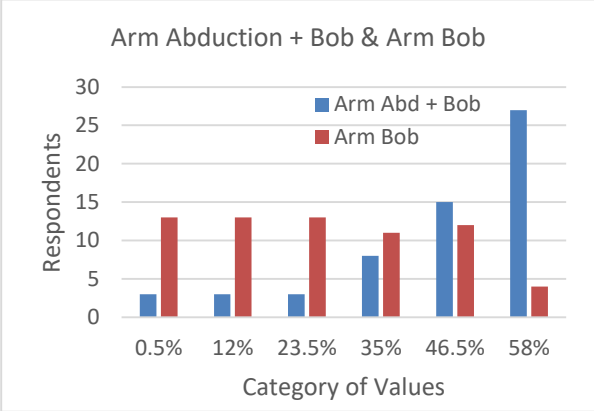

Figure 7-1 - Arm Abduction + Bob & Arm Bob Comparison

Arm swing was perceived to decrease. However, when decreased arm swing was combined with increased arm abduction, as seen in Figure 7-9, results show a slight upward trend but not as clear as arm abduction alone. As the total number of '58%' selections for combined arm abduction and swing were smaller than those for arm and abduction and bob we shall classify arm swing as potentially less perceptually important but more likely not modified quite correctly yet.

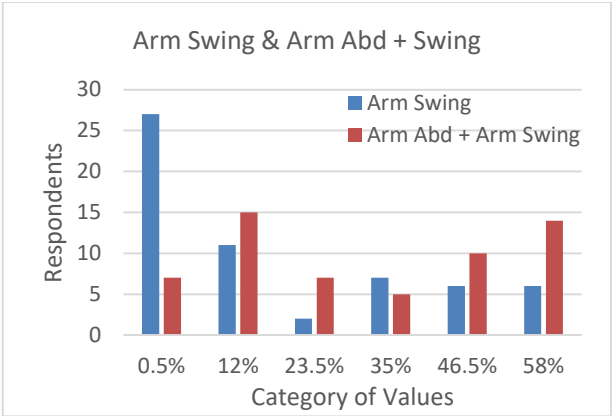

Figure 7-9 - Arm Swing & Arm Abduction + Arm Swing Comparison

The modified upper combination set of parameters in Figure 4-11 improved perceptual identification by decreasing instead of increasing arm swing and torso twist demonstrating that these were of perceptual significance. Arm bob was not decreased but left to increase and yet Figure 5-7 still shows a significant improvement which indicates that arm bob is low in terms of perception. Figure 7-10 demonstrates that the second combination of parameter strengths received was significantly more believable.

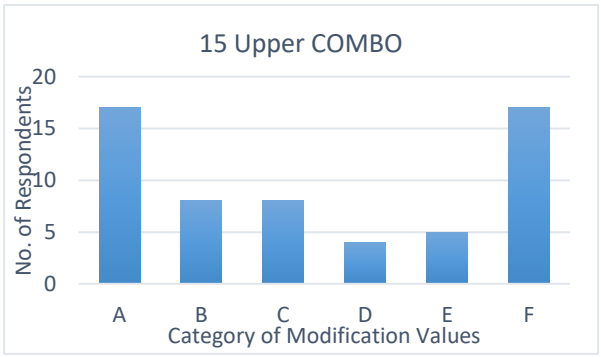

Figure 4-11- Upper Body Combination point-light results

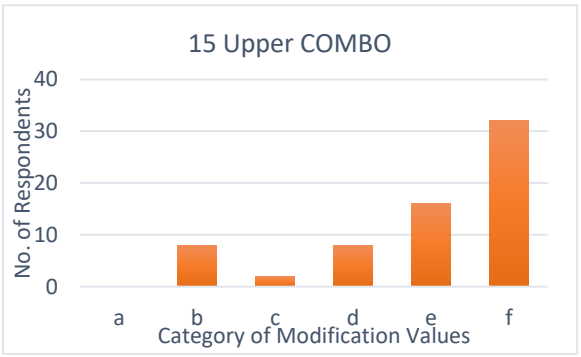

Figure 5-7- Upper Body Combination obese mesh results

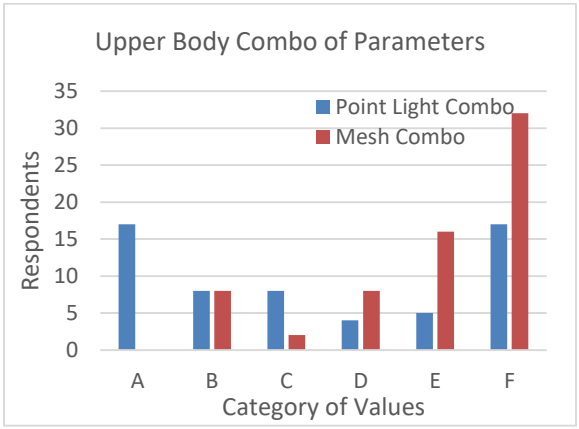

Figure 7-10- Upper Body Combinations of Parameters Compared

7.1.10. Lower body combination

In the point-light video survey, decreased speed-cadence, increased walking base and increased hip twist were modelled as a lower body combination of parameters. This was with an expectation that viewers would show an upward trend of identification of obese walkers. The upward trend demonstrates this to be true, however, the penultimate strength dipped.

However, hip twist was considered more convincing in this combination of parameters when retested as a decreasing effect in section 4.4.9. The only parameter changed from Figure 4-12 was hip twist which produced the more convincing lower combo results seen in Figure 5-11. This shows an upward trend of identification of obese walkers with values at the strongest preference peaking at 'D', which follows the results of preferred walking speed, suggesting that this is the more dominant parameter. Reductions in speed create the largest perceptual effect. Increased walking base skewed more results to the 'E' and 'F' values suggesting it as a strong secondary parameter and the hip twist the weakest parameter,

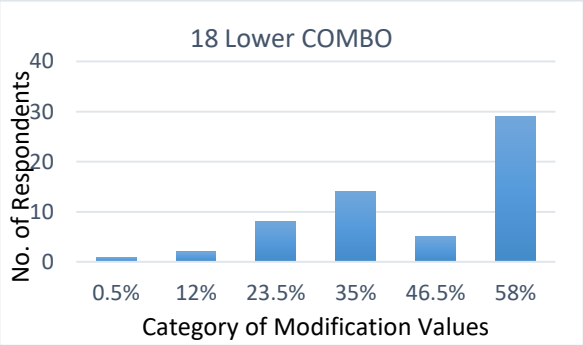

Figure 4-12- Lower Body Combination point-light results

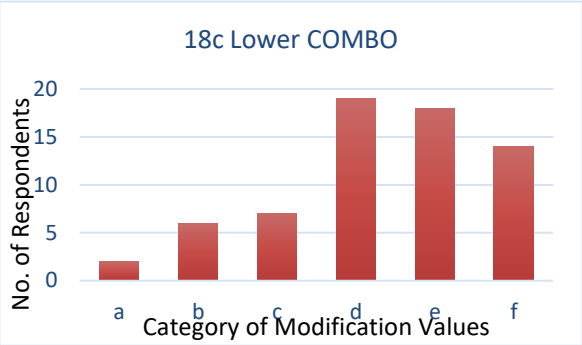

Figure 5-11- Lower Body Combination obese mesh results

7.1.11. Whole body combination

The point-light video survey in Figure 4-12 decreased walking speed and increased hip twist, torso twist, walking base, arm abduction, arm bob and arm swing were modelled as a total body combination of parameters. This was with an expectation that viewers would show an upward trend of identification of obese walkers. The upward trend demonstrates this to be true, with a much greater preference for the three strongest combinations.

The mesh survey in Figure 5-12 decreased hip and torso twist and arm swing. This provided a smoother upward trend of identification with obese walkers.

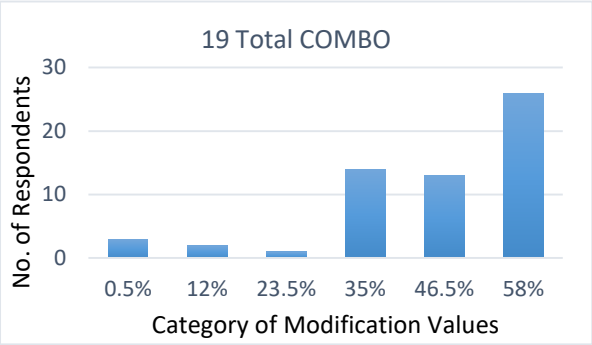

Figure 4-12- Lower Body Combination point-light results

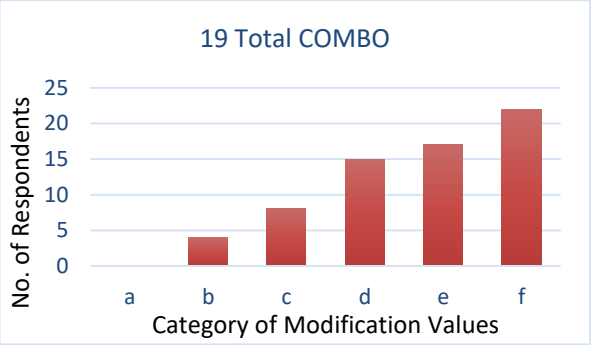

Figure 5-12- Total Combination obese mesh results

This could indicate that the upper body parameters of, torso twist and arm swing have a significant effect on perception of obesity, however, without modifying perceptually dominant lower body parameters such as walking speed, we cannot determine which has the stronger effect.

Comparing the most perceptually dominant parameters from the upper body and lower body shows similar peak identification numbers which suggests that both halves of the body may be equally important when perceiving obesity.

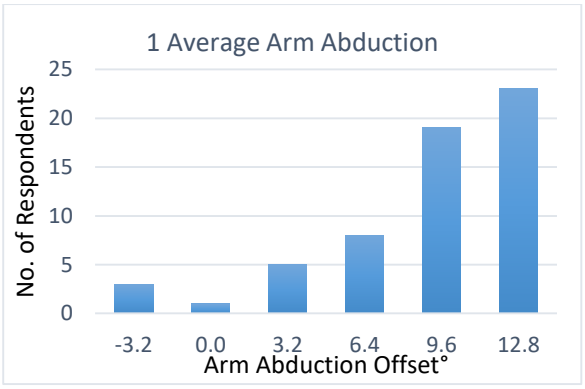

Figure 4-4- Increased Arm Abduction point-light results

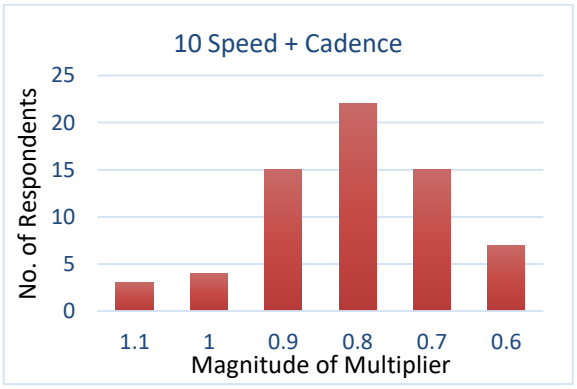

Figure 5-9- Speed and Cadence obese mesh results

7.2. Analysis & Results Summary

The results demonstrate a series of motion parameters that, when exaggerated from a normal walk, are identifiable as that of an obese walker. Following a series of data capture and analysis we deduced an order of perceptual dominance to certain motion parameters. These are summarised as follows.

7.2.1. Summary of Point Light Survey

Having analysed the results of the point light perceptual survey we can deduce an order of preference for a number of motion parameters and combinations. A number of parameters were also identified as needing to be retested:

Table 7-1 - Summary of Point Light Perceptual Survey Results

Perceptual Order	Video Parameter	Highest Votes	Perceived Preferred Direction of Change	Action
1	Lower body combination	29	Increase	
2	Increased Arm (swing)	27	Decrease	Retest decreasing swing with increasing abduction
2	Increased Arm Abduction & (bob)	27	Increase	Retest Arm Bob only
4	Whole body combination	26	Increase	
5	Increased Arm Abduction	23	Increase	
6	Upper body combination	17	Mixed	
	Increased Hip (twist) & Torso (twist)	16	Mixed/ Unclear	Retest with character mesh
	Reduced Walking Speed/ Cadence	15	Mixed/ Unclear	Retest with different camera angle
	Increased Arm Abduction & (swing)	15	Mixed/ Unclear	Retest with decreasing swing
	Increased Spinal Erectness	14	Mixed/ Unclear, Poorly Modelled	Abandon

These results informed the selection of parameters for the character mesh perceptual survey.

7.2.2. Summary of Mesh Survey

The second perceptual survey retested a number of motion parameters and combinations to give an indication of perceptual dominance.

Table 7-2 - Summary of Character Mesh Perceptual Survey Results

Perceptual Order	Video Parameter	Highest Votes	Perceived Preferred Direction of Change	Notes
1	Upper body combination	32		Much improved
2	Decreased Walking Speed/ Cadence	22		Much clearer
2	Whole body combination	22		
4	Lower body combination	19		Lower highest category, however, higher cluster of votes
4	Increased Walking Base	19		
6	Decreased Hip Twist	18	Mixed/ Increased	Abandoned
7	Increased Torso Twist	17	Mixed/ Unclear	Abandoned
8	Increased Arm Abduction & decreased Arm Swing	15	Mixed/ Unclear	Inconclusive
9	Increased Hip & Torso Twist	14	Mixed/ Unclear	Abandoned
10	Increased Arm Bob	13	Mixed/ Unclear	Weak parameter

From these two tables we can list the motion parameters perceptual strengths in the following order of dominance:

1. Decreased Preferred Walking Speed
2. Increased Average Arm Abduction
3. Increased Walking Base
4. Decreased Arm Bob Magnitude
5. Decreased Arm Swing Magnitude

The perceptual surveys demonstrate that people expect walking speed to decrease over increases in obesity. This validates observations previous findings (Spyropoulos et al., 1991;

DeVita and Hortobágyi, 2003; Hulens et al., 2003; Vismara et al., 2007; Tompkins et al., 2008; Lai et al., 2008; Browning, 2012; da Silva-Hamu et al., 2013; Pataky et al., 2014).

Increases in walking base is also perceived to increase over obesity which also validates previous findings (Spyropoulos et al., 1991; Browning and Kram, 2007; Sarkar et al., 2011; Wu et al., 2012; Vartiainen et al., 2012).

As previous research focussed on lower body gait, the perception that arm abduction raises and arm bob and swing magnitude reduces over obesity is a new contribution to knowledge.

Previous research focussed on the actual correlation between anthropometrics and gait parameters however these tests demonstrate the perceived correlation which is a different contribution to knowledge.

7.2.3. Summary of Anthropometrics and Gait Analysis

These motion parameters are listed in order of perceptual dominance and the direction and strength of correlation with anthropometrics. r^2 estimates of effect size are included and their effect size classification according to Cohen (1988; 1992) Benchmark:

Table 7-3 - Appearance to Motion Parameter Correlations by Perceptual Dominance

Perceptual Order	Gait Parameter	Perceived Change	Actual Change	Correlation & Effect Size
1	Preferred Walking Speed	decrease	increase over **Height**	r^2= 0.149 (small)
2	Average Arm Abduction	increase	increase over **Chest Circumference**	r^2= 0.486 (large)
3	Walking Base	increase	increase over **WtHR**	r^2= 0.236 (medium)
4	Arm Bob Magnitude	decrease	slight increase over **Height**	r^2= 0.082 (small)
5	Arm Swing Magnitude	decrease	increase over **BF%**	r^2= 0.089 (small)

This framework can be utilised in an animation tool to model automatic and believable changes to gait based on changes to height and body shape.

8. DATA-DRIVEN ANIMATION MODIFIER

The scripted animation tool was now capable of deforming the topological morphology along a general body fat percentage scale as well as changing the structural height of a virtual character. Uniquely the variation in appearance will then modify multiple gait parameters. In part the tool builds upon Gleicher (2001) to motion warp plus inverse kinematics to slow down all keys whilst still offering the flexibility of IK control to reposition the feet.

Part of the inspiration for this tool was Troje's (2002) synthesized walker demonstration which featured sliders to vary motion by classifiers such as gender. Whilst this approach also used twenty male (and twenty female) motion captured walkers and analysed limb lengths (height was normalised), body morphology was not directly recorded or analysed. Gait parameters were not specifically being extracted and modified. In reality these separate datasets were being trained with pattern recognition to classify variations in structural and dynamic motion overall, as opposed to a more discrete biomechanical framework. Our scripted tool can modify these as they directly relate to a single or multiple anthropometric features such as height and body fat percentage. Our tool can be expanded to separately alter different gait parameters by different anthropometric generating greater character and locomotion generation.

Troje (2008) later went on to allow users to train the demonstration to classify the motion by their perceived weight mood, strength and any other. Our perceptual tests allowed us to analyse movements on a gait parameter basis as opposed to overall.

Our slider based scripted animation tool matches the simplicity of Neff & Kim (2009) making it as easy to edit motion styles, however crucially these modifications are not just based on artistic judgements but correlated with recorded anthropometric data.

Whilst our appearance to motion framework doesn't directly try and modify motion to avoid self-mesh penetration as Ho et al. (2013) does, by analysing correlations between anthropometrics such as chest and bicep circumference it is able to do this, mimicking real world attempts to avoid chafing.

By taking the results of the most perceptually dominant motion parameters and their strengths, as previously seen in Table 7-3, it was possible to update the scripted animation tool to modify the five parameters according to the predictive formulas.

The following section explains the changes that were made to the appearance modifier and the scripted motion modifier tool to be able to fully implement the scripted framework. Figure 8-1 shows the simple interface which allows modification of Body Fat Percentage and Height and the script running to modify gait parameter keyframes. Additional sliders are not visible or not fully enabled but in future can allow modification of separate anthropometrics to modify separate gait parameters. This was not implemented yet as it could alter the perceived overall metric of Body Fat Percentage in unpredictable ways.

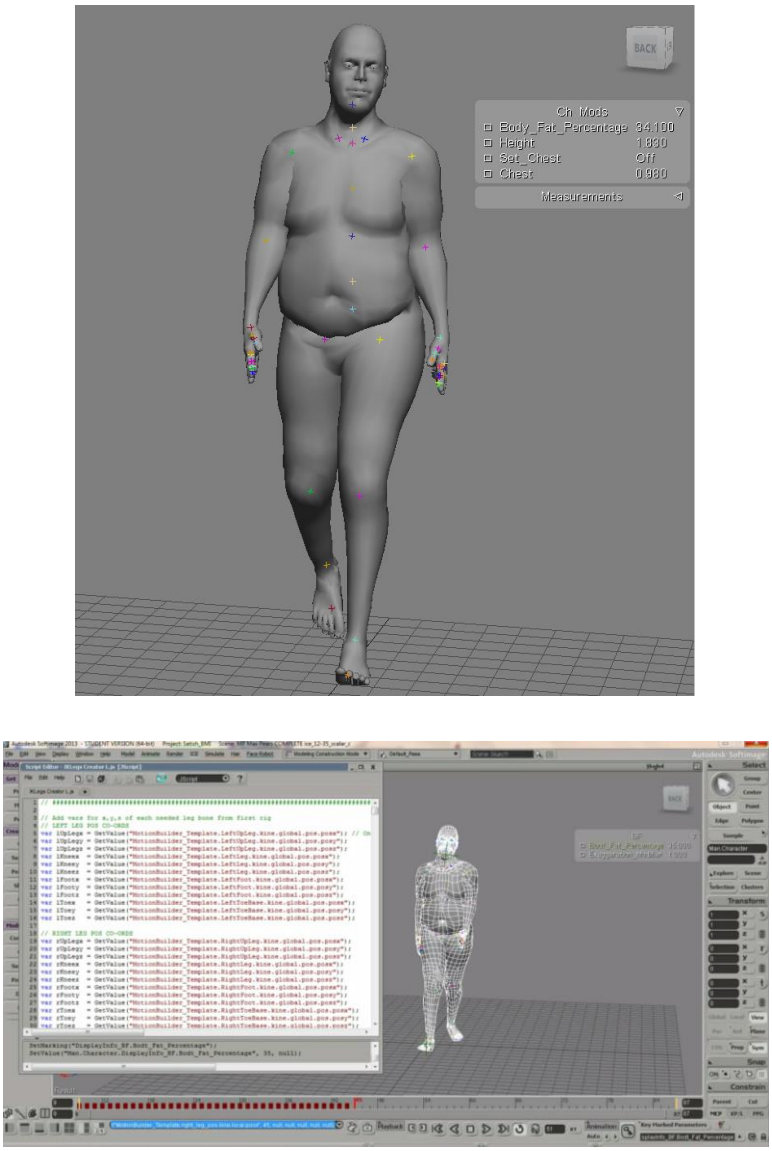

Figure 8-1 - Body Fat %, Height Slider Interface and Running Script

Finally the framework and animation tool is tested and validated in a live video based perceptual polling.

8.1. Scripted Animation Tool, Framework Modification

8.1.1. Preferred walking speed over Height

This was previously modelled but as the data showed the biggest correlation with speed was over height, the script needed to be modified to accommodate a height slider and skeletal scaler as seen in Figure 8-1.

```
65  //Scale Height before doing anything.
66  var ScaleHeight = ChHeight / leanHeight
67  // get local cordinates and move positions relative to character (effect: lengthen bones)
68  // LENGTHEN HEIGHT OF HIPS
69  var HipsLy  = GetValue("MotionBuilder_Template.Hips.kine.local.posy"); //may need small correction for feet to reach ground
70  SetValue("MotionBuilder_Template.Hips.kine.local.posy", HipsLy*ScaleHeight, null);
71  // LENGTHEN LEGS
72  var LeftLegLx    = GetValue("MotionBuilder_Template.LeftLeg.kine.local.posx");
73  SetValue("MotionBuilder_Template.LeftLeg.kine.local.posx", LeftLegLx*ScaleHeight, null);
```

Figure 8-2 - Height Slider and Skeletal scaler

The new formula was integrated:

$$Walking\ Speed = -1.07 + (1.3 * Height)$$

Equation 11 - Predicted Walking Speed by Height

8.1.2. Arm Abduction over Chest Circumference

This motion parameter was previously modelled but as the data showed the biggest correlation of arm abduction was over chest circumference, the arm abduction script was updated to integrate the new formula:

$$Average\ Arm\ Abduction\ Position = -31.42 + (39.97 * Chest\ Circumference)$$

Equation 12 - Predicted Average Arm Abduction by Chest Circumference

Based on mocap data analysis, the highest correlation was over Chest Circumference. For the purpose of this test, the chest circumference of the obese virtual characters blend shape was matched to the predicted dimensions at 35% Body Fat by recorded data.

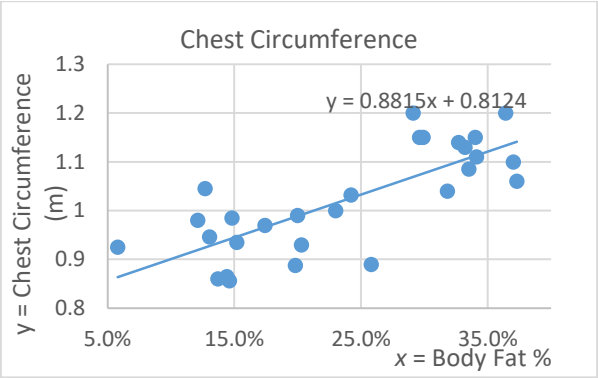

Figure 8-3 - Chest Circumference by Body Fat %

As the character deformed between 12%-35% body fat and beyond, the chest circumference of the obese character blend shape increases linearly between 0.98m-1.12m. The Body Fat % slider therefore also drives Chest Circumference as seen in Figure 8-1, however future modifications could integrate separate sliders for body sections. The reason that chest circumference, waist and hip circumferences were not allowed to be modified separately on the virtual characters obese blend shape, was because this could create the perception of a different Body Fat Percentage which would conflict with other parameters.

8.1.3. Walking Base over WtHR

Walking base had previously been modelled but as the data showed the biggest correlation that could be applied to virtual characters was over Waist-to-Hip Ratio, so the walking base script was updated to integrate the new formula:

$$Walking\ Base = -167.59 + (268.26 * WtHR)$$

Equation 13 - Predicted Walking Base by Waist to Hip Ratio

As previously mentioned, the waist and hip circumferences of the virtual character's obese blend shape were matched to the predicted value at 35% Body Fat so that as the Body Fat slider and deformation was applied the waist-to-hip ratio would linearly increase:

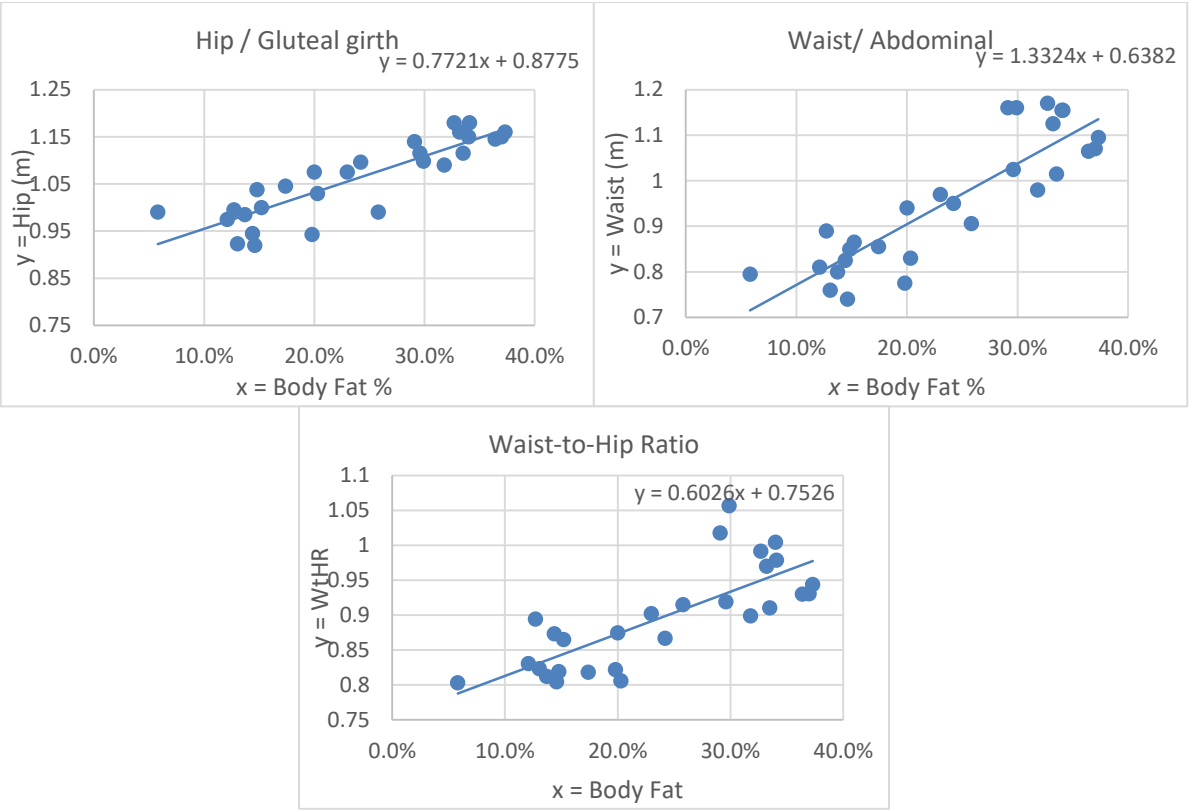

Figure 8-4 - Waist to Hip increases over Body Fat % (separate and combined)

8.1.4. Arm Bob Magnitude over Height

Arm bob magnitude had previously been modelled but as the data showed the biggest correlation that could be applied to virtual characters was over Height, the walking base script was updated to integrate the new formula:

$$Arm\ Bob\ Magnitude = -13.19 + (12.04 * Height)$$

Equation 14 - Predicted Arm Bob Magnitude by Height

8.1.5. Arm Swing Magnitude over BF%

Arm swing magnitude had also previously been modelled over body fat percentage, therefore the script simply needed updating with the formula based on the actual data captured:

$$Arm\ Swing\ Magnitude = 18.76 + (0.29 * BF)$$

Equation 15 - Predicted Arm Swing Magnitude by Body Fat Percentage

8.2. Final Perceptual Survey Design

Once the scripted animation tool had been updated with the formulas based on the actual data analysed, and the appearance modifications, the final test was to validate the appearance to motion framework and the scripted animation tools application of it. This was achieved by creating a final perceptual video poll.

The video comprised of four obese character meshes based on an obese participant codenamed 'AE'. The obese character meshes were scaled from 1.77m to 1.83m to match AE's height. The obese character mesh videos were driven by the walks put in the following randomised order:

A. MP's lean motion capture data
B. Keyframe animated in an obese style
C. MP's lean walk modified by scripted animation tool to deform five motion parameters
D. AE's obese motion capture data

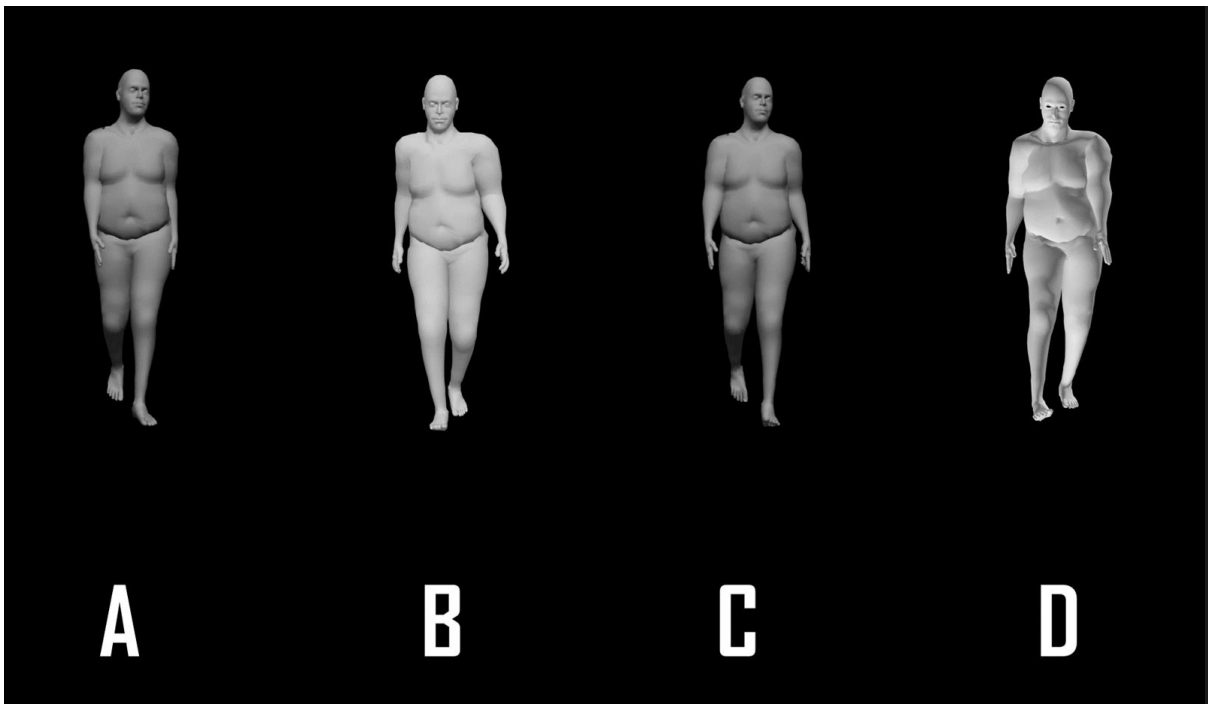

Figure 8-5 - Perceptual Video Poll to Validate the Appearance to Motion Parameter Framework

All characters were rendered out and edited together at 1080 x 1920 with plain grey shading, on a black background, walking towards the camera as this had proved the most effective approach previously. The four characters' order was randomised and they were edited together, side by side and labelled A,B,C,D in order of appearance.

8.2.1. Lean Motion Capture (A)

This data was derived from the previously used lean motion captured participants 'MP' who had the following attributes.

Table 8-1 MP's Lean Anthropometric Measurements

Metric	Metric
Ref No.	**MP**
Height (m)	1.758
BodyMass (weight kg)	70
Age (years	21
Fixed Speed (to 1.2m/s)	1.40
BMI =	**23**
STRUCTURAL LENGTHS	
Foot to hip (cm)	**95**
CIRCUMFERENCE	
Neck	0.37
Chest	0.98
Bicep/ arm girth relaxed	0.32
Waist/ Abdominal	0.81
Upper Body Total	**2.48**
Hip / Gluteal girth	0.975
Thigh	0.525
Calf	0.37
Lower Body Total	**1.87**
CIRCUMFERENCE TOTAL	**4.35**
WtHR =	**0.83**
BODY FAT PERCENTAGE	
InBody	**12.1%**

His character was scaled to match AE's comparative height of 1.83m.

8.2.2. Keyframe animated in obese style (B)

This data was keyframed by Stephie Johnson, a recent Teesside University animation graduate, who had not previously seen the other character walks and did not have access to the findings of my previous studies. Stephie was provided with the scaled obese character model and rig and was briefed to keyframe animate a walk cycle that matched her perception of the character's body shape and height. She was also asked to record the time it took to animate it, to compare the efficiency of this approach with the scripted animation tool.

8.2.3. Scripted Animation Tool (C)

This data was derived from the previously used lean motion captured participants 'MP' and then modified using the scripted animation tool to match 1.83m in height and 34.1% Body Fat.

8.2.4. Obese Motion Capture Data (D)

This data was derived from one of the motion captured participants 'AE' who had the following attributes.

Table 8-2 AE's Obese Anthropometric Measurements

Metric	
Ref No.	**AE**
Height (m)	1.83
BodyMass (weight kg)	112.4
Age (years	22
BMI =	**34**
STRUCTURAL LENGTHS	
Foot to hip (cm)	**1.03**
CIRCUMFERENCE	
Neck	0.435
Chest	1.11
Bicep/ arm girth relaxed	0.345
Waist/ Abdominal	1.155
Upper Body Total	**3.045**
Hip / Gluteal girth	1.18
Thigh	0.65
Calf	0.455
Lower Body Total	**2.285**
CIRCUMFERENCE TOTAL	**5.33**
WtHR =	**0.98**
BODY FAT PERCENTAGE	
InBody	**34.1%**

As AE fell on the obese side of the BMI and BF% scale his motion capture walk was considered ideal to test the scripted animation tool. Unlike other obese participants, AE also had above average height, and since this was a parameter that had been determined to be perceptually dominant, we chose his data and scaled the other comparative characters to match his height of 1.83m. His motion captured walk data was retargeted to the same obese character mesh as the previous video survey.

8.3. Polling Methodology

The looping video was screened on a large projector screen in front of 96 participating 3rd Year games design students at Teesside University on 24/11/16 as part of a lecture on research. The poll was conducted before this research project's aims and findings were fully explained.

Figure 8-6 - Turning Point live polling system

Turning Point (2016) was used to live poll students' opinion on which videos produced the most believable walking motion that matched the height and body shape of the character mesh. Students were requested to ignore any variations in lighting or glitchy mesh deformations. Anonymous participation in the polling was considered as consent and they were free to withdraw participation at any time. A videogame prize was offered as an incentive for participation and was awarded randomly. Turning Point assigned the following answer point values:

1st video rank awarded 4 points each

2nd video rank awarded 3 points each

3rd video rank awarded 2 points each

4th video rank awarded 1 points each

8.4. Polling Results

The results of the live polling were collated immediately and are as follows

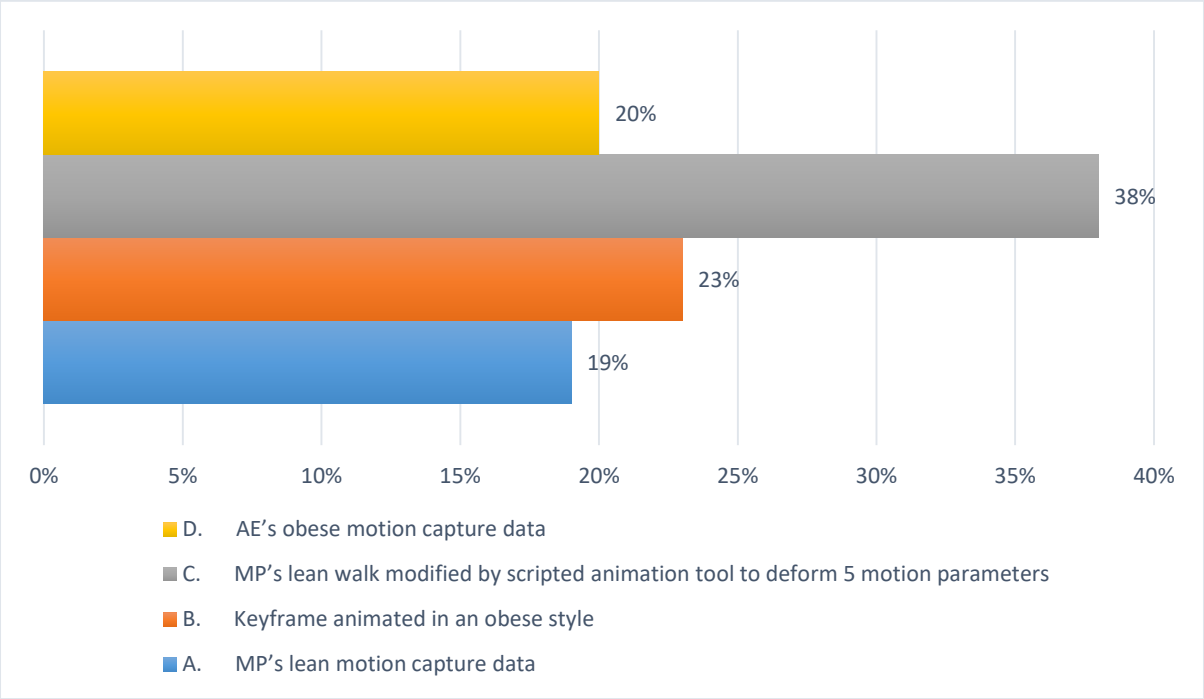

Figure 8-7 - Live Poll of Most Believable Motion Deformation Technique to Generate Obese Motion

The results of the live polling show that a 38% majority of viewers selected the appearance to motion framework and the scripted animation tool to be the most believable method to generate locomotion that matched the height and morphology of the obese character mesh.

Surprisingly in second ranking they selected the keyframe animated walk. Despite the animation not being polished, the parameter it most heavily exaggerated was walking speed, which had previously been determined to have the strongest effect on the perception of obese motion.

Thirdly the audience chose the actual obese motion. It was expected that this would have ranked highest, however there may be a number of factors which caused a lower ranking. AE's taller height caused challenges when rescaling the character non-linearly. Variations in leg length meant greater IK leg wobble was produced which could have proved slightly distracting. And whilst much of the framework and tool deforms appearance and motion

according to linear trendlines, there remains a huge human variation in body morphologies and walking styles that don't immediately fit perceptions of obesity.

Lastly as to be expected, the shorter, lean walk was chosen as the least believable match to the taller obese character mesh.

9. CONCLUSIONS

Our three main contributions to knowledge included an empirical study analysing perceived and actual changes of gait over body morphology, a framework of appearance to locomotion parameters that could be used to generate diverse, believable motion and a scripted animation tool that believably retargets lean gait to obese to different body morphologies.

Our empirical study collated, analysed and tested a range of published sources validating previously observed parameters such as preferred walking speed (Spyropoulos et al., 1991; DeVita and Hortobágyi, 2003; Hulens et al., 2003; Vismara et al., 2007; Tompkins et al., 2008; Lai et al., 2008; Browning, 2012; da Silva-Hamu et al., 2013; Pataky et al., 2014). Increases in walking base was validated (Spyropoulos et al., 1991; Browning and Kram, 2007; Sarkar et al., 2011; Wu et al., 2012; Vartiainen et al., 2012). Step width or walking base was also validated (Spyropoulos et al., 1991; Browning and Kram, 2007).

We found that the traditional anthropometric, Body Mass Index, is not always the most effective measurement when correlating appearance parameters with motion parameters. BMI incorporates height and mass but struggles to differentiate between fat mass and muscle mass. It fails to represent body shape the way Waist Circumference, Waist to Chest Ratio or Waist-to-Hip Ratio can. Keys (1972) noted that BMI was more appropriate for population studies and inappropriate for individual evaluation whilst Deurenberg et al. (2001) found that 8% of all men were incorrectly classified as obese using standard BMI cutoff points. BMI is also a difficult metric to map onto virtual characters as they have no mass. When reviewing our own data we found that a variety of different anthropometric parameters were more effective at providing correlations with gait parameters.

Our analysis verified Spyropoulos' (1991) observation that Average Preferred Walking Speed decreased and Walking Base increased over body morphology. Unfortunately McGraw's (2000) observation that posture became more erect over increases in body morphology could not be accurately tested and verified.

Based on the empirical data collected and analysed we have defined and validated a framework of anthropometric to locomotive gait correlations ordered by perceptual dominance and effect size. This framework can be used by animators and motion capture artists to efficiently and dynamically generate a diverse range of characters that not only vary in body morphology but also have varying walking styles that believably match their body shape.

Table 9-1- Effectiveness of Anthropometrics compared to BMI

Gait Parameter	**Anthropometric**	R^2	**Anthropometric**	R^2
Average Arm Abduction Position	Chest Circumference	0.4864	BMI	0.4222
Arm Swing Magnitude	Chest Circumference	0.3606	BMI	0.0128
Arm Bob Magnitude	Height	0.0819	BMI	5E-05
Average Preferred Walking Speed	Height	0.1486	BMI	0.0009
Walking Base	Mass	0.2356	BMI	0.1991

We hypothesised that by studying existing research and undertaking our own empirical study we can identify the most perceptually dominant motion parameters. Our research found that the following parameters were prioritised as perceptually dominant:

1. Decreased Preferred Walking Speed
2. Increased Average Arm Abduction
3. Increased Walking Base
4. Decreased Arm Bob Magnitude
5. Decreased Arm Swing Magnitude

This hypothesis was posed as the question was centred on whether we believe certain parameter correlations to be more influential in our perception of gait than actual scientific correlations.

By ordering the parameters by correlation effect size we can see some differences between what is perceived to be more influential and what actually is:

- Average Arm Abduction Position
↑ Arm Swing Magnitude
- Walking Base
↓ Average Preferred Walking Speed
↓ Arm Bob Magnitude

We found that people perceived a reduction in arm swing magnitude to be more influential to the perception of obese gait in comparison to the other ordered parameters. This could suggest that people expect certain characteristics to change more so, than ones that actually do. This challenges the validity of relying on perceptual based motion classification and synthesis (Troje, 2008).

Future work could include testing a framework of anthropometric to gait correlation prioritised by perceptually dominance versus a framework prioritised by actual correlation effect sizes.

We also hypothesised that by analysing changes in actual locomotion over changes in anthropometrics we can create a relaxed model of locomotion generation for obese characters. Our research found that the following anthropometric parameters, ordered by perceptual dominance, had the following effects on gait parameters.

Table 9-2 - Appearance to Motion Parameter Correlations by Perceptual Dominance

Perceptual Order	Gait Parameter	Perceived Change	Actual Change	Correlation & Effect Size
1	Preferred Walking Speed	decrease	increase over **Height**	r^2= 0.149 (small)
2	Average Arm Abduction	increase	increase over **Chest Circumference**	r^2= 0.486 (large)
3	Walking Base	increase	increase over **WtHR**	r^2= 0.236 (medium)
4	Arm Bob Magnitude	decrease	slight increase over **Height**	r^2= 0.082 (small)
5	Arm Swing Magnitude	decrease	increase over **BF%**	r^2= 0.089 (small)

Whilst we struggled to accurately record and verify McGraw et al. (2000) and de Souza (2005b) changes to spinal curvature over increases in obesity, our research in changes in upper body gait over increases in obesity is also a novel contribution to knowledge. As seen below in Figure 9-1, changes to upper body gait parameters are more influential in the perception of obese gait than lower body gait.

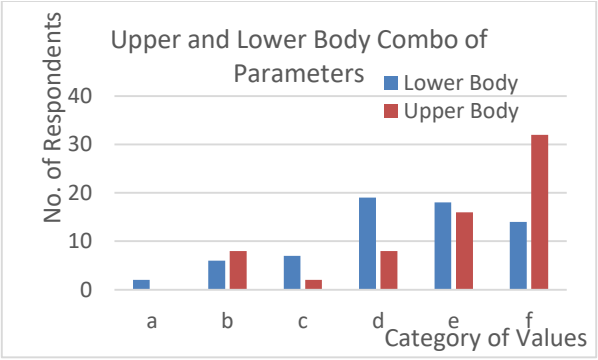

Figure 9-1 - Comparison of Upper and Lower Body Combo of Parameters

The framework was implemented in the final version of the scripted animation and validated with a perceptual poll. The scripted animation tool was ranked at 38%, a more believable generator of tall and obese motion than an actual obese motion captured walk.

The research provides animators and motion capture artists with a framework to generate a diverse range of characters that walk in a way that relates to their body shape. For animators and motion capture artists with limited or singular captures of walking data, this

empowers them to create a wide range of characters, saving them production time and improving believability.

Our final major contribution was the development of a scripted animation tool to test and apply the framework. This tool proved effective at believably retargeting lean locomotion data to taller or larger body morphology by modifying five gait parameters using a combination of motion warping plus IK, leg adjustments, foot constraints, and phase identification and amplification. These techniques have been used by the likes of Ho et al. (2013), Neff & Kim (2009) and Kim & Neff (2012) however none of these are correlated with anthropometric datasets and our tool has been tested to be more believable at modifying lean motion to obese motion than motion captured obese motion.

A number of alternative approaches exist that were considered outside of the scope of this process and approach as they were physics based or used machine learning.

Taylor & Hinton (2009) presented a model using Conditional Restricted Boltzmann Machines (CRBM) trained on Carngie Mellon University's (CMU) dataset to synthesize new motion with stride length and speed variables being manipulatable. In addition this system could transition and blend between styles. However as the CMU database contained no appearance data these variations are not constrained in any meaningful way to anthropometric variables. As the CRBM allowed a multiplicative three-way interaction between units, an anthropometric variable could serve as the third unit. Whilst Taylor & Hinton claimed their system could generate realistic motion, without available videos it is hard to assess how effectively this method avoids the perceived unnaturalness and foot sliding issues common to synthesized motion.

Kenwright (2011) uses centre of mass to balance synthesized characters using priority weighted inverse kinematic constraints. Whilst it was capable of creating a diverse range of actions its focus on centre of mass did not take into account conservation of energy or self-avoidance of mesh penetration. As the method is physics-based it once again falls victim to the production of unnatural poses that would need to be manually modified by an animator.

Holden et al. (2016) builds upon previous deep learning work by the likes of Taylor & Hinton (2009) to synthesize new editable motion trained on a motion capture database that breaks motion down into components and can add constraints whilst keeping the motion natural. This system allows the construction of the style of one motion to the timing of another. So whilst the neural network is not trained on motion with corresponding anthropometric data, this offers the possibility of combining our data driven method with the flexibility of deep learning frameworks.

Most recently Holden et al. (2017) presents a real-time character control mechanism using a neural network architecture. This Phase-Functioned Neural Network produces controllable motions trained from a large dataset of locomotions. Whilst highly adaptable to user control, variable terrain and edges, the neural network is trained on a variety of motions with no recording, analysis or correlation with anthropometrics. However by combining our data driven approach this could in future extend the systems capability beyond locomotion.

These were initially not considered due to the potential for unnatural motion, however the flexibility of their methods means it would be worthy to consider hybridising these approaches with ours.

Based on the empirical data collected and analysed we have defined and validated a framework of anthropometric to locomotive gait correlations ordered by perceptual dominance and effect size. This framework can be used by animators and motion capture artists to efficiently and dynamically generate a diverse range of characters that not only vary in body morphology but also have varying walking styles that believably match their body shape.

10. RECOMMENDATIONS & FUTURE WORK

Whilst the research could be considered a success against its original objectives, upon reviewing the project as a whole a number of areas remain that are ripe for future exploration.

Initially we analysed gait parameters that viewers perceived to give the impression of obese gait. However further analysis of the data, could be undertaken to understand if and how people of different gender, age and experience view these parameters. As this study was exploratory, it would be desirable to expand the sample size to at least 109. This would make results more reliable for the appearance and locomotion data.

The questionnaire asked participants to identify whether they were a member of the public or have a background in animation or biomechanics. Whilst this data was not analysed, it could be revisited to assess whether those with a background in movement were better able to detect modified motion.

It would be highly interesting to capture a larger useable sample of female participants. Whilst female body morphology obviously differs from males, female gait also differs significantly to male gait (Kozlowski and Cutting, 1977). Therefore any changes in appearance to gait correlations may also change. Whilst five female participants were motion captured, this was considered too small a sample size, but could form a basis to expand the research. In addition to gender it may also be interesting to explore the effects of sexuality on the masculine or feminine qualities of a walking style.

As many motion capture volunteers were sourced from Teesside University the average age was quite young at 27 years old, so this would be another potential area to expand the research to include younger and older participants.

Whilst it is unforeseeable that different racial ethnicities have distinct walking styles, population data for certain countries or regions might reveal socio-economic and dietary trends that influence walking styles.

Whilst the data modifies motion in relation to people's body shape, potentially it could also be used to adjust motion based on personality types. Satchell et al. (2016) recently determined a correlation between aggressive personality types and exaggerated gait swagger. This data could be added to the framework as another optionally adjustable motion modifier.

This research was started on the observation of distinct walk cycles of obese people. Whilst a range of body morphologies were recorded, the highest BMI of a participant was 34. It is believed that even more characteristic walk cycles could be observed and modelled from those who the World Health Organisation (1995; 2000) had classified with a BMI of 40 being labelled as Obesity III; morbidly obese.

Another reason for the distinctiveness of severely obese gait could be the increased likelihood of gait impairments. Whilst we only record participants who had no gait impairments, this might prove a future area of observation, especially if they are more likely to occur with those of large body morphologies.

Capturing more morbidly obese participants would require the anticipation of further breaks during the motion capture process due to potential health risks or fatigue. However this brings to mind another area for potential expansion of the model; average time for walking fatigue, as this could also improve the believability of the framework at the extreme end of the anthropometric scales. Based on average time for fatigue, the framework could blend the motion into a tired idle clip for a recovery time, before blending back into the walk cycle, further improving believability.

Much of the research was focussed on tracking changes in locomotion over a linear anthropometric such as body fat percentage or BMI. However the results of the research show that certain anthropometrics have larger effects on localised areas of locomotion than others. Further work could be undertaken to determine the effects of anthropometric data on each of the major limbs. This would provide much finer control on the generation of character appearance and individual locomotion.

Whilst the bio-electrical impedance method of recording body fat percentage was fast and non-invasive it would be desirable to try previously inaccessible measurement methods

such as hydro-densitometry or the Body Volume Index method (see Appendix C). The BVI method also appears to automatically record body limb circumference data, which would enable automatic and faster data correlations with localised motion parameters.

As McGraw et al. (2000) and de Souza (2005b) had previously observed changes in spinal curvature over increases in BMI we were disappointed to find that due to the tautness of the motion capture suits we were unable to accurately record and measure this anthropometric parameter. We hypothesise that this is to maintain balance over the centre of mass so in future it would be desirable to find an alternative method to measure and model this parameter.

The motion capture process proved accurate to a sub-millimeter level of tracking, however there are a number of areas for errors to creep into the process. Spinal erectness had already proved difficult to capture, and on participants with larger amounts of adipose tissue, the mocap suit could have slid more. It would be interesting to quantify the degree of marker slippage and inaccuracy caused by larger adipose areas on the body.

Perry (2012) was used as photographic reference for male body shapes of body fat classifications in the absence of any consensus on how people accumulate body fat in different areas of their body over time. This may extend outside of the boundaries of this research project however it would be highly useful to collect and analyse large datasets of body circumferences over periods of weight gain.

As Dobbyn et al. (2006) had been exploring clothing variation to virtual characters it could be beneficial to also add clothing to the data driven framework. Whilst all participants had to wear the simple and tight motion capture suits further explorations could measure and model the effects of changes in clothes, bags and weaponry to the centre of gravity and average walking and running speeds. These are the typical additions added to virtual characters in video games.

Whilst the research focussed on changes to locomotion over increases in body morphology, other action clips commonly recorded in motion capture for use in games and animation include running and jumping. Recording and analysing changes to these motion parameters over increases in body morphology could expand the usefulness of the framework and

implementation in character and crowd simulation systems. This could be achieved by a hybridised physics based motion system. The motion capture data also included measurements for centre of gravity and mass so it would be interesting to relate changes in parameters such as walking base and arm swing to these physical parameters.

Whilst the animation tool is based on data driven observations of body morphology it would be useful to track these changes more closely and have them simulated directly back into the virtual locomotion system. This could be done by modelling adipose oscillation. Muscle activation could also be measured and then simulated beneath the fat layer. A combination of skeletal, muscular and adipose layers could then present a data driven alternative to Weta Digital's Tissue System (2017).

Currently the animation tool is scripted in JavaScript to modify keyframe animation data within the Softimage animation package. This can take a couple of minutes to fully run, however the applications for the animation framework could be applied to game engines. The animation tool could therefore benefit from optimisation or recoding to run in real-time.

The tool also has the potential for further development to incorporate path planning and random character generation. In addition to incorporating these well researched areas, further research could explore the volume or width of personal body space and character avoidance that varies not just by crowd density but also by increases in body morphologies.

Ultimately the research aimed to discover whether it was possible to modify a lean walk cycle based on analysed data to appear obese, to an equally believable degree as actual obese motion. It succeeded - even appearing more believable than actual obese motion. The aim was to save animators time keyframing obese motion or modifying lean motion to appear obese. However one final test could be to test whether a lean actor can act obese and appear to be as believable as the tool. This final test could also extend to any future expansions to include women, children, ethnicities and personalities.

11. REFERENCES

Abate, N., Burns, D., Peshock, R.M., Garg, A. and Grundy, S.M. (1994) 'Estimation of adipose tissue mass by magnetic resonance imaging: validation against dissection in human cadavers', *Journal of Lipid Research, 35*(8), pp. 1490-1496.

Allen, B., Curless, B. and Popović, Z. (2004) 'Exploring the Space of Human Body Shapes: Data-Driven Synthesis Under Anthropometric Control'. In *Proceedings of Conference on Digital Human Modeling for Design and Engineering. SAE Technical Paper 2004-01-2188*.

American Council on Exercise (2003) *ACE Personal Trainer Manual.* 3rd edn. Healthy Learning.

Army, U.S., (2011) 'Standards of medical fitness', *Washington, DC: Department of the Army, 4*.

Ashwell, M., Gunn, P. and Gibson, S. (2012) 'Waist-to-height ratio is a better screening tool than waist circumference and BMI for adult cardiometabolic risk factors: systematic review and meta-analysis', *Obesity Reviews, 13*(3), pp. 275-286.

Ashwell, M. (2011) 'Charts based on body mass index and waist-to-height ratio to assess the health risks of obesity: a review', *Open Obesity Journal, 3*, pp. 78-84.

Association of Life Insurance Medical Directors (1912) 'actuarial society of America', *Medico-Actuarial Mortality Investigation, 1*, p. 38.

Aubel, A. and Thalmann, D., 2000. Realistic deformation of human body shapes. In *Computer Animation and Simulation 2000. Eurographics.* Springer, Vienna, pp. 125-135.

August, B. and Count, E. (1981) *The Complete Bonnie August's Dress Thin System: 642 Ways to Correct Figure Faults with Clothes.* Rawson: Wade Publishers.

Autodesk (2015) *Softimage* (Version 2015) [Computer Program] Available at http://www.autodesk.com/products/softimage/overview (Accessed 18/02/17).

Azuola, F., Badler, N.I., Ho, P.H., Kakadiaris, I., Metaxas, D. and Ting, B.J. (1994) 'Building anthropometry-based virtual human models', In *Proceedings of the IEEE IMAGE VII Conference*, Tucson, AZ.

Barreira, T.V., Harrington, D.M., Staiano, A.E., Heymsfield, S.B. and Katzmarzyk, P.T. (2011) 'Body adiposity index, body mass index, and body fat in white and black adults', *The Journal of the American Medical Association, 306*(8), pp. 828-830.

Bates, C. (2010) *Throw out the scales! 3D body scanner will tell you if you're overweight... and reveal all your lumps and bumps* [Webpage]. Available at:

http://www.dailymail.co.uk/health/article-1320086/3D-body-scanner-tell-youre-overweight--reveal-lumps-bumps.html#ixzz3dWMnRvCP (Accessed: 18/02/17).

Baty (2015) *Harpenden Skinfold Caliper* [Hardware]. Available at: http://www.harpenden-skinfold.com/measurements.html (Accessed: 18/02/17).

Baumgartner, R.N., Heymsfield, S.B., Lichtman, S., Wang, J. and Pierson, R.N.,Jr (1991) 'Body composition in elderly people: effect of criterion estimates on predictive equations', *The American Journal of Clinical Nutrition, 53*(6), pp. 1345-1353.

Becque, M.D., Katch, V.L. and Moffatt, R.J. (1986) 'Time course of skin-plus-fat compression in males and females', *Human Biology*, pp. 33-42.

Bergman, R.N., Stefanovski, D., Buchanan, T.A., Sumner, A.E., Reynolds, J.C., Sebring, N.G., Xiang, A.H. and Watanabe, R.M. (2011) 'A better index of body adiposity', *Obesity, 19*(5), pp. 1083-1089.

Bergsma–Kadijk, J.A., Baumeister, B. and Deurenberg, P. (1996) 'Measurement of body fat in young and elderly women: comparison between a four-compartment model and widely used reference methods', *British Journal of Nutrition, 75*(05), pp. 649-657.

Bindiganavale, R. (2000) 'Building parameterized action representations from observation', DPhil thesis, University of Pennsylvania.

Björntorp, P. (1984) 'Hazards in subgroups of human obesity', *European Journal of Clinical Investigation, 14*(4), pp. 239-241.

Bjorntorp, P. (1985) 'Obesity and the risk of cardiovascular disease', *Annals of Clinical Research, 17*(1), pp. 3-9.

Boulic, R., Capin, T., Huang, Z., Kalra, P., Lintermann, B., Magnenat-Thalmann, N., Moccozet, L., Molet, T., Pandzic, I. and Saar, K. (1995) 'The HUMANOID environment for interactive animation of multiple deformable human characters', *Computer Graphics Forum, 14*(3), pp. 337-348.

Boyd, E. (1935) *The Growth of the Surface Area of the Human Body*. University of Minnesota Press, Milford.

Browning, R.C. and Kram, R. (2007) 'Effects of obesity on the biomechanics of walking at different speeds', *Medicine and Science in Sports and Exercise, 39*(9), p. 1632-1641.

Brožek, J., Grande, F., Anderson, J.T. and Keys, A. (1963) 'Densitometric analysis of body composition: revision of some quantitative assumptions*', *Annals of the New York Academy of Sciences, 110*(1), pp. 113-140.

Choi, K. and Ko, H. (1999) 'On-line motion retargetting', *Computer Graphics and Applications.* In *Proceedings. Seventh Pacific Conference on. IEEE*, pp. 32-42.

Christou, D.D., Gentile, C.L., DeSouza, C.A., Seals, D.R. and Gates, P.E. (2005) 'Fatness is a better predictor of cardiovascular disease risk factor profile than aerobic fitness in healthy men', *Circulation,* 111(15), pp. 1904-1914.

Cohen, J. (1988) *Statistical power analysis for the behavioral sciences* 2ND edn. Hillsdale, NJ: Lawrence Earlbaum Associates. pp.20-26.

Cohen, J. (1992). 'A power primer', *Psychological bulletin, 112*(1), p.155-159.

Connell, L.J., Ulrich, P.V., Brannon, E.L., Alexander, M. and Presley, A.B. (2006) 'Body Shape Assessment Scale: Instrument Development Foranalyzing Female Figures', *Clothing and Textiles Research Journal, 24*(2), pp. 80-95.

COSMED (2015) *COSMED - BOD POD GS: Gold Standard Body Composition* [Hardware]. Available at: http://www.bodpod.com/en/products/body-composition/adult-children-bod-pod-gs (Accessed: 18/02/17).

Cutting, J.E. and Kozlowski, L.T. (1977) 'Recognizing friends by their walk: Gait perception without familiarity cues', *Bulletin of the Psychonomic Society, 9*(5), pp. 353-356.

Cutting, J.E., Proffitt, D.R. and Kozlowski, L.T. (1978) 'A biomechanical invariant for gait perception', *Journal of Experimental Psychology: Human Perception and Performance, 4*(3), p. 357-372.

da Silva-Hamu, T.C.D., Formiga, C.K.M.R., Gervásio, F.M., Ribeiro, D.M., Christofoletti, G. and de França Barros, J. (2013) 'The impact of obesity in the kinematic parameters of gait in young women', *International Journal of General Medicine, 6*, p. 507-513.

Davis, R.B., Ounpuu, S., Tyburski, D. and Gage, J.R. (1991) 'A gait analysis data collection and reduction technique', *Human Movement Science, 10*(5), pp. 575-587.

de Heras Ciechomski, P., Schertenleib, S., Maïm, J., Maupu, D. and Thalmann, D. (2005) 'Real-time shader rendering for crowds in virtual heritage', *VAST.* (5), pp. 1-8.

de Souza, S.A.F., Faintuch, J., Valezi, A.C., Sant'Anna, A.F., Gama-Rodrigues, J.J., de Batista Fonseca, I.C., and de Melo, R.D. (2005b) 'Postural changes in morbidly obese patients', *Obesity Surgery, 15*(7), pp. 1013-1016.

de Souza, S.A.F., Faintuch, J., Valezi, A.C., Sant'Anna, A.F., Gama-Rodrigues, J.J., de Batista Fonseca, I.C., Souza, R.B. and Senhorini, R.C. (2005a) 'Gait cinematic analysis in morbidly obese patients', *Obesity Surgery, 15*(9), pp. 1238-1242.

Dempster, P. and Aitkens, S. (1995) 'A new air displacement method for the determination of human body composition', *Medicine and Science in Sports and Exercise, 27*(12), pp. 1692-1697.

Deurenberg, P., Weststrate, J.A. and Seidell, J.C. (1991) 'Body mass index as a measure of body fatness: age-and sex-specific prediction formulas', *British Journal of Nutrition, 65*(02), pp. 105-114.

Deurenberg, P., Yap, M. and Van Staveren, W.A. (1998) 'Body mass index and percent body fat: a meta analysis among different ethnic groups', *International Journal of Obesity, 22*(12), pp. 1164-1171.

Deurenberg, P., Andreoli, A., Borg, P., Kukkonen-Harjula, K., de Lorenzo, A., van Marken Lichtenbelt, W.D., Testolin, G., Vigano, R. and Vollaard, N. (2001) 'The validity of predicted body fat percentage from body mass index and from impedance in samples of five European populations', *European Journal of Clinical Nutrition, 55*(11), pp. 973-979.

Deurenberg-Yap, M., Schmidt, G., Van Staveren, W. and Deurenberg, P. (2000) 'The paradox of low body mass index and high body fat percentage among Chinese, Malays and Indians in Singapore', *International Journal of Obesity and Related Metabolic Disorders, 24*(8), pp. 1011-1017.

DeVita, P. and Hortobágyi, T. (2003) 'Obesity is not associated with increased knee joint torque and power during level walking', *Journal of Biomechanics, 36*(9), pp. 1355-1362.

Dobbelsteyn, C.J., Joffres, M.R., MacLean, D.R. and Flowerdew, G. (2001) 'A comparative evaluation of waist circumference, waist-to-hip ratio and body mass index as indicators of cardiovascular risk factors. The Canadian Heart Health Surveys', *International Journal of Obesity and Related Metabolic Disorders: Journal of the International Association for the Study of Obesity, 25*(5), pp. 652-661.

Dobbyn, S., McDonnell, R., Kavan, L., Collins, S. and O'Sullivan, C., (2006) 'Clothing the masses: real-time clothed crowds with variation'. *Eurographics Short Papers*, pp. 103-106.

Douty, H. (1968) 'Silhouette photography for the study of visual somatometry and body image', *National Textile and Clothing Meeting, Minneapolis, Minnesota.*

Du Bois, D. and Du Bois, E.F. (1989) 'A formula to estimate the approximate surface area if height and weight be known. 1916', *Nutrition (Burbank, Los Angeles County, Calif.), 5*(5), pp. 303-11.

Durnin, J. and Womersley, J. (1974) 'Body fat assessed from total body density and its estimation from skinfold thickness: measurements on 481 men and women aged from 16 to 72 years', *British Journal of Nutrition, 32*(1), pp. 77-97.

Eknoyan, G. (2008) 'Adolphe Quetelet (1796-1874)--the average man and indices of obesity', *Nephrology, Dialysis, Transplantation: Official Publication of the European Dialysis and Transplant Association - European Renal Association, 23*(1), pp. 47-51.

Elliott, D. and Smith, D. (1993) 'Football stadia disasters in the United Kingdom: learning from tragedy?', *Organization & Environment, 7*(3), pp. 205-229.

Essa, S. (2012) *Gait Analysis.* Available at: http://www.slideshare.net/shimaa2022/gait-analysis-15743497 (Accessed: 18/02/17).

Fan, J., Dai, W., Qian, X., Chau, K. and Liu, Q. (2007) 'Effects of shape parameters on the attractiveness of a female body', *Perceptual and Motor Skills, 105*(1), pp. 117-132.

Fan, J., Dai, W., Liu, F. and Wu, J. (2005) 'Visual perception of male body attractiveness', *Proceedings. Biological Sciences / the Royal Society, 272*(1560), pp. 219-226.

Feng, A., Huang, Y., Xu, Y. and Shapiro, A., (2014). 'Fast, automatic character animation pipelines.' *Computer Animation and Virtual Worlds, 25*(1), pp.3-16.

Freedman, D.S., Thornton, J.C., Pi-Sunyer, F.X., Heymsfield, S.B., Wang, J., Pierson, R.N., Blanck, H.M. and Gallagher, D. (2012) 'The body adiposity index (hip circumference÷ height1. 5) is not a more accurate measure of adiposity than is BMI, waist circumference, or hip circumference', *Obesity, 20*(12), pp. 2438-2444.

Gallagher, D., Visser, M., Sepulveda, D., Pierson, R.N., Harris, T. and Heymsfield, S.B. (1996) 'How useful is body mass index for comparison of body fatness across age, sex, and ethnic groups?', *American Journal of Epidemiology, 143*(3), pp. 228-239.

GE Healthcare (2013) *Lupar DPX NT - DXA for Bone Health* [Hardware]. Available at: http://www3.gehealthcare.com.au/en-au/products/categories/bone_health/dxa/dpx_nt (Accessed: 18/02/2017).

Gehan, E.A. and George, S.L. (1970) 'Estimation of human body surface area from height and weight', *Cancer Chemotherapy Reports. Part 1, 54*(4), pp. 225-235.

Gibbons, W.J., Fruchter, N., Sloan, S. and Levy, R.D. (2001) 'Reference values for a multiple repetition 6-minute walk test in healthy adults older than 20 years', *Journal of Cardiopulmonary Rehabilitation and Prevention, 21*(2), pp. 87-93.

Ginsberg, H.N. (2000) 'Insulin resistance and cardiovascular disease', *The Journal of Clinical Investigation, 106*(4), pp. 453-458.

Gleicher, M. (1997) 'Motion editing with spacetime constraints', *Proceedings of the 1997 symposium on Interactive 3D graphics.* ACM, pp. 139-140.

Gleicher, M. (1998) 'Retargetting motion to new characters', *Proceedings of the 25th annual conference on Computer graphics and interactive techniques.* ACM, pp. 33-42.

Gleicher, M. (2001) 'Comparing constraint-based motion editing methods', *Graphical Models, 63*(2), pp. 107-134.

Gosselin, D., Sander, P.V. and Mitchell, J.L. (2005) 'Drawing a crowd', *ShaderX3 - Advanced Rendering with DirectX and OpenGL,* pp. 505-517.

Green, S.B. (1991). 'How many subjects does it take to do a regression analysis?' *Multivariate Behavioral Research*, *26*(3), pp. 499-510.

Han, T., McNeill, G. and Baras, P. (1995) 'Waist circumference relates to intra-abdominal fat mass better than waist: hip ratio', *Proceedings of the Nutrition Society, 54*, p. 182.

Haycock, G.B., Schwartz, G.J. and Wisotsky, D.H. (1978) 'Geometric method for measuring body surface area: a height-weight formula validated in infants, children, and adults', *The Journal of Pediatrics, 93*(1), pp. 62-66.

Health and Kinesiology Facilities. (2015) [Webpage] Available at: http://www.tamuk.edu/cehp/hkn/facilities.html (Accessed: 18/02/17).

Hecker, C., Raabe, B., Enslow, R.W., DeWeese, J., Maynard, J. and van Prooijen, K. (2008) 'Real-time motion retargeting to highly varied user-created morphologies', *ACM Transactions on Graphics*, *27*(3) pp. 1-11.

Height, M. and Tables, W. (1983) 'Metropolitan life foundation', *Statistical Bulletin, 64*(1), pp. 2-9.

Heitmann, B.L. and Frederiksen, P. (2009) 'Thigh circumference and risk of heart disease and premature death: prospective cohort study', *British Medical Journal,* 339: b3292.

Hertzmann, A., O'Sullivan, C. and Perlin, K. (2009) 'Realistic human body movement for emotional expressiveness', *ACM SIGGRAPH 2009 Courses.* ACM, pp. 1-20.

Heymsfield, S.B., Martin-Nguyen, A., Fong, T.M., Gallagher, D. and Pietrobelli, A. (2008) 'Body circumferences: clinical implications emerging from a new geometric model', *Nutrition & Metabolism, 5*(24).

Ho, E.S., Shum, H.P., Cheung, Y. and Yuen, P.C. (2013) 'Topology Aware Data-Driven Inverse Kinematics', *Computer Graphics Forum.* Wiley Online Library, pp. 61-70.

Hodgdon, J.A. and Beckett, M.B. (1984) *Prediction of Percent Body Fat for US Navy Women from Body Circumferences and Height,* San Diego: Naval Health Researcher Center.

Hodgins, J.K., O'Brien, J.F. and Tumblin, J. (1998) 'Perception of human motion with different geometric models', *Visualization and Computer Graphics, IEEE Transactions on, 4*(4), pp. 307-316.

Holden, D., Komura, T. and Saito, J., (2017) 'Phase-functioned neural networks for character control', *ACM Transactions on Graphics (TOG), 36*(4), p.42.

Holden, D., Saito, J. and Komura, T., (2016). 'A deep learning framework for character motion synthesis and editing'. *ACM Transactions on Graphics (TOG), 35*(4), p.138.

Houtkooper, L.B., Lohman, T.G., Going, S.B. and Howell, W.H. (1996) 'Why bioelectrical impedance analysis should be used for estimating adiposity', *The American Journal of Clinical Nutrition, 64*(3 Suppl), pp. 436-448.

Hsu, E., Pulli, K. and Popović, J., (2005) 'Style translation for human motion.' In *ACM Transactions on Graphics (TOG), 24*(3), pp. 1082-1089). ACM.

Hulens, M., Vansant, G., Claessens, A., Lysens, R. and Muls, E. (2003) 'Predictors of 6-minute walk test results in lean, obese and morbidly obese women', *Scandinavian Journal of Medicine & Science in Sports, 13*(2), pp. 98-105.

InBody Co., Ltd. (2014) *InBody 720* [Hardware]. Available at: http://www.inbody.com/global/product/InBody720.aspx (Accessed: 19/06/2015).

Insurance, Metropolitan Life (1959) 'New weight standards for men and women', *Statistical Bulletin Metropolitan Life Foundation, 40*, pp. 1-4.

Jackson, A.S. and Pollock, M.L. (1985) 'Practical assessment of body-composition', *Physician and Sportsmedicine, 13*(5), pp. 76-90.

Johansson, G. (1973) 'Visual perception of biological motion and a model for its analysis', *Attention, Perception, & Psychophysics, 14*(2), pp. 201-211.

Johansson, G. (1976) 'Spatio-temporal differentiation and integration in visual motion perception', *Psychological Research, 38*(4), pp. 379-393.

Kadaba, M.P., Ramakrishnan, H. and Wootten, M. (1990) 'Measurement of lower extremity kinematics during level walking', *Journal of Orthopaedic Research, 8*(3), pp. 383-392.

Kahn, B.B. and Flier, J.S. (2000) 'Obesity and insulin resistance', *The Journal of Clinical Investigation, 106*(4), pp. 473-481.

Kasap, M. and Magnenat-Thalmann, N. (2007) 'Parameterized human body model for real-time applications', *Cyberworlds, 2007. CW'07. International Conference on.* IEEE, pp. 160-167.

Kasap, M. and Magnenat-Thalmann, N. (2008) 'Modeling individual animated virtual humans for crowds', *ACM SIGGRAPH ASIA 2008 courses.* ACM, pp. 1-8.

Kasap, M. and Magnenat-Thalmann, N. (2009) 'Sizing avatars from skin weights', *Proceedings of the 16th ACM Symposium on Virtual Reality Software and Technology.* ACM, pp. 123-126.

Kasap, M. and Magnenat-Thalmann, N. (2010) 'Customizing and Populating Animated Digital Mannequins for Real-Time Application', *Cyberworlds (CW), 2010 International Conference on.* IEEE, pp. 368-374.

Kaur, A. (2014) *Gait.* [Lecture slides] Available at: http://www.slideshare.net/AmritKaur7/gait-34715786?related=2 (Accessed: 18/02/17).

Kenwright, B., (2012), 'Synthesizing Balancing Character Motions'. In *VRIPHYS,* pp. 87-96.

Keys, A. (1955) 'Body composition and its change with age and diet', *Weight Control*, pp. 18-28.

Keys, A. (1955) 'Obesity and heart disease', *Journal of Chronic Diseases, 1*(4), pp. 456-461.

Keys, A. and Brozek, J. (1953) Body fat in adult man. *Physiological Reviews*, *33*(3), pp. 245-325.

Keys, A., Fidanza, F., Karvonen, M.J., Kimura, N. and Taylor, H.L. (1972) 'Indices of relative weight and obesity', *Journal of Chronic Diseases, 25*(6), pp. 329-343.

Keys, A. (1954) 'Obesity and degenerative heart disease', *American Journal of Public Health and the Nation's Health, 44*(7), pp. 864-871.

Kim, Y. and Neff, M., (2012). 'Automating Expressive Locomotion Generation'. *Trans. Edutainment, 7*, pp.48-61.

Kissebah, A.H. and Krakower, G.R. (1994) 'Regional adiposity and morbidity', *Physiological Reviews,* 74(4), pp. 761-811.

Ko, S., Stenholm, S., Metter, E.J. and Ferrucci, L. (2012) 'Age-associated gait patterns and the role of lower extremity strength–results from the Baltimore Longitudinal Study of Aging', *Archives of Gerontology and Geriatrics, 55*(2), pp. 474-479.

Kohout, J., Kelnhoffer, P., Cholt, D., Kohoutová, E., Clapworthy, G., Zhao, Y., Tao, Y., Gonzalez-Garcia, G. and Dong, F. (2012) 'Fibre-based models of muscle wrapping'. Virtual Physiological Human.

Korenfeld, Y., Ngwa, T., Friedman, L., Romero-Corral, A., Xu, L., Albuquerque, F., Sert-Kuniyoshi, F., Okcay, A., Somers, V. and Lopez-Jimenez, F. (2009) 'Validation of a novel 3D body scanner for

obesity anthropometric measurements', *AHA 26th Princeton Conference on Cerebrovascular Disease, Houston, Texas, USA March.*

Kozlowski, L.T. and Cutting, J.E. (1977) 'Recognizing the sex of a walker from a dynamic point-light display', *Perception & Psychophysics, 21*(6), pp. 575-580.

Kozlowski, L.T. and Cutting, J.E. (1978) 'Recognizing the gender of walkers from point-lights mounted on ankles: Some second thoughts', *Attention, Perception, & Psychophysics, 23*(5), p. 459.

Krakauer, N.Y. and Krakauer, J.C. (2012) 'A new body shape index predicts mortality hazard independently of body mass index', *PLoS One, 7*(7), p. e39504.

Krakauer, N.Y. and Krakauer, J.C. (2014) 'Dynamic association of mortality hazard with body shape', *PloS One, 9*(2), p.e88793.

Kushner, R.F., Gudivaka, R. and Schoeller, D.A. (1996) 'Clinical characteristics influencing bioelectrical impedance analysis measurements', *The American Journal of Clinical Nutrition, 64*(3 Suppl), pp. 423-427.

Lai, P.P., Leung, A.K., Li, A.N. and Zhang, M., (2008) 'Three-dimensional gait analysis of obese adults'. *Clinical biomechanics*, *23*, pp.S2-S6.

Lee, S., Sifakis, E. and Terzopoulos, D. (2009) 'Comprehensive biomechanical modeling and simulation of the upper body', *ACM Transactions on Graphics (TOG), 28*(4), pp. 1-17.

Lee, Y., Terzopoulos, D. and Waters, K. (1995) 'Realistic modeling for facial animation', *Proceedings of the 22nd annual conference on Computer graphics and interactive techniques.* ACM, pp. 55-62.

Lukaski, H.C., Bolonchuk, W.W., Hall, C.B. and Siders, W.A. (1986) 'Validation of tetrapolar bioelectrical impedance method to assess human body composition', *Journal of Applied Physiology, 60*(4), pp. 1327-1332.

Lyard, E. and Magnenat-Thalmann, N. (2008) 'Motion adaptation based on character shape', *Computer Animation and Virtual Worlds, 19*(3-4), pp. 189-198.

Macmillan, N.A. and Creelman, C.D. (2004) *Detection theory: A user's guide.* 2ND edn. Hillsdale, NJ: Lawrence Earlbaum Associates.

Maessen, M.F., Eijsvogels, T.M., Verheggen, R.J., Hopman, M.T., Verbeek, A.L. and de Vegt, F. (2014) 'Entering a new era of body indices: the feasibility of a body shape index and body roundness index to identify cardiovascular health status', *PLoS One*, *9*(9), p.e107212.

Magnenat-Thalmann, N., Seo, H. and Cordier, F. (2004) 'Automatic modeling of virtual humans and body clothing', *Journal of Computer Science and Technology, 19*(5), pp. 575-584.

Maïm, J., Haegler, S., Yersin, B., Mueller, P., Thalmann, D. and Gool, L.V. (2007) 'Populating ancient pompeii with crowds of virtual romans', *Proceedings of the 8th International Symposium on Virtual Reality, Archeology and Cultural Heritage-VAST,* pp. 26-30.

Maisey, D.S., Vale, E.L., Cornelissen, P.L. and Tovee, M.J. (1999) 'Characteristics of male attractiveness for women', *Lancet, 353*(9163), p. 1500.

Martin, A., Drinkwater, D., Clarys, J., Daniel, M. and Ross, W. (1992) 'Effects of skin thickness and skinfold compressibility on skinfold thickness measurement', *American Journal of Human Biology, 4*(4), pp. 453-460.

McCrory, M.A., Gomez, T.D., Bernauer, E.M. and Mole, P.A. (1995) 'Evaluation of a new air displacement plethysmograph for measuring human body composition', *Medicine and Science in Sports and Exercise, 27*(12), pp. 1686-1691.

McDonnell, R., Larkin, M., Dobbyn, S., Collins, S. and O'Sullivan, C. (2008) 'Clone attack! Perception of crowd variety', *ACM Transactions on Graphics 27*(3), pp.1-8.

McGraw, B., McClenaghan, B.A., Williams, H.G., Dickerson, J. and Ward, D.S. (2000) 'Gait and postural stability in obese and nonobese prepubertal boys', *Archives of Physical Medicine and Rehabilitation, 81*(4), pp. 484-489.

Minott, J. (1972) *Pants and Skirts Fit for Your Shape.* Hampshire: Burgess Publishing Company.

Mokdad, A.H., Serdula, M.K., Dietz, W.H., Bowman, B.A., Marks, J.S. and Koplan, J.P. (1999) 'The spread of the obesity epidemic in the United States, 1991-1998', *Journal of the American Medical Association, 282*(16), pp. 1519-1522.

Moody, A. (2013) 'Adult anthropometric measures, overweight and obesity', *England: The Health and Social Care Information Centre, Vol 1. Ch 10, edn. 2013*. Available at: http://content.digital.nhs.uk/catalogue/PUB16076/HSE2013-Ch10-Adult-anth-meas.pdf (Accessed: 18/02/17).

Mosteller, R.D. (1987) 'Simplified calculation of body-surface area', *The New England Journal of Medicine, 317*(17), p. 1098.

MRI Scan - NHS Choices (2013) [Hardware]. Available at: http://www.nhs.uk/conditions/MRI-scan/Pages/Introduction.aspx (Accessed: 18/02/17).

Muth, N.D. (2009) 'What are the guidelines for percentage of body fat loss', *American Council on Exercise (ACE). Ask the Expert Blog* [Webpage] Available at:

https://www.acefitness.org/acefit/healthy-living-article/59/112/what-are-the-guidelines-for-percentage-of/ (Accessed: 18/02/17).

Muyor, J.M., López-Miñarro, P.A. and Alacid, F. (2011) 'Spinal posture of thoracic and lumbar spine and pelvic tilt in highly trained cyclists', *Journal of Sports Science & Medicine, 10*(2), pp. 355-361.

National Institutes of Health (US) (1994) *Bioelectrical impedance analysis in body composition measurement: program and abstracts: December 12-14, National Institutes of Health.* NIH Office of Medical Applications of Research.

Neff, M. and Kim, Y., (2009) 'Interactive editing of motion style using drives and correlations.' In *Proceedings of the 2009 ACM SIGGRAPH/Eurographics Symposium on Computer Animation,* pp. 103-112. ACM.

Newman, C. (2004) 'Why are we so fat', *National Geographic, 206*(2), pp. 46-62.

Nunez, C., Kovera, A.J., Pietrobelli, A., Heshka, S., Horlick, M., Kehayias, J.J., Wang, Z. and Heymsfield, S.B. (1999) 'Body composition in children and adults by air displacement plethysmography', *European Journal of Clinical Nutrition, 53*(5), pp. 382-387.

Ogawa, H., Fujitani, K., Tsujinaka, T., Imanishi, K., Shirakata, H., Kantani, A., Hirao, M., Kurokawa, Y. and Utsumi, S. (2011) 'InBody 720 as a new method of evaluating visceral obesity', *Hepato-Gastroenterology, 58*(105), pp. 42-44.

Oshita, O. (2017) 'Lattice-guided human motion deformation for collision avoidance', In *Proceedings of the Tenth International Conference on Motion in Games (MIG), ACM, 12.*

Pataky, Z., Armand, S., Müller-Pinget, S., Golay, A. and Allet, L., (2014) 'Effects of obesity on functional capacity'. *Obesity, 22*(1), pp.56-62.

Paton, N., Macallan, D., Jebb, S., Pazianas, M. and Griffin, G. (1995) 'Dual-energy X-ray absorptiometry results differ between machines', *The Lancet, 346*(8979), pp. 899-900.

Perlin, K. (1995) 'Real time responsive animation with personality', *Visualization and Computer Graphics, IEEE Transactions on Visualization and Computer Graphics, 1*(1), pp. 5-15.

Perry, M. (2013) *Body Fat Percentage Pictures Of Men & Women* [Webpage]. Available at: http://www.builtlean.com/2012/09/24/body-fat-percentage-men-women/ (Accessed: 18/02/17).

Phillips, C.M., Tierney, A.C., Perez-Martinez, P., Defoort, C., Blaak, E.E., Gjelstad, I.M., Lopez-Miranda, J., Kiec-Klimczak, M., Malczewska-Malec, M. and Drevon, C.A. (2013) 'Obesity and body fat classification in the metabolic syndrome: impact on cardiometabolic risk metabotype', *Obesity, 21*(1), pp. 154-161.

Pittenger, J.B. and Shaw, R.E. (1975) 'Aging faces as viscal-elastic events: Implications for a theory of nonrigid shape perception', *Journal of Experimental Psychology: Human Perception and Performance, 1*(4), p. 374-382.

Pollick, F.E., Hale, J.G. and McAleer, P. (2003) 'Visual perception of humanoid movement'. *Proceedings Third International Workshop on Epigenetic Robotics: Modeling Cognitive Development in Robotic Systems, 101*, pp.107-114.

Pouliot, M., Després, J., Lemieux, S., Moorjani, S., Bouchard, C., Tremblay, A., Nadeau, A. and Lupien, P.J. (1994) 'Waist circumference and abdominal sagittal diameter: best simple anthropometric indexes of abdominal visceral adipose tissue accumulation and related cardiovascular risk in men and women', *The American Journal of Cardiology, 73*(7), pp. 460-468.

Pražák, M., McDonnell, R., Kavan, L. and O'Sullivan, C. (2009) 'A perception based metric for comparing human locomotion', *Eurographics Ireland: 9th Irish Workshop on Computer Graphics,* pp. 75-80.

Pražák, M., McDonnell, R. and O'Sullivan, C. (2010) 'Perceptual evaluation of human animation timewarping', *ACM SIGGRAPH ASIA 2010 Sketches*, *30*, pp. 1-30.

Ravussin, E., Burnand, B., Schutz, Y. and Jequier, E. (1982) 'Twenty-four-hour energy expenditure and resting metabolic rate in obese, moderately obese, and control subjects', *The American Journal of Clinical Nutrition, 35*(3), pp. 566-573.

Reitsma, P.S.A. and Pollard, N.S. (2003) 'Perceptual metrics for character animation: sensitivity to errors in ballistic motion', *ACM Transactions on Graphics (TOG).* ACM, pp. 537-542.

Ren, L., Patrick, A., Efros, A.A., Hodgins, J.K. and Rehg, J.M. (2005) 'A data-driven approach to quantifying natural human motion', *ACM Transactions on Graphics (TOG).* ACM, pp. 1090-1097.

Rimm, E.B., Stampfer, M.J., Colditz, G.A., Chute, C.G., Litin, L.B. and Willett, W.C. (1990) 'Validity of self-reported waist and hip circumferences in men and women', *Epidemiology, 1*(6), pp. 466-473.

Rose, C., Cohen, M.F. and Bodenheimer, B. (1998) 'Verbs and adverbs: Multidimensional motion interpolation', *Computer Graphics and Applications, IEEE, 18*(5), pp. 32-40.

Rose, C., Guenter, B., Bodenheimer, B. and Cohen, M.F. (1996) 'Efficient generation of motion transitions using spacetime constraints', *Proceedings of the 23rd annual conference on Computer graphics and interactive techniques.* ACM, pp. 147-154.

Rosenbaum, D.A. (2009) *Human motor control.* San Diego: Academic press.

Ross, R., Dagnone, D., Jones, P.J., Smith, H., Paddags, A., Hudson, R. and Janssen, I. (2000) 'Reduction in obesity and related comorbid conditions after diet-induced weight loss or exercise-induced weight loss in men: a randomized, controlled trial', *Annals of Internal Medicine, 133*(2), pp. 92-103.

Ross, R., Leger, L., Morris, D., de Guise, J. and Guardo, R. (1992) 'Quantification of adipose tissue by MRI: relationship with anthropometric variables', *Journal of Applied Physiology (Bethesda, Md.: 1985), 72*(2), pp. 787-795.

Ross, R., Shaw, K.D., Martel, Y., de Guise, J. and Avruch, L. (1993) 'Adipose tissue distribution measured by magnetic resonance imaging in obese women', *The American Journal of Clinical Nutrition, 57*(4), pp. 470-475.

Sarkar, A., Singh, M., Bansal, N. and Kapoor, S., (2011) 'Effects of obesity on balance and gait alterations in young adults', *Indian J Physiol Pharmacol, 55*(3) pp.227–233.

Sarmini, M. (2005) *Understanding Normal & Pathological Gait.* [Lecture Slides] Available at: http://www.medschool.lsuhsc.edu/physical_medicine/PPT/Normal_Pathological_Gait.ppt (Accessed: 18/02/17).

Saunders, J.B., Inman, V.T. and Eberhart, H.D. (1953) 'The major determinants in normal and pathological gait', *The Journal of Bone and Joint Surgery. American Volume, 35*(3), pp. 543-558.

Satchell, L.P., Morris, P.H., Mills, C., O'Reilly, L., Marshman, P. & Akehurst, E. (2016) 'Evidence of big five and aggressive personalities in gait biomechanics', *Journal of Nonverbal Behavior. 41*(1), pp.33-44.

Scheepers, F., Parent, R.E., Carlson, W.E. and May, S.F. (1997) 'Anatomy-based modeling of the human musculature', *Proceedings of SIGGRAPH 97,* ACM, pp. 163-172.

Seidell, J.C., Bjorntorp, P., Sjostrom, L., Sannerstedt, R., Krotkiewski, M. and Kvist, H. (1989) 'Regional distribution of muscle and fat mass in men--new insight into the risk of abdominal obesity using computed tomography', *International Journal of Obesity, 13*(3), pp. 289-303.

Seltzer, F. (1984) 'Measurements of overweight', *Statistical Bulletin, 65*, pp. 20-23.

Seo, H., Cordier, F. and Magnenat-Thalmann, N. (2003) 'Synthesizing animatable body models with parameterized shape modifications', *Proceedings of the 2003 ACM SIGGRAPH/Eurographics symposium on Computer animation.* Eurographics Association, pp. 120-125.

Shaw, R. and McIntyre, M. (1974) 'Algoristic foundations to cognitive psychology', *Cognition and the Symbolic Processes*, pp. 305-362.

Sheldon, W.H., Stevens, S.S. and Tucker, W.B. (1940) *The varieties of human physique*. New York: Harper & Brothers Publishers.

Shewhorak, S. (2014) *Animex Gait Perception Survey.* Available at: http://goo.gl/forms/7XBXzJbtR3 (Accessed: 18/02/17).

Shewhorak, S. (2014) *Walking Gait Perception Survey 2.* Available at: http://goo.gl/forms/GlcePZeOv4 (Accessed: 18/02/17).

Shin, H.J., Lee, J., Shin, S.Y. and Gleicher, M. (2001) 'Computer puppetry: An importance-based approach', *ACM Transactions on Graphics (TOG), 20*(2), pp. 67-94.

Simon, H.B. (2013) *Waist-to-hip ratio* [Webpage]. Available at: http://pennstatehershey.adam.com/content.aspx?productId=10&pid=10&gid=000137 (Accessed: 18/02/17).

Siri, W.E. (1961) 'Body composition from fluid spaces and density: analysis of methods', *Techniques for Measuring Body Composition, 61*, pp. 223-244.

Slinde, F. and Rossander-Hulthen, L. (2001) 'Bioelectrical impedance: effect of 3 identical meals on diurnal impedance variation and calculation of body composition', *The American Journal of Clinical Nutrition, 74*(4), pp. 474-478.

Spyropoulos, P., Pisciotta, J.C., Pavlou, K.N., Cairns, M.A. and Simon, S.R. (1991) 'Biomechanical gait analysis in obese men', *Archives of Physical Medicine and Rehabilitation, 72*(13), pp. 1065-1070.

Stommel, M. and Schoenborn, C.A. (2009) 'Accuracy and usefulness of BMI measures based on self-reported weight and height: findings from the NHANES & NHIS 2001-2006', *BMC Public Health*, *9*, p. 421.

Tahrani, A., Boelaert, K., Barnes, R., Palin, S., Field, A., Redmayne, H., Aytok, L. and Rahim, A. (2008) 'Body volume index: time to replace body mass index?' *Endocrine Abstracts*, *15*, p. 104.

Tak, S. and Ko, H. (2005) 'A physically-based motion retargeting filter', *ACM Transactions on Graphics (TOG), 24*(1), pp. 98-117.

Taylor, G.W. and Hinton, G.E., (2009) 'Factored conditional restricted Boltzmann machines for modeling motion style'. In *ACM Proceedings of the 26th annual international conference on machine learning*, pp. 1025-1032.

Tecchia, F., Loscos, C. and Chrysanthou, Y. (2002) 'Visualizing Crowds in Real-Time', *Computer Graphics Forum. 21*(4), pp. 753-765.

Thalmann, D., Grillon, H., Maim, J. and Yersin, B. (2009) 'Challenges in Crowd Simulation', *CyberWorlds, 2009. CW'09. International Conference on.* IEEE, pp. 1-12.

Thomas, D.M., Bredlau, C., Bosy-Westphal, A., Mueller, M., Shen, W., Gallagher, D., Maeda, Y., McDougall, A., Peterson, C.M. and Ravussin, E. (2013) 'Relationships between body roundness with body fat and visceral adipose tissue emerging from a new geometrical model', *Obesity, 21*(11), pp. 2264-2271.

Tompkins, J., Bosch, P.R., Chenowith, R., Tiede, J.L. and Swain, J.M. (2008) 'Changes in functional walking distance and health-related quality of life after gastric bypass surgery', *Physical Therapy, 88*(8), pp. 928-935.

Torresani, L., Hackney, P. and Bregler, C., (2007) 'Learning motion style synthesis from perceptual observations'. In *Advances in Neural Information Processing Systems,* pp. 1393-1400.

Troje, N.F. (2002) 'Decomposing biological motion: a framework for analysis and synthesis of human gait patterns', *Journal of Vision, 2*(5), pp. 371-387.

Troje, N. F. (2008) Retrieving information from human movement patterns. In: Shipley, T. F. and Zacks, J. M. (eds.) *Understanding Events: How Humans See, Represent, and Act on Events*. Oxford University Press, pp. 308-334.

Turning Technologies (2016) *Turning Point.* [Hardware] Available at: http://www.turningtechnologies.co.uk/response-options/ (Accessed: 14/02/2017).

Ulijaszek, S.J. and Kerr, D.A. (1999) 'Anthropometric measurement error and the assessment of nutritional status', *British Journal of Nutrition, 82*(03), pp. 165-177.

van der Kooy, K., Leenen, R., Seidell, J.C., Deurenberg, P. and Hautvast, J.G. (1993) 'Effect of a weight cycle on visceral fat accumulation', *The American Journal of Clinical Nutrition, 58*(6), pp. 853-857.

Vartiainen, P., Bragge, T., Lyytinen, T., Hakkarainen, M., Karjalainen, P.A. and Arokoski, J.P., (2012) 'Kinematic and kinetic changes in obese gait in bariatric surgery-induced weight loss.' *Journal of biomechanics, 45*(10), pp.1769-1774.

Vismara, L., Romei, M., Galli, M., Montesano, A., Baccalaro, G., Crivellini, M. and Grugni, G. (2007) 'Clinical implications of gait analysis in the rehabilitation of adult patients with "Prader-Willi" Syndrome: a cross-sectional comparative study ("Prader-Willi" Syndrome vs matched obese patients and healthy subjects)', *Journal of NeuroEngineering and Rehabilitation, 4*, p. 14.

Visser, M., Gallagher, D., Deurenberg, P., Wang, J., Pierson, R.N.,Jr and Heymsfield, S.B. (1997) 'Density of fat-free body mass: relationship with race, age, and level of body fatness', *The American Journal of Physiology-Endocrinology And Metabolism, 272*(5), pp. 781-787.

Vukobratović, M. and Juričić, D., (1969) Contribution to the Synthesis of Biped Gait. *IEEE Transactions on Biomedical Engineering,* (1), pp.1-6.

Wang, J. and Bodenheimer, B. (2004) 'Computing the duration of motion transitions: an empirical approach', *Proceedings of the 2004 ACM SIGGRAPH/Eurographics symposium on Computer animation.* Eurographics Association, pp. 335-344.

Wang, J., Aulet, M., Thornton, J., Lichtman, S., Heymsfield, S. And Pierson, R. (1991) 'Body-Fat By Dual Photon-Absorptiometry (Dpa)-Comparisons With Traditional Methods In Caucasions (C), Blacks (B) And Asians (A)', *American Journal of Human Biology, 4(*4), pp.501-510.

Wang, J., Thornton, J.C., Russell, M., Burastero, S., Heymsfield, S. and Pierson, R.N.,Jr (1994) 'Asians have lower body mass index (BMI) but higher percent body fat than do whites: comparisons of anthropometric measurements', *The American Journal of Clinical Nutrition, 60*(1), pp. 23-28.

Wang, J., Gallagher, D., Thornton, J.C., Yu, W., Horlick, M. and Pi-Sunyer, F.X., (2006) 'Validation of a 3-dimensional photonic scanner for the measurement of body volumes, dimensions, and percentage body fat'. *The American journal of clinical nutrition, 83*(4), pp.809-816.

Ward, R. and Anderson, G. (1993) 'Examination of the skinfold compressibility and skinfold thickness relationship', *American Journal of Human Biology, 5*(5), pp. 541-548.

Webb, D. (1996) 'Maximum walking speed and lower limb length in hominids', *American Journal of Physical Anthropology, 101*(4), pp. 515-525.

Wells, J.C. and Fewtrell, M.S. (2006) 'Measuring body composition', *Archives of Disease in Childhood, 91*(7), pp. 612-617.

The Welsh Health Survey. (2009) Cardiff: Statistical Publication Unit.

Weta Digital (2017) *Tissue System* [Computer Program] https://www.youtube.com/watch?v=r45e5Xky35k (Accessed: 18/02/2017)

Wetsman, A. and Marlowe, F. (1999) 'How universal are preferences for female waist-to-hip ratios? Evidence from the Hadza of Tanzania', *Evolution and Human Behavior, 20*(4), pp. 219-228.

Whitney, D.E. (1969) 'Resolved motion rate control of manipulators and human prostheses', *IEEE Transactions on Man-Machine Systems*, *10*(2), pp.47-53.

Winter, D.A., Ruder, G.K. and MacKinnon, C.D. (1990) 'Control of balance of upper body during gait', in 'Control of balance of upper body during gait' *Multiple muscle systems.* New York: Springer, pp. 534-541.

Witkin, A. and Kass, M. (1988) 'Spacetime constraints', *ACM Siggraph Computer Graphics.* ACM, pp. 159-168.

Witkin, A. and Popovic, Z. (1995) 'Motion warping', *Proceedings of the 22nd annual conference on Computer graphics and interactive techniques.* ACM, pp. 105-108.

Womersley, J. and Durnin, J. (1977) 'A comparison of the skinfold method with extent of 'overweight'and various weight-height relationships in the assessment of obesity', *British Journal of Nutrition, 38*(02), pp. 271-284.

WHO (1995) 'Physical status: The use of and interpretation of anthropometry, Report of a WHO Expert Committee' *World Health Organization Technical Report Series, 854*.

WHO (2000) 'Obesity: preventing and managing the global epidemic*'. World Health Organization Technical Report Series, 894*.

WHO (2008) *STEPwise Approach to Surveillance (STEPS)* [Webpage] Available at: http://www.who.int/chp/steps/en/ (Accessed: 14/02/2017).

WHO (2011) 'Waist circumference and waist-hip ratio', Report of a WHO Expert Consultation Geneva: World Health Organization, pp.8-11.

Wu, X., Lockhart, T.E. and Yeoh, H.T., (2012) 'Effects of obesity on slip-induced fall risks among young male adults.' *Journal of biomechanics, 45*(6), pp.1042-1047.

Zhou, S., Chen, D., Cai, W., Luo, L., Low, M.Y.H., Tian, F., Tay, V.S.H., Ong, D.W.S. and Hamilton, B.D. (2010) 'Crowd modeling and simulation technologies', *ACM Transactions on Modeling and Computer Simulation (TOMACS), 20*(4).

12. APPENDIX A – INFORMATION GUIDE

Teesside University

Teesside University is sponsoring this project for the purposes of research governance

Information Guide

for Motion Capture Participants

Aim of the Research

We are looking to improve the realism of computer generated characters in games and films by the way the look and move. To do this we shall need to record the look of real people of all shapes and sizes and also the unique way that they walk. Aside from making games and films look more believable, your participation will help medical specialists better understand how changes in our weight affect the way we walk.

The Process

Upon arrival to the University's own Motion Capture lab you shall be asked to submit the attached consent form. We shall also talk through the procedure and you are welcome to ask any questions.
Using scales and a tape measure, the researcher shall take the following measurements:

1. Height
2. Weight
3. Age
4. Foot to hip length
5. Chest circumference
6. Waist / Abdominal circumference
7. Hip circumference
8. Thigh circumference (right)
9. Calf circumference (right)
10. Bicep circumference (right)
11. Neck circumference (right)

This shall produce your **BMI** value and your **Waist-to-Hip Ratio**; useful measurements to roughly estimate your body weight and health.

Your **Body Fat Percentage** shall be measured by gripping and stepping on a sterilised InBody 720 monitor for 60 seconds. Participants with pacemakers are not advised to use this machine as a small electrical current may interfere with it. Readings are more accurate when taken barefoot but can be taken wearing socks for those who feel uncomfortable:

You shall be provided with a printed **Body Composition Analysis** sheet showing your weight, BMI, Body Fat Percentage and a number of other interesting measurements that may be useful to track your health and fitness improvements over time.

It would be useful to bring **shorts** and tight fitting **t-shirt** to change into for the motion capture.

We shall fit some bands with ping-pong style markers to areas like your head, back, arms, waist and feet using Velcro bands or harnesses to your clothing or small sticker patches onto your skin.

We shall then take reference photos of you standing with your arms outstretched from the front, back and sides. You may opt out of photography if you are not comfortable with this.

For practise you shall be asked to walk back and forth along a 5m path at a comfortable speed to get a natural walking pace.

Once this preparation is complete, you shall be recorded walking the 5m in both directions at a comfortable speed. You shall then be asked to walk at a variety of speeds (3-6) from slow to fast. If you feel any pain or discomfort at walking at the fixed speed you may opt out. You are also free to withdraw from part or all of the experiment at any time.

The process should take approximately 2 hours so you can select a morning or afternoon slot. Refreshments and comfortable seating will be provided in the private lab environment.

Who We are Looking For and Why

We are ideally looking for a particular type of person for the following reasons:

- **18-40 years old**
  - Old enough to consent for participation
  - Within a range likely not to have any walking problems or illnesses

- **No walk impairing illnesses or injuries**
  - Illnesses such as osteoporosis can have an effect on your natural walking style
  - We must ensure that participants are at no risk of injury

Any Potential Risks and Mitigations

Photography of your body appearance shall be taken in the private lab. Once each session is complete the blurring of identifying facial features shall be prioritised as the first task to maintain your privacy.

The fitting, measurement and photography parts of the preparation process will be performed by same sex technicians in the private motion capture laboratory. Any physical contact as part of the process will only be made with your consent.

The experiment is designed not to be strenuous, uncomfortable or painful. You will be asked to walk at a fixed speed but this will not be excessive and you are welcome to opt out of this if you feel any discomfort.

How We Ensure Your Data and Identity is Kept Private

It is a legal requirement under the Data Protection Act 1998 (DPA) that personal data must be lawfully and confidentially processed respecting your privacy. Your data shall be stored and anonymised according to this law's eight principles:

1. Your personal data shall be processed fairly and lawfully
2. Your personal data shall be obtained only for the research project described and shall not be shared for use on other internal projects or external public resources (unless completely anonymised).
3. The data we shall collect is to be adequate, relevant and not excessive for the described purposes for which they are intended.
4. Your personal data shall be accurate and, where necessary, kept up to date.
5. Your personal data shall not be kept for longer than is necessary for the research project which is likely to be completed no longer than May 2015.
6. Your personal data shall be processed in accordance with the rights of data subjects under this Act.
7. Appropriate technical measures shall be taken against unauthorised or unlawful processing of personal data and against accidental loss or destruction of, or damage to, personal data e.g. password encryption and data storage in private folders
8. Personal data shall not be transferred to a country or territory outside the European Economic Area. Your data shall not be hosted on international servers as a public data research nor will it be shared with any other international research teams as this is a restricted project.

The biomechanics lab is on ground floor of the **Olympia Building** at **Teesside University**.

If you have any questions about the process or appointment slots please feel free to contact the researcher at:

Satish.Shewhorak@gmail.com

APPENDIX B – CONSENT FORM

Teesside University

Teesside University is sponsoring this project for the purposes of research governance

12.1. Consent Form

Motion Capture Participants

Participant ID No: _____

Project: 'A Data Driven Approach to Motion Diversification in relation to Body Morphology'

Researcher: Satish Shewhorak (BSc, MA)

Please initial all boxes

1. I confirm that I have read and understand the information sheet for the above study. I have had the opportunity to consider the information, ask questions and have had these answered satisfactorily. ☐
2. I understand that my participation is voluntary and that I am free to withdraw at any time without giving any reason. ☐
3. I consent to the use of reference photography/ video and motion capture. ☐
4. I agree to take part in the above study. ☐
5. I declare that I have no illnesses or injuries that may affect my ability to walk naturally such as osteoperosis, broken or strained bones, asthma. ☐

Name of Participant	Date	Signature
Name of Person taking consent.	Date	Signature

APPENDIX C – OTHER ANTHROPOMETRICS

C.1 Mass

Visceral Adipose Tissue (VAT) is deposited around the internal abdominal organs and is linked to increased cardiovascular disease and type 2 diabetes (Ginsberg, 2000; Kahn, 2000; Ross et al, 2000; Mokdad et al., 2000). As VAT is deposited primarily around the central abdominal area this can have a significant impact on the external perception of body shape. This may also be reflected in Waist Circumference and Waist to Hip Ratio.

Subcutaneous Adipose Tissue (SAT) builds up beneath the skin layer and has a prominent impact on the external perception of overall body shape. SAT does not come with the same health risks as VAT. SAT is used in skinfold calliper pinches to estimate overall BF%. This may also be reflected in body volume and circumferences.

Fat Free Mass (FFM) is the total body mass excluding fat tissue. This includes skeleton, muscles, ligaments, organs and water content. Levels of FFM can vary in an individual and between other people, which affects the representational accuracy of BMI when talking about body shape.

C.2 Circumferences

Another type of measurement for body shapes relates to circumferences of particular body areas.

Hip Circumference (HC) also helps measure central abdominal fatness in (cm). It is measured around the widest portion of the buttocks, with the tape parallel to the floor (WHO, 2011).

Waist circumference (WC) is highly correlated with central abdominal fatness explaining 80-90% of variance in total body fat (Han et al., 1995; Seidell et al., 1989; Pouliot et al., 1994; Ross et al., 1992; 1993; Van der Kooy et al., 1993).
The correct position for measuring waist circumference is midway between the uppermost border of the iliac crest and the lower border of the rib cage (WHO, 2008 cited in WHO, 2011). In practice it can be difficult for obese patients to accurately locate those bony

landmarks so the navel is often used instead which can introduce measurement error. HC and WC can be easily combined into Waist to Hip Ratio, however WC alone remains a useful metric being more effective at predicting abdominal fat than WtHR or BMI. Waist circumference does not take into account height which can bias people taller or shorter than the national average.

Thigh Circumference (ThC) helps measure lower body shape in (cm). A tape measure is used to measure the midpoint of the thigh. Thighs may feature more muscular tissue than fat, so thinner thighs could actually double the risk of heart disease (Heitmann and Freriksen, 2009) as opposed to necessarily indicating increased obesity. Increased thigh muscles could also have a direct effect on gait parameters.

Sum of Five circumferences (CSum) is simply the sum total of the HC, WC, ThC, arm and calf circumference. These expand with, and can loosely represent body volume. Waist, hip and arm/ calf circumferences had the highest associations with whole-body VAT, SAT and skeletal muscle volumes respectively (Heymsfield et al., 2008).

C.3 Ratios

Ashwell Shape Chart categorises health based on shape rather than just weight and height, as BMI does. The chart seen in Figure 12-1 uses WHtR as a proxy for abdominal obesity classifying WHtR into three bands of health risks (Ashwell, 2011). This chart suggests that to achieve a healthy body shape people should keep their waist circumference measurement to less than half their height.

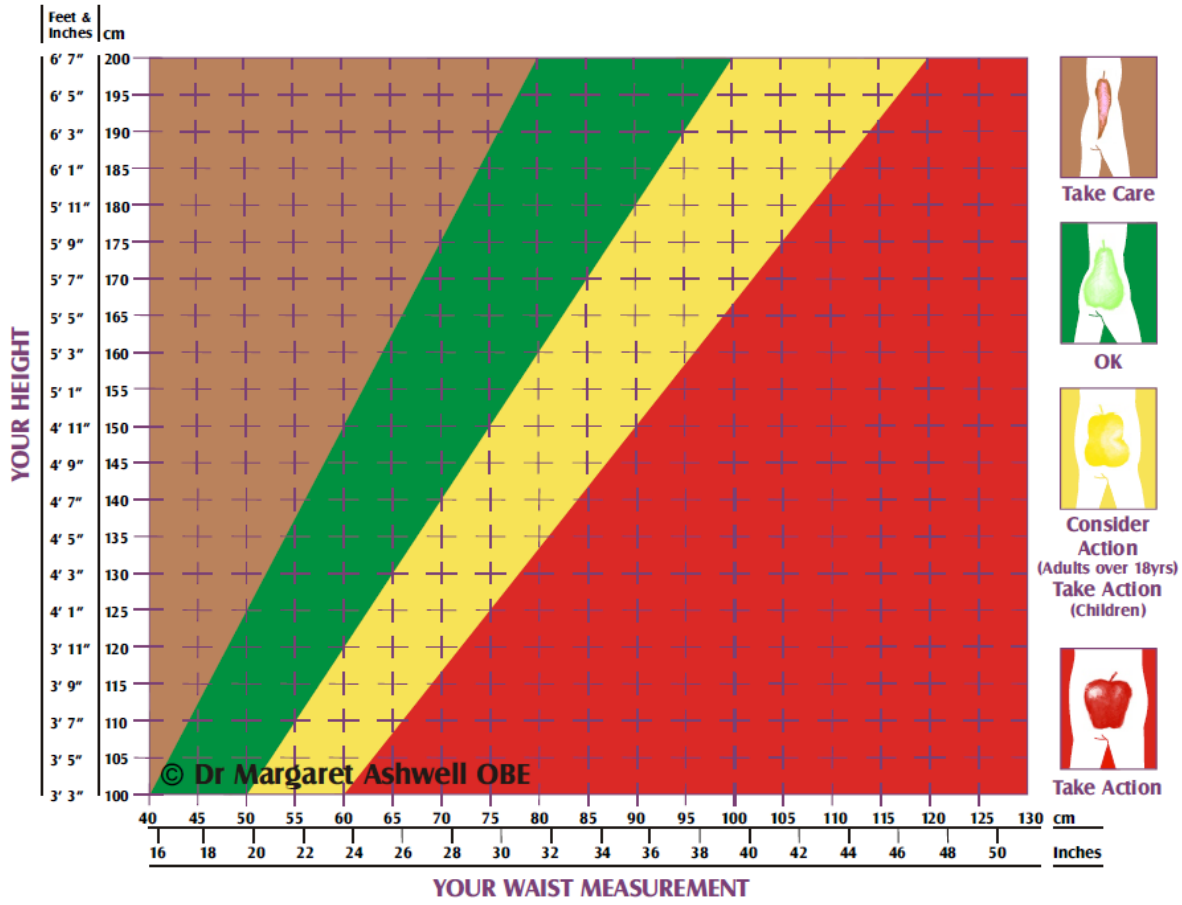

Figure 12-1- The Ashwell® Shape Chart based on waist-to-height ratio. (Ashwell, 2011).

The chart also suggests that the four WHtR bands could be represented as a chilli, pear, pineapple and apple body shape. However, these shape classifications have not been validated in either sex.

Waist to Chest Ratio (WCR) is the ratio of the waist circumference to chest (Maisey et al., 1999). This ratio provides a useful estimation of the proportion of upper-body shape. Whilst medically WCR is less important for determining health than WtHR or BMI, WCR has a stronger effect when it comes to the perception of a more attractive male body shape (Fan et al., 2005).

C.4 Linear Anthropometric Indecises

Quetelet Index (QI) was devised in the 1850s by Adolphe Quetelet, a social scientist and statistician, interested in classifying anthropometrics and their correlations to issues and trends in wider society (Eknoyan, 2008). It is an index of adiposity measured as:

$$QI = Mass / Height^2$$

Equation 16 - Quetelet Index (BMI)

However, its usefulness in the field of public health was only popularised when it was later re-termed as the Body Mass Index.

Attempts to classify the weight of a person as a percentage of the average weight of others of the same height, age and sex against population data led to the first developments of "standard height-weight" tables by the life insurance industry (ALIMD, 1912; cited in Eknoyan, 2008).
These kind of tables listed the average weights of insurance applicants of given a sex and height at approximately 25 years old (Keys, 1953; 1954; 1955a; 1955b).

Metropolitan Life tables were developed (MLIC, 1959; cited in Keys et al., 1972) to calculate Ideal Body Weight (IBW) to height for health insurance purposes and became a widely used measurement. They provided "ideal" weight for ranges of height, according to sex and three categories of body frame; small, medium and large. However, no instructions on how to measure frame size were included so many people erroneously chose their own frame size.
These Metropolitan Life tables were updated (MLIC, 1983) using elbow breadth to determine frame size. The idea behind this was to differentiate between people of the same weight but differences in skeletal-muscle mass and fat mass, which implies that the real target of measurement is body fat percentage rather than IBW (Seltzer, 1984).

C.5 Body Shape Scales / Surface Anthropometrics

Somatypes were three body types developed by Sheldon et al. (1940) by measuring nude students and classifying their body shapes into somatypes; endomorphic, mesomorphic, and ectomorphic. However, he believed the ratio of these body shapes did not increase with weight gain, and that a person's somatype determined their psychological character. Sheldon's somatypes have been widely discredited now.

Body Build and Posture Scales was developed by Douty (1968) by projecting body silhouettes from the front and side onto grids, in a technique called somatography, to rate body shape and posture to a 5-point Body Build Scale, however, this relied on scaling up only an hourglass body shape and did not take into account other body shape profiles.

Body I.D. Scale was developed by August and Count (1981) and featured five body shapes; circle, pear, rectangle, inverted triangle with secondary descriptions for body areas classified from the side view. However, these shape classifications could only be determined visually by experts.

Body Surface Area (BSA) uses height and weight measurements to estimate surface area SA (m^2) of the body and is used in medical tasks and dosage recommendations. Various formulas have been developed over the years (Boyd, 1935; Dubois and DuBois, 1916; Gehan and George, 1970; Haycock et al., 1978) all giving slightly different results which makes the lack of standardization problematic. The Mosteller (1987) formula is most commonly used due to its simplicity:

$$BSA_{(m2)} = (Height_{(cm)} \times Weight_{(kg)} / 3600)^{½}$$

Equation 17 - Body Surface Area

Volume Height Index (VHI) is the total body volume divided by the square of a person's height. It could be argued that volume is more related to shape than weight based indices such as BMI as the weight of skeletal, muscular and adipose mass can vary for the same BMI. VHI is noted for being a better at predictor of body shape attractiveness than BMI or WHtR (Fan et al., 2005; 2007).

$$VHI = Volume / Height^2$$

Equation 18 - Volume Height Index

Body Adiposity Index (BAI) is a method of predicting body fat without using weight but just HC and height (Bergman et al., 2011)

$$BAI = (Hip\ Circumference_{(cm)} / (Height_{(M)})^{1.5}) - 18$$

Equation 19 - Body Adiposity Index

Whilst Freedman et al. (2012) challenged the claim that BAI was more accurate than BMI at predicting body fat percentage, BAI is still a useful metric when correlating real world observations of humans with virtual characters that have no mass or weight.
It is also possible to estimate BF% from BMI and BAI, however, this would introduce two levels of estimation and is not considered accurate enough (Barreira et al., 2011).

A Body Shape Index (ABSI) was developed to improve upon BMI by taking Waist Circumference into consideration as a representation of body fat distribution and the risks of abdominal obesity (Krakauer and Krakauer, 2012). It was claimed to be a more effective predictor of mortality than BMI (Krakauer and Krakauer, 2014), however, Maessen et al. (2014) challenged this. ABSI is calculated as:

$$ABSI = Waist\ Circumference\ /\ BMI^{2/3}\ Height^{1/2}$$

Equation 20 - A Body Shape Index

Body Roundness Index (BRI) was developed to quantify geometric body shape using height, WC and HC. It was an attempt to improve upon BMI by measuring body girth in relation to height. By considering height, BRI also improves upon HC, WC and WtHR as taller individuals have larger WC or HCs, it also improves upon these metrics, BMI and WHtR, with slightly better predictions of BF% and %VAT (Thomas et al., 2013). However, it is relatively unpopular.

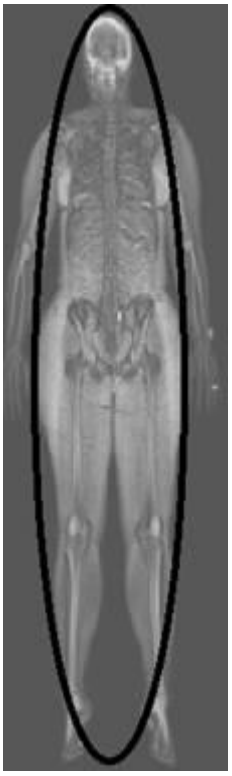

Figure 12-2- Image of BRI Scan (Thomas et al., 2013)

BRI quantifies body shape as:

$$BRI = 364.2 – (365:5 \times eccentricity)$$

Equation 21 - Body Roundness Index

Body Shape Assessment Scale (BSAS©) was developed by Connell et al. (2006) through investigating body scans and adaptation of the parameters from Douty (1968), Minott (1972) and August and Count (1981). This helped inform the development of The Body Measurement Software (BMS©) by $[TC]^2$ to automatically analyse body shapes from future scans. It is a nine parameter classification scale for body shape using front and side views. However, whilst body shape variation is continuous, BSAS is an ordinal scale.

Body Volume Index (BVI) is a relatively new measurement devised in 2000 that automatically assesses body shape through abdominal volume and infers the location and distribution of fat (Tahrani et al., 2008). It is used with a 3D full body scanner and automatically measures BMI, WC, WtHR volumetric and body compositional data. Korenfeld et al. (2009) investigated the reliability of the BVI scanner in comparison to manual

measurements and found it to be a reliable, valid and reproducible method to measure WC and HC.

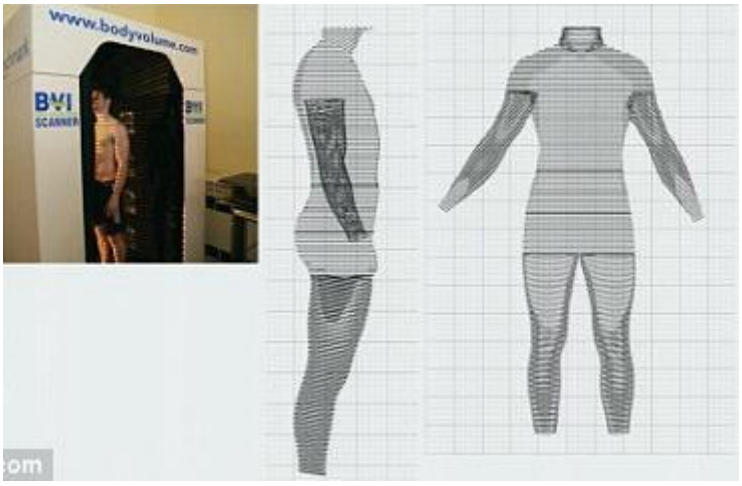

Figure 12-3- BVI Scanner and Model (Bates, 2010)

However, this index is still in development and evaluation and requires proprietary full body scanners that are not yet available.

C.6 Measurements

Underwater Weighing (UWW) also known as hydrostatic body composition analysis or hydro-densitometry is a way of measuring body density. This can then be used to estimate BF%. The subject is weighed under water with corrections made for any air that could not be exhaled before measuring. UWW also relies on equations for Caucasian populations to convert to BF% (Siri, 1961; Brožek, 1963; Jackson and Pollock, 1985; Womersley and Durnin, 1977). UWW is considered more invasive to participants and not currently available at Teesside University.

Figure 12-4 - Underwater Weighing (Health and Kinesiology Facilities, 2015)

Whole-body air displacement also known as air plethysmography is another method for measuring densitometry (for conversion to BF%) and gives comparable results to UWW (Dempster and Aitken, 1995; McCrory et al., 1995; Nunez et al., 1999).

Figure 12-5 - BodPod Air Displacement (COSMED, 2015)

Bodpod® is a commonly used air displacement device which avoids some of the discomfort of submersion underwater but still involves some disrobing and exhaling as much air from the lungs as possible, which can be uncomfortable for obese participants. It is also currently unavailable at Teesside University.

Dual energy X-ray Absorptiometry (DXA) is a direct method of measuring bone mineral density but can also be used to measure body composition and fat composition with a high degree of accuracy. It is also independent of age or sex. However, results can differ between machines (Paton et al., 1995).

Figure 12-6- DXA machine (GE, 2013)

Magnetic Resonance Imagery (MRI) has been used to scan internal body composition. MRI technology measures "imaging slices" to differentiate between volumes of FM and FFM. It can do this in regions of the body inaccessible with other anthropometric methods. However, MRI estimates volume rather than mass of adipose tissue and has to assume a constant density to FM. MRI can also only measure total FM versus densitometry and multicomponent methods which measure adipose tissue mass (Wells and Fewtrell, 2006). When compared with dissection of cadavers the mean difference in accuracy was only 0.076kg (Abate et al., 1994). MRI is a highly accurate and non-toxic method often used as reference when assessing other indices. However, scanners are expensive, require highly skilled technicians to capture and cleanup data and they are typically reserved for medical purposes.

Figure 12-7 - MRI Scan (MRI Scan - NHS Choices, 2013)

Figure 12-8 - MRI coloured results (Newman, 2004)

Computed Tomography (CT / CAT Scans) operates in a similar fashion to a DXA scanner. They use x-ray images from different angles to produce virtual slices which can be combined into a 3D model of the body. CT has a high contrast resolution which allows differentiation

between tissue density of less than 1%. Like MRI image artefacts can be introduced which takes trained technicians time to clean up. Whilst CT is non-invasive it is regarded as a moderate to high radiation technique. Radiation doses are higher than conventional X-ray machines which can cause cancerous damage to body cells.

APPENDIX D – MOTION PARAMETER CODE

```
// 19- WalkingSpeed + Cad, HipRoty+TorRotx , WalkBase, ArmAbd+ bob+ ArmSwing
OpenScene("D:\\Scenes\\MP COMPLETE camera_setup_H_test.scn", null, null);

// general Variables
var cmToSi = 0.1;           // value to multiply by to convert cm (centimeters) to SI units
var mToSi  = cmToSi*100;    // value to multiply by to convert m (meters) to SI units

// Modifier / changeable Variables
var ChHeight    = GetValue("DisplayInfo_Ch_Mods.Height");               // Char Height in m (meters)
var ChBF        = GetValue("DisplayInfo_Ch_Mods.Body_Fat_Percentage");  // body fat %
var GetChest    = GetValue("DisplayInfo_Ch_Mods.Set_Chest");
var ChChest     = 0.98;                                                 // (m)  curent using lean character (MP) data

// baseline values from (or calculated from) lean character data or mocap of lean character to be used to make modifier values from Calculated Values
var leanWalkingSpeed = 1.2154;  // ??? check all these baselines???
var leanArmAbduction = 7.7564;  // *** CHANGED ***
var leanStepWidth    = 55.0658; // (cm)
var leanArmBobMag    = 7.97632;
var leanArmSwing     = 22.269;

var leanHeight       = 1.758;
var leanWtHR         = 0.83;
var bf35WtHR         = 0.95;    // large BF% WtHR estimated
var leanChest        = 0.98;
var bf35Chest        = 1.14;    // large BF% Chest estimated *** CHANGED ***

function interpolate(a, b, t) {
    return (1-t)*a + t*b;
}
function reverseinterpolate(a, b, c) {
    return (c-a)/(b-a);
}

var scaleT = reverseinterpolate(12,35, ChBF)            // find linearly how far between BF% 12 & 35
var WtHR = interpolate(leanWtHR, bf35WtHR, scaleT);     // calculate linerly WtHR
if (GetChest == true){
    ChChest = GetValue("DisplayInfo_Ch_Mods.Chest");    // get chest value from SI if GetChest is True
}else{
    ChChest = interpolate(leanChest, bf35Chest, scaleT); // calculate linerly Chest
}

// var ChWaist       = 0.81;                           // (m)  curent using lean character data
// var ChHip         = 0.975;                          // (m)  curent using lean character data
// var WtHR          = ChWaist/ChHip;                  //= 0.83;

// Calculated Values
var walkingSpeed = -1.07 + (1.3 * ChHeight);            // Speed (m/s)
var armAbduction = -31.424 + (39.98 * ChChest);         // Avg Arm Abduction *** CHANGED ***
var walkingBase  = -167.59 + (268.26 * WtHR);           // Walking Base (cm)
var armBobMag    = -13.19 + (12.04 * ChHeight);         // Arm Bob Magnitude
var armSwing     = 18.76 + (0.29 * ChBF);               // Arm Swing Magnitude

// modifyer values for script some convet to SI units
var SiWalkingSpeed = walkingSpeed/leanWalkingSpeed;
var SiArmAbduction = armAbduction-leanArmAbduction;
var SiStepWidth    = (walkingBase-leanStepWidth)*cmToSi;// convert Walking base from metric to SI units and adjust for baseline
var SiArmBobMag    = armBobMag/leanArmBobMag;           // works as multiplyer value!
var SiArmSwing     = armSwing/leanArmSwing;             // should works as multiplyer value!
```

```
59
60  FirstFrame(null);                                    // set to first frame to build
    IK without distortion
61
62  //Scale Height before doing anything.
63  var ScaleHeight = ChHeight / leanHeight
64  // get local cordinates and move positions relative to character (effect: lengthen bones)
65  // LENGTHEN HEIGHT OF HIPS
66  var HipsLy  = GetValue("MotionBuilder_Template.Hips.kine.local.posy"); //may need small
    correction for feet to reach ground
67  SetValue("MotionBuilder_Template.Hips.kine.local.posy", HipsLy*ScaleHeight, null);
68  // LENGTHEN LEGS
69  var LeftLegLx   = GetValue("MotionBuilder_Template.LeftLeg.kine.local.posx");
70  SetValue("MotionBuilder_Template.LeftLeg.kine.local.posx", LeftLegLx*ScaleHeight, null);
71  var LeftFootLx  = GetValue("MotionBuilder_Template.LeftFoot.kine.local.posx");
72  SetValue("MotionBuilder_Template.LeftFoot.kine.local.posx", LeftFootLx*ScaleHeight,
    null);
73  var LeftToeBaseLx   = GetValue("MotionBuilder_Template.LeftToeBase.kine.local.posx");
74  SetValue("MotionBuilder_Template.LeftToeBase.kine.local.posx",
    LeftToeBaseLx*ScaleHeight, null);
75  var RightLegLx  = GetValue("MotionBuilder_Template.RightLeg.kine.local.posx");
76  SetValue("MotionBuilder_Template.RightLeg.kine.local.posx", RightLegLx*ScaleHeight,
    null);
77  var RightFootLx = GetValue("MotionBuilder_Template.RightFoot.kine.local.posx");
78  SetValue("MotionBuilder_Template.RightFoot.kine.local.posx", RightFootLx*ScaleHeight,
    null);
79  var RightToeBaseLx  = GetValue("MotionBuilder_Template.RightToeBase.kine.local.posx");
80  SetValue("MotionBuilder_Template.RightToeBase.kine.local.posx",
    RightToeBaseLx*ScaleHeight, null);
81  // LENGTHEN SPINE
82  var SpineLx = GetValue("MotionBuilder_Template.Spine.kine.local.posx");
83  SetValue("MotionBuilder_Template.Spine.kine.local.posx", SpineLx*ScaleHeight, null);
84  var Spine1Lx    = GetValue("MotionBuilder_Template.Spine1.kine.local.posx");
85  SetValue("MotionBuilder_Template.Spine1.kine.local.posx", Spine1Lx*ScaleHeight, null);
86  var Spine2Lx    = GetValue("MotionBuilder_Template.Spine2.kine.local.posx");
87  SetValue("MotionBuilder_Template.Spine2.kine.local.posx", Spine2Lx*ScaleHeight, null);
88  var Spine3Lx    = GetValue("MotionBuilder_Template.Spine3.kine.local.posx");
89  SetValue("MotionBuilder_Template.Spine3.kine.local.posx", Spine3Lx*ScaleHeight, null);
90  var Spine4Lx    = GetValue("MotionBuilder_Template.Spine4.kine.local.posx");
91  SetValue("MotionBuilder_Template.Spine4.kine.local.posx", Spine4Lx*ScaleHeight, null);
92  var NeckLx  = GetValue("MotionBuilder_Template.Neck.kine.local.posx");
93  SetValue("MotionBuilder_Template.Neck.kine.local.posx", NeckLx*ScaleHeight, null);
94  var HeadLx  = GetValue("MotionBuilder_Template.Head.kine.local.posx");
95  SetValue("MotionBuilder_Template.Head.kine.local.posx", HeadLx*ScaleHeight, null);
96  // LENGTHEN ARMS
97  var LeftForeArmLx   = GetValue("MotionBuilder_Template.LeftForeArm.kine.local.posx");
98  SetValue("MotionBuilder_Template.LeftForeArm.kine.local.posx",
    LeftForeArmLx*ScaleHeight, null);
99  var LeftHandLx  = GetValue("MotionBuilder_Template.LeftHand.kine.local.posx");
100 SetValue("MotionBuilder_Template.LeftHand.kine.local.posx", LeftHandLx*ScaleHeight,
    null);
101 var RightForeArmLx  = GetValue("MotionBuilder_Template.RightForeArm.kine.local.posx");
102 SetValue("MotionBuilder_Template.RightForeArm.kine.local.posx",
    RightForeArmLx*ScaleHeight, null);
103 var RightHandLx = GetValue("MotionBuilder_Template.RightHand.kine.local.posx");
104 SetValue("MotionBuilder_Template.RightHand.kine.local.posx", RightHandLx*ScaleHeight,
    null);
105 //SCALE HANDS
106 var LeftHandLsx = GetValue("MotionBuilder_Template.LeftHand.kine.local.sclx");
107 SetValue("MotionBuilder_Template.LeftHand.kine.local.sclx", LeftHandLsx*ScaleHeight,
    null);
108 var LeftHandLsy = GetValue("MotionBuilder_Template.LeftHand.kine.local.scly");
109 SetValue("MotionBuilder_Template.LeftHand.kine.local.scly", LeftHandLsy*ScaleHeight,
    null);
110 var LeftHandLsz = GetValue("MotionBuilder_Template.LeftHand.kine.local.sclz");
111 SetValue("MotionBuilder_Template.LeftHand.kine.local.sclz", LeftHandLsz*ScaleHeight,
    null);
112 var RightHandLsx    = GetValue("MotionBuilder_Template.RightHand.kine.local.sclx");
113 SetValue("MotionBuilder_Template.RightHand.kine.local.sclx", RightHandLsx*ScaleHeight,
```

```
    null);
114 var RightHandLsy    = GetValue("MotionBuilder_Template.RightHand.kine.local.scly");
115 SetValue("MotionBuilder_Template.RightHand.kine.local.scly", RightHandLsy*ScaleHeight,
    null);
116 var RightHandLsz    = GetValue("MotionBuilder_Template.RightHand.kine.local.sclz");
117 SetValue("MotionBuilder_Template.RightHand.kine.local.sclz", RightHandLsz*ScaleHeight,
    null);
118
119 //TORSO POS CO-ORDS
120 var Hipsx   = GetValue("MotionBuilder_Template.Hips.kine.global.pos.posx"); // On
    current frame
121 var Hipsy   = GetValue("MotionBuilder_Template.Hips.kine.global.pos.posy");
122 var Hipsz   = GetValue("MotionBuilder_Template.Hips.kine.global.pos.posz");
123 var Spinex  = GetValue("MotionBuilder_Template.Spine.kine.global.pos.posx");
124 var Spiney  = GetValue("MotionBuilder_Template.Spine.kine.global.pos.posy");
125 var Spinez  = GetValue("MotionBuilder_Template.Spine.kine.global.pos.posz");
126 var Spine1x = GetValue("MotionBuilder_Template.Spine1.kine.global.pos.posx");
127 var Spine1y = GetValue("MotionBuilder_Template.Spine1.kine.global.pos.posy");
128 var Spine1z = GetValue("MotionBuilder_Template.Spine1.kine.global.pos.posz");
129 var Spine2x = GetValue("MotionBuilder_Template.Spine2.kine.global.pos.posx");
130 var Spine2y = GetValue("MotionBuilder_Template.Spine2.kine.global.pos.posy");
131 var Spine2z = GetValue("MotionBuilder_Template.Spine2.kine.global.pos.posz");
132 var Spine3x = GetValue("MotionBuilder_Template.Spine3.kine.global.pos.posx");
133 var Spine3y = GetValue("MotionBuilder_Template.Spine3.kine.global.pos.posy");
134 var Spine3z = GetValue("MotionBuilder_Template.Spine3.kine.global.pos.posz");
135 var Spine4x = GetValue("MotionBuilder_Template.Spine4.kine.global.pos.posx");
136 var Spine4y = GetValue("MotionBuilder_Template.Spine4.kine.global.pos.posy");
137 var Spine4z = GetValue("MotionBuilder_Template.Spine4.kine.global.pos.posz");
138 // NECK POS CO-ORDS
139 var Neckx   = GetValue("MotionBuilder_Template.Neck.kine.global.pos.posx");
140 var Necky   = GetValue("MotionBuilder_Template.Neck.kine.global.pos.posy");
141 var Neckz   = GetValue("MotionBuilder_Template.Neck.kine.global.pos.posz");
142 // LEFT ARM POS CO-ORDS
143 var LeftShoulderx   =
    GetValue("MotionBuilder_Template.LeftShoulder.kine.global.pos.posx"); // On current frame
144 var LeftShouldery   =
    GetValue("MotionBuilder_Template.LeftShoulder.kine.global.pos.posy");
145 var LeftShoulderz   =
    GetValue("MotionBuilder_Template.LeftShoulder.kine.global.pos.posz");
146 var LeftArmx        = GetValue("MotionBuilder_Template.LeftArm.kine.global.pos.posx");
147 var LeftArmy        = GetValue("MotionBuilder_Template.LeftArm.kine.global.pos.posy");
148 var LeftArmz        = GetValue("MotionBuilder_Template.LeftArm.kine.global.pos.posz");
149 var LeftForeArmx    =
    GetValue("MotionBuilder_Template.LeftForeArm.kine.global.pos.posx");
150 var LeftForeArmy    =
    GetValue("MotionBuilder_Template.LeftForeArm.kine.global.pos.posy");
151 var LeftForeArmz    =
    GetValue("MotionBuilder_Template.LeftForeArm.kine.global.pos.posz");
152 var LeftHandx       = GetValue("MotionBuilder_Template.LeftHand.kine.global.pos.posx");
153 var LeftHandy       = GetValue("MotionBuilder_Template.LeftHand.kine.global.pos.posy");
154 var LeftHandz       = GetValue("MotionBuilder_Template.LeftHand.kine.global.pos.posz");
155 // RIGHT ARM POS CO-ORDS
156 var RightShoulderx  =
    GetValue("MotionBuilder_Template.RightShoulder.kine.global.pos.posx");
157 var RightShouldery  =
    GetValue("MotionBuilder_Template.RightShoulder.kine.global.pos.posy");
158 var RightShoulderz  =
    GetValue("MotionBuilder_Template.RightShoulder.kine.global.pos.posz");
159 var RightArmx       = GetValue("MotionBuilder_Template.RightArm.kine.global.pos.posx");
160 var RightArmy       = GetValue("MotionBuilder_Template.RightArm.kine.global.pos.posy");
161 var RightArmz       = GetValue("MotionBuilder_Template.RightArm.kine.global.pos.posz");
162 var RightForeArmx   =
    GetValue("MotionBuilder_Template.RightForeArm.kine.global.pos.posx");
163 var RightForeArmy   =
    GetValue("MotionBuilder_Template.RightForeArm.kine.global.pos.posy");
164 var RightForeArmz   =
    GetValue("MotionBuilder_Template.RightForeArm.kine.global.pos.posz");
165 var RightHandx      = GetValue("MotionBuilder_Template.RightHand.kine.global.pos.posx");
166 var RightHandy      = GetValue("MotionBuilder_Template.RightHand.kine.global.pos.posy");
```

```
var RightHandz      = GetValue("MotionBuilder_Template.RightHand.kine.global.pos.posz");

// LEFT LEG POS CO-ORDS
var lUpLegx = GetValue("MotionBuilder_Template.LeftUpLeg.kine.global.pos.posx"); // On current frame
var lUpLegy = GetValue("MotionBuilder_Template.LeftUpLeg.kine.global.pos.posy");
var lUpLegz = GetValue("MotionBuilder_Template.LeftUpLeg.kine.global.pos.posz");
var lKneex  = GetValue("MotionBuilder_Template.LeftLeg.kine.global.pos.posx");
var lKneey  = GetValue("MotionBuilder_Template.LeftLeg.kine.global.pos.posy");
var lKneez  = GetValue("MotionBuilder_Template.LeftLeg.kine.global.pos.posz");
var lFootx  = GetValue("MotionBuilder_Template.LeftFoot.kine.global.pos.posx");
var lFooty  = GetValue("MotionBuilder_Template.LeftFoot.kine.global.pos.posy");
var lFootz  = GetValue("MotionBuilder_Template.LeftFoot.kine.global.pos.posz");
var lToex   = GetValue("MotionBuilder_Template.LeftToeBase.kine.global.pos.posx");
var lToey   = GetValue("MotionBuilder_Template.LeftToeBase.kine.global.pos.posy");
var lToez   = GetValue("MotionBuilder_Template.LeftToeBase.kine.global.pos.posz");
// RIGHT LEG POS CO-ORDS
var rUpLegx = GetValue("MotionBuilder_Template.RightUpLeg.kine.global.pos.posx");
var rUpLegy = GetValue("MotionBuilder_Template.RightUpLeg.kine.global.pos.posy");
var rUpLegz = GetValue("MotionBuilder_Template.RightUpLeg.kine.global.pos.posz");
var rKneex  = GetValue("MotionBuilder_Template.RightLeg.kine.global.pos.posx");
var rKneey  = GetValue("MotionBuilder_Template.RightLeg.kine.global.pos.posy");
var rKneez  = GetValue("MotionBuilder_Template.RightLeg.kine.global.pos.posz");
var rFootx  = GetValue("MotionBuilder_Template.RightFoot.kine.global.pos.posx");
var rFooty  = GetValue("MotionBuilder_Template.RightFoot.kine.global.pos.posy");
var rFootz  = GetValue("MotionBuilder_Template.RightFoot.kine.global.pos.posz");
var rToex   = GetValue("MotionBuilder_Template.RightToeBase.kine.global.pos.posx");
var rToey   = GetValue("MotionBuilder_Template.RightToeBase.kine.global.pos.posy");
var rToez   = GetValue("MotionBuilder_Template.RightToeBase.kine.global.pos.posz");


//Create Hip root rings to to limit LEFT leg rotation
GetPrim("Null", null, null, null);
// get primitive null
SetValue("null.null.primary_icon", 2, null);
// change icon to rings
SetValue("null.Name", "left_leg_root_rot", null);
// rename null "left_leg_root_rot"
MakeLocal("left_leg_root_rot.display", siNodePropagation);
// change colour to pink for visability
SetValue("left_leg_root_rot.display.wirecolorr", 0.878, null);
SetValue("left_leg_root_rot.display.wirecolorg", 0, null);
SetValue("left_leg_root_rot.display.wirecolorb", 0.878, null);
MatchTransform("left_leg_root_rot", "MotionBuilder_Template.LeftUpLeg", siTrn, null);
// Match rotation rings pos to left leg up pos
MatchTransform("left_leg_root_rot", "MotionBuilder_Template.hips", siRot, null);
// Match rotation rings rot to hip rot
ParentObj("MotionBuilder_Template.Hips", "left_leg_root_rot");
// make hips parent

//Create Hip root rings to to limit RIGHT leg rotation
GetPrim("Null", null, null, null);
// get primitive null
SetValue("null.null.primary_icon", 2, null);
// change icon to rings
SetValue("null.Name", "right_leg_root_rot", null);
// rename null "right_leg_root_rot"
MakeLocal("right_leg_root_rot.display", siNodePropagation);
// change colour to pink for visability
SetValue("right_leg_root_rot.display.wirecolorr", 0.878, null);
SetValue("right_leg_root_rot.display.wirecolorg", 0, null);
SetValue("right_leg_root_rot.display.wirecolorb", 0.878, null);
MatchTransform("right_leg_root_rot", "MotionBuilder_Template.RightUpLeg", siTrn, null);
// Match rotation rings pos to left leg up pos
MatchTransform("right_leg_root_rot", "MotionBuilder_Template.hips", siRot, null);
// Match rotation rings rot to hip rot
ParentObj("MotionBuilder_Template.Hips", "right_leg_root_rot");
// make hips parent

```

```
// RUN COMMANDS TO BUILD IK LEGS
// Left IK Leg
var IKLbone;
var IKLeff;
var IKLLegChain = Create2DSkeleton(lUpLegx, lUpLegy, lUpLegz, lKneex, lKneey, lKneez, 1, 0, 0, 4, IKLbone, IKLeff);         // Create Upper IK Leg() should contain original null's kine.global.pos on Frame1
var IKLLegShin  = AppendBone (IKLLegChain.Effector, lFootx, lFooty, lFootz);                                                // Append Lower IK Leg
ParentObj("MotionBuilder_Template.left_leg_root_rot", IKLLegChain.Root);                                                    // Parent whole IK Leg to FK Leg
var IKLFootbone;
var IKLFooteff;
var IKLFootChain = Create2DSkeleton(lFootx, lFooty, lFootz, lToex, lToey, lToez, 1, 0, 0, 4, IKLFootbone, IKLFooteff);      // Create IK Foot from heel to toe() should contain original null's kine.global.pos on Frame

// Make a local vector and transform to global to apply
SelectObj("MotionBuilder_Template.LeftToeBase", null, true);
var oObj    = Application.Selection(0);
var oTrans  = oObj.Kinematics.Global.Transform;
oTrans.SclX = 1;
oTrans.SclY = 1;
oTrans.SclZ = 1;
var oVector = XSIMath.CreateVector3();
oVector.X   = -0.2;
oVector.Y   = 0;
oVector.Z   = 0;
// Convert toe's globalpos from local to global Vector space
var oGlobalPos = XSIMath.MapObjectPositionToWorldSpace( oTrans, oVector );
DeselectAll();

var IKLFootToe  = AppendBone (IKLFootChain.Effector, oGlobalPos.X, oGlobalPos.Y, oGlobalPos.Z);
ParentObj(IKLLegChain.Effector,IKLFootChain.Root);
                                    // toeRoot to Heel end eff // Might not need .Name

// Left Leg Control Box
GetPrim("Null", null, null, null);                                                  // get primitive null
SetValue("null.null.primary_icon", 4, null);                                        // change icon to box
SetValue("null.Name", "left_leg_pos", null);                                        // rename null "left_leg_pos"
MakeLocal("left_leg_pos.display", siNodePropagation);                               // change colour to red for visability
SetValue("left_leg_pos.display.wirecolorr", 0.878, null);
SetValue("left_leg_pos.display.wirecolorg", 0, null);
SetValue("left_leg_pos.display.wirecolorb", 0, null);
MatchTransform("left_leg_pos", "MotionBuilder_Template.eff", siTrn, null);  // Match Control Box pos to IK heel eff pos

// Left Toe
GetPrim("Null", null, null, null);                                                  //get primitive null
SetValue("null.null.primary_icon", 4, null);                                        // change icon to box
SetValue("null.Name", "left_toe_pos", null);                                        // rename null "left_leg_pos"
MakeLocal("left_toe_pos.display", siNodePropagation);                               // change colour to red for visability
SetValue("left_toe_pos.display.wirecolorr", 0.878, null);
SetValue("left_toe_pos.display.wirecolorg", 0, null);
SetValue("left_toe_pos.display.wirecolorb", 0, null);
MatchTransform("left_toe_pos", "MotionBuilder_Template.eff1", siTrn, null); // Match(pos) to leg eff on rig1

// Right IK Leg
```

```
var IKRbone;
var IKReff;
var IKRLegChain = Create2DSkeleton(rUpLegx, rUpLegy, rUpLegz, rKneex, rKneey, rKneez, 1, 0, 0, 4, IKRbone, IKReff);         // Create Upper IK Leg() should contain original null's kine.global.pos on Frame1
var IKRLegShin  = AppendBone (IKRLegChain.Effector, rFootx, rFooty, rFootz);                                                 // Append Lower IK Leg
ParentObj("MotionBuilder_Template.right_leg_root_rot", IKRLegChain.Root);                                                   // Parent whole IK Leg to FK Leg
var IKRFootbone;
var IKRFooteff;
var IKRFootChain = Create2DSkeleton(rFootx, rFooty, rFootz, rToex, rToey, rToez, 1, 0, 0, 4, IKRFootbone, IKRFooteff);      // Create IK Foot from heel to toe() should contain original null's kine.global.pos on Frame1

// Values in local space
SelectObj("MotionBuilder_Template.RightToeBase", null, true);                // make a local vector and transfrom to global to apply
var oObj = Application.Selection(0);
var oTrans = oObj.Kinematics.Global.Transform;
oTrans.SclX = 1;
oTrans.SclY = 1;
oTrans.SclZ = 1;
var oVector = XSIMath.CreateVector3();
oVector.X = 0.2;
oVector.Y = 0;
oVector.Z = 0;
// Convert to global space
var oGlobalPos = XSIMath.MapObjectPositionToWorldSpace( oTrans, oVector );
DeselectAll();

var IKRFootToe  = AppendBone (IKRFootChain.Effector, oGlobalPos.X, oGlobalPos.Y, oGlobalPos.Z);
ParentObj(IKRLegChain.Effector
,IKRFootChain.Root);
    // toeRoot to Heel end eff

// Right leg Control Box
GetPrim("Null", null, null, null);
SetValue("null.null.primary_icon", 4, null);
SetValue("null.Name", "right_leg_pos", null);
MakeLocal("right_leg_pos.display", siNodePropagation);
SetValue("right_leg_pos.display.wirecolorr", 0.878, null);
SetValue("right_leg_pos.display.wirecolorg", 0, null);
SetValue("right_leg_pos.display.wirecolorb", 0, null);
MatchTransform("right_leg_pos", "MotionBuilder_Template.eff2", siTrn, null);                                                // Match control box(pos) to leg IK eff on rig0

// Right toe
GetPrim("Null", null, null, null);
SetValue("null.null.primary_icon", 4, null);
SetValue("null.Name", "right_toe_pos", null);
MakeLocal("right_toe_pos.display", siNodePropagation);
SetValue("right_toe_pos.display.wirecolorr", 0.878, null);
SetValue("right_toe_pos.display.wirecolorg", 0, null);
SetValue("right_toe_pos.display.wirecolorb", 0, null);
MatchTransform("right_toe_pos", "MotionBuilder_Template.eff3", siTrn, null);




// make heel control boxes children of hips
ParentObj("MotionBuilder_Template.Hips", "left_leg_pos");                                                                    // Parent control box to hips
ParentObj("B:MotionBuilder_Template.Hips", "right_leg_pos");

ParentObj("MotionBuilder_Template.Hips",
```

```
"left_toe_pos");                                                    // Parent control box to hips
ParentObj("B:MotionBuilder_Template.Hips", "right_toe_pos");

// constrain effectors position to new controls
ApplyCns("Position", "MotionBuilder_Template.eff", "MotionBuilder_Template.left_leg_pos", null);              // Heel IK eff pos constrained to CB(the constraining obj)
ApplyCns("Position", "MotionBuilder_Template.eff2", "MotionBuilder_Template.right_leg_pos", null);

// DEL?
ApplyCns("Position", "MotionBuilder_Template.eff1", "MotionBuilder_Template.left_toe_pos", null);              //true means constraint comp is on (offset is preserved)
ApplyCns("Position", "MotionBuilder_Template.eff3", "MotionBuilder_Template.right_toe_pos", null);

// LOOPS THROUGH AND SAVES CB KEYS ON EVERY MATCHING POS TO FK POS ####################
// USED TO SAY // var CurrentFrameNo    = FirstKey("MotionBuilder_Template.Hips.kine.global.pos.posy");
var firstKeyf       = 9;                // set start to stop overshoot and overwrite when wrap round is on.
var lastKeyf        = 88;               // NEED TO FIX THIS TO DETECT LAST KEY
FirstFrame(null);                       // USED TO SAY //
SetValue("PlayControl.Current", 9, null); // NEED TO FIX THIS TO DETECT FIRST KEY

for (var i=firstKeyf; i<lastKeyf ; i++) //each frame
    {
    // (match translation (local pos) of CB heel and toe effectors to FK heel and toes)
    MatchTransform("MotionBuilder_Template.left_leg_pos", "MotionBuilder_Template.LeftFoot",  siRT, null);     // MatchTransform CB to FK heel null
    MatchTransform("MotionBuilder_Template.right_leg_pos", "MotionBuilder_Template.RightFoot", siRT, null);

    MatchTransform("MotionBuilder_Template.left_toe_pos", "MotionBuilder_Template.LeftToeBase", siRT, null);   // use toe pos
    // Values in local space
    SelectObj("MotionBuilder_Template.LeftToeBase", null, true);    // make a local vector and transfrom to global to apply
    var oObj = Application.Selection(0);
    var oTrans = oObj.Kinematics.Global.Transform;
    oTrans.SclX = 1;
    oTrans.SclY = 1;
    oTrans.SclZ = 1;
    var oVector = XSIMath.CreateVector3();
    oVector.X = -0.2;
    oVector.Y = 0;
    oVector.Z = 0;
    // Convert to global space
    var oGlobalPos = XSIMath.MapObjectPositionToWorldSpace( oTrans, oVector );
    DeselectAll();
    Translate("MotionBuilder_Template.left_toe_pos", oGlobalPos.X, oGlobalPos.Y, oGlobalPos.Z, siAbsolute, siGlobal, siObj, siXYZ, null, null, null, null, null, null, null, null, 0, null); // translate to compensate for offset

    MatchTransform("MotionBuilder_Template.right_toe_pos", "MotionBuilder_Template.RightToeBase", siRT, null);  // use toe pos
    // Values in local space
    SelectObj("MotionBuilder_Template.RightToeBase", null, true);                // make a local vector and transfrom to global to apply
    var oObj = Application.Selection(0);
    var oTrans = oObj.Kinematics.Global.Transform;
    oTrans.SclX = 1;
    oTrans.SclY = 1;
    oTrans.SclZ = 1;
    var oVector = XSIMath.CreateVector3();
    oVector.X = 0.2;
```

```
375       oVector.Y = 0;
376       oVector.Z = 0;
377       // Convert to global space
378       var oGlobalPos = XSIMath.MapObjectPositionToWorldSpace( oTrans, oVector );
379       DeselectAll();
380       Translate("MotionBuilder_Template.right_toe_pos", oGlobalPos.X, oGlobalPos.Y,
          oGlobalPos.Z, siAbsolute, siGlobal, siObj, siXYZ, null, null, null, null, null,
          null, null, null, null, 0, null); // translate to compensate for offset
381
382       //Saves local pos key on where the effectors have been match translated to
383       SaveKey("MotionBuilder_Template.left_leg_pos.kine.local.posx");
384       SaveKey("MotionBuilder_Template.left_leg_pos.kine.local.posy");
385       SaveKey("MotionBuilder_Template.left_leg_pos.kine.local.posz");
386
387       SaveKey("MotionBuilder_Template.right_leg_pos.kine.local.posx");
388       SaveKey("MotionBuilder_Template.right_leg_pos.kine.local.posy");
389       SaveKey("MotionBuilder_Template.right_leg_pos.kine.local.posz");
390
391       SaveKey("MotionBuilder_Template.left_toe_pos.kine.local.posx");
392       SaveKey("MotionBuilder_Template.left_toe_pos.kine.local.posy");
393       SaveKey("MotionBuilder_Template.left_toe_pos.kine.local.posz");
394
395       SaveKey("MotionBuilder_Template.right_toe_pos.kine.local.posx");
396       SaveKey("MotionBuilder_Template.right_toe_pos.kine.local.posy");
397       SaveKey("MotionBuilder_Template.right_toe_pos.kine.local.posz");
398
399       // USED TO SAY // CurrentFrameNo = i;
400       NextFrame();
401       };
402
403
404
405
406
407
408
409   Refresh(20); // forces viewport to update. can be any frame but not current or first.
      This fixes misalignment strange bug
410
411   FirstFrame(null); // SetValue("PlayControl.Current", 9, null);
412   // ########### Loop through and remove FK null pos | LOOP REMOVED; DOES NOT NEED TO BE
      LOOPED
413   RemoveAllAnimation("MotionBuilder_Template.LeftUpLeg",      null , siUnspecified,
      siAnySource, siAllParam, null, null, null);
414   RemoveAllAnimation("MotionBuilder_Template.LeftLeg",        null , siUnspecified,
      siAnySource, siAllParam, null, null, null);
415   RemoveAllAnimation("MotionBuilder_Template.LeftFoot",       null , siUnspecified,
      siAnySource, siAllParam, null, null, null);
416   RemoveAllAnimation("MotionBuilder_Template.LeftToeBase",    null , siUnspecified,
      siAnySource, siAllParam, null, null, null);
417
418   RemoveAllAnimation("MotionBuilder_Template.RightUpLeg",     null , siUnspecified,
      siAnySource, siAllParam, null, null, null);
419   RemoveAllAnimation("MotionBuilder_Template.RightLeg",       null , siUnspecified,
      siAnySource, siAllParam, null, null, null);
420   RemoveAllAnimation("MotionBuilder_Template.RightFoot",      null , siUnspecified,
      siAnySource, siAllParam, null, null, null);
421   RemoveAllAnimation("MotionBuilder_Template.RightToeBase",   null , siUnspecified,
      siAnySource, siAllParam, null, null, null);
422
423
424
425
426
427   // MUST BE ON A FRAME WHERE THERE IS NO DISTORTION (I.E. THE FIRST FRAME) (done above)
428   ParentObj("MotionBuilder_Template.bone",  "MotionBuilder_Template.LeftUpLeg");
429   ParentObj("MotionBuilder_Template.bone1", "MotionBuilder_Template.LeftLeg");
430   ParentObj("MotionBuilder_Template.bone2", "MotionBuilder_Template.LeftFoot");
      // Parents FK nulls to IK heel
```

```
ParentObj("MotionBuilder_Template.bone3", "MotionBuilder_Template.LeftToeBase");
// ADDED THIS TO TRY KEEP COPY TO RIG2 IN PLACE

ParentObj("MotionBuilder_Template.bone4", "MotionBuilder_Template.RightUpLeg");
ParentObj("MotionBuilder_Template.bone5", "MotionBuilder_Template.RightLeg");
ParentObj("MotionBuilder_Template.bone6", "MotionBuilder_Template.RightFoot");
ParentObj("MotionBuilder_Template.bone7", "MotionBuilder_Template.RightToeBase");
// ADDED THIS TO TRY KEEP COPY TO RIG2 IN PLACE

// NEW CODE INSERTED HERE
######################################################################

/* get primative null, change icon to box & rename "Global_Control_SRT" */
GetPrim("Null", null, null, null);
SetValue("null.null.primary_icon", 4, null);
SetValue("null.null.size", 40, null);
SetValue("null.Name", "Global_Control_SRT", null);
/* change colour to red for visability */
MakeLocal("Global_Control_SRT.display", siNodePropagation);
SetValue("Global_Control_SRT.display.wirecolorr", 0.878, null);
SetValue("Global_Control_SRT.display.wirecolorg", 0, null);
SetValue("Global_Control_SRT.display.wirecolorb", 0, null);

/* Match all Transformations (SRT) to hips */
MatchTransform("Global_Control_SRT", "MotionBuilder_Template.Hips", siSRT, null);

/* give hips a shadow icon for visability */
SetValue("MotionBuilder_Template.Hips.shadow_icon", 9, null);
SetValue("MotionBuilder_Template.Hips.shadow_offsetY", 5, null);
SetValue("MotionBuilder_Template.Hips.shadow_scaleX", 40, null);
SetValue("MotionBuilder_Template.Hips.shadow_scaleY", -20, null);
SetValue("MotionBuilder_Template.Hips.shadow_scaleZ", 20, null);

// PARENTING ######################
/* make "Global_Control_SRT" child of "MotionBuilder_Template1" */
ParentObj("MotionBuilder_Template", "Global_Control_SRT");

/* REmove any scaling animation, copy all animation pos and rot from "hips" to
"Global_Control_SRT" */
RemoveAnimation("MotionBuilder_Template.Hips.kine.local.sclx,
MotionBuilder_Template.Hips.kine.local.sclz,
MotionBuilder_Template.Hips.kine.local.scly", 77, null, null, null, null);
CopyAnimation("MotionBuilder_Template.Hips", null, null, null, null, null);
PasteAnimation("MotionBuilder_Template.Global_Control_SRT", null);
/* remove ALL animation from "hips" */
RemoveAnimation("MotionBuilder_Template.Hips.kine.local.posx,
MotionBuilder_Template.Hips.kine.local.posy,MotionBuilder_Template.Hips.kine.local.posz,M
otionBuilder_Template.Hips.kine.local.rotx,MotionBuilder_Template.Hips.kine.local.roty,Mo
tionBuilder_Template.Hips.kine.local.rotz,MotionBuilder_Template.Hips.kine.local.sclx,Mot
ionBuilder_Template.Hips.kine.local.scly,MotionBuilder_Template.Hips.kine.local.sclz",
75, null, null, null, null);

/* make "Hips" Child of "Global_Control_SRT" */
ParentObj("MotionBuilder_Template.Global_Control_SRT", "MotionBuilder_Template.Hips");

/* set ALL pos and rot values to ZERO. THIS IS IMPORTANT! any modifications to hip rot
can now be made after this step */
Rotate("MotionBuilder_Template.Hips", 0, 0, 0, siAbsolute, siPivotSym, siObj, siX,
null, null, null, null, null, null, null, 0, null);
Rotate("MotionBuilder_Template.Hips", 0, 0, 0, siAbsolute, siPivotSym, siObj, siY,
null, null, null, null, null, null, null, 0, null);
Rotate("MotionBuilder_Template.Hips", 0, 0, 0, siAbsolute, siPivotSym, siObj, siZ,
null, null, null, null, null, null, null, 0, null);
Translate("MotionBuilder_Template.Hips", 0, 0, 0, siAbsolute, siPivotSym, siObj, siX,
null, null, null, null, null, null, null, null, null, 0, null);
Translate("MotionBuilder_Template.Hips", 0, 0, 0, siAbsolute, siPivotSym, siObj, siY,
null, null, null, null, null, null, null, null, null, 0, null);
Translate("MotionBuilder_Template.Hips", 0, 0, 0, siAbsolute, siPivotSym, siObj, siZ,
null, null, null, null, null, null, null, null, null, 0, null);
```

```
482
483   /* make "Spine" Child of "Global_Control_SRT" */
484   ParentObj("MotionBuilder_Template.Global_Control_SRT", "MotionBuilder_Template.Spine");
485   /* make "leg_pos" controls Children of "Global_Control_SRT" */
486   ParentObj("MotionBuilder_Template.Global_Control_SRT",
      "MotionBuilder_Template.left_leg_pos");
487   ParentObj("MotionBuilder_Template.Global_Control_SRT",
      "MotionBuilder_Template.right_leg_pos");
488   /* make "toe_pos" controls Children of "Global_Control_SRT" */
489   ParentObj("MotionBuilder_Template.Global_Control_SRT",
      "MotionBuilder_Template.left_toe_pos");
490   ParentObj("MotionBuilder_Template.Global_Control_SRT",
      "MotionBuilder_Template.right_toe_pos");
491   /* make leg effectors controls Children of "Global_Control_SRT" */
492   ParentObj("MotionBuilder_Template.Global_Control_SRT", "MotionBuilder_Template.eff");
493   ParentObj("MotionBuilder_Template.Global_Control_SRT", "MotionBuilder_Template.eff2");
494
495   //set expression to limit rotation of legs
496   SetExpr("MotionBuilder_Template.left_leg_root_rot.kine.local.roty", "cond(
      MotionBuilder_Template.Hips.kine.local.roty < 0 , 0 -
      MotionBuilder_Template.Hips.kine.local.roty , 0 )", null);
497   SetExpr("MotionBuilder_Template.right_leg_root_rot.kine.local.roty", "cond(
      MotionBuilder_Template.Hips.kine.local.roty > 0 , 0 -
      MotionBuilder_Template.Hips.kine.local.roty , 0 )", null);
498
499   // fix leg twist
500   Rotate("MotionBuilder_Template.RightLeg", 0, 0, 0, siAbsolute, siPivotSym, siObj, siX,
      null, null, null, null, null, null, null, 0, null);
501   // Rotate("MotionBuilder_Template.LeftLeg", 0, 0, 180, siAbsolute, siPivotSym, siObj,
      siX, null, null, null, null, null, null, null, 0, null);
502   Rotate("MotionBuilder_Template.root", 0, -90, 0, siAbsolute, siPivotSym, siObj, siXYZ,
      null, null, null, null, null, null, null, 0, null); // straightens weird knee kink
503   Rotate("MotionBuilder_Template.root2", 0, 90, 180, siAbsolute, siPivotSym, siObj,
      siXYZ, null, null, null, null, null, null, null, 0, null); // straightens weird knee kink
504
505   // Duplicate rig0 to create rig1 with IK rigs
506   Duplicate("B:Max_Pears_setb_n", null, 2, 1, 1, 0, 0, 1, 0, 1, null, null, null, null,
      null, null, 0, 0, 0, null, 0);    // 5th value from end is posx offset translation
507
508
509
510
511
512
513   //
      ==========================================================================================
      ==========================================================================
514
515
516   // 16- WALKING BASE
517   // HEEL local vars
518   var LeftLegCB_1posx     = "MotionBuilder_Template.left_leg_pos.kine.local.posx";
519   var LeftLegCB_2posx     = "MotionBuilder_Template1.left_leg_pos.kine.local.posx";
520   var RightLegCB_1posx    = "MotionBuilder_Template.right_leg_pos.kine.local.posx";
521   var RightLegCB_2posx    = "MotionBuilder_Template1.right_leg_pos.kine.local.posx";
522
523   // loop whole operation not just ssmodkey MG
524   var keyCounter          = LeftLegCB_1posx;  // arbitrarily chosen LeftLegCB_1posx as
      all have keys
525   CurrentWBFrameNo        = FirstKey(keyCounter);
526   LastWBKey               = LastKey(keyCounter);
527   var newKeyPos           = 0;
528   while (CurrentWBFrameNo <= LastWBKey)
529       {
530       // before modify step width for each frame. HEEL global vars
531       var HeelPosL_1posx =
          GetValue("MotionBuilder_Template.left_leg_pos.kine.global.posx");
532       var HeelPosR_1posx =
          GetValue("MotionBuilder_Template.right_leg_pos.kine.global.posx");
```

```
533
534         // WALKING BASE VALUES
535             // var stepWidth    = -1;           // A
536             // var stepWidth    = 0;            // B (Lean 12%)
537             // var stepWidth    = 1;            // C
538             // var stepWidth    = 2;            // D (Trendline 35%)
539             // var stepWidth    = 3;            // E
540             // var stepWidth    = 4;            // F
541         var stepWidth = SiStepWidth;            // now use SiStepWidth (SI unit version of
            stepWidth which is set in cm at the top)
542
543         // Modify each HEEL local key at a time
544         ssModKeyOPsingle(LeftLegCB_1posx, LeftLegCB_2posx, stepWidth,
            CurrentWBFrameNo);        // 15- LEFT LEG CB.posx
545         ssModKeyONsingle(RightLegCB_1posx, RightLegCB_2posx, stepWidth,
            CurrentWBFrameNo);      // 15- RIGHT LEG CB.posx
546
547         // after step width applied. Char2's HEEL global pos
548         var HeelPosL_2posx  =
            GetValue("MotionBuilder_Template1.left_leg_pos.kine.global.posx");
549         var HeelPosR_2posx  =
            GetValue("MotionBuilder_Template1.right_leg_pos.kine.global.posx");
550         var HeelMoveL       = HeelPosL_2posx -
            HeelPosL_1posx;                                 // Local difference that heel is
            moved out
551         var HeelMoveR       = HeelPosR_2posx -
            HeelPosR_1posx;                                 // Local difference that heel is
            moved out
552
553         // TRANSLATING TOES
554         Translate("MotionBuilder_Template1.left_toe_pos",  HeelMoveL, 0, 0, siRelative,
            siGlobalSym, siObj, siXYZ, null, null, null, null, null, null, null, null, null, 0,
            null);
555         Translate("MotionBuilder_Template1.right_toe_pos", HeelMoveR, 0, 0, siRelative,
            siGlobalSym, siObj, siXYZ, null, null, null, null, null, null, null, null, null, 0,
            null);
556
557         var lToePos_2posx   = "MotionBuilder_Template1.left_toe_pos.kine.local.pos.posx";
558         var rToePos_2posx   = "MotionBuilder_Template1.right_toe_pos.kine.local.pos.posx";
559
560         // Single key at a time. Move TOE local pos out by local difference of heels
561         ssModKeyOPsingle(lToePos_2posx, lToePos_2posx, HeelMoveL,
            CurrentWBFrameNo);            // 15- LEFT LEG CB.posx
562         ssModKeyONsingle(rToePos_2posx, rToePos_2posx, HeelMoveR,
            CurrentWBFrameNo);            // 15- RIGHT LEG CB.posx
563
564         CurrentWBFrameNo = NextKey(keyCounter,
            CurrentWBFrameNo);                              // Increment frame
565
            }
                // end of loop
566
567
568
569
570     // HIP ROTATION Y
571     var GCSRT_2roty     =
        "MotionBuilder_Template1.Global_Control_SRT.kine.local.ori.euler.roty";       // Global
        Hips
572     var Hips_2roty      =
        "MotionBuilder_Template1.Hips.kine.local.ori.euler.roty";                     //
        Additive Hips
573     var avgPosHipsy     =
        avgPosFinder(GCSRT_2roty);                                                    //
        Average position
574     // 13- TORSO Rotx TWIST
575     var Spine4_1rotx    = "MotionBuilder_Template.Spine4.kine.local.ori.euler.rotx";
576     var Spine4_2rotx    =
        "MotionBuilder_Template1.Spine4.kine.local.ori.euler.rotx";                   //
```

```
    Commented out below
577 var avgPosTRx       = avgPosFinder(Spine4_1rotx);
578 // 7b- ARM BOB ROTz (minus is outwards, positive is inward abduction)
579 var LeftArm_1rotz   = "MotionBuilder_Template.LeftArm.kine.local.ori.euler.rotz";
580 var LeftArm_2rotz   =
    "MotionBuilder_Template1.LeftArm.kine.local.ori.euler.rotz";                  //
    Commented out below
581 var avgPosAALz      = avgPosFinder(LeftArm_1rotz);
582 var RightArm_1rotz  = "MotionBuilder_Template.RightArm.kine.local.ori.euler.rotz";
583 var RightArm_2rotz  =
    "MotionBuilder_Template1.RightArm.kine.local.ori.euler.rotz";                 //
    Commented out below
584 var avgPosAARz      = avgPosFinder(RightArm_1rotz);
585 // 6- ARM SWING ROTy
586 var LeftArm_1roty   = "MotionBuilder_Template.LeftArm.kine.local.ori.euler.roty";
587 var LeftArm_2roty   =
    "MotionBuilder_Template1.LeftArm.kine.local.ori.euler.roty";                  //
    Commented out below
588 var avgPosAALy      = avgPosFinder(LeftArm_1roty);
589 var RightArm_1roty  = "MotionBuilder_Template.RightArm.kine.local.ori.euler.roty";
590 var RightArm_2roty  =
    "MotionBuilder_Template1.RightArm.kine.local.ori.euler.roty";                 //
    Commented out below
591 var avgPosAARy      = avgPosFinder(RightArm_1roty);
592
593
594 // 11a- MAGMODS at Diff Strengths [DATA] MAYBE SPACE OUT MORE. RECHECK INCREMENTS ARE
    LINEAR OR CURVED
595 // 13- MAGMODS Hips roty and Torso rotx
596     // var magModHyTx       = 1.25;         // A
597     // var magModHyTx       = 1;            // B
598     // var magModHyTx       = 0.75;         // C
599     // var magModHyTx       = 0.50;         // D
600     // var magModHyTx       = 0.25;         // E
601        var magModHyTx       = 0;            // F
602
603 // ARM ABDUCTION VALUES
604     // var dataPosAvgDiff   = -3.19355;     // A
605     // var dataPosAvgDiff   = 0;            // B (Lean 12%)
606     // var dataPosAvgDiff   = 3.19355;      // C
607     // var dataPosAvgDiff   = 6.3871;       // D (Trendline 35%)
608     // var dataPosAvgDiff   = 9.58065;      // E
609     // var dataPosAvgDiff   = 12.7742;      // F
610        var dataPosAvgDiff = SiArmAbduction; // uses modifyer value from top
611
612 // magMods ARM BOB at Diff Strengths [DATA]
613     // var magModAAz        = 0.55;         // A
614     // var magModAAz        = 1;            // B 12% Original Lean
615     // var magModAAz        = 1.45;         // C
616     // var magModAAz        = 1.895681358;  // D 35% trendl exag
617     // var magModAAz        = 2.34;         // E slight exag
618     // var magModAAz        = 2.79 ;        // F
619        var magModAAz = SiArmBobMag;
620
621 // 6- magMods ARM SWING at Diff Strengths [NO DATA]
622     // var magModAAy        = 1.25;         // A under exag
623     // var magModAAy        = 1.00;         // B slight under exag
624     // var magModAAy        = 0.75;         // C 12% Original Lean
625     // var magModAAy        = 0.50;         // D slight exag
626     // var magModAAy        = 0.25;         // E 35%  exag
627     // var magModAAy        = 0.00;         // F very exag
628        var magModAAy        = SiArmSwing;
629
630
631
632 ssModKeyT(LeftArm_1roty, LeftArm_2roty, magModAAy, avgPosAALy);                   //
    6- LEFT ARM SWING Roty
633 ssModKeyT(RightArm_1roty, RightArm_2roty, magModAAy, avgPosAARy);                 //
    6- RIGHT ARM SWING Roty
```

```
634
635 ssModKey(LeftArm_1rotz, LeftArm_2rotz, dataPosAvgDiff, magModAAz, avgPosAALz);      //
    7b- LEFT ARM BOB Rotz
636 ssModKey(RightArm_1rotz, RightArm_2rotz, dataPosAvgDiff, magModAAz, avgPosAARz);    //
    7b- RIGHT ARM BOB Rotz
637
638 // MODKEY FUNCTION
    ################################################################################
639 function ssModKey(objectStringFrom, objectStringTo, avgPosDiff, magMod,
    averagePos)                 // rig1, rig2, theor diff between avg pos, mag multiplier,
    actual average position
640     {
641         CurrentFrameNo          =
            FirstKey(objectStringFrom);                                          // After
            deletion current frame set back to start
642         aLastKey                =
            LastKey(objectStringFrom);                                           // Does this
            need resetting? Isn't it still correct?
643         var newKeyPos = 0;
644
645         while (CurrentFrameNo   <= aLastKey)
646             {
647             var CurrentKeyVal   = GetValue(objectStringFrom,
                CurrentFrameNo);                        // Gets current key value
648             newKeyPos           = (((CurrentKeyVal - averagePos) * magMod) + averagePos
                - avgPosDiff);  // avgPosDiff is MINUS as rig has ARMS goings upwards
                towards 0
649             SaveKey(objectStringTo, CurrentFrameNo, newKeyPos );
650             CurrentFrameNo      = NextKey(objectStringFrom,
                CurrentFrameNo);                         // Increment frame no on Rig1
651             }
652     }
653
654 // MODKEY 1 FUNCTION
    ################################################################################
655 function ssModKeyT(objectStringFrom, objectStringTo, magMod,
    averagePos)                     // rig1, rig2, mag multiplier, actual average position
656     {
657         CurrentFrameNo          =
            FirstKey(objectStringFrom);                                  // After deletion
            current frame set back to start
658         aLastKey                =
            LastKey(objectStringFrom);                                   // Does this need
            resetting? Isn't it still correct?
659         var newKeyPos = 0;
660
661         while (CurrentFrameNo   <= aLastKey)
662             {
663             var CurrentKeyVal   = GetValue(objectStringFrom,
                CurrentFrameNo);                    // Gets current key value
664             newKeyPos           = (((CurrentKeyVal - averagePos) * magMod ) +
                averagePos);
665             SaveKey(objectStringTo, CurrentFrameNo, newKeyPos);
666             CurrentFrameNo      = NextKey(objectStringFrom,
                CurrentFrameNo);                     // Increment frame no on Rig1
667             }
668     }
669
670
671
672
673
674 // Average Pos calculator
    ################################################################
675 function avgPosFinder
    (objectStringFrom)                                                       // (deleted
    objectStringTo as it seemed unecessary)
676 {
677     var CurrentFrameNo          = FirstKey(objectStringFrom);
```

```
678         var aLastKey                = LastKey(objectStringFrom);
679         var i                       = 0;
680         var sumKeyVal               =
            0;                                                          // Needed declaring
            outside
681
682         while (CurrentFrameNo       <=
            aLastKey)                                                   // Better as a For loop?
683             {
684                 var CurrentKeyVal   = GetValue(objectStringFrom,
                    CurrentFrameNo);                    // Gets current key value
685                 sumKeyVal           = CurrentKeyVal + sumKeyVal;
686                 CurrentFrameNo      = NextKey(objectStringFrom,
                    CurrentFrameNo);                    // Increment frame no on Rig1
687
                    i++;
                            // Increments the count
688             }
689         return (sumKeyVal /
            i);                                                                 // Returns
            a value to variable used to execute command
690     }
691
692     // MODKEY FUNCTION
        ###############################################################################
693     function ssModKeyDiff(objectStringFrom, objectStringTo, magMod,
        averagePos)                     // rig1, rig2, mag multiplier, actual average position
694         {
695             CurrentFrameNo          =
                FirstKey(objectStringFrom);                                 // After deletion
                current frame set back to start
696             aLastKey                =
                LastKey(objectStringFrom);                                  // Does this need
                resetting? Isn't it still correct?
697             var newKeyPos = 0;
698
699             while (CurrentFrameNo   <= aLastKey)
700                 {
701                 var CurrentKeyVal   = GetValue(objectStringFrom,
                    CurrentFrameNo);                                // Gets current key value
702                 newKeyPos           = (((CurrentKeyVal - averagePos) * magMod) + averagePos
                    - CurrentKeyVal);   // only adds the difference
703                 SaveKey(objectStringTo, CurrentFrameNo, newKeyPos);
704                 CurrentFrameNo      = NextKey(objectStringFrom,
                    CurrentFrameNo);                                // Increment frame no on Rig1
705                 }
706         }
707
708     // MODKEY OFFSET POSITIVE FUNCTION no loop
        ###############################################################################
709     function ssModKeyOPsingle(objectStringFrom, objectStringTo, avgPosDiff,
        CurrentFrameNo)     // rig1, rig2,
710         {
711         var CurrentKeyVal   = GetValue(objectStringFrom,
            CurrentFrameNo);                        // Gets current key value
712         newKeyPos           = (CurrentKeyVal +
            avgPosDiff);                                    // avgPosDiff is POSITIVE as rig
            has LEGS due to rig
713         SaveKey(objectStringTo, CurrentFrameNo, newKeyPos );
714         }
715
716     // MODKEY OFFSET NEGATIVE FUNCTION no loop
        ###############################################################################
717     function ssModKeyONsingle(objectStringFrom, objectStringTo, avgPosDiff,
        CurrentFrameNo)     // rig1, rig2, theor diff between avg pos, mag multiplier, actual
        average position
718         {
719         var CurrentKeyVal   = GetValue(objectStringFrom,
            CurrentFrameNo);                        // Gets current key value
```

```
720         newKeyPos           = (CurrentKeyVal -
            avgPosDiff);                                    // avgPosDiff is NEGATIVE as rig
            has LEGS due to rig
721         SaveKey(objectStringTo, CurrentFrameNo, newKeyPos );
722         }
723
724
725
726
727
728
729     //
            ##########################################################################################
            ##############
730
731     // DUPLICATE IKmod rig2 to create IKmod slowdown rig3 with IK rigs
732     Duplicate("B:Max_Pears_setb_n1", null, 2, 1, 1, 0, 0, 1, 0, 1, null, null, null, null,
            null, null, 0, 0, 0, null, 0);   // 5th value from end is posx offset translation
733
734     // UPDATE IF I CHANGE VALUES IN 10!
735         // var speedMod     = 1.1;          // A SLOWER
736         // var speedMod     = 1.0;          // B 12%
737         // var speedMod     = 0.9;          // C NO CHANGE
738         // var speedMod     = 0.805025734;  // D 35%
739         // var speedMod     = 0.7;          // E
740         // var speedMod     = 0.6;          // F FASTER
741            var speedMod = SiWalkingSpeed;   // uses modifier value from top
742
743     // LIST ALL ANIMATED BONES
744
745
746     // GCSRT HIP ROTATION
747     var GCSRT_2rotx = "MotionBuilder_Template1.Global_Control_SRT.kine.local.ori.euler.rotx";
748     //var GCSRT_2roty =
            "MotionBuilder_Template1.Global_Control_SRT.kine.local.ori.euler.roty";     // DECLARED
            L396 Additive hip rotation now added
749     var GCSRT_2rotz = "MotionBuilder_Template1.Global_Control_SRT.kine.local.ori.euler.rotz";
750     var GCSRT_3rotx = "MotionBuilder_Template2.Global_Control_SRT.kine.local.ori.euler.rotx";
751     var GCSRT_3roty = "MotionBuilder_Template2.Global_Control_SRT.kine.local.ori.euler.roty";
752     var GCSRT_3rotz =
            "MotionBuilder_Template2.Global_Control_SRT.kine.local.ori.euler.rotz";       // For
            Pelvic Rotation Magnification later (not direct slowdown)
753
754     // GCSRT POSITION
755     var GCSRT_2posx = "MotionBuilder_Template1.Global_Control_SRT.kine.local.pos.posx";
756     var GCSRT_2posy = "MotionBuilder_Template1.Global_Control_SRT.kine.local.pos.posy";
757     var GCSRT_2posz = "MotionBuilder_Template1.Global_Control_SRT.kine.local.pos.posz";
758     var GCSRT_3posx = "MotionBuilder_Template2.Global_Control_SRT.kine.local.pos.posx";
759     var GCSRT_3posy = "MotionBuilder_Template2.Global_Control_SRT.kine.local.pos.posy";
760     var GCSRT_3posz =
            "MotionBuilder_Template2.Global_Control_SRT.kine.local.pos.posz";             // HIPS
            POS SHOULDNT BE SLOWED ONLY GCSRT
761
762     // ADDITIVE HIP ROTATION
763     //var Hips_2roty =
            "MotionBuilder_Template1.Hips.kine.local.ori.euler.roty";                     //
            DECLARED L397 Additive hip rotation now added
764     var Hips_3roty = "MotionBuilder_Template2.Hips.kine.local.ori.euler.roty";
765
766     // Spine
767     var Spine_2rotx = "MotionBuilder_Template1.Spine.kine.local.ori.euler.rotx";
768     var Spine_2roty = "MotionBuilder_Template1.Spine.kine.local.ori.euler.roty";
769     var Spine_2rotz = "MotionBuilder_Template1.Spine.kine.local.ori.euler.rotz";
770     var Spine_3rotx = "MotionBuilder_Template2.Spine.kine.local.ori.euler.rotx";
771     var Spine_3roty = "MotionBuilder_Template2.Spine.kine.local.ori.euler.roty";
772     var Spine_3rotz = "MotionBuilder_Template2.Spine.kine.local.ori.euler.rotz";
773     // Spine1
774     var Spine1_2rotx = "MotionBuilder_Template1.Spine1.kine.local.ori.euler.rotx";
775     var Spine1_2roty = "MotionBuilder_Template1.Spine1.kine.local.ori.euler.roty";
```

```
776   var Spine1_2rotz = "MotionBuilder_Template1.Spine1.kine.local.ori.euler.rotz";
777   var Spine1_3rotx = "MotionBuilder_Template2.Spine1.kine.local.ori.euler.rotx";
778   var Spine1_3roty = "MotionBuilder_Template2.Spine1.kine.local.ori.euler.roty";
779   var Spine1_3rotz = "MotionBuilder_Template2.Spine1.kine.local.ori.euler.rotz";
780   // Spine2
781   var Spine2_2rotx = "MotionBuilder_Template1.Spine2.kine.local.ori.euler.rotx";
782   var Spine2_2roty = "MotionBuilder_Template1.Spine2.kine.local.ori.euler.roty";
783   var Spine2_2rotz = "MotionBuilder_Template1.Spine2.kine.local.ori.euler.rotz";
784   var Spine2_3rotx = "MotionBuilder_Template2.Spine2.kine.local.ori.euler.rotx";
785   var Spine2_3roty = "MotionBuilder_Template2.Spine2.kine.local.ori.euler.roty";
786   var Spine2_3rotz = "MotionBuilder_Template2.Spine2.kine.local.ori.euler.rotz";
787   // Spine3
788   var Spine3_2rotx = "MotionBuilder_Template1.Spine3.kine.local.ori.euler.rotx";
789   var Spine3_2roty = "MotionBuilder_Template1.Spine3.kine.local.ori.euler.roty";
790   var Spine3_2rotz = "MotionBuilder_Template1.Spine3.kine.local.ori.euler.rotz";
791   var Spine3_3rotx =
      "MotionBuilder_Template2.Spine3.kine.local.ori.euler.rotx";                    //
      Sideways Torso rotation
792   var Spine3_3roty = "MotionBuilder_Template2.Spine3.kine.local.ori.euler.roty";
793   var Spine3_3rotz = "MotionBuilder_Template2.Spine3.kine.local.ori.euler.rotz";
794   // Spine4
795   //var Spine4_2rotx =
      "MotionBuilder_Template1.Spine4.kine.local.ori.euler.rotx";                  // DECLARED
      ABOVE
796   var Spine4_2roty = "MotionBuilder_Template1.Spine4.kine.local.ori.euler.roty";
797   var Spine4_2rotz = "MotionBuilder_Template1.Spine4.kine.local.ori.euler.rotz";
798   var Spine4_3rotx = "MotionBuilder_Template2.Spine4.kine.local.ori.euler.rotx";
799   var Spine4_3roty = "MotionBuilder_Template2.Spine4.kine.local.ori.euler.roty";
800   var Spine4_3rotz = "MotionBuilder_Template2.Spine4.kine.local.ori.euler.rotz";
801   // Neck
802   var Neck_2rotx = "MotionBuilder_Template1.Neck.kine.local.ori.euler.rotx";
803   var Neck_2roty = "MotionBuilder_Template1.Neck.kine.local.ori.euler.roty";
804   var Neck_2rotz = "MotionBuilder_Template1.Neck.kine.local.ori.euler.rotz";
805   var Neck_3rotx = "MotionBuilder_Template2.Neck.kine.local.ori.euler.rotx";
806   var Neck_3roty = "MotionBuilder_Template2.Neck.kine.local.ori.euler.roty";
807   var Neck_3rotz = "MotionBuilder_Template2.Neck.kine.local.ori.euler.rotz";
808   // Head
809   var Head_2rotx = "MotionBuilder_Template1.Head.kine.local.ori.euler.rotx";
810   var Head_2roty = "MotionBuilder_Template1.Head.kine.local.ori.euler.roty";
811   var Head_2rotz = "MotionBuilder_Template1.Head.kine.local.ori.euler.rotz";
812   var Head_3rotx = "MotionBuilder_Template2.Head.kine.local.ori.euler.rotx";
813   var Head_3roty = "MotionBuilder_Template2.Head.kine.local.ori.euler.roty";
814   var Head_3rotz = "MotionBuilder_Template2.Head.kine.local.ori.euler.rotz";
815   // RightShoulder
816   var RightShoulder_2rotx =
      "MotionBuilder_Template1.RightShoulder.kine.local.ori.euler.rotx";
817   var RightShoulder_2roty =
      "MotionBuilder_Template1.RightShoulder.kine.local.ori.euler.roty";
818   var RightShoulder_2rotz =
      "MotionBuilder_Template1.RightShoulder.kine.local.ori.euler.rotz";
819   var RightShoulder_3rotx =
      "MotionBuilder_Template2.RightShoulder.kine.local.ori.euler.rotx";
820   var RightShoulder_3roty =
      "MotionBuilder_Template2.RightShoulder.kine.local.ori.euler.roty";
821   var RightShoulder_3rotz =
      "MotionBuilder_Template2.RightShoulder.kine.local.ori.euler.rotz";
822   // RightArm
823   var RightArm_2rotx = "MotionBuilder_Template1.RightArm.kine.local.ori.euler.rotx";
824   //var RightArm_2roty =
      "MotionBuilder_Template1.RightArm.kine.local.ori.euler.roty";            //DECLARED ABOVE
825   //var RightArm_2rotz =
      "MotionBuilder_Template1.RightArm.kine.local.ori.euler.rotz";            //DECLARED ABOVE
826   var RightArm_3rotx = "MotionBuilder_Template2.RightArm.kine.local.ori.euler.rotx";
827   var RightArm_3roty = "MotionBuilder_Template2.RightArm.kine.local.ori.euler.roty";
828   var RightArm_3rotz = "MotionBuilder_Template2.RightArm.kine.local.ori.euler.rotz";
829   // RightForeArm - NOT SURE WHY I HAD PREVIOUSLY LEFT THIS OUT???
830   var RightForeArm_2rotx =
      "MotionBuilder_Template1.RightForeArm.kine.local.ori.euler.rotx";
831   var RightForeArm_2roty =
```

```
"MotionBuilder_Template1.RightForeArm.kine.local.ori.euler.roty";
var RightForeArm_2rotz =
"MotionBuilder_Template1.RightForeArm.kine.local.ori.euler.rotz";
var RightForeArm_3rotx =
"MotionBuilder_Template2.RightForeArm.kine.local.ori.euler.rotx";
var RightForeArm_3roty =
"MotionBuilder_Template2.RightForeArm.kine.local.ori.euler.roty";
var RightForeArm_3rotz =
"MotionBuilder_Template2.RightForeArm.kine.local.ori.euler.rotz";
// RightHand
var RightHand_2rotx = "MotionBuilder_Template1.RightHand.kine.local.ori.euler.rotx";
var RightHand_2roty = "MotionBuilder_Template1.RightHand.kine.local.ori.euler.roty";
var RightHand_2rotz = "MotionBuilder_Template1.RightHand.kine.local.ori.euler.rotz";
var RightHand_3rotx = "MotionBuilder_Template2.RightHand.kine.local.ori.euler.rotx";
var RightHand_3roty = "MotionBuilder_Template2.RightHand.kine.local.ori.euler.roty";
var RightHand_3rotz = "MotionBuilder_Template2.RightHand.kine.local.ori.euler.rotz";
// LeftShoulder
var LeftShoulder_2rotx =
"MotionBuilder_Template1.LeftShoulder.kine.local.ori.euler.rotx";
var LeftShoulder_2roty =
"MotionBuilder_Template1.LeftShoulder.kine.local.ori.euler.roty";
var LeftShoulder_2rotz =
"MotionBuilder_Template1.LeftShoulder.kine.local.ori.euler.rotz";
var LeftShoulder_3rotx =
"MotionBuilder_Template2.LeftShoulder.kine.local.ori.euler.rotx";
var LeftShoulder_3roty =
"MotionBuilder_Template2.LeftShoulder.kine.local.ori.euler.roty";
var LeftShoulder_3rotz =
"MotionBuilder_Template2.LeftShoulder.kine.local.ori.euler.rotz";
// LeftForeArm - NOT SURE WHY I HAD PREVIOUSLY LEFT THIS OUT???
var LeftForeArm_2rotx = "MotionBuilder_Template1.LeftForeArm.kine.local.ori.euler.rotx";
var LeftForeArm_2roty = "MotionBuilder_Template1.LeftForeArm.kine.local.ori.euler.roty";
var LeftForeArm_2rotz = "MotionBuilder_Template1.LeftForeArm.kine.local.ori.euler.rotz";
var LeftForeArm_3rotx = "MotionBuilder_Template2.LeftForeArm.kine.local.ori.euler.rotx";
var LeftForeArm_3roty = "MotionBuilder_Template2.LeftForeArm.kine.local.ori.euler.roty";
var LeftForeArm_3rotz = "MotionBuilder_Template2.LeftForeArm.kine.local.ori.euler.rotz";
// LeftArm
var LeftArm_2rotx = "MotionBuilder_Template1.LeftArm.kine.local.ori.euler.rotx";
// var LeftArm_2roty = "MotionBuilder_Template1.LeftArm.kine.local.ori.euler.roty";
//DECLARED ABOVE
// var LeftArm_2rotz = "MotionBuilder_Template1.LeftArm.kine.local.ori.euler.rotz";
//DECLARED ABOVE
var LeftArm_3rotx = "MotionBuilder_Template2.LeftArm.kine.local.ori.euler.rotx";
var LeftArm_3roty = "MotionBuilder_Template2.LeftArm.kine.local.ori.euler.roty";
var LeftArm_3rotz = "MotionBuilder_Template2.LeftArm.kine.local.ori.euler.rotz";
// LeftHand
var LeftHand_2rotx = "MotionBuilder_Template1.LeftHand.kine.local.ori.euler.rotx";
var LeftHand_2roty = "MotionBuilder_Template1.LeftHand.kine.local.ori.euler.roty";
var LeftHand_2rotz = "MotionBuilder_Template1.LeftHand.kine.local.ori.euler.rotz";
var LeftHand_3rotx = "MotionBuilder_Template2.LeftHand.kine.local.ori.euler.rotx";
var LeftHand_3roty = "MotionBuilder_Template2.LeftHand.kine.local.ori.euler.roty";
var LeftHand_3rotz = "MotionBuilder_Template2.LeftHand.kine.local.ori.euler.rotz";

// LEGS ######################
// Left Leg control box
// var LeftLegCB_2posx  = "MotionBuilder_Template1.left_leg_pos.kine.local.posx";
//DECLARED ABOVE L415
var LeftLegCB_2posy = "MotionBuilder_Template1.left_leg_pos.kine.local.posy";
var LeftLegCB_2posz = "MotionBuilder_Template1.left_leg_pos.kine.local.posz";
var LeftLegCB_3posx = "MotionBuilder_Template2.left_leg_pos.kine.local.posx";
var LeftLegCB_3posy = "MotionBuilder_Template2.left_leg_pos.kine.local.posy";
var LeftLegCB_3posz = "MotionBuilder_Template2.left_leg_pos.kine.local.posz";
// Right Leg control box
//var RightLegCB_2posx = "MotionBuilder_Template1.right_leg_pos.kine.local.posx";
//DECLARED ABOVE L417
var RightLegCB_2posy = "MotionBuilder_Template1.right_leg_pos.kine.local.posy";
var RightLegCB_2posz = "MotionBuilder_Template1.right_leg_pos.kine.local.posz";
var RightLegCB_3posx = "MotionBuilder_Template2.right_leg_pos.kine.local.posx";
var RightLegCB_3posy = "MotionBuilder_Template2.right_leg_pos.kine.local.posy";
```

```
var RightLegCB_3posz = "MotionBuilder_Template2.right_leg_pos.kine.local.posz";
// Left Toe Control Boxes
//var lToePos_2posx     = "MotionBuilder_Template1.left_toe_pos.kine.local.pos.posx";
var lToePos_2posy       = "MotionBuilder_Template1.left_toe_pos.kine.local.pos.posy";
var lToePos_2posz       = "MotionBuilder_Template1.left_toe_pos.kine.local.pos.posz";
var lToePos_3posx       = "MotionBuilder_Template2.left_toe_pos.kine.local.pos.posx";
var lToePos_3posy       = "MotionBuilder_Template2.left_toe_pos.kine.local.pos.posy";
var lToePos_3posz       = "MotionBuilder_Template2.left_toe_pos.kine.local.pos.posz";
// Right Toe Control Boxes
//var rToePos_2posx     = "MotionBuilder_Template1.right_toe_pos.kine.local.pos.posx";
var rToePos_2posy       = "MotionBuilder_Template1.right_toe_pos.kine.local.pos.posy";
var rToePos_2posz       = "MotionBuilder_Template1.right_toe_pos.kine.local.pos.posz";
var rToePos_3posx       = "MotionBuilder_Template2.right_toe_pos.kine.local.pos.posx";
var rToePos_3posy       = "MotionBuilder_Template2.right_toe_pos.kine.local.pos.posy";
var rToePos_3posz       = "MotionBuilder_Template2.right_toe_pos.kine.local.pos.posz";

// LIST ALL SSRETIMEKEYS
// ENSURE GCSRT IS THERE
// Execute retime commands for every bone on rig1 and rig2
// ssRetimeKey function ######################################################

// GCSRT Hip Rotation
ssReTimeKey(GCSRT_2rotx,GCSRT_3rotx,speedMod);
ssReTimeKey(GCSRT_2roty,GCSRT_3roty,speedMod);
ssReTimeKey(GCSRT_2rotz,GCSRT_3rotz,speedMod);
// GCSRT Hip/ CHARACTER Pos
ssReTimeKey(GCSRT_2posx,GCSRT_3posx,speedMod);
ssReTimeKey(GCSRT_2posy,GCSRT_3posy,speedMod);
ssReTimeKey(GCSRT_2posz,GCSRT_3posz,speedMod);
// Added Hip twist
ssReTimeKey(Hips_2roty,Hips_3roty,speedMod);

// Spine
ssReTimeKey(Spine_2rotx,Spine_3rotx,speedMod);
ssReTimeKey(Spine_2roty,Spine_3roty,speedMod);
ssReTimeKey(Spine_2rotz,Spine_3rotz,speedMod);
// Spine1
ssReTimeKey(Spine1_2rotx,Spine1_3rotx,speedMod);
ssReTimeKey(Spine1_2roty,Spine1_3roty,speedMod);
ssReTimeKey(Spine1_2rotz,Spine1_3rotz,speedMod);
// Spine3
ssReTimeKey(Spine2_2rotx,Spine2_3rotx,speedMod);
ssReTimeKey(Spine2_2roty,Spine2_3roty,speedMod);
ssReTimeKey(Spine2_2rotz,Spine2_3rotz,speedMod);
// Spine3
ssReTimeKey(Spine3_2rotx,Spine3_3rotx,speedMod);
ssReTimeKey(Spine3_2roty,Spine3_3roty,speedMod);
ssReTimeKey(Spine3_2rotz,Spine3_3rotz,speedMod);
// Spine4
ssReTimeKey(Spine4_2rotx,Spine4_3rotx,speedMod);
ssReTimeKey(Spine4_2roty,Spine4_3roty,speedMod);
ssReTimeKey(Spine4_2rotz,Spine4_3rotz,speedMod);
// Neck
ssReTimeKey(Neck_2rotx,Neck_3rotx,speedMod);
ssReTimeKey(Neck_2roty,Neck_3roty,speedMod);
ssReTimeKey(Neck_2rotz,Neck_3rotz,speedMod);
// Head
ssReTimeKey(Head_2rotx,Head_3rotx,speedMod);
ssReTimeKey(Head_2roty,Head_3roty,speedMod);
ssReTimeKey(Head_2rotz,Head_3rotz,speedMod);

// RightShoulder
ssReTimeKey(RightShoulder_2rotx,RightShoulder_3rotx,speedMod);
ssReTimeKey(RightShoulder_2roty,RightShoulder_3roty,speedMod);
ssReTimeKey(RightShoulder_2rotz,RightShoulder_3rotz,speedMod);
// RightForeArm # Don't know why I had previously left this out?
ssReTimeKey(RightForeArm_2rotx,RightForeArm_3rotx,speedMod);
ssReTimeKey(RightForeArm_2roty,RightForeArm_3roty,speedMod);
ssReTimeKey(RightForeArm_2rotz,RightForeArm_3rotz,speedMod);
```

```
955   // RightArm
956   ssReTimeKey(RightArm_2rotx,RightArm_3rotx,speedMod);
957   ssReTimeKey(RightArm_2roty,RightArm_3roty,speedMod);
958   ssReTimeKey(RightArm_2rotz,RightArm_3rotz,speedMod);
959   // RightHand
960   ssReTimeKey(RightHand_2rotx,RightHand_3rotx,speedMod);
961   ssReTimeKey(RightHand_2roty,RightHand_3roty,speedMod);
962   ssReTimeKey(RightHand_2rotz,RightHand_3rotz,speedMod);
963
964   // LeftShoulder
965   ssReTimeKey(LeftShoulder_2rotx,LeftShoulder_3rotx,speedMod);
966   ssReTimeKey(LeftShoulder_2roty,LeftShoulder_3roty,speedMod);
967   ssReTimeKey(LeftShoulder_2rotz,LeftShoulder_3rotz,speedMod);
968   // LeftArm
969   ssReTimeKey(LeftArm_2rotx,LeftArm_3rotx,speedMod);
970   ssReTimeKey(LeftArm_2roty,LeftArm_3roty,speedMod);
971   ssReTimeKey(LeftArm_2rotz,LeftArm_3rotz,speedMod);
972   // LeftForeArm # Don't know why I had previously left this out?
973   ssReTimeKey(LeftForeArm_2rotx,LeftForeArm_3rotx,speedMod);
974   ssReTimeKey(LeftForeArm_2roty,LeftForeArm_3roty,speedMod);
975   ssReTimeKey(LeftForeArm_2rotz,LeftForeArm_3rotz,speedMod);
976   // LeftHand
977   ssReTimeKey(LeftHand_2rotx,LeftHand_3rotx,speedMod);
978   ssReTimeKey(LeftHand_2roty,LeftHand_3roty,speedMod);
979   ssReTimeKey(LeftHand_2rotz,LeftHand_3rotz,speedMod);
980
981   /* RightUpLeg
982   ssReTimeKey(RightUpLeg_2rotx,RightUpLeg_3rotx,speedMod);
983   ssReTimeKey(RightUpLeg_2roty,RightUpLeg_3roty,speedMod);
984   ssReTimeKey(RightUpLeg_2rotz,RightUpLeg_3rotz,speedMod);
985   // RightLeg
986   ssReTimeKey(RightLeg_2rotx,RightLeg_3rotx,speedMod);
987   ssReTimeKey(RightLeg_2roty,RightLeg_3roty,speedMod);
988   ssReTimeKey(RightLeg_2rotz,RightLeg_3rotz,speedMod);
989   // RightFoot
990   ssReTimeKey(RightFoot_2rotx,RightFoot_3rotx,speedMod);
991   ssReTimeKey(RightFoot_2roty,RightFoot_3roty,speedMod);
992   ssReTimeKey(RightFoot_2rotz,RightFoot_3rotz,speedMod);
993   // LeftUpLeg
994   ssReTimeKey(LeftUpLeg_2rotx,LeftUpLeg_3rotx,speedMod);
995   ssReTimeKey(LeftUpLeg_2roty,LeftUpLeg_3roty,speedMod);
996   ssReTimeKey(LeftUpLeg_2rotz,LeftUpLeg_3rotz,speedMod);
997   // LeftLeg
998   ssReTimeKey(LeftLeg_2rotx,LeftLeg_3rotx,speedMod);
999   ssReTimeKey(LeftLeg_2roty,LeftLeg_3roty,speedMod);
1000  ssReTimeKey(LeftLeg_2rotz,LeftLeg_3rotz,speedMod);
1001  // LeftFoot
1002  ssReTimeKey(LeftFoot_2rotx,LeftFoot_3rotx,speedMod);
1003  ssReTimeKey(LeftFoot_2roty,LeftFoot_3roty,speedMod);
1004  ssReTimeKey(LeftFoot_2rotz,LeftFoot_3rotz,speedMod);*/
1005
1006  // Right Leg
1007  ssReTimeKey(LeftLegCB_2posx,LeftLegCB_3posx,speedMod);
1008  ssReTimeKey(LeftLegCB_2posy,LeftLegCB_3posy,speedMod);
1009  ssReTimeKey(LeftLegCB_2posz,LeftLegCB_3posz,speedMod);
1010
1011  // Left Leg
1012  ssReTimeKey(RightLegCB_2posx,RightLegCB_3posx,speedMod);
1013  ssReTimeKey(RightLegCB_2posy,RightLegCB_3posy,speedMod);
1014  ssReTimeKey(RightLegCB_2posz,RightLegCB_3posz,speedMod);
1015
1016  // Right Toe
1017  ssReTimeKey(lToePos_2posx,lToePos_3posx,speedMod);
1018  ssReTimeKey(lToePos_2posy,lToePos_3posy,speedMod);
1019  ssReTimeKey(lToePos_2posz,lToePos_3posz,speedMod);
1020
1021  // Left Toe
1022  ssReTimeKey(rToePos_2posx,rToePos_3posx,speedMod);
1023  ssReTimeKey(rToePos_2posy,rToePos_3posy,speedMod);
```

```
ssReTimeKey(rToePos_2posz,rToePos_3posz,speedMod);



// PASTE SSRETIMEKEY
function ssReTimeKey(objectStringFrom, objectStringTo, timeMod)
    {
    try
        {   // DELETES all keys on rig2. COULD I REPLACE WITH RemoveAllAnimation TO SPEED UP??????????
        var CurrentFrameNo      = FirstKey(objectStringTo);
        var aLastKey            = LastKey(objectStringTo);

        while (CurrentFrameNo   <= aLastKey)
            {
            RemoveKey(objectStringTo, CurrentFrameNo);
            CurrentFrameNo      = NextKey(objectStringTo, CurrentFrameNo );
            }
        }
    catch (err){}

    try //Retiming section
    ##########################################################################################################
        {
        CurrentFrameNo          = FirstKey(objectStringFrom);                   // After deletion current frame set back to start
        aLastKey                = LastKey(objectStringFrom);                    // Does this need resetting? Isn't it still correct?

        while (CurrentFrameNo   <= aLastKey)
            {
            var modFrameNo      = CurrentFrameNo / timeMod;                     // Divides frame no by scaleMod
            var CurrentKeyVal   = GetValue(objectStringFrom, CurrentFrameNo);   // Gets current key value
            SaveKey(objectStringTo, modFrameNo, CurrentKeyVal );                // ASSUMING MODKEYVAL WORKS. IF NOT REVERT TO CURRENTKEYVAL
            CurrentFrameNo      = NextKey(objectStringFrom, CurrentFrameNo );   //
            }
        }
    catch (err){}
    }



// ########################################## NULLSPHERES
##############################################

// HIDE BOTH CHARACTERS
SelectObj("Max_Pears_setb_n", "BRANCH", null);
ToggleSelection("Max_Pears_setb_n1", "BRANCH", null);
//ToggleSelection("Max_Pears_setb_n2", "BRANCH", null);
ToggleVisibility(null, null, null);

// MAKE BACKGROUND BLACK
// SetValue("Preferences.SceneColors.backgroundcol", 0, null);
SetDisplayMode("Camera", "shaded");


//ParentObj("B:Camera_Interest", "Camera");
FirstFrame();                           // Jump to FirstFrame
SelectObj("Camera_Interest", null, true);
//Rotate(null, 0, 45, 0, siRelative, siLocalSym, siObj, siXYZ, null, null, null, null, null, null, null, 0, null);                                  // Rotx Camera_Interest 0
Rotate(null, 0, 0, 0, siRelative, siLocalSym, siObj, siXYZ, null, null, null, null, null, null, null, 0, null);                                  // Rotx Camera_Interest 0
SaveKey("Camera_Interest.kine.local.rotx,Camera_Interest.kine.local.roty,Camera_Interest.kine.local.rotz", 9, null, null, null, false, null);   // SaveKey
```

```
1081
1082  // NEED TO CHANGE THE ROTY TO 360 FOR PANAROUND
1083  LastFrame();                              // Jump to LastFrame
1084  // SelectObj("Camera_Interest", null, true);
1085  //Rotate(null, 0, 45, 0, siRelative, siLocalSym, siObj, siXYZ, null, null, null, null,
      null, null, null, 0, null);                                    // Rotx Camera_Interest 0
1086  Rotate(null, 0, 0, 0, siRelative, siLocalSym, siObj, siXYZ, null, null, null, null,
      null, null, null, 0, null);                                    // Rotx Camera_Interest 0
1087  SaveKey("Camera_Interest.kine.local.rotx,Camera_Interest.kine.local.roty,Camera_Interest.
      kine.local.rotz", 87, null, null, null, false, null);  // Or change frame no
1088
1089  // FRAME WALKERS FULLY
1090  SelectObj("Camera_Interest", null, true);
1091  Translate(null, 0, -1, 0, siRelative, siLocalSym, siObj, siXYZ, null, null, null, null,
      null, null, null, null, null, 0, null);
1092  SelectObj("Camera", null, true);
1093  Translate(null, 0, 0, 7, siRelative, siLocalSym, siObj, siXYZ, null, null, null, null,
      null, null, null, null, null, 0, null);
1094
1095  // Deform mesh
1096  SetValue("Camera.camvis.constructionlevel", false, null);
1097  SetValue("Camera.camvis.custominfo", true, null);
1098  SetValue("Camera.camvis.gridaxisvis", false, null);
1099  // Hide nulls and control objects in User view
1100  //
      SelectObj("MotionBuilder_Template1.eff,MotionBuilder_Template1.root1,MotionBuilder_Templa
      te1.eff1,MotionBuilder_Template1.eff2,MotionBuilder_Template1.root3,MotionBuilder_Templat
      e1.eff3", null, true);
1101  // ToggleVisibility(null, null, null);
1102  // SetValue("Views.ViewD.UserCamera.camvis.objnulls", false, null);
1103  // SetValue("Views.ViewD.UserCamera.camvis.objctrlwaves", false, null);
1104  // SetValue("Views.ViewD.UserCamera.camvis.objctrlother", false, null); */
1105
1106  SetMarking("DisplayInfo_BF.Bodt_Fat_Percentage");
1107  SetValue("Man2.Character.DisplayInfo_BF.Bodt_Fat_Percentage", ChBF, null);
1108  SelectObj("MotionBuilder_Template2.eff,MotionBuilder_Template2.root1,MotionBuilder_Templa
      te2.eff1,MotionBuilder_Template2.eff2,MotionBuilder_Template2.root3,MotionBuilder_Templat
      e2.eff3", null, true);
1109  ToggleVisibility(null, null, null);
1110
1111  // measurement readouts
1112  SetValue("DisplayInfo_Measurements.Body_Fat_Percentage", ChBF, null);
1113  SetValue("DisplayInfo_Measurements.WtHR", WtHR, null);
1114  SetValue("DisplayInfo_Measurements.Chest", ChChest, null);
1115  SetValue("DisplayInfo_Measurements.Height", ChHeight, null);
1116  SetValue("DisplayInfo_Measurements.ArmSwing", armSwing, null);
1117  SetValue("DisplayInfo_Measurements.ArmBob", armBobMag, null);
1118  SetValue("DisplayInfo_Measurements.StepWidth", walkingBase, null);
1119  SetValue("DisplayInfo_Measurements.armAbduction", armAbduction, null);
1120  SetValue("DisplayInfo_Measurements.WalkingSpeed", walkingSpeed, null);
```